University of Reading

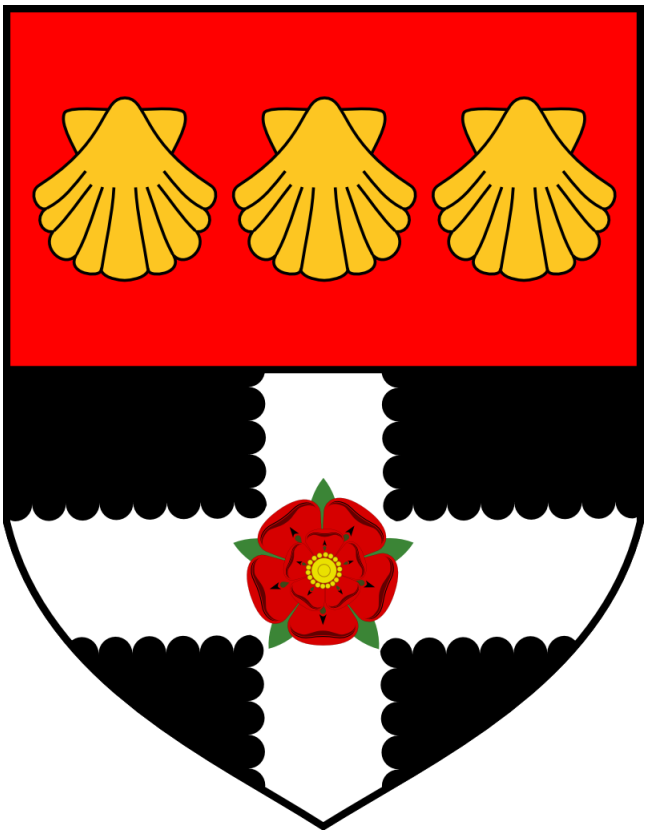

Generation and functional testing of novel biologics targeting glycoprotein receptors in platelets

A thesis submitted for the degree of Doctor of Philosophy

Institute for Cardiovascular and Metabolic Research

School of Biological Sciences

Eva Maria Soriano Jerez

March 2022

DECLARATION

I confirm that this is my own work and the use of all material from other sources has been properly and fully acknowledged.

Signed: Eva Maria Soriano Jerez

Date: March 2022.

ABSTRACT

Glycoprotein receptor VI (GPVI) is the major collagen receptor in platelets. Ligand binding induces GPVI clustering, which initiates a tyrosine kinase-based signalling cascade via an immunoreceptor tyrosine-based activation motif (ITAM). GPVI has been shown to play roles in both the initiation and growth of thrombi, although GPVI deletion is not associated with significant bleeding. Therefore, targeting the GPVI pathway is a potential route to overcome the bleeding risk associated with current therapies.

G6b-B is a glycoprotein receptor with restricted expression to platelets membrane surface that inhibits platelet activation by ITAM receptors. Crosslinking with G6b-B antibodies prevents platelet activation. We hypothesize that it will be possible to overcome the bleeding risk of current antithrombotics, which target other platelet activation pathways, by inhibiting GPVI-mediated pathway molecules or activating G6b-B using novel biologics, such as Affimers.

To inhibit the GPVI pathway we generated novel anti-human GPVI monoclonal antibodies (mAbs) and their F(ab) fragments (developed prior to the start of this project by Emfret Analytics Würzburg, Germany). The aim was to determine their mode of action and to which epitopes or regions of the protein they bind. Four new anti-GPVI mAbs and their F (ab) fragments were characterised. Among the mAbs, E7 was the only antibody to fully block GPVI activity. A9 caused a minor inhibition suggestive of either direct competition for the CRP binding site, binding close enough to cause steric hindrance to its binding.

GPVI-mediated platelet activation was inhibited by all four F(ab) fragments suggesting these have potential as a novel α-GPVI therapy.

Structural characterization of these anti-GPVI mAbs (E12, E7, E2, D3 and A9) with GPVI was assessed with three complementary approaches, namely bio-layer interferometry (BLI), crystallography, and epitope mapping. BLI showed that none of the mAbs are monomer or dimer specific. Crystallographic studies were not successful and will need further future optimisation. GPVI chimeras were generated to identify that the mAbs were binding to the GPVI D1 domain, which is the ligand binding domain. Additional studies will be needed for a full structural characterization of these mAbs bound to GPVI which protein-based therapeutics are required to demonstrate during their development phase.

Our other aim was to develop new biologics (Affimers) to target and activate the ITIM-receptor G6b-B, which constitutively inhibits platelet activation by ITAM-like receptors. The potential antithrombotic effect of G6b-B and whether G6b-B stimulation could lead to less reactive platelets, reducing the risk, or severity of thrombosis has not been extensively studied until now. Here we targeted for the first time an inhibitory pathway to downregulate GPVI by targeting G6b-B. Three Affimers were identified to bind G6b-B. Preliminary functional studies showed that these Affimers did not induce G6b-B to inhibit platelet activation through the GPVI activation pathway in classical *in vitro* platelet function assays (namely aggregometry). However, preliminary *in vitro* flow studies with Affimer 24 showed some potential to influence thrombus size on CRP coated surfaces.

In conclusion, in this thesis we provide an insight of the first functional and structural characterization of new mAbs targeting human GPVI, with some showing potential as good candidates for antiplatelet therapy. Additionally, we show the first attempt to target an inhibitory pathway as anti-platelet therapy by developing Affimers against G6b-B.

Further research is needed to explore whether G6b-B stimulation could lead to less reactive platelets reducing the risk, or severity of thrombotic disease without causing substantial bleeding.

ACKNOWLEDGEMENTS

Firstly, I would like to express my heartfelt gratitude to my supervisor and mentor Craig Hughes. I could never imagine that you, the person, whom I was not able to see well in our first zoom meeting, were going to turn in one of the most important persons in my life. Your constant and encouraging support on the good and the bad day has been crucial for this achievement. I do not have words to express my gratitude for sharing this journey and challenging me to grow up as a scientist. Thank you, Craig!

Massive thanks to my second supervisor in Reading, Jon Gibbins, and Alice Pollitt and Chris Jones for your support, advice, and discussions. Thanks also to all the members of the lab for the great shared experience and all the lab discussions. Thanks to Tanya, Neline, Amanda, Renato, Alex, Kirk, Jo, Yasmin, Amro, Daniel, Taysseer, Fahd, Abdul, Zannah and Salihah.

Thank to my lab mates, Sophie, Safa, Carly, Gemma, Danni, Charlie, Isabella and Ilaria, for being there always for me, for sharing tears and laughs. This experience would not be the same without you!

I also would like to thank my other supervisors in my second lab Bernard Nieswandt and David Stegner for their great help, advice and understanding. Special thanks to Bernard Nieswandt for providing the antibodies that make possible part of this thesis.

I would like to extend my thanks to Prof Michael Douglas, Prof. Andrew Herr, Dr Mike Tomlinson, and Dr Christian Tiede, for the constructs.

A very special thanks to all the TAPAS ESRs to share this experience together Ale, Isabella, Ilaria, Natalie, Helena, Xueqing, Jingnan, Zahra, Chu, Hilaire and Stefano. Also, all the TAPAS supervisors and members. Especially I would like to thank Isabella, for her help with the thrombus flow experiments and Dr Marcin Sowa for sharing this experience from the very beginning, that first of September in 2018. It was great to find such a special friend and share all the good and bad experiences of a challenging PhD because easy things aren't made for us!

Huge thanks to Danni, Charlie, and Prof. Kim Watson for all their support and help with protein purification and crystallography and for sharing the lab space together. Especially Danni, thank you for being so patient with me and always being there for me.

I would like to extend my thanks to Prof Steve Watson, Dr Alex Slater and Dr Eleyna Martin for their help, support, training and all the emails during these years, thank you for being always an email away.

Finally, thank to my family for believing in me and supporting me throughout the years of my education. Thank you to my parents, Francisco, and Maria for all the sacrifices that they have made for giving me better opportunities and for teaching me that with hard work, I can do all that I want. Thank you to all my siblings, especially my small sister, Mercedes, for being always so thoughtful. Massive thanks to my boyfriend, fiancé and now husband, Daniel, for being the best partner to team with, even more, if you have to plan a wedding in a different country. From the very beginning, he was encouraging me to pursue my dreams, no matter the distance or the country. It only took six years and a pandemic to start living together! Thank you for being so patient and kind with me, especially these last months and thank you, for all the cool backgrounds for my slides and for helping me with my figures. Thanks to my friends Carmen, Eva and Malva who have been there for me no matter the distance and for sending me papers when I didn't have access!

I also would like to thank the European Union's Horizon 2020 research and innovation programme: Targeting Platelet Adhesion Receptors in Thrombosis (TAPAS) under the Marie Skłodowska-Curie grant agreement No. 766118 for supporting this work and making it possible. And thank you to all the blood donors that made possible this work!

PUBLICATIONS

Soriano Jerez, E.M., J.M. Gibbins, and C.E. Hughes. 2021. Targeting platelet inhibition receptors for novel therapies: PECAM-1 and G6b-B. *Platelets*. 32:761-769.

d'Alessandro E, Becker C, Bergmeier W, Bode C, Bourne JH, Brown H, (…), **Soriano EM**, Sowa MA, (…), Ten Cate H; Scientific Reviewer Committee. Thrombo-Inflammation in Cardiovascular Disease: An Expert Consensus Document from the Third Maastricht Consensus Conference on Thrombosis. Thromb Haemost. 2020 Apr;120(4):538-564. doi: 10.1055/s-0040-1708035. Epub 2020 Apr 14. PMID: 32289858.

Helena C Brown, Sarah Beck, Stefano Navarro, Ying Di, **Eva M Soriano Jerez**, Jana Kaczmarzyk, Steven G. Thomas, Valbona Mirakaj, Steve P Watson, Bernhard Nieswandt, David Stegner. Antibody-mediated depletion of human CLEC-2 in a novel humanised mouse model. bioRxiv 2021.10.03.462933; doi: https://doi.org/10.1101/2021.10.03.462933

PRESENTATIONS

1.1 Oral communication

BSHT Annual Scientific meeting 2022. January 2022.

Eva M. Soriano Jerez, S. Navarro, B. Nieswandt, D. Stegner, Jonathan M. Gibbins, C. E. Hughes. Novel inhibitory GPVI antibodies block the GPVI ligand binding domain.

School of Biological Sciences PhD Symposium (University of Reading, UK). June 2021.

Eva M. Soriano Jerez, S. Navarro, B. Nieswandt, D. Stegner, Jonathan M. Gibbins, C. E. Hughes. Targeting human GPVI with novel monoclonal antibodies inhibits platelet function.

BSHT Annual Scientific meeting 2021. March 2021.

Eva M. Soriano Jerez, S. Navarro, B. Nieswandt, D. Stegner, Jonathan M. Gibbins, C. E. Hughes. Targeting human GPVI with novel monoclonal antibodies inhibits platelet function.

1.2 Poster presentation

2nd Platelet Society Online Meeting (Keele University, UK). March 2021.

Eureka! Symposium 2019 (University of Würzburg, Germany). October 2019

1st Platelet Society Meeting, University of Cambridge, UK October 2019.

School of Biological Sciences PhD Symposium (University of Reading, UK). June 2019.

ABBREVIATIONS

αIIbβ3	Glycoprotein IIb/IIIa
Abs	Antibodies
ACD	Acid-citrate-dextrose
ADP	Adenosine diphosphate
ADAM	A-Disintegrin-And-Metalloproteinase
AMP	Adenosine monophosphate
ANOVA	Analysis of variance
ATP	Adenosine triphosphate
BLI	Bio-layer interferometry
BSA	Bovine serum albumin
Ca^{2+}	Calcium ion
cAMP	Cyclic adenosine monophosphate
cGMP	Cyclic guanosine monophosphate
CD31	Cluster of differentiation 31
CD32a	Cluster of differentiation 32a
CD39	Cluster of Differentiation 39
CLEC-2	C-type lectin-like receptor 2
COX	Cyclooxygenase enzyme
CRP	Collagen-related peptide
CV	Column volume
CVD	Cardiovascular diseases
DMEM	Dulbecco's Modified Eagle's Medium
DMSO	Dimethyl sulfoxide
DNA	Deoxyribonucleic acid
DTT	Dithiothreitol
EDTA	Ethylenediamine tetra-acetic acid
ELISA	Enzyme-linked immunosorbent assay
EMA	European Medical Agency

ENTPD1	Ectonucleoside triphosphate diphosphohydrolase 1
ESAM	Endothelial cell specific adhesion molecule
Fab	Fragment antigen binding domain
FACS	Fluorescence-activated cell sorting
FBS	Fetal bovine serum
Fc	Fragment crystallizable
FcRγ	Fc receptor γ-chain
FDA	Food and Drug Administration
FXa	Activated Factor X
GAPDH	Glyceraldehyde-3-phosphate dehydrogenase
GFP	Green fluorescent protein
GP	Glycoprotein
GPO	Glycine-proline-hydroxyproline
GPVI	Glycoprotein VI
GST	Glutathione-S-transferase
HCAbs	heavy-chain antibodies
HEK293T	Human endothelial kidney 293T cells
hemITAM	Hemi-immunoreceptor-tyrosine-based activation motif
Ig	Immunoglobulin
IPTG	Isopropyl β-D-1-thiogalactopyranoside
ITAM	Immunoreceptor Tyrosine-based Activation Motif
ITIM	Immunoreceptor Tyrosine-based Inhibitory Motif
ITSM	Immunoreceptor Tyrosine-based Switch Motif
k_a	Association constant
K_D	Affinity constant
k_d	Dissociation constant
kDa	Kilodalton
LAT	Linker of Activated T cells
LTA	Light transmission aggregometry
M	Molar

mAb	Monoclonal antibody
MFI	Median fluorescence intensity
mg	milligram
mL	Millilitre
µg	Microgram
µL	Microliter
µM	Micromolar
MWCO	Molecular weight cut-off
NaCl	Sodium chloride
Nb	Nanobody
NO	Nitric oxide
ns	Not significant
PCR	Polymerase chain reaction
PDB	Protein Data Bank
PE	Phosphatidylethanolamine
PECAM-1	Platelet endothelial cell adhesion molecule-1
PGI_2	Prostaglandin I_2
PKA	Protein kinase A
PKC	Protein kinase C
PLCγ2	Phospholipase Cγ2
PRP	Platelet-rich plasma
PS	Phosphatidylserine
PVDF	Polyvinylidene difluoride
RPM	Revolutions per minute
scFvs	single -chain variable fragments
SDS-PAGE	Sodium dodecyl sulphate–polyacrylamide gel electrophoresis
SELEX	Sequential Evolution of Ligands by Exponential Enrichment
SFK	Src family kinase
SH2	Src Homology 2
SH3	Src Homology 3

Syk	spleen tyrosine kinase
TAE	Tris-acetate-EDTA
TBS-T	Tris-buffered saline with Tween 20
TxA_2	Thromboxane A_2
V_{HH}	variable domain
v/v	Volume/Volume
vWF	Von Willebrand factor
WB	Western blot
WP	Washed platelet
WT	Wild type

Contents

Chapter 1

General introduction

1 CHAPTER 1. GENERAL INTRODUCTION

1.1 Platelets

Platelets, or thrombocytes, are the smallest cells in the blood (~2 μm diameter) and anucleate. They play a critical role in the maintenance of vascular integrity, haemostasis, and thrombosis. Their main function lies in their ability to aggregate upon blood vessel damage, preventing bleeding (haemostasis). However, unregulated, or inappropriate platelet activation can result in pathological thrombus formation (thrombosis) in a diseased vessel, such as those affected by atherosclerosis. This can lead to ischaemia in acute coronary heart disease and stroke. Platelets have also been shown to play a role in the immune system and inflammation (Herter et al., 2014). Furthermore, in the recent decades, platelets have also been shown to be involved in several other pathological processes such as hypertension (Camilletti et al., 2001), cancer (Labelle et al., 2011), diabetes (Nusca et al., 2021), autoimmune diseases (Verschoor and Langer, 2013) and more recently COVID-19 (Esparza-Ibarra et al., 2021; Zhang et al., 2020).

Platelets are produced primarily in the bone marrow from megakaryocytes (Italiano et al., 1999). However, in recent years more studies have shown evidence of megakaryocytes in lungs and a potential role for them in producing platelets *in situ* (Banerji et al., 1964; Lefrancais et al., 2017). Some authors have suggested that these give rise to a subpopulation of platelets which play larger roles in inflammation, angiogenesis, and immune responses as a result of their genesis in an environment primed to induce immune cell activation (Lefrancais et al., 2017). This also suggests that platelets formed in the bone marrow, a sterile environment, are less prone to play roles in these processes and therefore perhaps, are more primed for haemostasis (Banerji et al., 1964; Lefrancais et al., 2017; Levine et al., 1990). Each megakaryocyte produces an average of 1000-1500

platelets. Platelets have a short lifespan, circulating in blood for 7 to 10 days in humans (Cohen and Leeksma, 1956) following formation and separation from the megakaryocyte. Normal platelet count ranges from 1.5 – 4.0x10^{11} platelets per litre of blood in healthy adult humans (Giles, 1981). During their circulating life, platelets decrease in size, ribonucleic acid (RNA) content and reactivity (Holinstat, 2017; van der Meijden and Heemskerk, 2019). Platelet clearance from circulation is carried out by neutrophils and macrophages and transported to the spleen and liver for removal from the body (Grozovsky et al., 2010). Up regulation or down regulation of platelet biogenesis can lead to two different platelet disorders: thrombocytopenia is low platelet count (<1.5x10^{11}/L) and normal or smaller size; and thrombocytosis is higher platelet count (>4.5x10^{11}/L) (Mohan et al., 2020).

1.1.1 Platelet's structure

Platelets have discoid form when circulating within the blood vessels and they undergo structural changes upon activation. They change from discoid to compact spheres with dendritic extensions. As cell fragments of their progenitor cells (megakaryocytes), platelets do not have nucleus, but they contain a series of distinguishable elements that confer them their abilities, such as, (1) RNA that can affect platelet responsiveness; (2) ribosomes; (3) mitochondria that generates the necessary energy for platelet activation and granules content release (Boudreau et al., 2014), (4) three type of platelet granules, α-granules (which contain factors involved in hemostasis, including p-selectin, von Willebrand Factor and fibrinogen); dense granules (which contain ADP and serotonin, as well as high levels of calcium) and lysosomes (which contain hydrolytic enzymes) (Blair and Flaumenhaft, 2009; Duran-Saenz et al., 2022; Rendu and Brohard-Bohn, 2001). The final important component in platelets structure is the open canalicular system (OCS),

formed by deep surface membrane invaginations that allows more contact with the outside, facilitates granules secretion, and plays a key role in the transport of membrane receptors (Selvadurai and Hamilton, 2018).

1.1.2 Platelet regulation

This section is a general introduction about how platelets are regulated under healthy conditions. Platelet activation and inhibition are in a balance, where circulating platelets are inhibited until inhibitory signals are removed or overcome by activation. After vascular endothelium injury, subendothelial matrix components are exposed and surrounding platelets adhere to the injury site aggregating to form a thrombus limiting blood loss (Aarts et al., 1988).

Under physiological conditions, circulating platelet activation is constantly inhibited by vascular endothelium. The best studied mechanisms are:

1. Ectonucleotidases (such as CD39/ENTPD1 which degrade ATP and ADP).
2. Thrombomodulin, a high affinity thrombin receptor presents on endothelial cell membrane. Thrombomodulin inactivates thrombin, an enzyme that catalyzes the conversion of fibrinogen to fibrin and activates procoagulant factors.
3. And the release of factors as prostaglandin I_2 (PGI_2; prostacyclin) and nitric oxide (NO). PGI_2 and NO activate protein kinases A and G (PKA, PKG) increasing intracellular levels of cAMP and cGMP, respectively (Figure 1.1).

Without these inhibitory mechanisms, platelets would become activated even in the absence of activating signals (Bye et al., 2016; van der Meijden and Heemskerk, 2019).

Following vascular injury or a plaque rupture, the first step in primary haemostasis is the adhesion of platelet membrane adhesion receptors (integrins α6β1, α2β1, αIIbβ3, and

glycoprotein (GP) Ib–V–IX complex) with their ligands, such as laminin (on the extracellular matrix), collagen (in vessel wall), fibrinogen (in blood plasma) and von Willebrand factor (vWF, on vessel wall and blood plasma), respectively. Platelet collagen receptors (integrin α2β1) stabilize adhesion and (GPVI) start platelet activation, and inside-out signalling (further explained below) that converts several platelet integrins, including αIIbβ3 and α2β1, into their high affinity forms (Lecut et al., 2004b). This also leads to the production and release of thromboxane A_2 (TxA_2) along with the contents of platelet alpha (fibrinogen, P-selectin, and vWF multimers) and dense granules (calcium, ATP, ADP, 5-HT, and epinephrine).

Consequently, intracellular calcium increases inducing platelet shape change, which facilitates primary haemostatic plug formation. These highly activated platelets generate thrombin on the surface that stabilizes the growing thrombus by cleaving fibrinogen to fibrin. Resting platelets are recruited to the growing plug and become activated by a core set of signalling mediators that support activation (ADP, TxA_2 and thrombin). ADP binds to $P2Y_{12}$; TxA_2 to TP; and thrombin interacts with the protease-activated receptor (PAR)-1 (cleaved by thrombin), P2y1 and PAR-4; all of them are important G-protein-coupled receptors. These bindings promote an intracellular cascade signalling that culminate in the activation of αIIbβ3 receptor that mediates platelet aggregation by the binding of fibrinogen (Bye et al., 2016; Induruwa et al., 2016).

Platelets have negative signalling mechanisms to limit thrombus growth and prevent the formation of occlusive thrombi, and include: immunoreceptor tyrosine-based inhibition motif (ITIM)–containing receptors (further explained below), endothelial cell-selective adhesion molecule (ESAM, downregulates αIIbβ3 activity) and cell surface receptors desensitization (Bye et al., 2016).

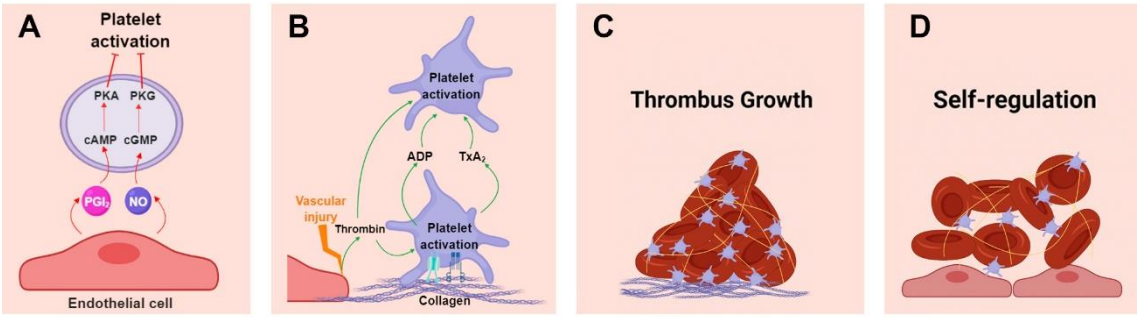

Figure 1.1 Platelet regulation and thrombus formation scheme.

A. *Platelet activation is suppressed by protein kinase A and G (PKA, PKG) which are activated by high levels of cAMP and cGMP, which themselves are produced via NO and PGI_2 released by healthy vascular endothelium.* ***B.*** *Following vascular injury, thrombin and collagen initiate platelet shape change and activation. Secreted ADP, and TxA_2 support this activation.* ***C.*** *Intracellular signalling mediates platelet aggregation and thrombus formation.* ***D****. Negative regulators limit thrombus growth (ITIM, ESAM and cell surface receptors desensitization).*

All these processes are tightly balance and the smallest changes can lead to bleeding or thrombotic problems. During pathologic platelet activation, in areas of diseased endothelium and atherosclerotic plaque rupture, platelets form an occlusive thrombus that obstructs blood flow leading to tissue damage (Ruggeri, 2002), which can lead to ischaemic heart disease and stroke, two of the leading cause of death worldwide (WHO, 2021a), further discussed below.

1.1.3 Clinical need

Cardiovascular diseases (CVD) are the leading cause of death worldwide (WHO, 2021a). From 1990 to 2019 the number of patients with CVD have increased from 12.1 million to 18.6 million (Roth et al., 2020). Constituting the 32% of the worldwide deaths in 2019, where ischaemic heart disease and stroke represented the 85% of them (WHO, 2021a).

Ischaemic means that an organ, in this case the heart, does not get enough supply of blood, which in most of the cases is due to the formation plaque, called atherosclerosis (2010). Atherosclerotic plaques build up inside the subendothelial layer of connective tissue in

arteries and consists of smooth muscle cells, endothelial cells, inflammatory cells, intracellular and extracellular lipids (Ross, 1993). Arterial thrombosis is usually preceded by an atherosclerotic plaque rupture where subendothelial collagens are exposed on its surface initiating platelet adhesion and aggregation leading to thrombus formation in the coronary and cerebral arteries causing myocardial infarction and stroke, respectively (Baumgartner, 1977; Fuster et al., 1992a; Fuster et al., 1992b; Hawiger, 1987).

Novel agents to prevent thrombotic complications are currently sought by researchers and the pharmaceutical industry. To this end, the underlying mechanisms of platelet adhesion, activation, and aggregation need to be understood to be able to develop new drugs that target crucial pathways and/or molecules to modulate the response and prevent them.

1.1.4 Current antiplatelet drugs

Under physiological conditions, haemostatic balance is achieved through procoagulant and anticoagulant factors in equilibrium. Platelet deregulation affects this balance leading to thrombotic disorders or bleeding.

Current oral antiplatelet therapy targets autocrine release mechanisms (TxA_2, ADP) and thrombin (Figure 1.2). The most frequently prescribed antiplatelet therapy is aspirin (acetylsalicylic acid), which irreversibly inhibits platelet cyclooxygenase 1 (COX) blocking the formation of TxA_2. Ticlopidine, clopidogrel, prasugrel and ticagrelor block $P2Y_{12}$, an ADP receptor, preventing its activation by ADP. Vorapaxar binds PAR-1 inhibitor that inhibits thrombin-induced aggregation. Dual antiplatelet treatment is the standard approach, combining aspirin with $P2Y_{12}$ blockers (Yousuf and Bhatt, 2011). However, these antiplatelets agents dysregulate the haemostatic balance leaving patients

at risk of systemic side-effects such as haemorrhage (Gurbel et al., 2016; Yeung and Holinstat, 2012).

Due to the side-effects of current therapies, new anti-platelet drugs, as well as novel targets for drugs are actively sought by the pharmaceutical industry. One approach could be to target primary platelet activation pathways such as the activation provided by the immunoreceptor tyrosine-based activation motif (ITAM)-containing collagen receptor complex GPVI-Fc receptor (FcR) γ-chain. As known from animal models, downregulation of GPVI signalling reduce aggregation and culminates in smaller arterial thrombi, without major bleeding complications other than moderate increased tail bleeding times (Kleinschnitz et al., 2007; Nieswandt et al., 2001). There is a need to translate these results to humans; promising results have been obtained with the humanized Fc fusion protein of the GPVI ectodomain, commercially known as Revacept, currently in phase II of clinical trials, (Ungerer et al., 2011); and the human GPVI-blocking F(ab) ACT017 (also known as Glenzocimab), also in phase II of clinical trials (Lebozec et al., 2017; Voors-Pette et al., 2019). Another approach to downregulate GPVI signalling would be to target the ITIM-containing receptor G6b-B (further discussed below) (Soriano Jerez et al., 2021). G6b-B is uniquely expressed in the platelet/megakaryocyte lineage (Senis et al., 2007) and constitutively inhibits platelet activation by ITAM-like receptors, GPVI and CLEC-2 (C-type lectin-like receptor-2) (Mori et al., 2008). G6b-B is constitutively phosphorylated under resting conditions (Senis et al., 2007), indicating that it may play an important role preventing activation of circulating platelets. Studies stimulating G6b-B, such as, cross-linking the receptor with polyclonal antibodies have shown to exert inhibition of both platelet activation and aggregation *in vitro* (Newland et al., 2007). This points to its potential as a target for antiplatelet therapy.

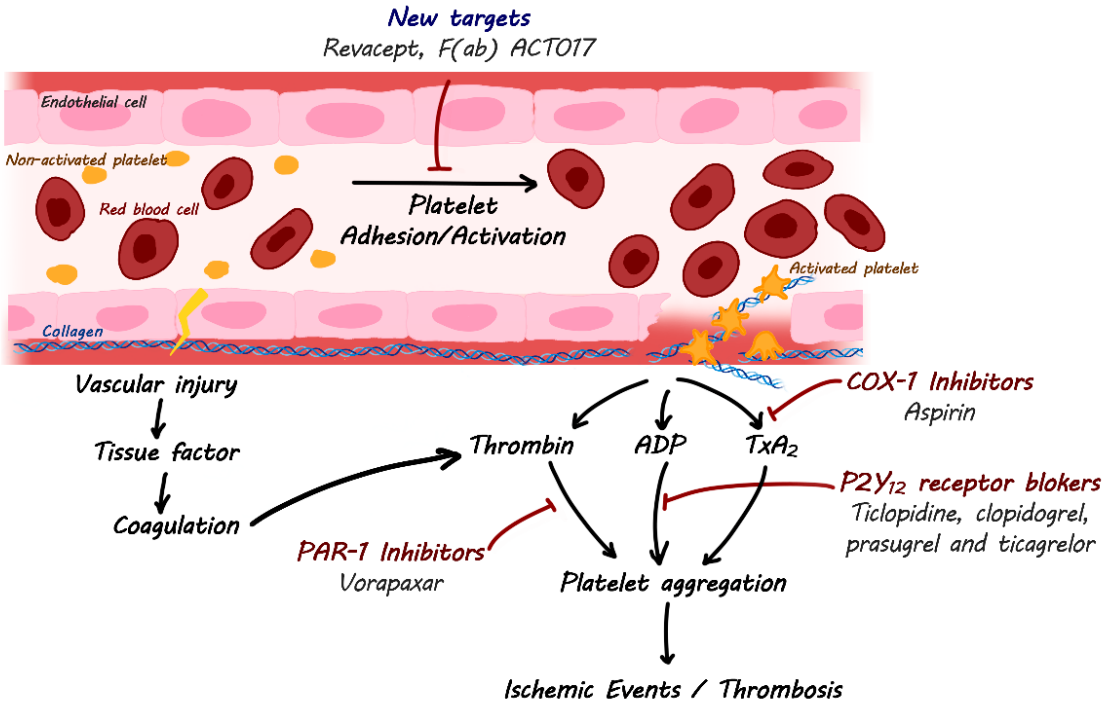

Figure 1.2. Current oral antiplatelet therapy targets scheme.

Current oral antiplatelet therapies mainly target autocrine release mechanisms (TxA_2, ADP) and thrombin and leave patients at risk of systemic side-effects such as haemorrhage. Targeting primary platelet activation pathways could be a new approach that overcomes these side-effects. The image shows a scheme of the process after vascular injury, but the mechanisms are the same after a plaque rupture.

1.1.5 ITAM & ITIM receptors on platelets

The immunoreceptor tyrosine-based activation motif (ITAM)-containing receptors and the immunoreceptor tyrosine-based inhibition motif (ITIM)- containing receptors are an important group of receptors in platelets. Human platelets contain three ITAM-containing receptors: the GPVI/FcRγ-chain complex, FcγRIIA and CLEC-2 (C-type lectin-like receptor-2 which bears a truncated form of an ITAM named hemITAM) (Watson et al., 2010); and five ITIM-containing receptors: Platelet Endothelial Cell Adhesion Molecule-1 (PECAM-1) or CD31, Carcino Embryonic Antigen-related Cell Adhesion Molecule 1 (CEACAM-1) and CEACAM-2, TREM-like transcript-1 (TLT-1) and G6b-B ,described to date (Figure 1.3).

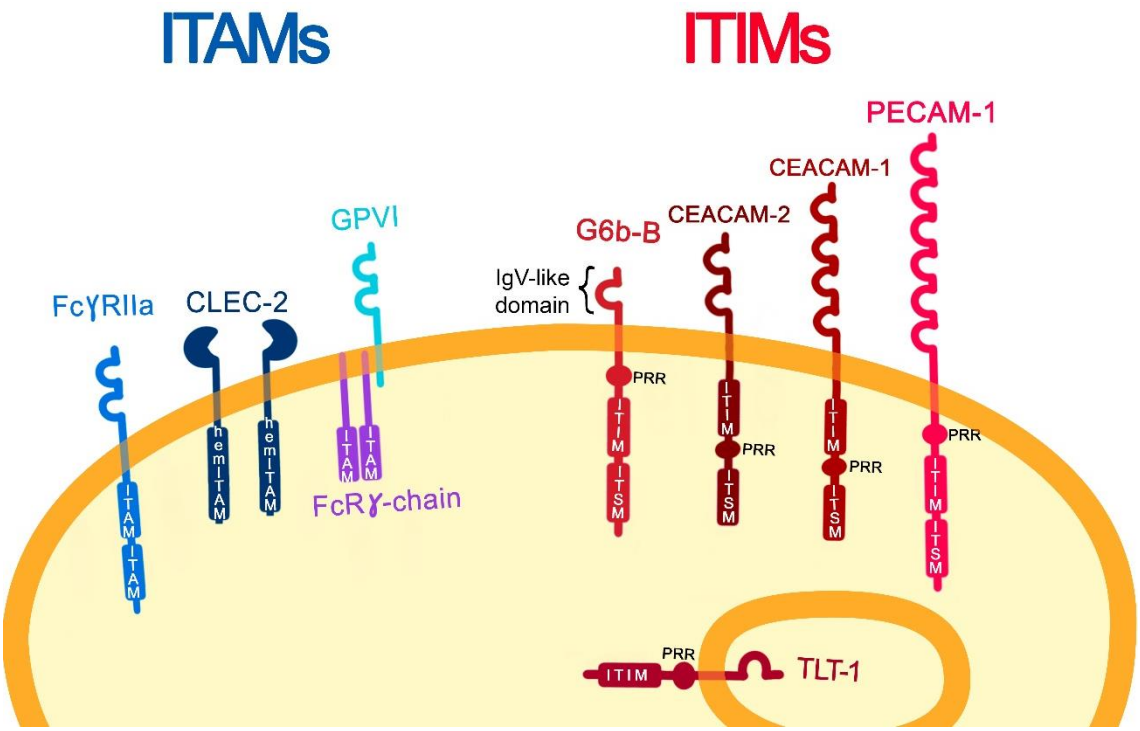

Figure 1.3. ITAM- and ITIM-bearing receptors on resting platelets.

Immunoreceptor tyrosine-based activation motif (ITAM)-bearing platelet receptors are represented on the left together with the hemITAM receptor, CLEC-2. On the right, immune-receptor tyrosine-based inhibitory-motif (ITIM)-bearing platelet receptors are shown. PRR (proline-rich region), and ITSM (immune-receptor immunoreceptor tyrosine-based switch-motif). Figure from publication (Soriano Jerez et al., 2021).

1.1.5.1 ITAM-containing receptors

The immunoreceptor tyrosine-based activation motif (ITAM) consists of two repeats of the conserved sequence of Yxx(I/L) (single letter abbreviation where x can denote any amino acid) commonly found within the cytoplasmic domain separated by 6-12 amino acids (Isakov, 1997; Lee and Bergmeier, 2016; Reth, 1989). Since their discovery, ITAMs have been shown to play a crucial role in generation intracellular signalling cascades leading to cell proliferation, cell death, cell survival, or effector functions including cytokine production and cellular cytotoxicity differentiation, and acquisition of unique effector functions (Billadeau and Leibson, 2002; Isakov, 1997). In human platelets ITAM

receptors we can find three different ITAM receptors, CLEC-2, the GPVI/FcRγ-chain complex and FcγRIIA. They share their signalling pathway to activate platelets, further explained in section 1.3.5, but they differ on their ligands.

FcγRIIA and GPVI will be described in detail in sections 1.2 Human platelet Fc receptor, FcγRIIA and 1.3 Glycoprotein receptor VI, respectively. CLEC-2 is not the focus of this project, but it is an important ITAM receptor, therefore here there are presented the main features about CLECL-2.

CLEC-2 type II transmembrane receptor (~32kDa) expressed on megakaryocytes, platelets, and dendritic cells (Suzuki-Inoue et al., 2006). CLEC-2 is expressed as a dimer and contains a single Yxx(I/L) sequence and that is the reason why it is called hemITAM (Robinson et al., 2006). Human platelets express 2,000-4,000 copies of CLEC-2 and mouse approximately ~40,000 (Burkhart et al., 2012; Gitz et al., 2014; Zeiler et al., 2014). CLEC-2 is the receptor for podoplanin, a protein which is not present in the blood vasculature, which is why CLEC-2 has minor contribution to normal haemostasis, but experiments with CLEC-2 deficient mouse showed that it may play a role on tumour metastasis, lymphangiogenesis and thrombus stabilization (Suzuki Inoue et al., 2010). A new endogenous ligand for CLEC-2 was identified recently, hemin, a product of haemolysis, released during red blood cell destruction (Bourne et al., 2021). CLEC-2 is also a ligand for the two exogenous ligands: the snake venom toxin rhodocytin and type 1 human immunodeficiency virus (HIV-1) (Meng et al., 2021). Fucoidan also was proposed as a ligand for CLEC-2 (Manne et al., 2013).

1.1.5.2 ITIM-containing receptors

The immunoreceptor tyrosine-based inhibition motif (ITIM) is a conserved sequence of amino acids (L/I/V/S)xYxx(L/V), this sequence is commonly found in pairs separated by 15 to 30 amino acid residues (Burshtyn et al., 1997; Vivier and Daeron, 1997). The ITIM was identified for the first time in the cytoplasmic tails of selected receptors on the surface of immune cells (Vivier and Daeron, 1997). ITIMs were named after their role opposing the activity of ITAM-bearing receptors in immune cell function (D'Ambrosio et al., 1995; Daeron, 1995). Since then, ITIM-containing receptors have been identified in several cell types of the haematopoietic lineage such as mast cells, NK cells, T cells, macrophages, megakaryocytes, and platelets (Newman, 1999). Some controversy has surrounded these receptors since their discovery as to whether they possess inhibitory function alone, or whether they can also positively regulate pathways. This is due to the similar, but distinct immunoreceptor tyrosine-based switch motif (ITSM) which has been described as an ITIM-like motif (TxYxxV/I) (Sidorenko and Clark, 2003). ITSM confers activatory and/or inhibitory properties to a receptor depending on associated signalling proteins (Sidorenko and Clark, 2003). Notably, ITIM receptors on platelets bear an ITIM consensus sequence followed by an ITSM which may confer on them inhibitory and activatory function.

PECAM-1 (130-kDa) is a transmembrane glycoprotein that belongs to the Ig gene superfamily (Newman et al., 1990; Stockinger et al., 1990). PECAM-1 expression has been detected on the surface of both vascular endothelial cells, and a number of haematopoietic cells, including platelets, monocytes, neutrophils, T-cells, and B-cells (Albelda et al., 1990). On human platelets PECAM-1 expression levels ranging from 5,000–20,000 copies per cell (Burkhart et al., 2012; Novinska et al., 2007; Zeiler et al., 2014), and in mouse ~5,500 copies (Zeiler et al., 2014). A key function of platelet

PECAM-1 is to inhibit signalling downstream of the collagen receptor GPVI, and other platelet activation pathways, such as those mediated by ADP and thrombin (Jones et al., 2009), thereby inhibiting platelet aggregation and thrombus formation *in vitro* (Patil et al., 2001) and *in vivo* (Falati et al., 2006). PECAM-1 was thought to be the only ITIM-containing receptor in megakaryocytes and platelets (Gibbins, 2002) until recently when proteomics and transcriptomics studies revealed other structurally distinct ITIM-containing receptors: CEACAM-1 and CEACAM-2, which are both expressed at low levels on platelet surface; TREM-like transcript-1 (TLT-1), which is the most highly expressed and is stored in the α-granules (Washington et al., 2004) and released upon platelet activation; and G6b-B.

G6b-B is a transmembrane protein and its expression is restricted to the platelet/megakaryocyte lineage (Senis et al., 2007), with approximately ~14,000 copies per cell in human (Burkhart et al., 2012), and ~30,000 in mouse (Zeiler et al., 2014), making it one of the most highly expressed platelet cell surface proteins. G6b-B constitutively inhibits platelet activation by the ITAM-bearing receptors GPVI and CLEC-2 (Mori et al., 2008). G6b-B will be described in detail in section 1.3 G6b-B.

An additional ITIM receptor, LAIR-1, is present on a variety of immune cells, while it is found on megakaryocytes, this protein has not been detected in platelets (Steevels et al., 2010).

1.2 Human platelet Fc receptor, FcγRIIA

Fc receptors (FcR) are present in most of the cells of the immune system, and they recognize the constant (Fc) region of antibodies present on immune complexes (ICs) and immunoglobulin (Ig) opsonized cells with high avidity (Karas et al., 1982; Rosenfeld et al., 1985). Human platelets present on the plasma membranes a member of the FcR that recognized IgGs, namely FcγRIIA (CD32a) (Arman and Krauel, 2015). This receptor is specific to higher primates and therefore it is not present in murine platelets (Daeron, 1997). Human platelets express on their surface 1000–4000 copies of the FcγRIIA, making platelets the richest source of FcγRIIA in the body (Karas et al., 1982). FcγRIIA level on platelet membrane is stable within donors, but variable between different donors (Rosenfeld et al., 1987; Tomiyama et al., 1992). FcγRIIA plays a role in host response to pathogens, and it has been associated with thrombotic disorders, such as heparin-induced thrombocytopenia (Arman and Krauel, 2015).

FcγRIIA is a type I transmembrane glycoprotein (~40 kDa) belonging to the Ig receptors superfamily. FcγRIIA contains two extracellular Ig-like domains. The second Ig-like domain contains the IgG-binding domain, there are two polymorphism at codon 131 (His-Arg (CAT/CGT)) of the FcγRIIA gene, which influences ligand binding by the receptor, FcγRIIA-His131 has higher binding affinity for human IgG_2 and IgG_3 antibodies (Tomiyama et al., 1992). In its cytoplasmic tail FcγRIIA contains an ITAM that is responsible for signalling transduction after receptor clustering. The ITAM sequence within the FcγRIIA is separated by 12 amino acids (Brooks et al., 1989). The FcγRIIA together with FcγRIIC are the only single-chain FcR with an ITAM, rather than a multichain complex (Daeron, 1997). Schematic representation of the FcγRIIA can be found on Figure 1.3.

1.2.1 Platelet activation by antibodies

Human platelets can be activated by aggregated IgGs, IgGs or their Fc fragments by binding to the FcγRIIA receptor. Other FcγRIIA ligands, reported in the literature consist of specific antiplatelet antibodies that are binding the same platelet (intraplatelet activation) or adjacent platelets (interplatelet activation) (Rubinstein et al., 1995); IgG-coated beads; IgG-opsonized pathogens and Immune complexes (ICs) (Arman and Krauel, 2015). IV.3 is a mouse anti-human FcγRIIA mAb, that in its monomeric form can block FcγRIIA function. However, when IV.3 is crosslinked with F(ab′)2 fragments of a secondary antibody induces FcγRIIA clustering and platelet activation (Rosenfeld et al., 1985).

1.3 Glycoprotein receptor VI

Glycoprotein VI (GPVI) is a transmembrane protein with expression restricted to the megakaryocyte lineage (platelets and megakaryocytes), with around 4,000-6,000 copies per platelet (Burkhart et al., 2012). GPVI is the major collagen receptor in platelets underlying platelet activation which initiates a signalling cascade leading to thrombus formation. The restricted expression of GPVI, together with its tightly regulated expression levels highlight its potential as a highly specific pharmacologic target for antiplatelet therapy (Best et al., 2003).

1.3.1 GPVI structure

GPVI is a type I transmembrane protein belonging to the immunoglobulin (Ig) receptor superfamily. In the human genome GPVI gene is found on chromosome 19 (Ezumi et al., 2000), composed of 8 exons which encode a protein composed of 319 amino acids with a N-terminal 20 amino acid signal sequence cleaved once it reaches the membrane. Its molecular weight is 62 kDa (Sugiyama et al., 1987). GPVI consists of two IgG-like extracellular domains formed by multiple disulfide bonds (D1 and D2, linked by a peptide linker), joined to a mucin-rich region that has a number of sites for O-linked glycosylation, a transmembrane region and a 51 amino acid cytoplasmic tail (Clemetson et al., 1999; Jandrot-Perrus et al., 2000; Miura et al., 2000). GPVI contains a metalloproteinase cleavage site (Gardiner et al., 2004), where its extracellular domain can be cleaved and released after prolonged activation by collagen (Stephens et al., 2005).

The cytosolic tail does not have enzymatic activity but is required for signal transmission and contains interaction sequences for calmodulin and the SH3 (Src homology 3) domain of Src family kinases. In the membrane proximal region there is a basic amino acid rich region that binds calmodulin constitutively in platelets and undergoes delayed dissociation upon activation (Andrews et al., 2002). Another proline rich motif can bind to the SH3 domain of the Src family tyrosine kinases (SFK) Fyn and Lyn, localising these kinases at the membrane and close to their substrates (Suzuki-Inoue et al., 2002).

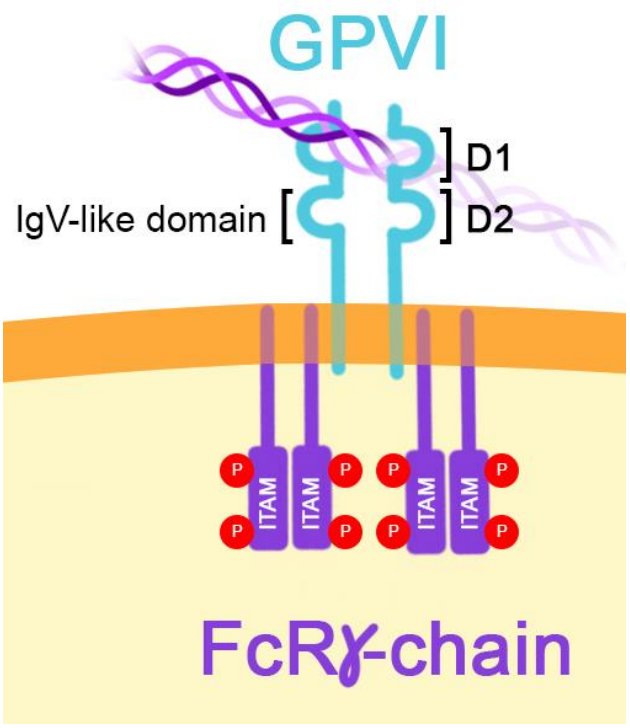

Figure 1.4. GPVI/FcRγ signalling complex.

Here GPVI is represented as a dimer in complex with FcRγ and binding collagen.

GPVI is present as a non-covalently linked complex with the Fc receptor (FcR) γ-chain. FcRγ-chain is essential for GPVI expression at the platelet surface (Nieswandt et al., 2000).The FcRγ-chain is associated with GPVI via a salt bridge between an aspartate and an arginine within the transmembrane domains of the two proteins, respectively (Berlanga et al., 2002; Zheng et al., 2001). The FcRγ-chain is a covalently linked homodimer, with each chain containing one copy of an immunoreceptor tyrosine-based activation motif (ITAM) characterized by two Yxx(L/I) motifs, separated by 6 - 12 amino acids. When the tyrosines within the ITAM are phosphorylated by the Src family kinases Fyn and Lyn, it facilitates the binding of the two SH2 domains of the non-receptor tyrosine kinase Syk (Reth, 1989).

On the platelet surface the GPVI-FcRγ-chain complex is present in both its monomeric and dimeric form (Miura et al., 2002). Molecular docking between GPVI crystal structure

and collagen-related peptide (CRP) showed that GPVI forms back-to-back dimers, the D1 domains display a 5.5 nm space where the collagen triple helix fits (Horii et al., 2006). On resting platelets, monomeric GPVI is the most predominant form, while on activated platelets it switches to predominantly dimers (Jung et al., 2012). The affinity for collagen is lower for monomeric GPVI than dimeric. Dimeric GPVI displays a unique conformation that has an increased affinity for collagen (Horii et al., 2006). Collagen binding to the small proportion of dimeric form on resting platelets initiates the formation of further high-affinity dimers, and clustering of the GPVI dimers. The data suggest that clustering increases both the avidity for collagen and signalling molecule recruitment, which may be crucial for the initiation and persistence of signalling, leading to efficient platelet activation during thrombus formation (Poulter et al., 2017).

1.3.2 GPVI structure-function relationship

Whether GPVI is a monomer, or a dimer is something that has been discussed within the platelet field for several years. The GPVI structure is known by X-ray crystallography since 2006 (Horii et al., 2006) however little is known about how this structure relates with its biological functions (Clark et al., 2021a).

New crystallographic structure recently released supports the work of Horii *et al*., which shows that the GPVI dimerization site is within the D2 domain, however the mechanism of dimerization differs. Slater *et al.*, showed a GPVI structure in complex with a nanobody in which dimerisation is due to a domain swap between the D2 domains and that a small loop in the D2 domain may be critical for collagen/CPR signalling. (Slater et al., 2021). Nevertheless, none of the dimers demonstrated to date could bind to collagen without disrupting the dimer (Feitsma et al., 2022).

Feitsma *et al.*, released recently a new crystallographic structure of GPVI in complex triple-helical collagen peptides where no GPVI ectodomain dimerization is observed and they suggest that the cooperative collagen-binding observed to date may be explained by avidity effects from clustering (Feitsma et al., 2022). The steric hindrance of the dimer observed in the crystal structure to bind collagen may be due to the short length of the collagen peptides used in these study (Feitsma et al., 2022). Nevertheless, in all these crystal structures the D1-D2 angle is rigid (Feitsma et al., 2022; Horii et al., 2006; Slater et al., 2021), so this does not discard the possibility that other residues within the D2 domain may be contributing to the binding, directly or by allosteric contributions.

Dimeric specific antibodies which block platelet activation suggest the possibility of a unique dimer specific conformation (Jung et al., 2012; Jung et al., 2009; Loyau et al., 2012). GPVI is activated by receptor clustering which agrees with the data that GPVI forms dimers (Clark et al., 2021a). A recent publication from Clark et al., showed that GPVI is present as a monomer at the platelet membrane surface at low levels and partially expressed as a dimer; and that binding to collagen and activation is independent of dimerization through the D2 domain with transfected cell line models and advanced microscopy techniques (Clark et al., 2021b). Clark et al., have suggested that as dimerization is not crucial for activation, therapeutic strategies targeting a dimeric conformation are unlikely to succeed (Clark et al., 2021b).

1.3.3 GPVI ligands

Fibrillar collagens (mainly types I and III) are the main ligands for GPVI, binding dimeric GPVI with high affinity through a glycine-proline-hydroxyproline (GPO) sequence (K_D of 5.76×10^{-7} M) (Miura et al., 2002; Smethurst et al., 2007). GPVI also binds the helical peptide based on this sequence called collagen-related peptide (CRP), containing 10

repeats of the GPO sequence (K_D of 5.26×10^{-6} M) (Miura et al., 2002; Morton et al., 1995). Recent studies suggest that collagenous substrates cause GPVI dimers to cluster, but the size number and density depends on the nature of the collagenous substrates and the GPO repetitions (Poulter et al., 2017).

Fibrinogen and fibrin have been recently described as human GPVI ligands, supporting thrombus growth and stabilization (Alshehri et al., 2015; Mammadova-Bach et al., 2015; Mangin et al., 2018; Onselaer et al., 2017). Both ligands bind to GPVI and activate human platelets and humanized mouse platelets, however fibrinogen does not appear to activate mouse platelets which suggests that it does not bind mouse GPVI (Alshehri et al., 2015; Induruwa et al., 2018; Mammadova-Bach et al., 2015; Mangin et al., 2018; Onselaer et al., 2017). The fact that GPVI is not activated by fibrinogen in suspension in the blood vessels may be due to low-affinity interaction and the inability to induce dimerization or higher order clustering. The nature of this interaction is still unknown with some authors report binding to monomeric GPVI, others to dimeric GPVI and others to neither monomeric nor dimeric. The differences between GPVI constructs applied in these studies, the lack of their structural knowledge and the use of non-standardised reagents, may be the main reason of this controversial result (Slater et al., 2018).

Additional ligands have been reported in different studies such as laminin (Inoue et al., 2006), fibronectin and vitronectin (Bultmann et al., 2010), the membrane protein EMMPRIN (CD147) (Seizer et al., 2009), adiponectin (Riba et al., 2008) and amyloid Aβ40 peptide (Elaskalani et al., 2018), but the majority have been described in a single study, and their significance remains uncertain.

Regarding exogenous ligands, a remarkable number of toxins and synthetic ligands activate GPVI: snake venom toxins (e.g., convulxin), diesel exhaust particles, small peptides, polysulfated sugars, and phosphorothioate antisense oligonucleotides (Rayes et al., 2019).

Anti-GPVI monoclonal antibodies (mAbs), such as JAQ1 (Nieswandt et al., 2000), can act as a GPVI agonist, activating platelets independently of FcγRIIA (CD32A). This activation is suggested to be due to clustering of GPVI, (Horii et al., 2006)since F(ab) fragments derived from the same mAb do not induce aggregation under the same conditions (Al-Tamimi et al., 2009). These mAbs induce activation-dependent shedding of GPVI *in vitro*.

1.3.4 GPVI ligand-binding site

Despite the fact that the GPVI structure was known from 2006, no structure of GPVI in complex with its ligand had been resolved until this March (Feitsma et al., 2022),(Foster et al., 2022) and all GPVI ligand-binding sites were suggested either by *in silico* predictions (Horii et al., 2006) or by a number of functional studies using anti-GPVI antibodies, GPVI mutants and/or transfected cell line models (Clark et al., 2021b; Lecut et al., 2004a; Schulte et al., 2001). Some of these studies suggested specific residues within the D1 domain where collagen or CRP might be binding (Figure 4.14, chapter 4) and some of them suggest the possibly of two different epitopes for CRP and collagen. Despite the variety of the approaches, all these studies provided evidence that D1 domain is the ligand-binding domain. GPVI ligand binding sites will be further discussed in Chapter 4 and in the General Discussion.

1.3.5 GPVI signalling pathway

As previously described in this section, firm platelet adhesion and activation depends largely on inside-out signalling provided by the immunoreceptor tyrosine-based activation motif (ITAM)-containing collagen receptor complex GPVI-FcRγ-chain. Exposed subendothelial collagen interaction with GPVI leads to tyrosine phosphorylation of the two YXX(L/I) motifs present in the ITAM by Src family kinases (SFK) Lyn and Fyn. GPVI has a conserved proline-rich region (PxxP) where SFK (Lyn and Fyn) can bind and become activated (Suzuki-Inoue et al., 2002). This is thought to be a "ready to go" state where Lyn and Fyn are constitutively associated with GPVI (Suzuki-Inoue et al., 2002), but they are not fully activated until GPVI is clustered by ligand binding. SFK phosphorylation takes place in lipid rafts, where GPVI is translocated upon ligand engagement (Locke et al., 2002; Wonerow et al., 2002), and induce the recruitment and activation of the tyrosine kinase Syk.

Syk binds the two phosphorylated tyrosines through its tandem SH2 domains. Then, Syk propagates the signal by phosphorylating the membrane scaffolding protein linker for activation of T-cells (LAT). LAT has many tyrosine residues that can be phosphorylated by tyrosine kinases, resulting in the formation of a multi-protein complex that leads to the activation of phospholipase Cγ2 (PLCγ2) (Pasquet et al., 1999) and, as a consequence, an intracellular Ca^{2+} rise (Figure 1.5). Then, αIIbβ3 is activated and mediates platelet aggregation by binding to fibrinogen. Second messengers (including ADP and TxA_2) are released from activated platelets to activate surrounding resting platelets synergizing the response.

In this way, the main GPVI role is to generate intracellular signals promoting integrin activation rather than to serve as an adhesion receptor.

1.3.6 GPVI role in haemostasis and thrombosis

Haemostasis is the healthy mechanism that maintains vascular integrity by preventing excessive blood loss upon blood vessel damage by thrombus formation, while thrombosis is the pathological thrombus formation.

GPVI does not seem to play a crucial role in haemostasis. In 1989 it was reported for first time that platelets from GPVI-deficient patients failed to aggregate in response to collagen and presented a mild bleeding tendency (Moroi et al., 1989), suggesting that GPVI is not essential for normal haemostasis. There is a 2.9% estimated frequency of GPVI-deficient patients in Chile (Nagy et al., 2020), where the majority have been found , with only 16 GPVI-deficient patients reported to date (Arthur et al., 2007; Matus et al., 2013). This may mean that this deficiency is rare or that it does not show up due to its low pathological prevalence.

Several studies have showed the key role that GPVI plays not only in platelet adhesion and activation by collagen, but also in arterial thrombosis, thrombus size, propagation and clot stabilization, with the GPVI interaction with fibrin(ogen) potentially being one of the reasons of this physiological role (Nieswandt et al., 2011).

Mouse models have been used to determine the role of GPVI in thrombosis because GPVI-deficient patients are exceptionally rare (Arthur et al., 2007; Matus et al., 2013)). These GPVI-deficient models have showed reduced mortality in thromboembolism models and are protected from induced thrombosis (Bender et al., 2011; Lockyer et al., 2006; Nieswandt et al., 2001). Additionally, other studies demonstrated GPVI binding to atheroma plaques (Cosemans et al., 2005; Reininger et al., 2010) and how its antagonization by Revacept reduces thrombus formation (Ungerer et al., 2013).

On the other hand, high levels of GPVI have been found on patient's platelets after ischemic stroke and transient ischemic attack (TIA) (Bigalke et al., 2010) as well as, elevated levels of shed GPVI after ischemic strokes (Al-Tamimi et al., 2011). Is there the possibility that high levels of GPVI increase the risk of suffering these pathologies?

Several studies reported GPVI interacting with fibrin and fibrinogen, although there is controversy about the nature of this binding (Slater et al., 2018). Nevertheless, it seems clear that this interaction plays a role in thrombus assembly and stabilization by promoting thrombin generation and recruiting circulating platelets in the forming clot (Mammadova-Bach et al., 2015). Additionally, GPVI-deficient mouse platelets were showed to have a delay in vessel occlusion and increase in embolization following $FeCl_3$ injury which was suggested to be due to loss of platelet activation by fibrin and therefore reduced thrombin generation (Alshehri et al., 2015).

Studies on proteins within the downstream GPVI signalling pathway, such as Src family kinases (SFKs) highly the role of the whole GPVI pathway on platelet aggregation. Studies with single and double-deficient mice platelets for Fgr, Fyn, Lyn and Src showed their importance on mediating GPVI signalling (Severin et al., 2012).

These studies highlight the implication of GPVI in thrombosis, thrombus growth, and thrombus stability. Together with its low impact on haemostasis, GPVI has great potential as an antithrombotic target (Dutting et al., 2012; Induruwa et al., 2016; Stegner et al., 2014).

1.3.7 GPVI endogenous inhibition

GPVI signalling (Figure 1.5) is regulated through shedding by A-Disintegrin-And-Metalloproteinase (ADAM)10/17 upon platelet activation (Gardiner et al., 2004; Gardiner et al., 2007). On resting platelets, G6b-B allows more specific intrinsic regulation than PGI_2 and NO by downregulating ITAM receptor activation (Newland et al., 2007). The cytoplasmic tail of G6b-B contains an ITIM (immune receptor tyrosine-based inhibitory motif, to be described in the next section) which is also phosphorylated by SFKs, but in this case creating docking sites for the SH2 domain-containing phosphatases: SHP1 and SHP2. Activation of these two phosphatases leads to inactivation of tyrosine kinases such as Syk and of downstream signalling pathways (Bye et al., 2016; Coxon et al., 2017).

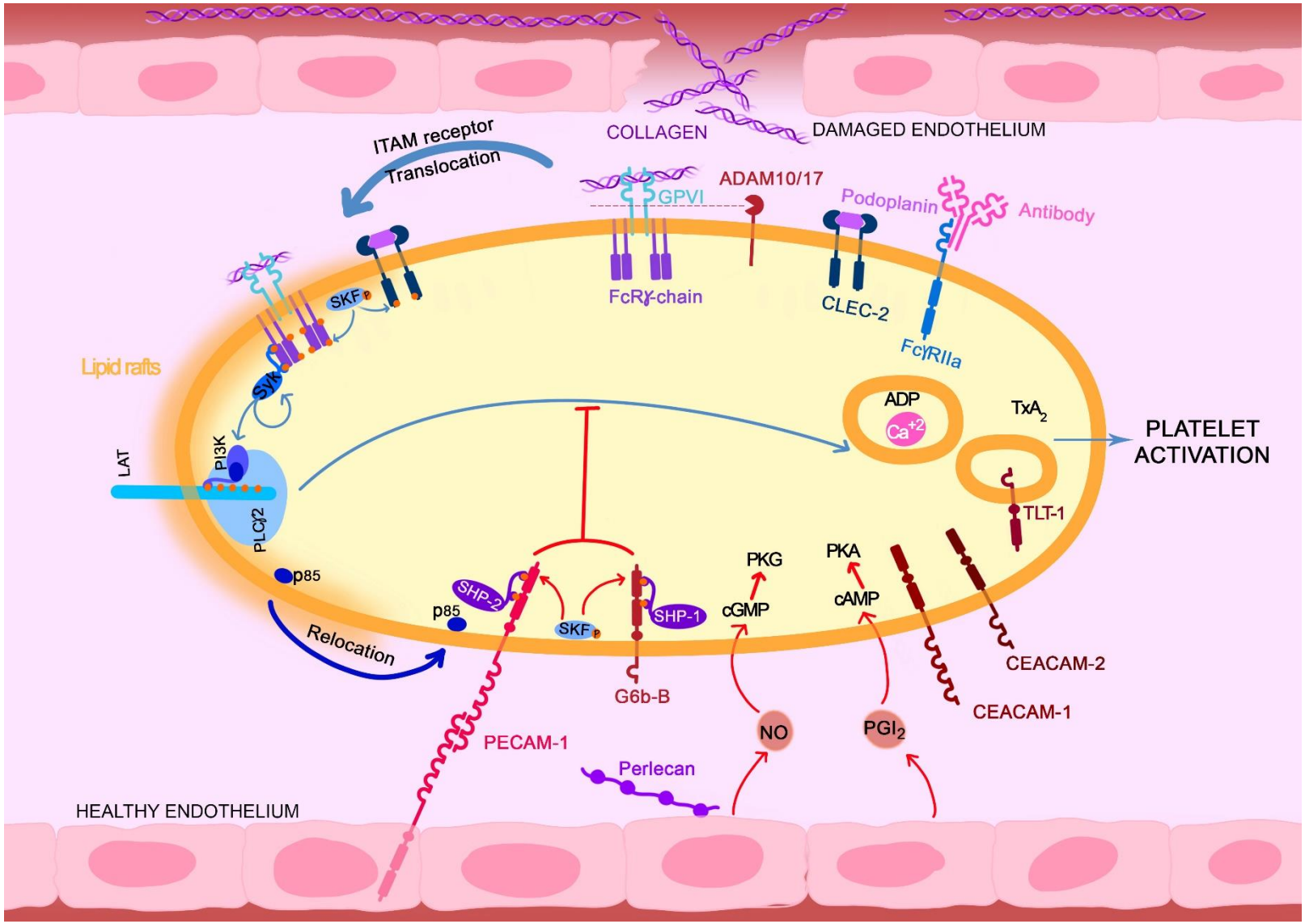
ITAM receptor
Translocation
COLLAGEN
DAMAGED ENDOTHELIUM
GPVI
ADAM10/17
Podoplanin
Antibody
FcRγ-chain
CLEC-2
FcγRIIa
SKF
Lipid rafts
Syk
ADP
Ca+2
TxA2
PLATELET ACTIVATION
LAT
PI3K
PLCγ2
TLT-1
p85
SHP-2
p85
SKF
SHP-1
cGMP
PKG
PKA
cAMP
CEACAM-2
CEACAM-1
Relocation
G6b-B
PECAM-1
NO
PGI2
Perlecan
HEALTHY ENDOTHELIUM

Figure 1.5. ITAM-ITIM activation.

ITAM-containing receptor (GPVI/FcRγ-chain/ CLEC-2/ FcγRIIA) are activated by their respective ligands (collagen/ podoplain/ antibodies). Then, ITAMs are translocated to lipid rafts where SFKs phosphorylate them. Syk is recruited, activated, and subsequently propagates the signal through the LAT signalosome, where p85/p110 are recruited to form PI3K. This results in PLCγ2 activation and further platelet activation. GPVI signalling is regulated through shedding by ADAM10/17. On the bottom, ITIM-receptor activation (PECAM-1/ G6b-B) recruits SFK, phosphorylating the ITIM/ITSM motifs, providing docking sites for of the phosphatases (SHP1/2 and SHIP1/2). This also results in relocation of molecules, such as p85, away from lipid rafts and therefore a reduction in the activation of Syk and the LAT signalosome, leading to platelet inactivation/maintenance of the resting state. Healthy endothelium contributes to platelet resting state, releasing PGI_2 and NO, that rise platelet intracellular levels of cAMP and cGMP, activating PKA and PKG, respectively.

1.4 G6b-B

G6b-B is a transmembrane protein exclusively expressed in megakaryocytes and platelets, with approximately ~14,000 copies per cell in human (Burkhart et al., 2012), and ~30,000 in mouse (Zeiler et al., 2014), making it one of the most highly expressed platelet cell surface proteins. G6b-B constitutively inhibits platelet activation by ITAM-like receptors, GPVI and CLEC-2 (Mori et al., 2008). G6B cross-linking with polyclonal antisera was shown to have an inhibitory effect on platelet aggregation, in a calcium-independent manner (Newland et al., 2007).

G6b-B physiological function was studied in a G6b knockout mouse model. G6b-B–deficient mice were markedly macrothrombocytopenic (characterized by oversized platelets and a low platelet count) and had a bleeding diathesis because of defective platelet production (Mazharian et al., 2012).

The extracellular matrix heparan sulfate (HS, a subgroup of glycosaminoglycan defined by their basic disaccharide unit) has recently been identified as a G6b-B ligand; this binding inhibits platelet and megakaryocyte function by inducing downstream signalling via the tyrosine phosphatases Shp1 and Shp2 (Vogtle et al., 2019).

1.4.1 G6b-B structure

G6b-B is a member of the immunoglobulin superfamily and is expressed as several splice-variants (de Vet et al., 2001). G6b-A and B contain transmembrane regions while the remaining three are secreted (de Vet et al., 2001). G6b-B is the only splicing variant that contains a transmembrane region, along with a cytoplasmic region containing the ITIM and an ITSM, and therefore the only isoform capable of intracellular signalling. ITIM/ITSM interact with the SH2 domain of the cytoplasmic protein tyrosine phosphatases SHP-1 and SHP-2 (de Vet et al., 2001). G6b-B is constitutively phosphorylated by Src family kinases (SFKs) and subsequently act as docking sites for SHP-1 and SHP-2 (de Vet et al., 2001; Senis et al., 2009; Senis et al., 2007). This leads to their activation, and the subsequent deactivation of tyrosine kinases such as Syk and of downstream signalling pathways.

G6b-B gene (*Mpig6b*) gene is located on chromosome 6 Open Reading Frame 25 and composed of 6 exons which encode a 26 kDa protein comprised of 241 amino acids (de Vet et al., 2001). However, when G6b-B is analysed by SDS–PAGE it migrates as a distinctive doublet at ~24–30 kDa due to its N-glycosylation (de Vet et al., 2001; Mazharian et al., 2012).

G6b-B consists of a single variable-type Ig-like (IgV) domain which is N-glycosylated (1 site in humans and 2 in mice), a proline-rich region (PRR) in the juxtamembrane region, an ITIM and an ITSM, Figure 1.6 (de Vet et al., 2001; Mazharian et al., 2012; Senis et al., 2007). The ITIM and ITSM separation on G6b-B is 26 amino acids (de Vet et al., 2001) and their sequences are $LLY_{194}ADL$ and $TIY_{220}AVV$.

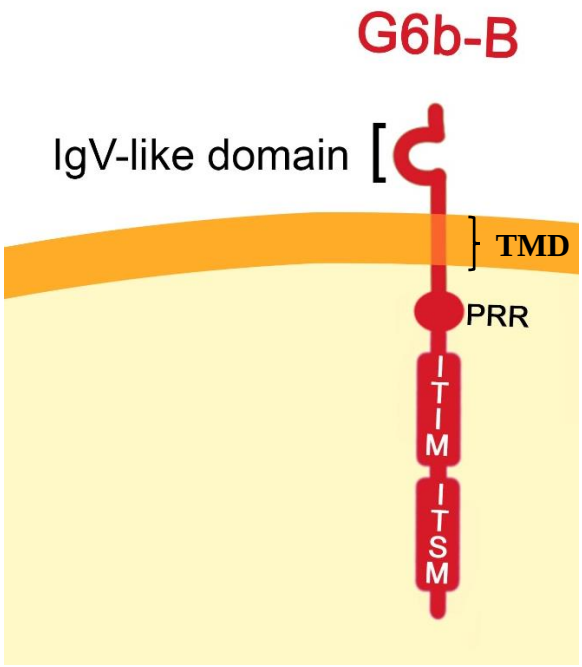

Figure 1.6. G6b-B schematic structure.

IgG-like domain; TMD, transmembrane domain; proline-rich region (PRR), immune-receptor tyrosine-based inhibitory-motif (ITIM), immune-receptor tyrosine-based switch-motif (ITSM).

1.4.2 G6b-B ligands

G6b-B has been described to bind the extracellular matrix heparan sulphate (HS), a subgroup of glycosaminoglycan defined by a basic disaccharide unit (Vogtle et al., 2019) and heparin (de Vet et al., 2005). Data from size-exclusion chromatography and X-ray crystallography suggest that ligand binding induces ectodomain dimerisation (Vogtle et al., 2019). However, this dimerisation is not enough to cluster G6b-B sufficiently into higher-order oligomers to induce robust downstream signalling (Vogtle et al., 2019). HS chains of vessel-wall, such as perlecan, may facilitate further G6b-B phosphorylation and downstream signalling via the tyrosine phosphatases SHP1 and SHP2, resulting in the inhibition of platelet activation (Vogtle et al., 2019).

1.4.3 G6b-B role in haemostasis and thrombosis

Studies on humans have shown that G6b-B deletion and loss-of-function mutations lead to megakaryocytic and myelofibrotic disorders (Hofmann et al., 2018), highlighting the importance of this receptor not only for platelet regulation but also for megakaryocyte function.

Most of the studies on G6b-B function have been based on transgenic gene-deficient mice. It has been shown that megakaryocytes lacking G6b-B have reduced proplatelet formation leading to oversized platelets, a low platelet count and bleeding diathesis (Mazharian et al., 2012). In addition, G6b-B-deficient megakaryocytes display an increase of metalloproteinase production, responsible for cell-surface receptor shedding, such as GPVI (Mazharian et al., 2012). This seems to be a compensatory mechanism to downregulate the receptors regulated by G6b-B, since G6b-B constitutively inhibits platelet activation by ITAM-like receptors, GPVI and CLEC-2. CLEC-2 is not shed in G6b-B-deficient platelets because it lacks the cleavage site (Mori et al., 2008). Furthermore, G6b-B is constitutively phosphorylated under resting conditions (Senis et al., 2007), indicating that it may play an important role preventing activation of circulating platelets. However, very few studies have explored the impact of G6b-B stimulation. Over 10 years ago, G6b-B cross-linking with polyclonal antibodies was shown to exert inhibition of platelet activation and aggregation *in vitro* (Newland et al., 2007). This points to its potential as a target for antiplatelet therapy. Further studies in this direction using *in vivo* models and with monoclonal antibodies or other tools would clarify whether G6b-B stimulation could lead to platelets less reactive reducing the risk, or severity of thrombosis.

1.5 Potential antithrombotic targets and approaches

For a drug to be effective, it must be able to reach the therapeutic target. That is why it is crucial to choose an accessible target to increase the chances of success. Modulating key regulators of the GPVI signalling pathway, both positive and negative, appears to be a good approach. However, it is as important to choose the correct pathway as it is to choose an accessible target; and that is why, in this project, we have focussed our efforts on the membrane receptors which regulate GPVI pathway, GPVI and G6b-B. Consequently, a suitable drug will not need to pass through the platelet membrane to reach its target and as platelet specific targets, off target effect as likely to be minimal.

GPVI's and G6b-B's potential as powerful and safe antithrombotic targets relies on the fact that:

- ✓ their expression is restricted to platelets and megakaryocytes, giving a high specificity.
- ✓ GPVI downregulation, blocking or genetic deficiency reduces pathological thrombus formation, showing antithrombotic potential.
- ✓ physiological haemostasis is preserved without bleeding complications, due to overlapping of activation signalling pathways, such as with the GPIb–V–IX complex.
- ✓ GPVI is a key regulator on platelet-dependent inflammatory processes.
- ✓ G6b-B constitutively inhibits platelet activation by the ITAM-bearing receptors GPVI and CLEC-2 (Mori et al., 2008).
- ✓ *Ex vivo* experiments with G6b-B crosslinking with antibodies showed promising platelet function inhibitory results (Newland et al., 2007).

Therefore, we can conclude that both, GPVI and G6b-B are biologically relevant for haemostasis, thrombosis, and platelet responsiveness, and worthy of consideration as targets for new antiplatelet therapy. The pertinent question then, would be how could we achieve GPVI inactivation and/or G6b-B activation therapeutically/ pharmacologically?

1.5.1 Small molecules

The classical way to address a molecular target would be to develop a small molecule suitable for oral therapy. Small molecules drugs are low molecular weight compounds capable of modulating biochemical processes for diagnostics, treatments or preventing diseases (Ngo and Garneau-Tsodikova, 2018). The attractiveness of small molecules lies in their relatively low molecular weight and simple chemical structures, their pharmacokinetics and pharmacodynamics which are usually easier to predict than for biologics; and that their development requires simpler synthesis, manufacture, characterization and regulation (Ngo and Garneau-Tsodikova, 2018): and they can be administered by a variety of routes, including oral therapy, which is indeed the most advantage over biologics in drug development (Makurvet, 2021). Small molecules are more economic sustainable to produce, which also effects patient access to them (Makurvet, 2021).

Despite the fact that the number of biologics approved for use as therapeutics has risen in recent decades, small molecule medicines continue to lead on the latest WHO Model List of Essential Medicines in 2021, and interestingly, in the case of anti-platelet medicines, aspirin (acetylsalicylic acid) and clopidogrel, both small molecules, were the only ones in the list (WHO, 2021b). However, small molecules tend to be less successful when targeting protein-protein interactions such as the GPVI-collagen interaction (Gurevich and Gurevich, 2014), but we can find exceptions in the literature, such as Tirofiban, and

Maraviroc. Tirofiban interacts with platelet integrin αIIbβ3 and inhibits platelet aggregation by blocking binding to fibrinogen, while Maraviroc inhibits interaction between human CCR5 and HIV-1 gp120 (Buchwald, 2010).

Regarding GPVI relatively few small molecules have been reported to direct interact with GPVI. Between them we can find natural products isolated from plants, such as, Honokiol and Glaucocalyxin A (GLA) (Lee et al., 2017; Li et al., 2013). Other compounds were found *by in silico* approaches, such as, structure-based repurposing; compounds that were originally used for other treatments. These compounds are Losartan (used for treating hypertension) and cinanserin (atypical pneumonia) (Taylor et al., 2014). Additionally, we can find compounds chemically engineered to target GPVI, such as, Compound 5 a novel inhibitor based on a tetrahydroisoindole scaffold (Bhunia et al., 2017). A recent publication from Foster et al., 2022, made a comprehensive comparison of these small molecules with functional assays and with *in silico* binding assays (Foster et al., 2022). However, the efficacy of all these small molecules is low and therefore these are unlikely to be good candidate for therapy.

1.5.2 Biologics

Biologics, biological medicines, biological products, biological therapies, biopharmaceuticals, and biologicals are all terms used indiscriminately, yet they refer to the same. According to the EMA (European Medicines Agency) a biological medicine is a medicine whose active substance is made by a living organism (EMA, 2021). The FDA (U.S. Food and Drug Administration) gives a more extended definition of biological products involving vaccines, blood and blood components, allergenics, somatic cells, gene therapy, tissues, and recombinant therapeutic proteins ((FDA), 2018). Consistent with these definitions a biologic ranges from sugars, proteins, or nucleic acids to complex

combinations of these substances, or even living entities such as cells and tissues ((FDA), 2018). Regardless of these general definitions, nowadays when we talk about a biologic, we refer to a subtype, complex molecules, such as, monoclonal antibodies and recombinant proteins. In this section we will explore some of these biologics, and the benefits and limitations of their use in the context of thrombosis.

1.5.2.1 Antibodies

Antibodies (Abs), or immunoglobulins (Igs), are the most widely used biologics. Abs are components of the immune system that are involve in cellular and humoral responses to antigens, both from the host and external. Abs produce as a part of a normal immune response are polyclonal, which means that they are produce by different B lymphocytes and therefore they bind different epitopes of the same molecule, or potentially the same epitope but with different affinities.

On the other hand, monoclonal Abs (mAbs) are produced by a single B lymphocyte clone and therefore only recognize a single epitope per antigen. These B lymphocytes can be immortalized by fusion with hybridoma cells, allowing for long-term generation of identical mAbs in a laboratory setting. Monoclonal and polyclonal Abs are the commercial terms of the IgGs obtained by this process. Polyclonal Abs are a mixture of mAbs made in an immune response, but each antibody comes from a specific single B lymphocyte. Monoclonal Abs come from the isolation of a single B lymphocyte which is used to grow and purify a specific antibody.

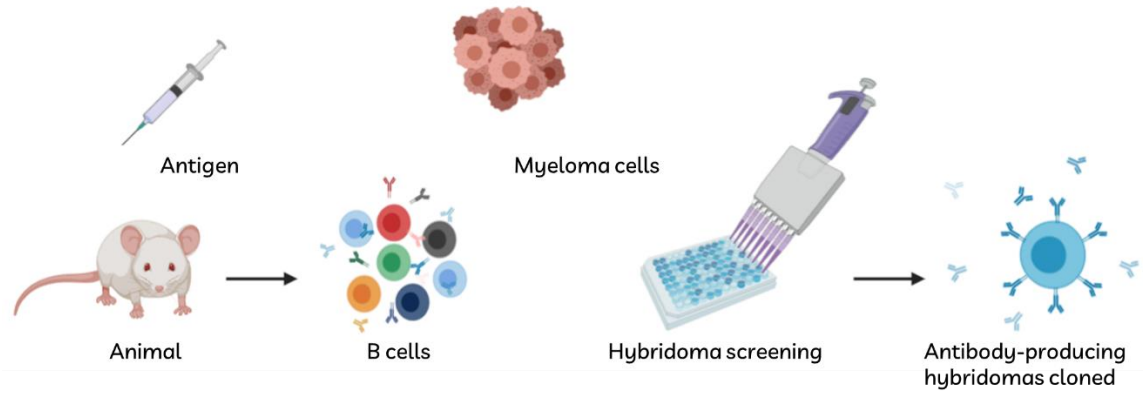

Figure 1.7. The process to generate the monoclonal antibody.

Monoclonal Abs are less likely than polyclonal Abs to cross-react with other proteins since they specifically detect a particular epitope on the antigen, while polyclonal detect a mixture of epitopes because they came from more than one B lymphocytes. For drug therapies, it is essential to achieve reproducibility and polyclonal Abs do not accomplish it, this is the main reason why mAbs are more extensively used for therapeutics compared to polyclonal. Some of the differences between mAbs and polyclonal are shown in Table 1.1.

Monoclonal Abs	Polyclonal Abs
Produced by a single B cell clone	Produced by a range of different B cells
Identical antibody molecules	Batch-to-batch variability
Bind to one epitope	Recognizes different epitopes
Production is slow	Production is quicker
Very expensive	Less expensive
System is only well developed for mouse and rat. More than 99% of the cells do not survive the fusion process.	Increased chance for cross reaction. Antibody response depends on the host animal. Sometimes requires multiple control samples to arrive at meaningful conclusions.

Table 1.1. Differences between monoclonal and polyclonal antibodies.

Immunoglobulins (Igs) are Y-shaped glycoproteins (~150 kDa) composed of two identical light chains and two identical heavy chains. The heavy chain and light chain of the heterodimer are linked through disulphide bonds. The two heavy chains are also

linked between them by disulphide bridges. Igs light chains have two domains, a constant domain (C_L) and a variable domain (V_L). Heavy chains contain 3 constant domains (C_H) and one variable domain (V_H). At the variable regions there is find a hypervariable region which is the responsible for antigen binding (Chiu et al., 2019).

Abs in mammalian species are highly conserved and can be divided in five classes that differ on their heavy chain constant domains (IgM, IgG, IgA, IgD, and IgE isotypes) (Schroeder and Cavacini, 2010). Igs have three functional components, two Fragment antigen binding domains (Fabs) and the fragment crystallizable (Fc). The two Fabs are linked to the Fc domain by a hinge region that allows the Fabs a large degree of conformational flexibility relative to the Fc (Figure 1.8) (Schroeder and Cavacini, 2010).

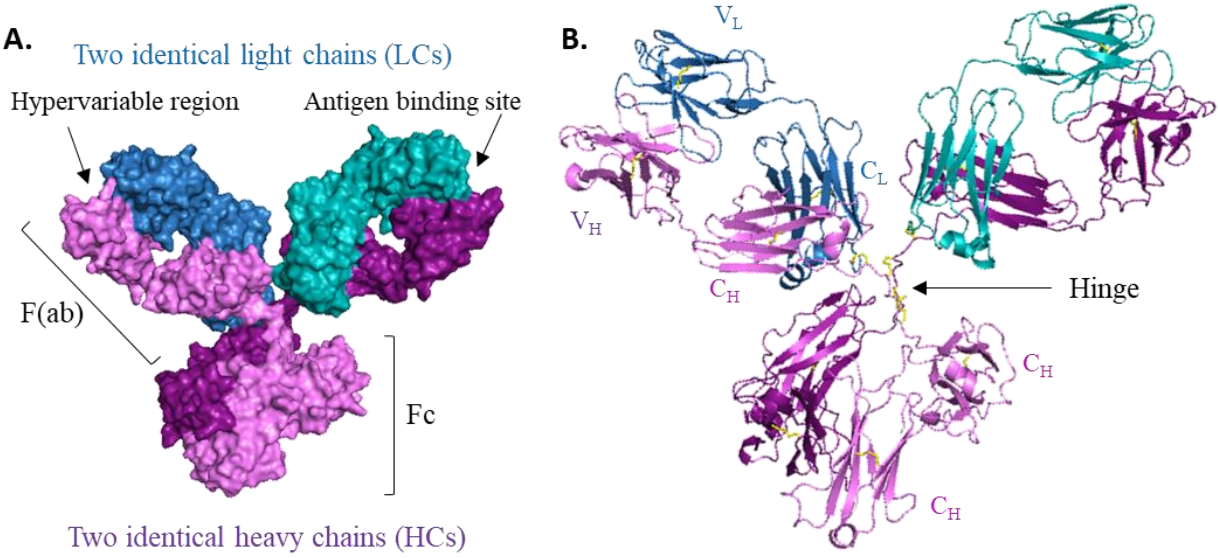

Figure 1.8. Antibody structure.

*Represented as a surface (**A.**) or cartoon (**B.**). IgG structure is composed of two heavy chains (HCs, in purple) and two light chains (LCs, in blue). LC have two regions constant domain (C_L) and a variable domain (V_L). HC consist of 3 constant domains (C_H) and one variable domain (V_H). At the V_L and V_H regions there is find a hypervariable region which is the responsible for antigen binding. IgGs have 3 functional regions: two Fragment antigen binding domains (Fabs), the fragment crystallizable (Fc), and the hinge region where the two Fabs linked to the Fc. Disulphide bridges binding the two HCs are showed in yellow (**B.**). Images were generated using PyMol (Protein Data Bank (PDB) ID: 1igy (Harris et al., 1997)).*

Antibodies are bivalent molecules because they have two identical antigen-binding sites and therefore antibodies can cross-link antigens. The nature of the cross-link depends on the antigen, if there are more than one antigenic determinants or only one, some examples are shown in Figure 1.9. Antigen cross-linking and binding efficiency is possible due to the flexible hinge region, which facilitates variation on the distance between the two antigen-binding sites (Alberts, 2002).

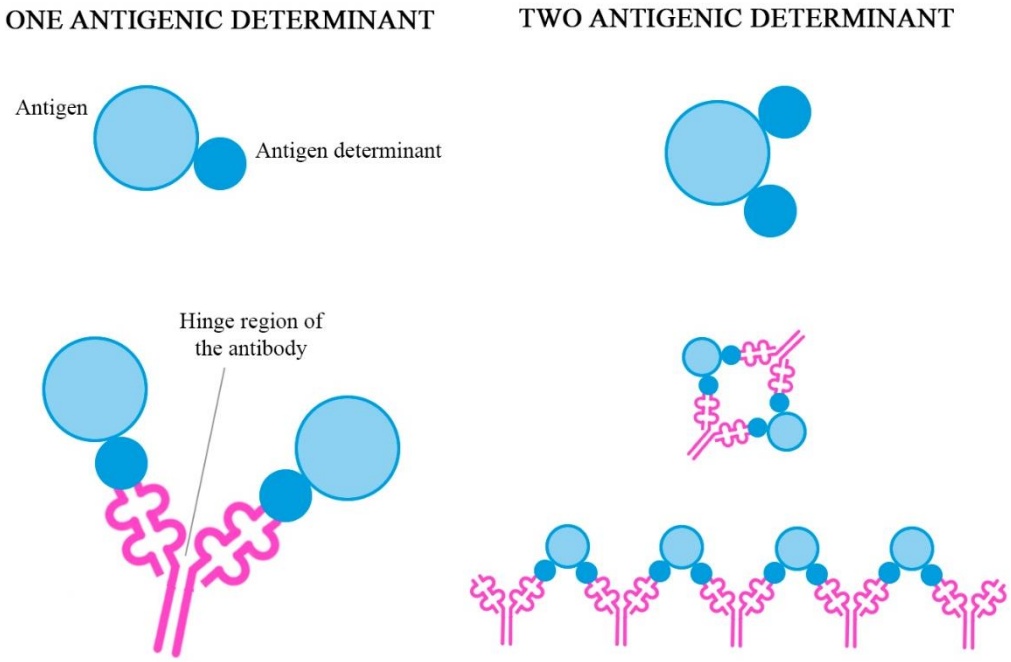

Figure 1.9. Antibody antigen interactions.
Antibodies can cross-link antigens differently depending on the number of binding sites on the antigen.

Antibody binding to its antigen is a reversible binding and it depends on both the antibody and the antigen. An antigen can have more than one antigenic determinant (polyvalent). The affinity of an antibody describes the strength of binding to a single antigen-binding site. However, when an antibody binds to a polyvalent antigen, or as bivalent molecule binds to two antigens, the strength of that binding is referred as avidity (Alberts, 2002).

Despite of the advantages of using mAbs as therapeutics, such as, their high specificity to the target or their ability to cross-link their targets, they have some limitations such as inadequate pharmacokinetics and tissue accessibility as well as adverse interactions with the immune system. However, in field of antibody engineering has developed different ways to overcome these limitations, such as modified antibodies (chimeric or humanized), antibody fragments or recombinant proteins (Chames et al., 2009).

1.5.2.1.1 Chimeric and humanized antibodies

To avoid adverse interactions with the immune system, there is the possibility of making chimeric or humanized antibodies. Chimeric antibodies have been engineered to be 70% human and possessed a fully human Fc portion. Humanized antibodies are 85–90% human and are less immunogenic than chimeric ones. Most of the approved mAbs in current use are either chimeric or humanized (Chames et al., 2009). However, modified antibodies still have some of the limitations generally associated with antibodies: difficult tissue accessibility and penetration, associated with their size (150 kDa), impaired interactions with the immune system, mainly due the non-specific binding between Fc portions of antibodies and Fc receptors on cells (such as macrophages, dendritic cells, neutrophils, NK cells and B cells): their high production costs, and inadequate pharmacokinetics, they are difficult to clear, having long half-life (Chames et al., 2009). Long half-life can be an advantage due to patients would need less frequently dosed, but if antibodies are not removed from circulation after their action, they can lead to impaired or unwanted effects.

1.5.2.1.2 Antibody fragments

Antibodies can be processed to obtain antibody fragments with the same affinity (Holliger and Hudson, 2005). The antibody Fc portion can be removed by an enzymatic digestion. Pepsin digestion results in a F(ab')2 fragment antibodies (110-100 kDa) with the two Fragment antigen binding domains (Fabs) meanwhile, papain digestion gives rise to two separate F(ab) fragments (55-50 kDa) (Carolyn S. Feldkamp, 1996). The single -chain variable fragments (scFvs, 30-25 kDa), are a third variant which have been engineered into a single polypeptide, they are recombinant molecules with the variable regions of light and heavy antigen-binding domains joined by a flexible linker sequence (Bird et al., 1988). All these antibody fragments are illustrated in Figure 1.10. Like the full antibody, antibodies fragments also have pros and cons when it comes to therapy, the key advantages and disadvantages of the antibody fragments are shown on Table 1.2.

Advantages	**Disadvantages**
Smaller size	Lack of an Fc region - risk of aggregation - increase the possibility of immunogenicity - loss of Fc-mediated functions
Lack of an Fc region	
Tissue penetration	
Therapeutic action by ligand binding	
scFvs Advantages	
ideal for large-scale production in microbial systems	
produced more quickly, in higher yields, and at lower costs	

Table 1.2. Key advantages and disadvantages of the antibody fragments.

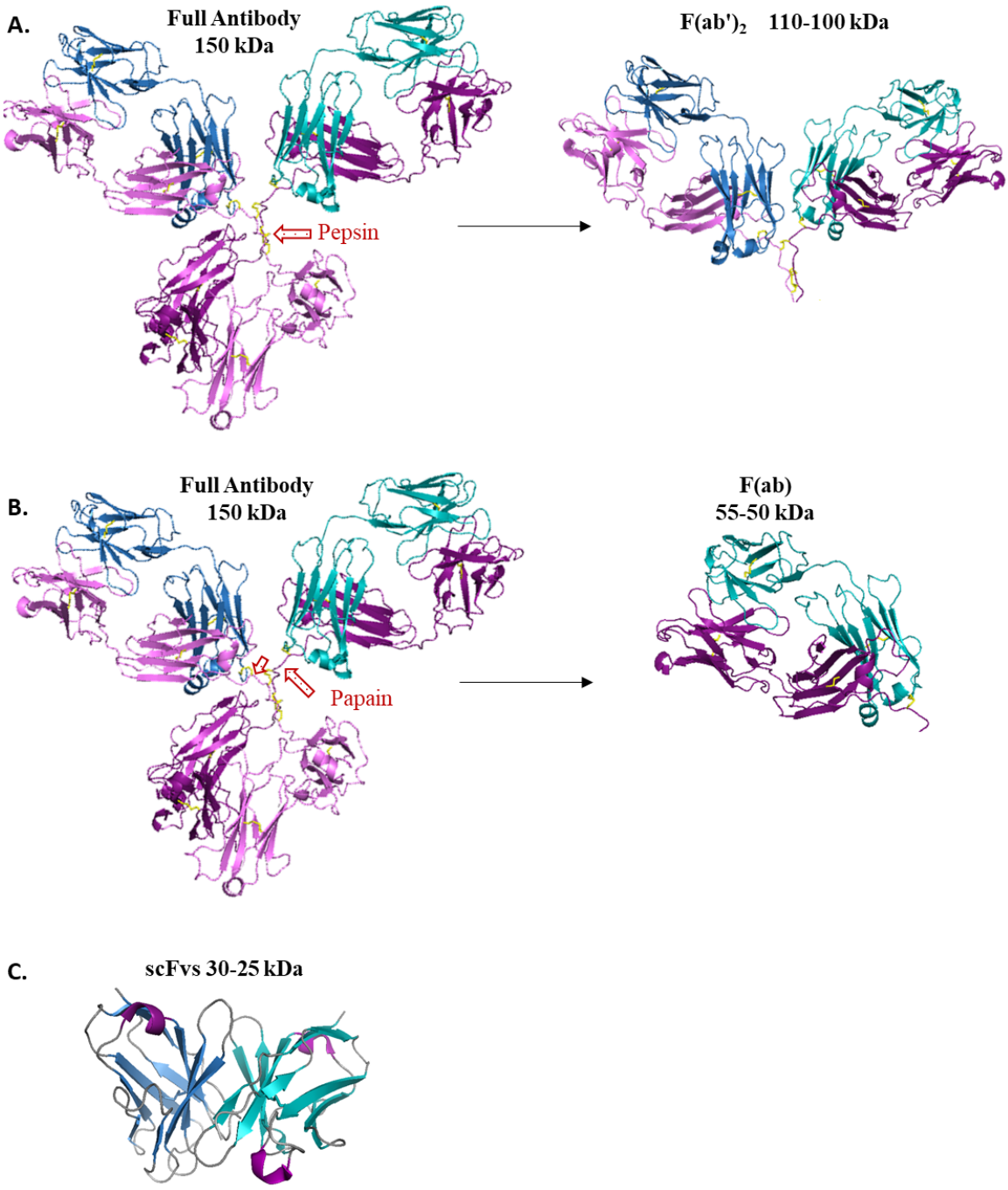

Figure 1.10. Antibody fragments.

*Antibodies Fc portion enzymatic digestion. (**A**)Pepsin digestion results in a F(ab')2 fragment antibodies (110-100 kDa). (**B**) Papain digestion resulting in two F(ab) fragments (55-50 kDa). (**C**) Antibody antigen-binding domains engineered into a single polypeptide (scFvs). Images were generated using PyMol with cartoon representation. (PDB IDs: 1igy and 1p4i_scFvs).*

1.5.2.1.3 Antibodies and antibodies derivates for antiplatelet therapy

An approach to target our proteins of interest (GPVI and G6b-B) would be to use a monoclonal antibody that inactivates GPVI or activates G6b-B to alter platelet aggregation. Specifically, a F(ab) fragment of a humanised antibody would most likely be required to avoid unwanted interactions with the immune system. This approach has been applied successfully with Abciximab, the first anti-αIIbβ3 antigen-binding fragment approved to inhibit platelet aggregation in cardiovascular disease (Faulds and Sorkin, 1994). The numbers of antibodies approved as therapeutic agents rise every year, with their success likely due to their high specificity, affinity and stability (Chames et al., 2009). Specifically relating to GPVI, recent literature has described two anti-GPVI Fab fragments (ACT017 and SAR264565) in clinical trial phase 2 and phase 1/2 respectively (Florian et al., 2017; Lebozec et al., 2017). Nevertheless, a key disadvantage of antibody therapy is that they are not suitable for oral therapy, therefore these anti-GPVI inhibitors can only be administered intravenously.

1.5.2.2 Recombinant proteins

Therapeutic recombinant proteins are proteins expressed in a production organism, such as bacteria or mammalian cells, and can also be used for the treatment or prevention of disease in humans or animals. The first recombinant protein was introduced in 1982, when recombinant human insulin became the first approved therapeutic peptide to be manufactured by recombinant fermentation in *E. coli* (Chance and Frank, 1993). Since then more than 200 recombinant proteins have been approved for therapeutical treatments (Fosgerau and Hoffmann, 2015).

A recombinant protein targeting GPVI is currently in phase II of clinical trials; the humanized Fc fusion protein of the GPVI ectodomain, commercially known as Revacept.

This recombinant protein is a dimeric fusion of the human GPVI extracellular domain and the human Fc-fragment. It binds to collagen and fibronectin at the atherosclerotic plaques preventing platelet adhesion and consecutive thrombus formation (Ungerer et al., 2011). Revacept is in clinical trials for two different diseases (Carotid Artery Stenosis and Coronary Artery Disease, results not published yet), where initial results trial reported a favourable safety profile with no bleeding complications.

1.5.2.3 Nanobodies

The *Camelidae* family possess a unique type of IgG in compared to conventional mammalian IgGs. These IgGs are formed by only two heavy chains which is why they are also known as heavy-chain antibodies (HCAbs). These antibodies also differ with conventional IgGs in the number of constant domains, *Camelidae* IgGs lack the first constant domain. At the N-terminus of the heavy chains, *Camelidae* IgGs contain the variable or antigen-binding domain, named as V_{HH}, these regions correspond with the Fragment antigen binding domains (Fabs) of the conventional IgGs Figure 1.11(Hamers-Casterman et al., 1993).

Nanobodies (Nb) are the recombinant single variable domain (V_{HH}) of this *Camelidae* HCAbs (Figure 1.11). They are produced by immunization of the *Camelidae* animals, followed by isolation of the peripheral blood lymphocytes and by selection through phage display. The V_{HH} domain is encoded by a gene fragment of ~360 bp, which allows amplification by PCR and the generation of immune libraries. When immunization is not possible immune libraries can be substitute by naive or synthetic libraries. Nanobodies are selected by phage display and the antigen-binders are then expressed at high levels in microorganisms, mammalian cells or plants (Muyldermans, 2013).

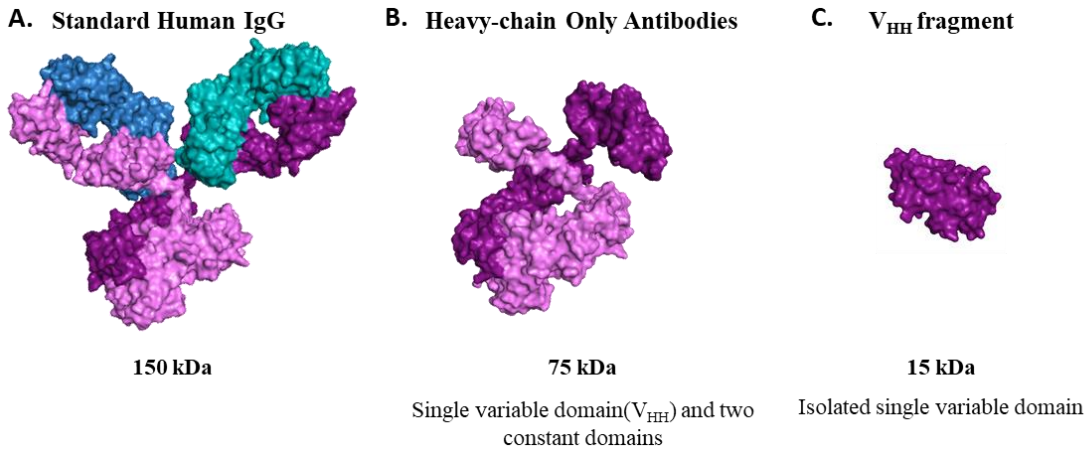

Figure 1.11. Antibody structure vs HCAbs vs V_{HH}.

*Represented as a surface (**A.**) IgG structure is composed of two heavy chains (purple) and two light chains (blue). (**B.**) Camelidae family heavy-chain antibodies (HCAbs) form only by two heavy chains and lack the first constant domain. (**C.**) Nanobodies: the recombinant single variable domain (V_{HH}). Images were generated using PyMol (PDB ID: 1igy).*

The application of nanobodies as therapeutics has some advantages compared with conventional antibodies and F(ab) fragments shown in Table 1.3.

Nanobodies advantages vs conventional antibodies	
Smaller size (~ 15 kDa) - deep and fast tissue penetration - rapid blood clearance	High specificity
	High affinity
	Soluble in aqueous solutions
Reversible refolding	Stability under extreme conditions
Low toxicity	Low immunogenicity
Suitable for oral administration	Proteolytic resistance
Economic to produce	Easy to produce

Table 1.3. Nanobodies advantages vs conventional antibodies.

A major advantage of nanobodies, which highlights them as an exciting alternative to conventional antibodies, is their suitability for oral therapy. This is due to their proteolytic resistance thereby retaining their activity as they pass through the gastrointestinal tract. An example of this is V565, an anti-TNFα oral nanobody currently in phase II of clinical trials (Nurbhai et al., 2019). However, the first nanobody approved by the FDA in 2019, Cablivi™, is an intravenous therapy (Duggan, 2018), although this may reflect the nature

of the target disorder, thrombotic thrombocytopenic purpura, and that it is used in combination with plasma exchange and immunosuppressive therapy (Duggan, 2018). Cablivi™ is a nanobody that binds to vWF and inhibits platelet adhesion to the vessel wall, controlling platelet aggregation and subsequent clot formation without increasing bleeding risk (Bartunek et al., 2013).

Regarding GPVI, a recent study showed a nanobody that inhibits platelets aggregation *in vitro* and thrombus formation under flow by direct binding to GPVI. Further studies and characterization of this nanobody (Nb2) will reveal its potential as an anti-platelet therapy (Slater et al., 2021).

A single nanobody is unlikely to cause receptor clustering and therefore less likely than the previously listed agents to act as agonists. However, nanobodies are easily engineered, which makes it possible to fuse them, for example, to cluster specific targets to activate/inactivate them, or even to generate a bispecific nanobodies to target more than one receptor to generate stronger responses. One example of this would be Nb2-4, four nanobodies (Nb2) linked in order to cluster GPVI or LUAS-4 a nanobody tetramer for CLEC-2, both developed at the University of Birmingham, (Watson Lab, University of Birmingham – unpublished data).

1.5.2.4 Aptamers

DNA or RNA aptamers are short, single-stranded (ssDNA or ssRNA) molecules that can selectively bind to a specific target, including proteins, peptides, carbohydrates, small molecules, toxins, and even live cells. This is due to their three-dimensional shape that allows them to bind to their target with high specificity and affinity (Hermann and Patel, 2000).

Aptamers are small, usually from 20 to 100 nucleotides, and they can be considered as nucleotide analogues of antibodies. Aptamer generation is significantly easier and cheaper than the production of antibodies. Aptamers are selected from a large oligonucleotide library through a process called SELEX, which stands for Sequential Evolution of Ligands by Exponential Enrichment (Tuerk and Gold, 1990). This selection consists of an iterative process, where non-binding aptamers are discarded and apatamers which bind to the target are expanded. Aptamers can be modified during SELEX or post-SELEX in order to make them more suitable for their application (Adachi and Nakamura, 2019).

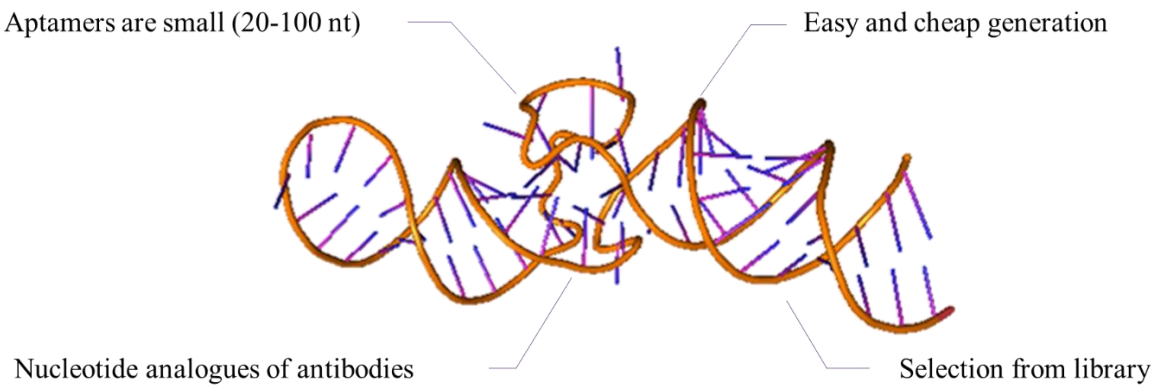

Figure 1.12. RNA Aptamer.

An example of an RNA aptamer with their key features. Image was generated using PyMol (PDB ID: 5ob3).

Aptamers advantages vs antibodies	
Small molecules (20-100 nucleotides)	Can bind to very small targets
Stable at ambient temperature	Reversible denaturation
High specificity	Non immunogenic, non toxic
Low time production	Low production cost (chemically synthetized)

Table 1.4. Aptamer advantages vs conventional antibodies.

Although they have promising characteristics to be good therapeutics, their relative novelty; aptamers were discovered for the first time 3 decades ago, has resulting in only one (Macugen/Pegaptanib sodium) to date to have been approved by the US FDA in 2004. Macugen binds to the vascular endothelial growth factor and stops intraocular blood vessel growth, for the treatment of age-related macular degeneration. Nonetheless, there are several aptamers with promising results in different stages of the clinical trials (Adachi and Nakamura, 2019).

1.5.2.5 Peptide Aptamers

Peptide Aptamers were described for the first time in 1996 and they consist of a short amino acid sequence (5-20 residue peptide loop) embedded onto a neutral scaffold (Colas et al., 1996). Protein scaffold is the term used to refer to a protein backbone that contains the peptide fragment that binds to the target (Reverdatto et al., 2015).

Since their first appearance more than 50 protein scaffolds have been engineered to allow peptide presentation, with different properties and sizes (Reverdatto et al., 2015). Two of these are the human stefin A and a cystatin consensus sequence, with have been named as Affimers.

1.5.2.6 Affimers

Affimers are non-antibody binding proteins derived from a scaffold engineered from human stefin A and a cystatin consensus sequence (Tiede et al., 2017). Affimers molecules are further reviewed in chapter 5. Affimers meet a number of advantages compared with antibodies shown in Table 1.5

Affimers advantages vs antibodies	
Small size (~12 kDa)	Non-immunogenic
Produce from synthetic libraries	High expression
Quick to develop times (3-4 weeks)	Simple and economic to manufacture
Excellent stability to acidity and high temperature	Easy to modify

Table 1.5. Affimers advantages vs antibodies.

While Affimers are in the early stages of development, promising results have been seen stabilizing fibrin networks with potential reduction on bleeding risk, with a fibrinogen binding Affimer (Kearney et al., 2019).

Activatory affimers targeting G6b-B may be a promising therapy, although this has yet to be attempted. Further research is needed to explore these ideas, and fully determine the potential success of targeting these receptors to prevent thrombotic disease without causing substantial bleeding.

1.6 Aims and hypothesis of the thesis

We hypothesize that it will be possible to overcome the bleeding risk of current antiplatelet drugs by modulating GPVI signalling pathway using novel biologics.

Aims of this project are (Figure 1.13):

- To develop new biologics (monoclonal antibodies (mAbs), F(ab) fragments) targeting human GPVI and Affimers targeting G6b-B. Novel GPVI mAbs were generated immediately prior to this project in the Würzburg laboratory, but as a part of this project we aimed to develop new biologics from scratch, choosing Affimers as a new and interesting approach.

- To assess their ability to modulate platelet function and signalling. Using classical platelet function assays, biochemistry, flow adhesion assays.

- To understand their mode of action focusing on the anti-human GPVI antibodies. Understanding whether the effect dimerization and mapping the epitopes where these antibodies bind.

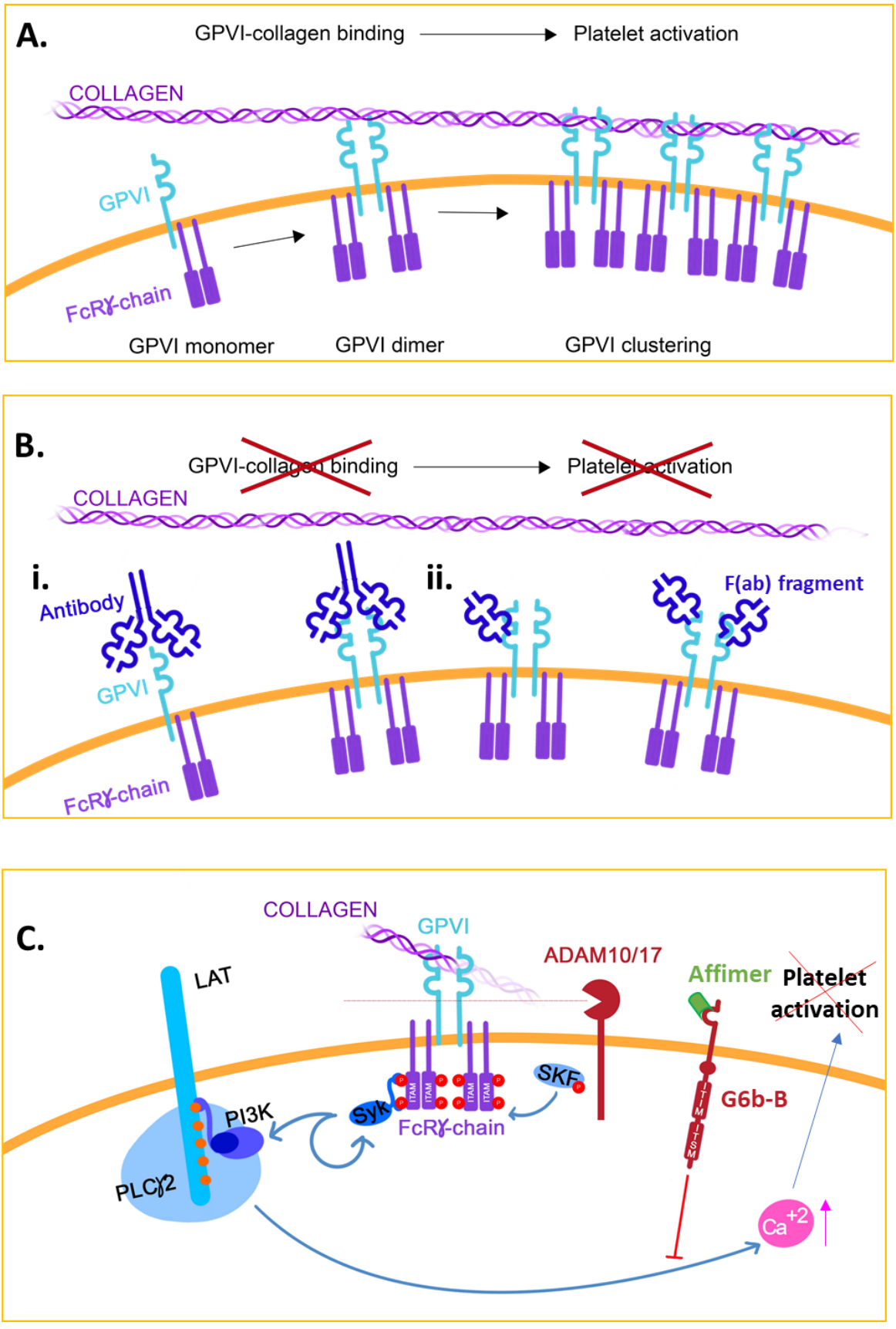

Figure 1.13. Aims.

A. *GPVI activation and clustering. Monomeric GPVI is the most predominant form, switching to dimers upon activation. Collagen binding to the small proportion of dimeric form on resting platelets initiates the formation of further high-affinity dimers, and clustering.* ***B.*** *GPVI inhibition: GPVI binding to* ***i.*** *mAbs or* ***ii.*** *F(ab) would block signalling transduction and further platelet activation.* ***C.*** *Other strategy will be target G6b-B (with Affimers) to inhibit GPVI pathway.*

Chapter 2

Materials and methods

2 CHAPTER 2. MATERIALS AND METHODS

2.1 Materials

2.1.1 Reagents

The agonist used in this work are provided in Table 2.1.

Agonist	Target	Source
Type I Horm Collagen	GPVI, α2β1	Nycomed (Munich, Germany)
Collagen-related peptide (CRP)	GPVI	Professor Richard Farndale (University of Cambridge, Cambridge, UK)
Thrombin	PAR-1, PAR-3, PAR-4	Merck
PAR1 activating peptide TRAP-6 (SFLLRN)	PAR-1	Bachem (Switzerland)
Human vWF	GPIb	ThermoFisher Scientific
Perlecan (Heparan sulfate proteoglycan)	G6b-B	Merck

Table 2.1. List of used agonists.

2.1.2 Antibodies

The anti-human GPVI monoclonal antibodies (Table 2.2) were generated by Emfret Analytics Würzburg, Germany. Antibodies and proteins purchased from commercial sources are presented at Table 2.3and Table 2.4.

Anti-GPVI mAbs		
Antibody	**Species**	**Isotype**
JAQ1	Rat	IgG2a ƙ
338E7 (E7)	Mouse	IgG1 ƙ
336E2 (E2)	Mouse	IgG2a ƙ
328D3 (D3)	Mouse	IgG1 ƙ
336A9 (A9)	Mouse	IgG1 ƙ
326E12 (E12/ EMF1)	Mouse	IgG

Table 2.2. Anti-human GPVI antibodies from Emfret Analytics Würzburg, Germany *and their isotypes. In brackets is denote the short name used throughout this thesis.*

Commercial antibodies				
Antibody	**Species**	**Purpose/ Application**	**Dilution**	**Source**
IV.3 Anti-human CD32	Mouse monoclonal IgG2b	Block FcγRIIA	3/10 μg/mL	StemCell Technologies
IgG from mouse serum I581-1MG	Mouse	Isotype control.	Depending on assay	Sigma
Human IgG1 Fc Recombinant Protein	Human	Affimer screening	--	Invitrogen
Primary antibodies				
Tubulin	Mouse	Western blotting	1:2000	ProteinTech
Phospho-tyrosine (4G10)	Mouse		1:1000	Millipore
His-tag	Mouse		1:5000	ProteinTech
GAPDH	Rabbit		1:5000	Abcam
Myc-Tag (9B11)	Mouse	Western blotting Flow cytometry	1:5000 1:100	Cell Signaling Technology
FITC- anti-human fibrinogen	Rabbit	Flow cytometry	1:100	Dako
APC Mouse Anti-Human CD62P	Mouse		1:100	BD Biosciences
PE/Cy5 Mouse Anti-Human CD62P	Mouse		1:100	
PE anti-human GPVI (HY101)	Mouse		2.5 μl/test	
PE/Cy5 Mouse Isotopy control	Mouse		1:100	

Table 2.3. Commercial antibodies used.

Secondary antibodies				
Antibody	**Species**	**Purpose/ Application**	**Dilution**	**Source**
Alexa Fluor 488 conjugated goat anti-mouse	Goat	Western blotting Flow cytometry	1:4000 1:500	Invitrogen
Alexa Fluor 488 conjugated anti-rat	Goat			
Alexa Fluor 647 conjugated anti-rabbit	Donkey	Western blotting	1:4000	

Table 2.4. Commercial secondary antibodies used.

2.1.3 Cell culture reagents

Reagent	Purpose/ Application	Dilution/ concentration	Source
Dulbecco's Modified Eagle's Medium (DMEM)	Lenti-X 293T cell growth	500 mL	Gibco
Foetal Bovine Serum (FBS)		10% (v/v)	
Penicillin /Streptomycin (P/S)		100u/mL	
L-Glutamine		2 mM	
Ultra-low IgG Fetal Bovine Serum	Fc fusion proteins	10% (v/v)	
PEI MAX® 40K	Lenti-X 293T cell transfection	Stock (1 mg/ml) 3:1 ratio of PEI to DNA (w/w)	Polysciences

Table 2.5. Cell culture reagents.

2.1.4 Bacterial cells

Bacterial cells used in this study are provided in Table 2.6.

Strain	Purpose	Source
DH5α Competent Cells	Cloning	ThermoScientific
T7 Express Competent (C2566H)	Protein expression (Affimer)	New England Biolabs

Table 2.6. List of E. coli strains.

2.1.5 Plasmids and constructs

All the plasmids and constructs used in this work can be found in Table 2.7.

2.1.5.1 G6b-B Fc fusion construct

Human G6b-B was previously cloned into pCDNA3 and was kindly provided by Prof Michael Douglas (University of Birmingham, UK). At the N-terminus there is the signal sequence from CD33 (MPLLLLLPLLWAGALA), to increase secretion, and a T7 antibody epitope (MASMTGGQQMG) to help with protein detection. At the C-terminus there is a human IgG1 Fc tag to purify the protein (Vogtle et al., 2019).

2.1.5.2 GPVI Fc fusion

Recombinant monomeric and dimeric GPVI containing the extracellular domains D1 and D2, the *N*- and *O*-glycosylation sites (monomeric GPVI) and the human IgG1 Fc fused domain (dimeric GPVI) were prepared from a modified SigpIg+ mammalian expression vector containing a N-terminal CD33 signal sequence (for extracellular secretion), the GPVI cDNA (D1 and D2) and a C-terminal Fc domain (human IgG1 for dimerisation) was supplied by Prof. Andrew Herr (Cincinnati Children's Hospital) (Onselaer et al., 2017).

2.1.5.3 GPVI Chimeras

Human-mouse, mouse-human and mouse GPVI were cloned into the pEF6a mammalian expression vector. Human-mouse, mouse-human and mouse sequences were designed with two flanking regions containing restriction sites for KpnI and NotI (although ultimately these were not used) and synthesised by Twist Bioscience (USA). Oligonucleotides were then inserted into the pEF6a mammalian expression vector using the Gibson Assembly (NEBuilder HiFi DNA Assembly commercial master mix, NEB).

Human-mouse, mouse-human and mouse sequences were prepared for the assembly by PCR with primers containing a 17/18 bp overlap complementary to the pEF6a vector (Table 2.8). The pEF6a vector was prepared for the reaction by digestion with KpnI and NotI. Cartoon representations of the constructs are shown in Figure 8.3.

Vector	Tags / Features	Source/ Additional info	Purpose
GPVI Fc (Figure 8.2.)			
modified SigpIg+ human GPVI	Human IgG_1 Fc tag	Prof. Andrew Herr (Cincinnati Children's Hospital).	GPVI production
GPVI chimeras (Figure 8.3.)			
pEF6a	C-terminal His_6 and Myc tag	Invitrogen	Negative control
pEF6a human GPVI		Dr Mike Tomlinson (University of Birmingham, UK) (Tomlinson et al., 2007).	Chimeras experiments.
pEF6a human mouse GPVI		N/A	
pEF6a mouse human GPVI			
pEF6a mouse GPVI			
pDNA3		Invitrogen	Negative control
pDNA3 FcRɣ chain		Dr Mike Tomlinson (University of Birmingham, UK) (Tomlinson et al., 2007)	GPVI expression on cell surface
G6b-B Fc (Figure 8.1.)			
Human G6b-B modified pCDNA3	Human IgG_1 Fc tag	Prof Michael Douglas (University of Birmingham, UK).	G6b-B production for Affimer selection.
G6b-B affimers (Figure 8.4.)			
pET11a-derived	C-terminal His_6 tag Modified with restriction sequence for NheI and NotI	Dr. Christian Tiede (University of Leeds, UK)	Affimer production
pET11a-2/2C	C-terminal His_6 tag	N/A	
pET11a-24/24C			
pET11a-34/34C			

Table 2.7. List of constructs.

All the used plasmids are resistant to Ampicillin.

2.1.6 Primers

Primers were design with SnapGene software or Benchling (online tool) and ordered from ThermoFisher Scientific (Table 2.8).

Primers	Sequence 5' → 3'
Fw GPVI Chimeras	CTCGGATCCGCCACCATGTCTCCA
Rv GPVI Chimera (HD1/MD2)	CGAGCGGCCGCCTAACTAGTGATTGA
Rv GPVI Chimera (MD1/HD2)	CGAGCGGCCGCTCAACTAGTGATTGA
Rv Mouse GPVI	CGAGCGGCCGCCTAGGCCAGTGGGAG
Fw afimers	TTAAGAAGGAGATATACATATGGCTAGCAACTCCCTGGAAATCGAAG
Rv afimers	GTGGTGATGATGGTGATGCGCGGCCGCAGCGTCACCAAC
Rv Cys afimers	GTGGTGATGATGGTGATGCGCGGCCGCACAAGCGTCACCAAC

Table 2.8. List of primers.

Underline can be found the matching sequences with the sequence of the protein and no underline the matching sequences plasmid needed for HIFI assembly.

2.2 Methods

2.2.1 Platelet preparation

Human blood samples from healthy drug free patients and collected in a 4.5 mL or 9 mL vacutainers containing 3.2% sodium citrate. Platelet-rich plasma (PRP) was prepared by centrifuging the whole blood at 102 g for 20 minutes at 20°C. After PRP isolation, acid citrate dextrose (ACD, 85 mM sodium citrate, 71 mM citric acid and 110 mM glucose) prewarmed at 30°C was added and washed platelets were prepared using two consecutive centrifugations to pellet the platelets, at 1413 g for 10 minutes in presence of 10 µL prostacyclin (PGI_2 125 µg/mL, solubilised in ethanol). Platelet count was determined

using a Sysmex counter (Sysmex, UK) and then; resuspended at $4x10^8$/mL in prewarmed (30°C) Tyrode's buffer (134 mM NaCl, 2.9 mM KCl, 0.34 mM Na_2HPO_4, 12 mM $NaHCO_3$, 20 mM HEPES, 1 mM $MgCl_2$ and 5 mM glucose pH 7.3). Platelets were rested for 30 minutes at 30°C to recover. Blood samples were collected under the University of Reading Research Ethics Committee procedures.

2.2.2 Platelet functional studies

2.2.2.1 Light transmission aggregometry (LTA).

Light transmission based real time aggregometry was measured using human washed platelets ($4x10^8$/mL) under stirring conditions (1200 rpm) at 37°C for 5 minutes in an AggRAM aggregometer (Helena Biosciences, Gateshead UK). Washed platelets ($4x10^8$/mL) were pre-treated for 10 minutes at 37°C with IV.3 (3/10 μg/mL) (FcγRIIA blocker, when necessary) and, an additional, 5 minutes at 37°C with the stated mAbs (10 μg/mL). Aggregation was induced with the stated agonists. Tyrode's buffer was used as a blank sample.

2.2.2.2 Plate-based aggregometry (PBA).

Human washed platelets ($4x10^8$/ml) were added to a 96-well half-area plate (Greiner) containing increasing concentrations of anti G6b-B affimers and incubated for 20 minutes. Platelets were then stimulated with agonist and the plate was shaken at 1200 rpm at 37°C for 5 minutes using a plate shaker (Quantifoil Instruments). Absorbance was measured at 450 nm using a Flexstation 3 plate reader. Tyrode's buffer was used as a positive control and resting platelets as a negative control.

2.2.2.3 Fibrinogen binding and P-selectin exposure.

Flow cytometry was used to measure fibrinogen binding (a marker of integrin activation) and P-selectin (CD62P) exposure (a marker of degranulation) by using PRP pre-treated for 10 minutes with F(ab) fragments and stimulated with CRP (3 µg/ml) and TRAP-6 (10 µM) in the presence of FITC-conjugated polyclonal rabbit anti-fibrinogen antibody and APC or PE conjugated mouse anti-human CD62P, and then incubated at room temperature for 20 minutes in the dark. Then, samples were fixed by adding filtered formyl saline (0.2% formaldehyde in 0.15 M NaCl). Negative controls for anti-fibrinogen and CD62P antibodies were established with their isotype controls (EDTA and APC or PE- Mouse IgG1 kappa Isotype Control, respectively). Median fluorescence intensities were measured for 5000 events per sample in the platelet gate (determined by forward and side scatter profiles, measuring cell size and cell granularity, respectively) on an BD Accuri™ C6 Plus Flow Cytometer (BD Biosciences, UK). Data was analysed using CSampler Plus Analysis Software.

2.2.2.4 *In vitro* thrombus formation under flow.

Washed coverslips were coated with three different microspots, one containing a combination of CRP (250 µg/mL), and VWF (12.5 µg/mL µg/mL), another with perlecan (25 µg/mL) and VWF (12.5 µg/mL) and the third one a combination of CRP (250 µg/mL) plus perlecan (25 µg/mL) and VWF (12.5 µg/mL µg/mL). The coated coverslips were incubated for 1 hour in a humid chamber at room temperature and then blocked with HEPES buffer (pH 7.45) containing 1% bovine serum albumin (BSA) for 30 minutes before being mounted into Maastricht microfluidic chambers.

For blood perfusion, 100 µL of citrated whole blood were pre-incubated for 10 minutes with either control Affimer or Affimer 24 (both at a final concentration of 50 µg/mL) for

10 minutes at 37°C. After the addition of 10 U/mL hirudin, which prevents clot formation in the tubings before the blood reaches the flow chamber by blocking thrombin, blood samples were perfused through microspot-containing flow chambers for 3.5 minutes at a wall-shear rate of 150 s^{-1}. Post-perfusion thrombi were stained for phosphatidylserine (PS) exposure (Alexa Fluor 568-annexin A5) and CD62P expression (Alexa Fluor 647 anti-CD62P mAb), followed by rinsing with HEPES buffer (pH 7.45) containing 2 mM $CaCl_2$ and 1 unit/mL heparin. The experiments were performed in duplicate, using blood obtained from 3 different healthy donors. From each microspot, two representative z stacks were acquired using a confocal Ti2 Fluorescence microscope.

2.2.3 Molecular biology methods

2.2.3.1 Polymerase Chain Reaction (PCR)

2.2.3.1.1 GPVI chimeras PCR

GPVI sequences were amplified and prepared for assembly by PCR using KOD Xtreme hot start DNA pol. Reaction volumes and conditions can be found on Table 2.9and Table 2.10, respectively. The PCR mixture was resolved by agarose gel electrophoresis and the amplified samples were excised and purified with a gel extraction kit according to manufacturer's instruction.

KOD Xtreme hot start DNA pol Mix	
2X Xtreme buffer	25 µL
dNTPs 2 mM	10 µL
20 µM Forward Primer	0.75 µL
20 µM Reverse Primer	0.75 µL
Template DNA	0.5 µL Plasmid DNA (~50 ng) 1 µL Genomic DNA (~200 ng)
KOD Xtreme pol.	1 µL
ddH_2O	Up to 50 µL

Table 2.9. KOD Xtrem hot start DNA pol PCR mix.

Reaction conditions			
Cycle step	Temperature	Time	Cycles
Initial denaturation	94°C	2 minutes	1
Denaturation	98°C	10 seconds	30
Annealing	T_m minus 5°C	30 seconds	
Extension	68°C	1 minute/Kbp	
Hold	4°C	Hold	

Table 2.10. Reaction conditions

2.2.3.1.2 Affimer PCR

Affimer sequences were amplified from the phage vectors and prepared for assembly by PCR using Phusion High-Fidelity PCR Master Mix, reaction volumes and conditions can be found on Table 2.11 and Table 2.12, respectively. The PCR mixture was resolved by agarose gel electrophoresis and the amplified samples were excised and purified with a gel extraction kit according to manufacturer's instruction.

Phusion High-Fidelity PCR Mix	
2X Phusion Master Mix	12.5 µL
10 µM Forward Primer	2 µL
10 µM Reverse Primer	2 µL
DMSO	0.75 µL
Template DNA	0.5 µL
ddH_2O	Up to 20 µL

Table 2.11. Phusion High-Fidelity PCR mix.

Reaction conditions			
Cycle step	Temperature	Time	Cycles
Initial denaturation	98°C	30 seconds	1
Denaturation	98°C	10 seconds	30
Annealing	54°C	20 seconds	
Extension	72°C	20 seconds	
Final Extension	72°C	10 minutes	1
Hold	4°C	Hold	

Table 2.12. Reaction conditions

2.2.3.2 Vector digestion

Vectors were digested overnight at 37°C. Reaction was in a total volume of 20 µL (1 µg of DNA, 1 µL of each restriction enzyme, 2µL of 10× CutSmart buffer (New England

Biolabs, NEB) and ddH_2O up to 20 µL). Digested DNA fragments were resolved via agarose gel electrophoresis. Digested fragments were excised from gel and purified using GenElute™ Gel Extraction Kit (Sigma-Aldrich) according to manufacturer's instruction.

2.2.3.3 Agarose gel electrophoresis

Agarose gel electrophoresis was carried out using 50 mL of 1-2% agarose (Fisher BioReagents) in 1×Tris-acetate-EDTA (TAE) buffer. SYBR® Safe DNA gel stain (Invitrogen) in dilution 1:10.000 was used in order to be able to visualize DNA. Samples were prepared using Gel Loading Dye Purple (6×) buffer (NEB). Gels with the samples and GeneRuler 1 kb Plus DNA Ladder (Thermo Scientific) were run in 1×TAE buffer at 100V for 45 minutes.

2.2.3.4 HiFi DNA Assembly

HiFi DNA Assembly was performed following manufacturer's instructions (NEB). Plasmid (previously digested by the corresponding restriction enzymes) and insert (prepare for reaction by PRC) were mixed in a 1:2 ratio and with the rest of the components as showed in Table 2.13. Samples were incubated at 50°C for 30 minutes and subsequently transformed.

HiFi DNA Assembly mix	
DNA ratio	Vector: insert (1:2) 0.03-0.2 pmols
NEBuilder HiFi DNA Assembly Master Mix	10 µL
ddH_2O	Up to 20 µL

Table 2.13. HiFi DNA Assembly mix.

2.2.4 Bacterial cell methods

2.2.4.1 Transformation

Aliquots of 50 µL of *E. coli* DH5α competent cells were transformed with 2-4 µL of plasmid DNA (usually 10 pg - 100 ng). Competent cells stored at -80°C were thawed on ice (20 - 30 minutes). After, adding the plasmid DNA, they were incubated on ice for 30 minutes. The cells were heat shocked for 45 seconds at 42°C and they were incubated again on ice 2 minutes. Cells were then incubated in 700µL of LB (Lysogeny broth) medium for 1 hour at 37°C with stirring (250 rpm). The preculture was spread on LB-Agar plates with Ampicillin (100 µg/mL). The plates were incubated at 37 ° C overnight.

Single transformed colonies of *E. coli* DH5α were inoculated in appropriate volume of LB medium supplemented with ampicillin (100 µg/mL) at 37°C overnight, with agitation (200 rpm).

2.2.4.2 Plasmid DNA isolation

The transformed cells were collected after centrifugation at maximum centrifuge speed for 5 minutes. Plasmid extraction was carried out using the GenElute™ Plasmid Miniprep or Maxiprep kit (Sigma-Aldrich), following the manufacturer's instructions, obtaining 50 µL or 3 mL of plasmid DNA respectively.

2.2.4.3 Glycerol stocks

Overnight bacterial cultures of positive transformed colonies were used to prepare glycerol stocks at final concentration of 50% (v/v) and stored at –80°C.

2.2.4.4 Bacterial protein expression (Affimers)

Affimers expression was carried out using the T7 expression system, which is widely used for recombinant protein production in bacteria owing to its high efficiency of transformation and protein expression. The gene of interest was inserted downstream of a T7 promoter and *lac* operon. The *lac* repressor prevents expression of the protein of interest until IPTG is added to the culture, allowing protein expression to be controlled (Kang et al., 2007).

Single colonies of the Affimers of interest from the LB-Agar plates with transformed T7 Express Competent bacteria were picked using a sterile pipette tip and then, used to inoculate a 5 mL overnight culture in LB medium supplemented with Ampicillin (100 µg/mL) and grown overnight at 37°C, 230 rpm. The following day, a 2 L flask with 200 mL prewarmed LB supplemented with Ampicillin (100 µg/mL) was inoculated with the 5 mL of the overnight culture. Cultures were grown at 37°C and 230 rpm until they reached an OD_{600} between 0.6–0.8 when IPTG (0.1 mM final concentration) was added to induce protein expression. The induced cultures were grown overnight at 25°C at 150 rpm. Cells were harvested by centrifugation at 4,816 g for 15 minutes. Supernatant was discarded and the pellet was used for protein purification (methods 2.2.6.3). This protocol for Affimer expression was previously described by (Tiede et al., 2014).

2.2.5 Mammalian cells methods

2.2.5.1 Cell culture

Lenti-X 293T cells were grown at 37°C, 5% CO_2 atmosphere in Dulbecco's Modified Eagle's Medium (DMEM), supplemented with 10% foetal bovine serum (FBS) or 10% ultra-low IgG Foetal Bovine Serum (for Fc protein expression), containing penicillin (100u/mL)/streptomycin (100 µg/ml) (P/S) and 2 mM L-Glutamine solution.

2.2.5.2 Transient transfection

Lenti-X 293T cells were transfected with PEI 'Max' 40 K (Polyscience). After testing other transfected reagents, such as calcium phosphate and traditional PEI, this was the most effective reagent with the least cytotoxicity. Cells were transfected with a 3:1 ratio of PEI to DNA (w/w). PEI 'Max' and DNA were diluted and then incubated for 30 minutes at room temperature. The mixture was carefully added to the cell dishes and incubated at 37°C, 5% CO_2 until needed for the corresponding experiments.

2.2.5.3 GPVI chimera expression

Lenti-X 293T cells were harvested and expanded into 6 well plates 24 - 48 hours before transfection, until cells were 60 - 80 % confluent. Cell medium was replaced 1 h before transfection. PEI 'Max' (9 µg) was diluted into 150 µl of DMEM (no FBS) and then added to the diluted DNA (3 µg). DNA-PEI 'Max' mix was incubated at room temperature for 30 minutes and then, carefully added to the cell dishes. To allow expression of GPVI at the cell surface cells were co-transfected with a FcRɣ chain expression plasmid in equal amount (Berlanga et al., 2002). Cells were incubated at 37°C, 5% CO_2 for 48 h prior to experiments with the mAbs.

2.2.5.4 GPVI chimera flow cytometry

Lenti-X 293T cells from each transfection ($1x10^6$/mL) were used to study mAbs binding to GPVI D1 or D2. Cells were incubated with the corresponding mAb (10 µg/mL), and the corresponding isotypes controls, in a volume of 50 µL for 1 hour at room temperature. Cells were then washed three times with 100 µL PBS 2% FBS and then stained with the secondary antibody in a volume of 50 µL for 1 hour at room temperature in the dark. Then, samples were washed three times with 100 µL PBS 2% FBS and fixed by adding filtered formyl saline (0.2% formaldehyde in 0.15 M NaCl). The percentage of positive

cells were measured for 10000 events per sample in the cells gate (determined by forward and side scatter profiles, measuring cell size and cell granularity, respectively) on an BD Accuri™ C6 Plus Flow Cytometer (BD Biosciences, UK). Data was analysed using CSampler Plus Analysis Software.

2.2.5.4.1 GPVI chimera flow cytometry with saponin

Lenti-X 293T cells from each transfection ($1x10^6$/mL) were used to confirm GPVI chimera expression in the presence of saponin. Cells were fixed in 100 µL 0.01 % formaldehyde and incubated for 15 minutes at room temperature. Cells were permeabilized in 100 µL 0.5 % saponin in PBS and incubated for 15 minutes at room temperature. Then, samples were washed three times with 100 µL PBS 0.5 % saponin. Cells were incubated with the corresponding mAb (10 µg/mL) in the presence of 0.5 % saponin, and the corresponding isotypes controls, in a volume of 50 µL for 1 hour at room temperature. Cells were then washed three times with 100 µL PBS 2% FBS and then stained with the secondary antibody (if needed) in a volume of 50 µL for 1 hour at room temperature in the dark. Then, samples were washed three times with 100 µL PBS 0.5 % saponin. The percentage of positive cells were measured for 10000 events per sample in the cells gate (determined by forward and side scatter profiles, measuring cell size and cell granularity, respectively) on an BD Accuri™ C6 Plus Flow Cytometer (BD Biosciences, UK). Data was analysed using CSampler Plus Analysis Software.

2.2.5.5 Protein overexpression

Lenti-X 293T cells were harvested and re-plated on ten 150 mm × 25 mm cell culture dishes 24 - 48 hours before transfection, until cells were 60 - 80 % confluent. One hour before transfection cell medium was replaced with 10% ultra-low IgG FBS containing medium. The expression plasmid containing the expression protein (GPVI-Fc or G6b-B-

Fc, 12 µg) was diluted into a 1 mL of DMEM (no FBS). PEI 'Max' (36 µg) was diluted into 1 mL of DMEM (no FBS) and then added to the diluted DNA. DNA-PEI 'Max' mix was incubated at room temperature for 30 minutes and then, carefully added to the cell dishes. Cells were incubated at 37°C, 5% CO_2. After 5 days the cell media, containing the protein of interest (GPVI-Fc or G6b-B-Fc) was collected and replace with fresh ultra-low IgG media and cultured for a further 3 days, when the media was collected again and replaced for another 3 days more before discarding the cells. Collected cell media was pooled and centrifuged (1000×g, 10 minutes at room temperature) to remove cell debris. The supernatant was stored at 4°C with 0.05% sodium azide and saved until purification.

2.2.6 Protein biochemistry

2.2.6.1 SDS-PAGE and Western Blotting

Samples were prepared by adding 10 µl of 6X sample buffer (12% (w/v) Sodium Dodecyl Sulphate (SDS), 30% (v/v) glycerol, 0.15M Tris-HCl (pH 6.8), 0.001% (w/v) Brilliant Blue R, 30% (v/v) β-mercaptoethanol), into 50 µl of sample. Then, the samples were boiled at 95°C for 5 minutes.

Proteins were resolved by electrophoresis through sodium dodecyl sulphate polyacrylamide gels SDS-PAGE gels (4-12% Bis-Tris NuPAGE gel (Invitrogen)) in 1× running buffer (25 mM Tris-HCl, 192 mM glycine, 0,1% SDS) under non-reducing conditions, unless otherwise stated. Pre-stained molecular weight markers (Precision Plus Protein Dual Colour Standards, Bio-Rad) were run alongside samples. Separated proteins were then electro-transferred onto polyvinylidene difluoride (PVDF) membranes using a semi-dry method at 25 V for 40 minutes or stained by InstantBlue Coomassie Dye (Expedeon). Membranes were then blocked with blocking buffer (5% BSA (bovine serum albumin) and 0.1% sodium azide in TBS-T (Tris-buffered saline (200 mM Tris, 1.37 M

NaCl; pH 7.6 containing 0.1% Tween-100)) for 1 hour prior to Western Blotting. The blocked membranes were then incubated with primary antibodies in blocking buffer for 1 hour at room temperature in the dark followed by washing for 5 minutes at a time, with three changes of TBS-T. The membranes were then incubated with fluorescent-conjugated secondary antibodies in TBS-T for 1 hour followed by washing for 5 minutes at a time, with three changes of TBS-T. The proteins were visualised using Typhoon FLA 9500.

Coomassie staining was performed by incubation of the polyacrylamide gel in Staining solution (0.1% Coomassie Brilliant Blue R-250, 50% methanol and 10% glacial acetic acid) for 1 hour with constant shaking. Afterwards, the gel was destained using Destaining solution (40% methanol and 10% glacial acetic acid), changing solution several times, until the background of the gel was clear. Alternatively, the polyacrylamide gels were stained with InstantBlue Coomassie (Expedeon) or Gel Code Blue Safe Satin (Thermo Scientific) and destained in distilled water.

2.2.6.2 Fc-fusion proteins purification by Immobilized protein A Affinity Chromatography

GPVI Fc-fusion and G6b-B Fc-fusion proteins were purified by protein A affinity chromatography. Purification was carried out using ÄKTA™ pure system (GE/cytivia) with a HiTrap™ Protein A HP (5 mL) column (GE Healthcare). The protein A column was washed by running 5 column volumes (CV) of ddH_2O and 5 CV of elution buffer (0.1 M glycine, pH 3.0) and then, equilibrated with 10 CV of binding buffer (0.15 M NaCl, 20 mM NaH_2PO_4, pH 7). The media containing the Fc protein was loaded into the column using sample pump P9S, twice to increase yields, and the column was subsequently washed with 5 CVs of binding buffer. Fc protein was eluted with 15 CV of

elution buffer and 1.5 mL eluted fractions were collected into a 96-well 2mL plate containing 200 µL of neutralization buffer (1M Tris-HCl, pH 9.0). A sample from each step was tested by SDS-PAGE and analysed using Coomassie staining. Eluted fractions containing the corresponding protein were spin concentrated to the appropriate volume and dialysed to exchange protein buffer, when necessary. The dialysis was performed 3 times at 4°C, using SnakeSkin™ Dialysis Tubing (Thermo Scientific, 10K MWCO) in fresh buffer each time.

2.2.6.3 Affimer purification by immobilized metal ion affinity chromatography (IMAC)

Harvested cells from Affimer expression were lysed in 4 mL Lysis buffer (BugBuster® Protein Extraction Reagent (Sigma) supplemented with Lysozyme (0.1mg/mL), 1% Triton-X, Benzonase® Nuclease (Novagen) 10U/mL, 1X Halt Protease Inhibitor Cocktail, EDTA-Free (100X) (Thermo Scientific)) for 1 h on a rotator at room temperature. Non-specific proteins were heat denatured by incubating the samples in a 50°C water bath for 20 min. Cell debris and insoluble proteins were pelleted by two consecutive centrifugations at 4816 xg and 12000 xg for 20 minutes each.

Affimers express a N-terminal 8x His tag which allowed affinity purification by immobilized metal ion affinity chromatography (IMAC). Purification was carried out using ÄKTA™ pure system (GE/cytivia) with a HisTrap™ HP (5 mL) column (cytiva). HisTrap column was washed by running 5 column volumes (CV) of ddH_2O and 5 CV of elution buffer (50 mM NaH_2PO_4, 500 mM NaCl, 300 mM Imidazole, pH 7.4) and then, equilibrated with 10 CV of binding buffer (50 mM NaH_2PO_4, 500 mM NaCl, 20 mM Imidazole, pH 7.4). The protein sample was loaded into the column using a 5 mL loading loop and subsequently washed with 5 CVs of binding buffer. His-tagged protein was then

eluted with 10 CV of elution buffer. A sample from each step tested by SDS-PAGE and analysed using Coomassie staining. Eluted fractions containing the corresponding protein were concentrated with Pierce™ Protein Concentrator PES, 3K MWCO (Molecular weight cut-off), 5-20 mL to the appropriated volume and dialysed to exchange protein buffer, when necessary. The dialysis was performed 3 times at 4°C, by changing the SnakeSkin™ Dialysis Tubing (Thermo Scientific) to fresh buffer each time.

2.2.6.4 Factor Xa Protease cleavage

Dimeric GPVI-Fc was cleaved with Factor Xa Protease (FXa, NEB) to remove the Fc portion and obtain monomeric GPVI. $CaCl_2$ to a final concentration of 2mM of was mixed with FXa/purified GPVI-Fc (1/1000) and incubated on a rotator at room temperature overnight. A sample was tested by SDS-PAGE and analysed using Coomassie staining to assess the level of cleavage.

2.2.6.5 Protein purification by Size Exclusion Chromatography

Following tagged purifications, the proteins were further purified from other small molecules and non-specific proteins by size exclusion chromatography (SEC, also referred as gel filtration) which allows the separation of proteins by size (Porath and Flodin, 1959) using an AKTA FPLC system. Samples were concentrated using a Pierce™ Protein Concentrator PES (Thermo Scientific) molecular weight cut-off (MWCO) of 10, 7 or 3K, depending on the size of the protein; and to a final volume of 5 mL or 0.5 mL depending on the SEC (Size Exclusion Chromatography) column used. Concentrated samples were loaded onto a pre-packed HiLoad 26/600 Superdex 200 prep grade column (GE Healthcare Life Sciences) or Superdex 75 Increase 10/300 GL (GE Healthcare) pre-equilibrated with 1.5 CV of Gel Filtration Buffer (20 mM Tris, 200 mM NaCl or 20 mM Tris, 140 mM NaCl for crystallography). Eluted fractions containing the corresponding

protein were concentrated to the appropriate volume and dialysed to exchange protein buffer, when necessary. Protein that was not used straight away was frozen into liquid nitrogen and stored at - 80°C.

2.2.6.6 Affimer Cysteine labelling

Affimers with a C-terminal cysteine were conjugated with Alexa Fluor™ 488 C5 Maleimide (Thermo Fisher Scientific) directly after IMAC elution as previously described by (Tiede et al., 2014). Tris (2-carboxyethyl) phosphine (TCEP) immobilised resin (Thermo Fisher Scientific) was washed 3 times with PBS containing 1 mM EDTA (150 µl per Affimer). Affimers were diluted in PBS to a final concentration of 40 µM and 150 µl were incubated together with the TCEP resin. After 1 hour on a rotor at room temperature, the solution was centrifuged at 1500 g for 1 minutes. Supernatant containing Affimer molecules with reduced cysteines ready for labelling were collected and transferred into a fresh tube containing 6 µL of 2 mM Alexa Fluor 488 C5 Maleimide (Thermo Fisher Scientific) and incubated for 2 hours at room temperature. Unlabelled fluorophore was removed using a Zeba™ Spin Desalting Column (7K MWCO, 0.5 mL, Thermo Fisher Scientific) according to the manufacturer's instructions. Final concentrations were measure using a NanoDrop One Spectrophotometer (Thermo Scientific) using the pre-configured methods for labelled proteins.

2.2.6.7 Bio-Layer Interferometry

The binding of the mAbs to monomeric and dimeric GPVI was measured by Bio-Layer Interferometry (BLI) on a ForteBio Octet® RED96 System (Octet K2) using anti-mouse Fc (AMC) biosensor probes (AMC Biosensors, Sartorius UK). The AMC Biosensors were hydrated in PBS buffer with 0.02% (v/v) Tween-20 (PBS/Tween20) 10 minutes at room temperature prior to use. Hydrated sensors were preconditioned using 3

regeneration cycles of 5 seconds 10 mM Glycine pH 1.7, 5 s PBS/Tween20 before an initial baseline was established in PBS/Tween20 for 60 seconds at 1000 rpm, 30 °C. All subsequent steps were carried out at 1000 rpm, 30 °C. The anti-GPVI mAbs (10μg/mL) diluted in PBS/Tween20 were immobilized on AMC biosensors for 5minutes at 1000 rpm, then sensors were washed for 30 seconds in PBS/Tween20 before establishing a pre-association baseline in new wells containing PBS/Tween20 for 60 sec. Association and dissociation of monomeric or dimeric GPVI (7.5 nM or 5 nM, respectively) diluted in PBS/Tween20 was measure for 5 minutes for each phase. As a control for any non-specific binding or baseline drift in the experiment, reference sensors and reference wells were included and subtracted prior to kinetic analysis of the data. Affinities (K_D) and kinetic parameters (k_a and k_d) were calculated using the Octet Data Analysis HT 11.1 software.

2.2.6.8 Crystallization Screening

Initial screenings of crystallization conditions were performed with the sitting drop vapour diffusion method using the monomeric GVPI-F(ab) fragment complex (mixed in a 1:1 ratio) purified as above. An Oryx8 Protein Crystallization Robot for Sitting Drop (Douglas Instruments) to dispense 0.2 μL of the screening buffer and 0.2 μL of the protein complex in SwissSci 2 Lens sitting drop crystallisation 96 well plates. The screening buffers tested can be found in Table 4.2 (all from Molecular Dimensions). Plates were stored at room temperature and visualized regularly with a phase contrast microscope. All crystallizations were set up, stored at 295°K and sent to the Research Complex at Harwell for X-ray diffraction.

2.2.7 Data analysis of data

Unless otherwise stated, data presented are mean ± standard deviation. Statistical analysis ware performed using GraphPad Prism 8 Software and statistical significance was determined by one-way ANOVA with Dunnett or Sidak post-test. Differences which reached statistical significance are stated with p values in the figure legends, if significance is not explicitly stated, differences were not statistically significant. Significance was taken for $p \leq 0.05$.

Chapter 3

Effect of novel anti-human GPVI monoclonal antibodies on platelet function

3 CHAPTER 3. EFFECT OF NOVEL ANTI-HUMAN GPVI MONOCLONAL ANTIBODIES ON PLATELET FUNCTION

3.1 Introduction

GPVI is the major collagen receptor. Ligand binding induces GPVI clustering, which initiates a tyrosine kinase-based signalling cascade via an immunoreceptor tyrosine-based activation motif. GPVI has been shown to play roles in both the initiation and growth of thrombi, although GPVI deletion is not associated with significant bleeding. Therefore, modulating GPVI pathway would be a prospect to overcome the bleeding risk associated with current therapies. Using novel monoclonal α-human GPVI antibodies (mAbs) and their F(ab) fragments, we aim to find an antiplatelet biologic that improves current antiplatelet therapies.

Similar strategies targeting GPVI that have achieved clinical trials are two anti-GPVI F(ab) fragments (ACT017 (Lebozec et al., 2017), in phase 1/2 and SAR264565 (Florian et al., 2017), in preclinical) and a recombinant dimeric GPVI-Fc fusion protein (Revacept (Ungerer et al., 2011), in phase 2). This has been already further discussed in section 1.1.4.

This chapter shows the characterization of 4 new monoclonal antibodies (mAbs) against GPVI generated by Emfret Analytics Würzburg, Germany.

3.1.1 Aims

The aims of this chapter are:

- to characterise the effect of the anti-GPVI mAbs and their F(ab)s on platelet function.

3.2 Results

3.2.1 Anti-GPVI mAbs induce platelet activation by the platelet receptor FcγRIIA.

The effect of the anti-GPVI mAbs on platelets was studied by Light Transmission Aggregometry (LTA), the standard method for evaluation of platelet function. In LTA, light transmission through the platelet suspension is monitored in an AggRAM, light transmission increases as the platelets become activated and form aggregates (Born, 1962; O'Brien, 1961).

Human washed platelets ($4x10^8$/mL, 37°C) responded to the anti-hGPVI IgG E7, E2, D3 and A9 (10 µg/mL) with partial or full aggregation in most of the tested donors (Figure 3.2. A, B, C, D, respectively). There were two possible explanations for this: 1.) that FcγRIIA was activating platelets by clustering following binding to the IgGs or 2.) the mAbs activate GPVI through receptor clustering. In order to investigate which was the reason, the anti-hGPVI mAbs were studied in the presence of mAb IV.3. The mAb IV.3 is a FcγRIIA receptor-blocker that has no effect on platelet aggregation alone (Figure 3.1.).

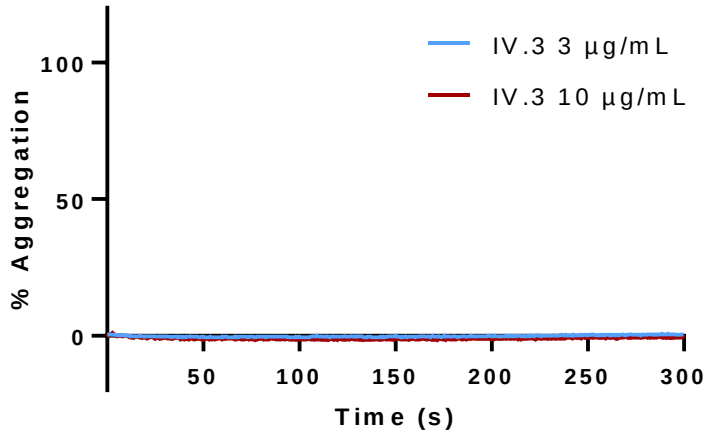

Figure 3.1. Representative traces for human washed platelets with the mAb IV.3.

Representative traces for human washed platelets ($4×10^8$ /ml) incubated with the mAb IV.3 (FcγRIIA blocker 3 or 10 µg/mL) for five minutes, then, aggregation was monitored using LTA for an additional five minutes.

Although platelet activation by the anti-hGPVI IgGs was variable (2-95%), this activation was significatively prevented in all cases (0-15%) when human washed platelets ($4x10^8$/mL) were pre-treated for 10 minutes at 37°C with IV.3 (3/10 μg/mL, Figure 3.2. A.ii., B.ii., C.ii., D.ii.).

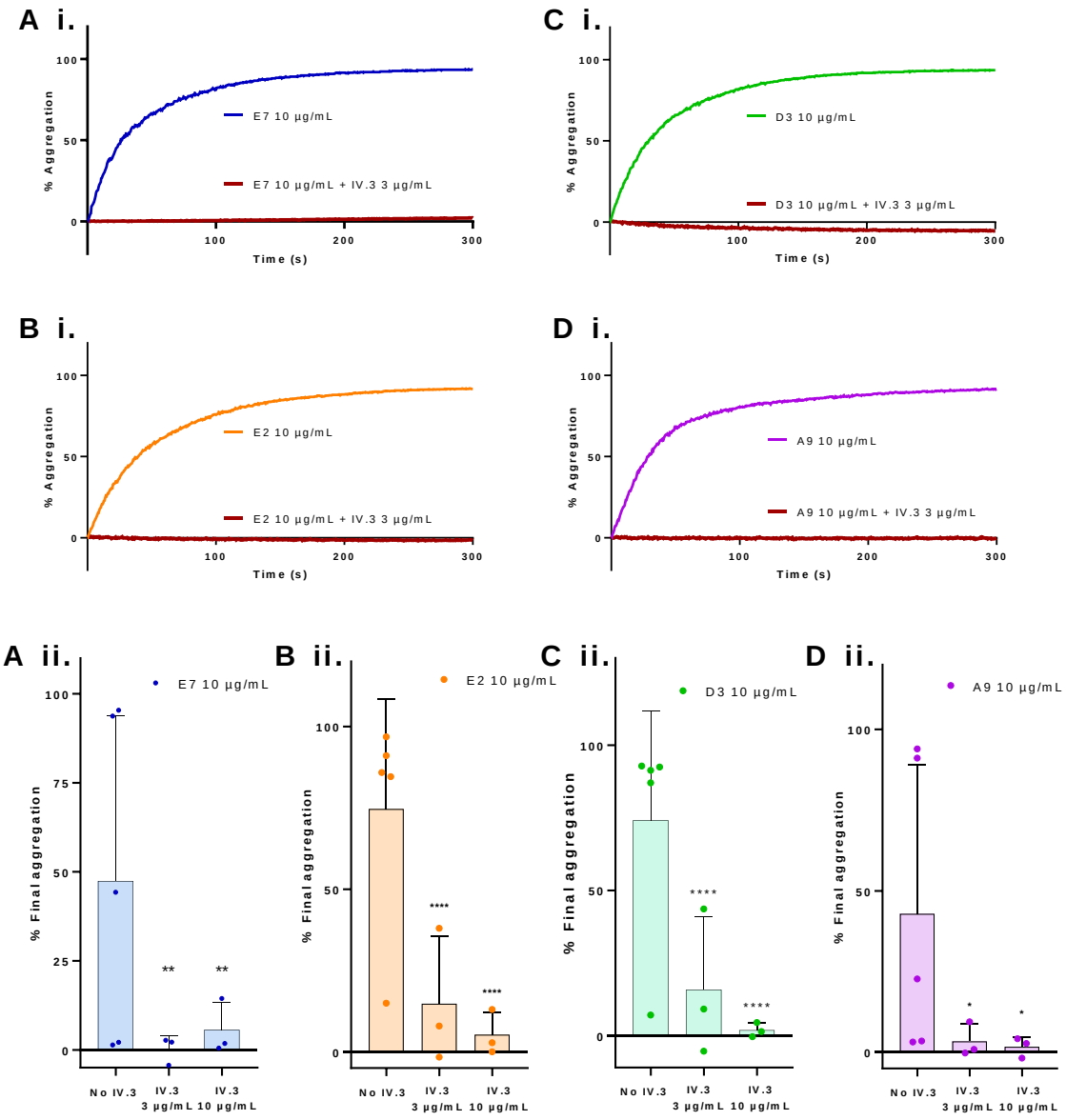

Figure 3.2. Representative aggregation traces of human washed platelets activated by the mAbs.

*Washed platelets (4×10^8 /ml) were incubated with the mAbs E7 (A. blue), E2 (B. orange), D3 (C. green) and A9 (D. purple) (10 µg/mL) for 5 minutes, then, aggregation was monitored using LTA for an additional 5 minutes. Red traces are representative traces for platelets preincubated for 10 minutes with 3 or 10 µg/mL of mAb IV.3 (FcγRIIA blocker) prior to incubation with the GPVI antibodies for 5 minutes. A i. to D i. are representative traces of one donor. A ii. to D ii. Quantified aggregation values for human washed platelets in presence of 10 µg/mL IgGs with IV.3 (3/10 µg/mL) or without it. Statistical significance was calculated using one-way ANOVA with Dunnett's post-test. Data are shown as mean ± SD n = 3-5. *p ≤ .05 **p ≤ .01, ****p ≤ .0001.*

To further confirm that this activation was through the FcγRIIA receptor, human washed platelets ($4x10^8$/mL) were also tested in presence of the anti-mouse GPVI (JAQ1), which has been already described to activate platelets independent to the FcγRIIA receptor (Nieswandt et al., 2000). So, we also tested this antibody as a control. JAQ1 (10 µg/mL) induce platelet aggregation in all the donors. The presence of the mAb IV.3 (3 µg/mL) for the previous 10 minutes at 37°C, do not prevent this aggregation (Figure 3.3.), showing that this aggregation is not due to non-specific activation by FcγRIIA.

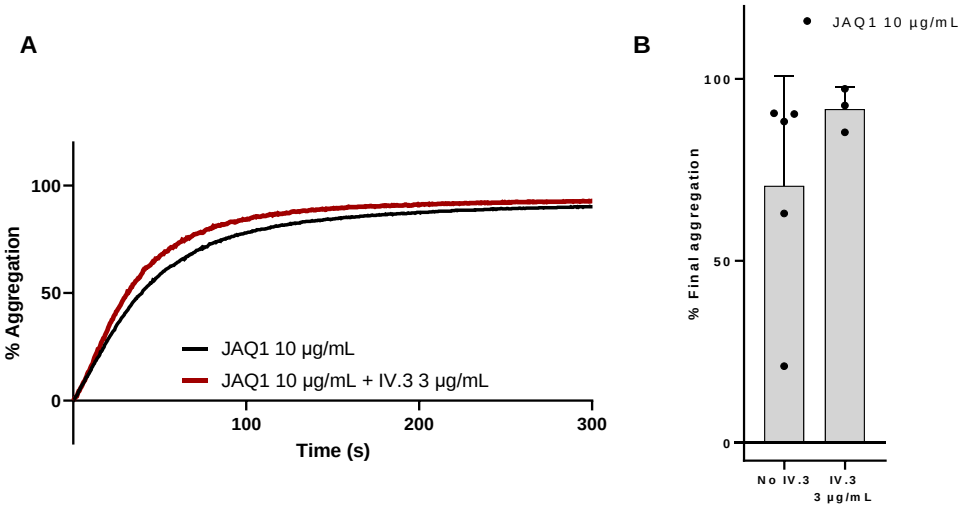

Figure 3.3. A. Representative aggregation traces of human washed platelets with JAQ1. *Human washed platelets ($4×10^8$/ml) were incubated with JAQ1 (10 µg/mL) for 5 minutes and the aggregation was monitored using LTA for an additional 5 minutes. Red trace is representative trace for platelets preincubated for 10 minutes with 3 µg/mL of mAb IV.3 (FcγRIIA blocker) prior to incubation with the GPVI antibodies for 5 minutes.* ***B.*** *Quantified aggregation values for human washed platelets in presence of 10 µg/mL JAQ1 with IV.3 (3 µg/mL) or without it (t = 300 s). Statistical significance was calculated using one-way ANOVA with Dunnett's post-test. Data are shown as mean ± SD and are representative of 3-5 experiments.*

3.2.2 The anti-GPVI mAb E7 inhibits GPVI mediated aggregation

Having established that the mAbs were not GPVI activators, the next step sought to identify whether they were inhibitory for GPVI. The anti-hGPVI IgG E7 (from here on it will be referred as E7) effect on platelet aggregation was studied in presence of GPVI agonists (collagen, physiological GPVI agonist and the collagen-related peptide (CRP), selective GPVI agonist). CRP is used because it only binds to GPVI meanwhile collagen, also binds to α2β1 integrin. Human washed platelets ($4x10^8$/mL) were pre-treated for 10 minutes at 37°C with IV.3 (3/10 μg/mL) (FcγRIIA blocker) and an additional 5 minutes with E7 IgG (10 μg/mL) prior to agonist stimulation. We observed that 10 μg/mL E7 IgG significantly inhibited the platelet aggregation stimulated by CRP (Figure 3.4. A/B). The maximum aggregation percentage was reduced from 92% to 16% (± 7%) when platelets were pre-treated with 3 μg/mL IV.3 and stimulated with 3 μg/mL CRP (Figure 3.4. A/B, $p \leq 0.0001$). Similar results were also observed after increasing CRP concentration to 10 μg/mL (Figure 3.4. B) confirming that it is not dose dependent. When platelets were stimulated with collagen (3/10 μg/mL) the percentage of maximum aggregation was also significantly reduced to 27% (± 13%) and 56% (± 34%), respectively (Figure 3.4, $p \leq 0.0001$, $p \leq 0.01$). However, depending on the donor, the inhibitory effect seen with E7 appeared to be dose dependent as it was overcome when platelets were stimulated with a higher concentration of collagen.

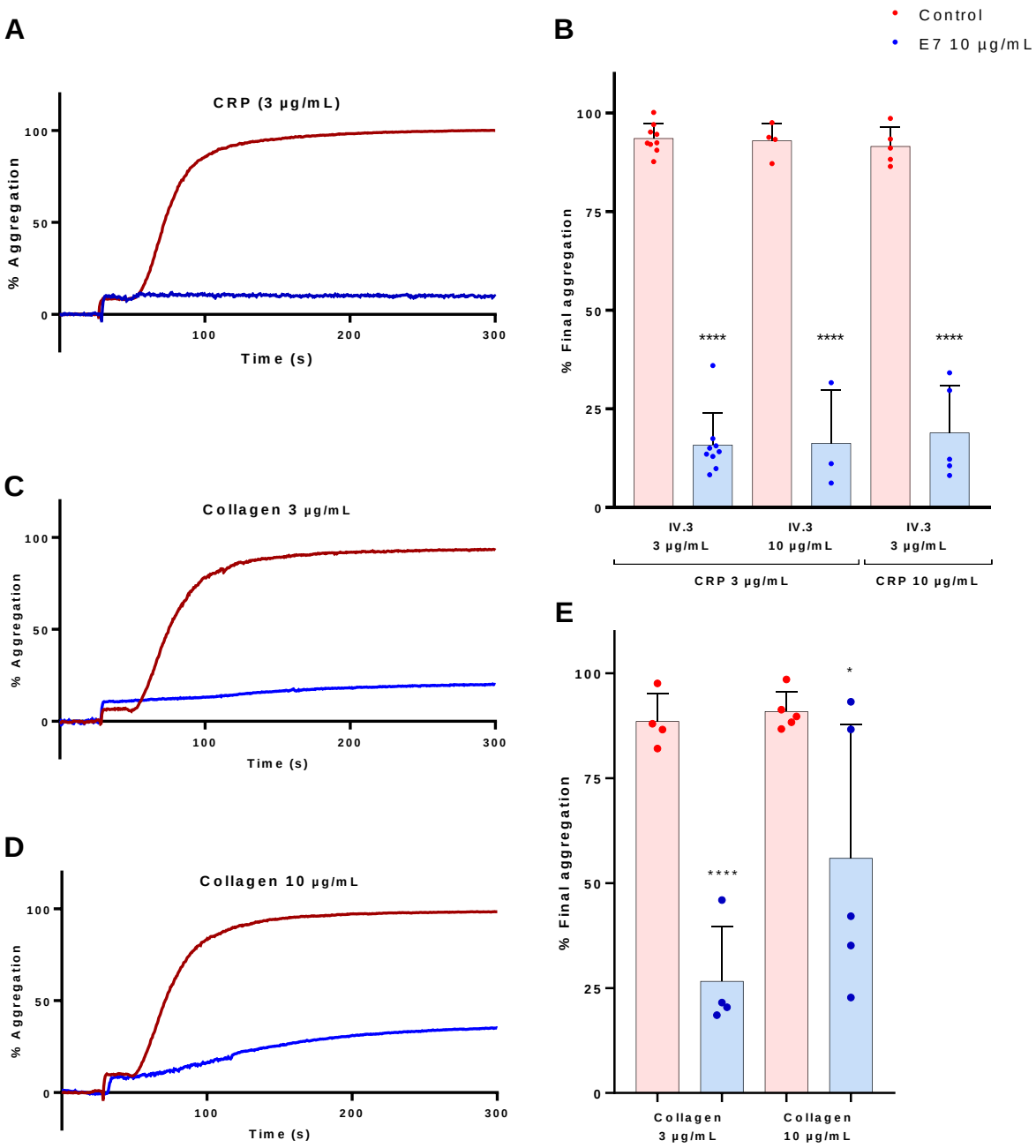

Figure 3.4. Representative aggregation traces of human washed platelets in presence of E7. *Human washed platelets (4×10^8/mL) were preincubated for 10 minutes with 3 or 10 µg/mL of IV.3 (FcγRIIA blocker) prior to incubation with E7 (10 µg/mL) for 5 minutes. Platelet aggregation was induced by the respective agonist (**A.** CRP 3 µg/mL, **C.** Collagen 3 µg/mL or **D.** Collagen 10 µg/mL) and was monitored for an additional 5 minutes. **B.** and **E.** Percentage final aggregation values. Statistical significance was calculated using one-way ANOVA for multiple comparisons. Data are shown as mean ± SD and are representative of 3-9 experiments. ****$p \leq 0.0001$, *$p \leq 0.01$.*

Platelet aggregation induced by thrombin was investigated, as a negative control, to confirm that the effect of E7 was specific to GPVI-mediated activation. As expected, E7 did not significantly effect thrombin induce platelet aggregation (Figure 3.5).

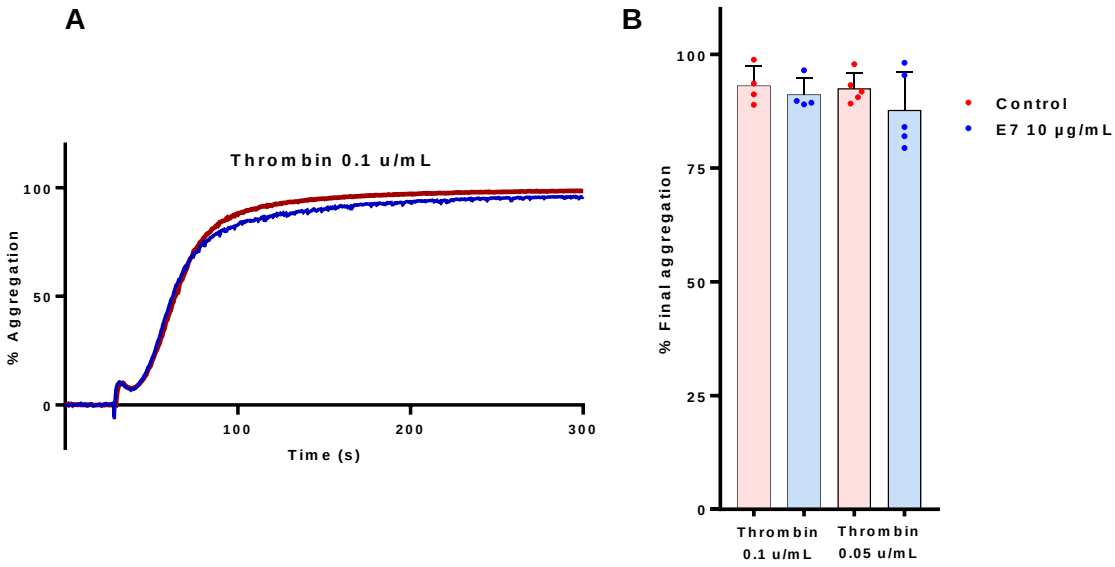

Figure 3.5. Representative aggregation traces of human washed platelets in presence of E7 stimulated by thrombin.

Human washed platelets (4×10^8/mL) preincubated for 10 minutes with 3 µg/mL of mAb IV.3 (FcγRIIA blocker) prior to incubation with E7 (10 µg/mL) for 5 minutes. Platelet aggregation was induced with thrombin (0.1 units/mL), and it was monitored for an additional 5 minutes. ***B.*** *Quantified aggregation values. Statistical significance was calculated using one-way ANOVA for multiple comparisons. Data are shown as mean ± SD and are representative of 4 experiments.*

A generic mouse IgG was used, as an additional negative control, to further confirm that these results are specific to E7 IgG (Figure 3.6).

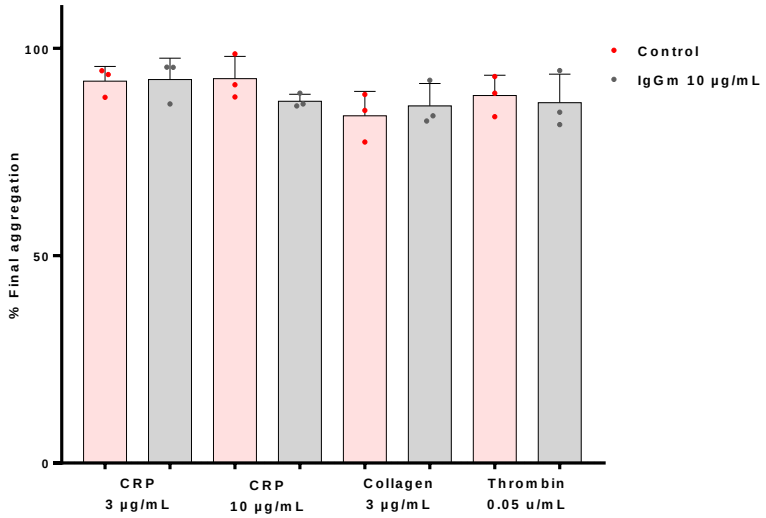

Figure 3.6. Quantified aggregation values of human washed platelets in presence of mouse IgG control.

Human washed platelets (4×10^8/mL) preincubated for 10 minutes with 3 µg/mL of mAb IV.3 (FcγRIIA blocker) prior to incubation with the mouse IgG control (10 µg/mL) for 5 minutes. Platelet aggregation was induced with the respective agonist (CRP 3/10 µg/mL, collagen 3 µg/mL or Thrombin 0.05 u/mL) and it was monitored for an additional 5 minutes. Statistical significance was calculated using one-way ANOVA for multiple comparisons. Data are shown as mean ± SD and are representative of 3 experiments.

3.2.3 E2 and D3 mAbs have no significant effect on GPVI mediated aggregation

The effect on platelet aggregation of the anti-hGPVI IgGs E2 and D3 were studied in the same way as E7, by LTA in presence of GPVI agonists (collagen and CRP) and Thrombin (PAR receptors agonist, to discard that they had an off-target effect). Human washed platelets ($4x10^8$/mL) were pre-treated for 10 minutes at 37°C with IV.3 (3 μg/mL) (FcγRIIA blocker) and, an additional, 5 minutes with E2 or D3 (10 μg/mL) prior to agonist stimulation. We observed that in presence of 10 μg/mL of any of this two mAbs (E2 or D3) platelet aggregation started earlier (potentiation) when platelets were stimulated with CRP (3 μg/mL), (Figure 3.7. A. (E2) and B. (D3)). However, this potentiation was restricted to onset as final percentage aggregation did not change significantly with respect to controls (Figure 3.7. G/H, respectively). In order to investigate the earlier start of aggregation, we analysed the time between the addition of the agonist and the beginning of the aggregation curve (lag phase) on section 3.2.5. Lag phase analysis showed that E2 and D3 decreased it by half (Figure 3.9).

E2 and D3 did not have any significative effect on platelets stimulated with GPVI physiological agonist (collagen, 3 μg/mL) (Figure 3.7. C. and G (E2); D. and H (D3)). Lower concentration of collagen (1 μg/mL) was used to investigated whether these mAbs (E2 and D3) could inhibit a lower concentration. However, we found no significant effect on percentage of final aggregation in samples with the mAbs E2 and D3 respect to controls (Figure 3.7. G/H, respectively). E2 and D3 did not showed any effect on platelet activation when stimulation was performed with Thrombin (0.1/0.05 u/mL), confirming that they did not have off-target effects (Figure 3.7. (E/F and G/H)).

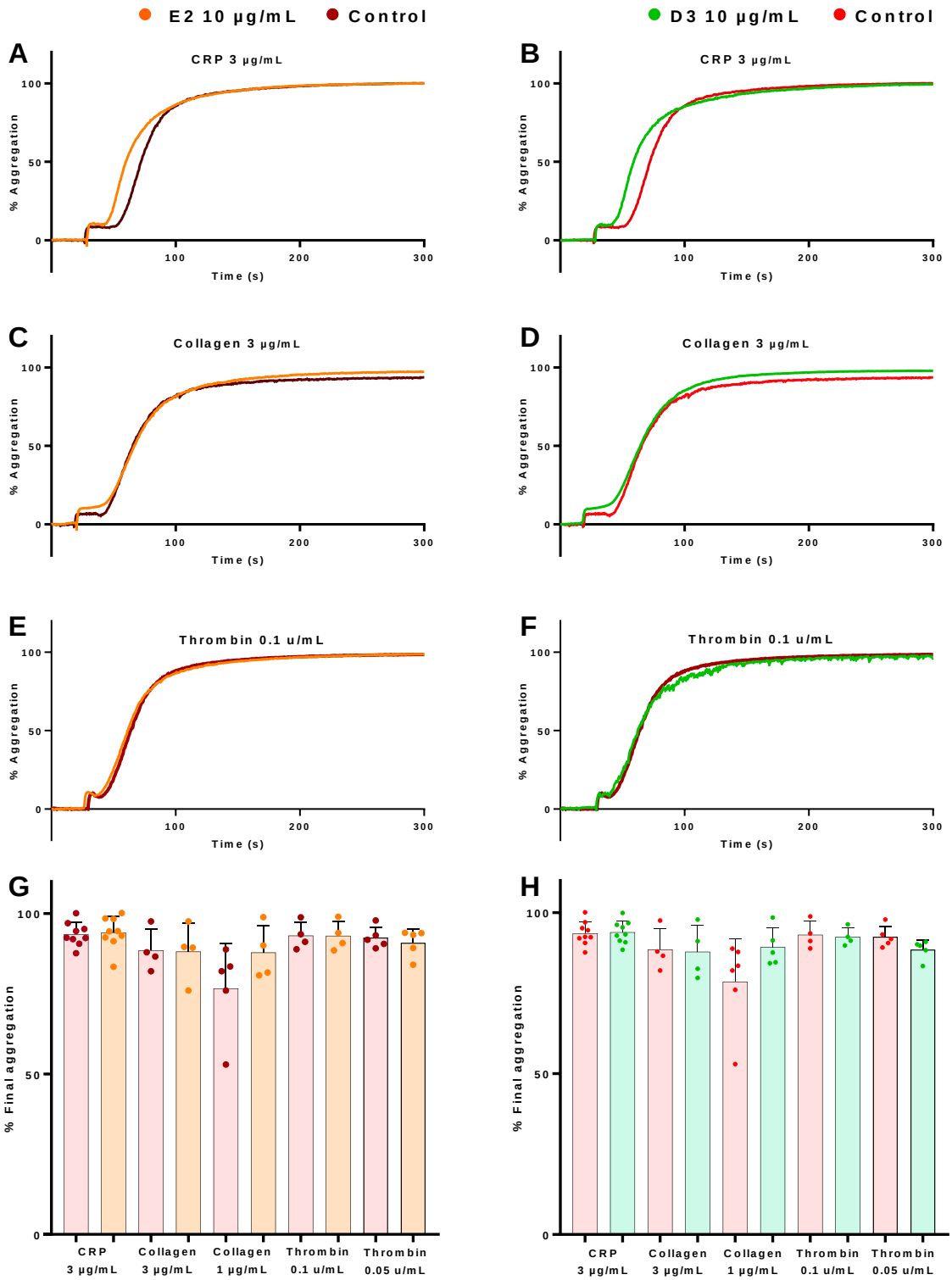

Figure 3.7. Representative aggregation traces of human washed platelets in presence of E2 and D3.

*Human washed platelets (4×10^8/mL) preincubated for 10 minutes with 3 µg/mL of mAb IV.3 (FcγRIIA blocker) prior to incubation with E2 or D3 (10 µg/mL) for 5 minutes. Platelet aggregation was induced by the respective agonist (**A.** and **B.** CRP 3 µg/mL, **C.** and **D.** Collagen 3 µg/mL or **E.** and **F**. Thrombin 0.1 u/mL) and it was monitored for an additional 5 minutes. **G.** and **H.** Quantified aggregation values. Statistical significance was calculated using one-way*

ANOVA for multiple comparisons. Data are shown as mean ± SD and are representative of 9-4 experiments.

3.2.4 A9 has a no significative effect on GPVI mediated aggregation

The effect of Anti-hGPVI IgG A9 on platelet function was studied in the same way as the rest of the mAbs by LTA in presence of GPVI agonists (collagen and CRP) and Thrombin (PAR receptors agonist, to discard that it had an off-target effect). Human washed platelets ($4x10^8$/mL) were pre-treated for 10 minutes at 37°C with IV.3 (3 μg/mL) (FcγRIIA blocker) and, an additional, 5 minutes with A9 (10 μg/mL) prior to agonist stimulation. In the presence of 10 μg/mL of A9 platelet aggregation was delayed when platelets were stimulated with CRP (3 μg/mL), (Figure 3.8). A. However, this delay did not affect final percentage aggregation (Figure 3.8 E). This phenomenon was studied by analysing the lag phase on section 3.2.5. where we observed that lag phase was doubled (Figure 3.9).

A9 (10 μg/mL) seemed to have a minimal effect on platelets stimulated with collagen (3 μg/mL). This effect was variable between donors, Figure 3.8 B and C. Maximum platelet aggregation percentage was reduced to 25, 30 and 50% in some donors (Figure 3.8 B and E) while not in others (Figure 3.8 C and E).

Platelet aggregation induced by Thrombin was investigated to confirm that the effect of A9 was specific to GPVI-mediated activation. No effect of A9 was found with Thrombin (0.1/0.05 u/mL, Figure 3.8 D and E).

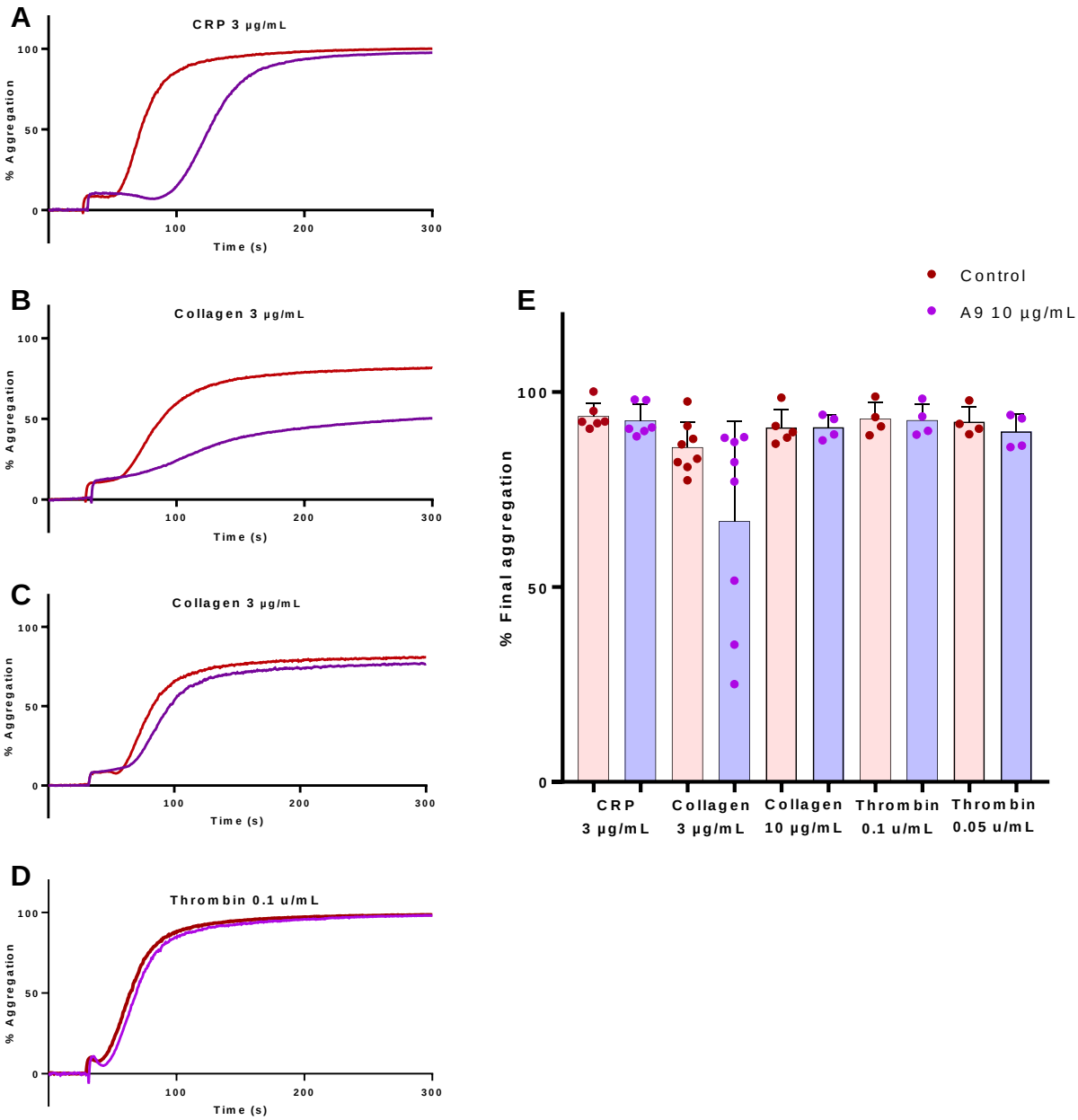

Figure 3.8. Representative aggregation traces of human washed platelets in presence of A9. *Human washed platelets (4×10^8/mL) preincubated for 10 minutes with 3 µg/mL of mAb IV.3 (FcγRIIA blocker) prior to incubation with A9 (10 µg/mL) for 5 minutes. Platelet aggregation was induced by the respective agonist (**A.** CRP 3 µg/mL, **B.** and **C.** and Collagen 3 µg/mL or **D.** Thrombin 0.1 u/mL) and it was monitored using LTA for an additional 5 minutes. **E.** Quantified aggregation values. Statistical significance was calculated using one-way ANOVA for multiple comparisons. Data are shown as mean ± SD and are representative of 8-4 experiments.*

3.2.5 Increased lag phase in response to GPVI activation by A9

Previous sections in this chapter showed that some of the mAbs affected to some extent the lag phase when platelets are stimulates with 3 µg/mL CRP. Lag phase was defined as the delay time occurring between the addition of the agonist and the beginning of the aggregation curve. Lag phase was analysed to see whether the mAbs modified it, given that their aggregation traces showed differences compared with controls (Figure 3.7 and Figure 3.8). Lag phase was quantified, and it manifested that the mAbs E2 and D3 significantly decrease it from 25.2 ± 10 s to 9.7 ± 4.5 s and 10.4 ± 4.5 s, respectively (Figure 3.9, ** $p<0.01$). On the other hand, the mAb A9 exhibited significant increase on lag phase (49.2 ± 20 s, Figure 3.9, **** $p<0.0001$). E7 was not included on this analysis due to it was inhibitory and therefore lag phase can be quantified.

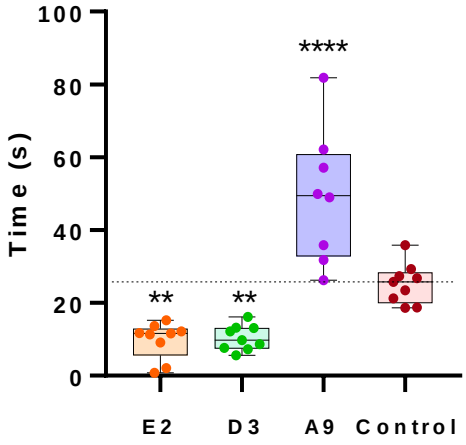

Figure 3.9. Lag phase quantification.

*Quantified aggregation values for human washed platelets (4×10^8/mL) in presence of the mAbs (10 µg/mL) with IV.3 (3 µg/mL) and stimulated with CRP 3 µg/mL. Statistical significance was calculated using one-way ANOVA with Dunnett's post-test. Data are shown as mean ± SD and are representative of 9 experiments, (**** $p<0.0001$, ** $p<0.01$).*

3.2.6 E7 IgG reduce tyrosine phosphorylation downstream of GPVI

Platelet activation by GPVI agonists initiates a series of tyrosine phosphorylations which propagate the signal (Pasquet et al., 1999). Accordingly, the hypothesis was that the antibodies which inhibit GPVI-mediated platelet aggregation would also inhibit the downstream signalling (i.e., tyrosine phosphorylation).

Washed platelets ($4x10^8$/mL) were incubated 10 minutes with IV.3 (3 μg/mL) and 5 minutes with the respective mAb (10 μg/mL). GPVI activations were performed with CRP (3 μg/mL). The reaction was stopped after 90 seconds of the addition of the CRP. Samples were resolved by SDS-PAGE and western blotting for tyrosine phosphorylation with 4G10 antibody. Samples in the presence of E7 significantly reduced total tyrosine phosphorylation (Figure 3.10). This results further confirm that E7 reduces platelet activation mediated by GPVI.

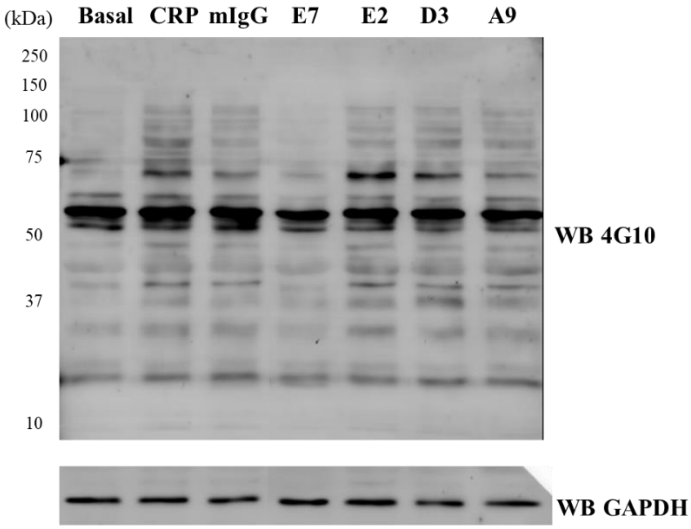

Figure 3.10. E7 IgG reduces tyrosine phosphorylation downstream of GPV.
Human washed platelets ($4×10^8$/mL) preincubated for 10 minutes with 3 μg/mL of mAb IV.3 (FcγRIIA blocker) prior to incubation with mAbs (10 μg/mL) for 5 minutes. Stimulation was induced by CRP 3 μg/mL. Stimulations were stopped at 90 seconds by the addition of lysis buffer and the whole-cell lysates were separated by SDS-PAGE and analysed by western blotting for pTyr (4G10), with GAPDH as a loading control. Representative blot from 3 independent experiments.

Table 3.1 is a summary showing the functional effect of the 4 mAbs tested.

Anti-GPVI mAbs					
Antibody	**E7**	**E2**	**D3**	**A9**	**JAQ1**
Induces platelet aggregation	Yes*	Yes*	Yes*	Yes*	Yes
Blocked by mAb IV.3	Yes*	Yes*	Yes*	Yes*	No
Effect on GPVI mediated aggregation	Reduced	Not significant	Not significant	Not significant	N/A
Effect on lag phase	N/A	Reduced	Reduced	Increased	N/A
Total cell phosphorylation	Reduced	Not significant	Not significant	Not significant	N/A

Table 3.1. MAbs functional activity summary.

**Variable between donors. N/A, no applicable or not tested.*

3.2.7 F(ab) fragment generation

The data above show an effect of the anti GPVI antibodies on platelet aggregation. However, there is also clearly an effect of the Fc portion of the antibodies binding to FcγRIIA receptor. Therefore, we generated F(ab) fragments to be able to assess mAbs effect on GPVI-dependent aggregation *in vitro* without activating them by the Fc region. F(ab) fragments were generated using a commercial F(ab) Preparation Kit.

F(ab) fragments were generated from 0.5 mL of the whole IgGs with immobilised Ficin cleavage for IgG_1 (E7, D3 and A9, Figure 3.11. A) or with immobilised Papain cleavage for IgG_2 (E2, Figure 3.11. B) and purified by NAb™ Protein A Plus Spin Column. The efficiency of F(ab) fragment generation was analysed by non-reducing and non-boiled SDS-PAGE (10%) with an expected apparent molecular weight of 45-50 kDa (Figure 3.11. C). F(ab) fragment concentrations were measured using a NanoDrop One Spectrophotometer (Thermo Scientific), obtaining ~200 µL at 0.25 mg/mL for F(ab) D3 (yield of 11%), ~700 µL at 0.27 mg/mL for F(ab) A9 (10.4% yield), ~700 µL at 0.569mg/mL for F(ab) E7 (23.7% yield) and ~700 µL at 0.417 mg/mL, giving a yield of 37.9%. We observed on SDS-PAGE gel the presence of the whole IgG on E2 fraction, and it was purified again by NAb™ Protein A Plus Spin Column obtaining ~700 µL at 0.285mg/mL (25.9% yield).

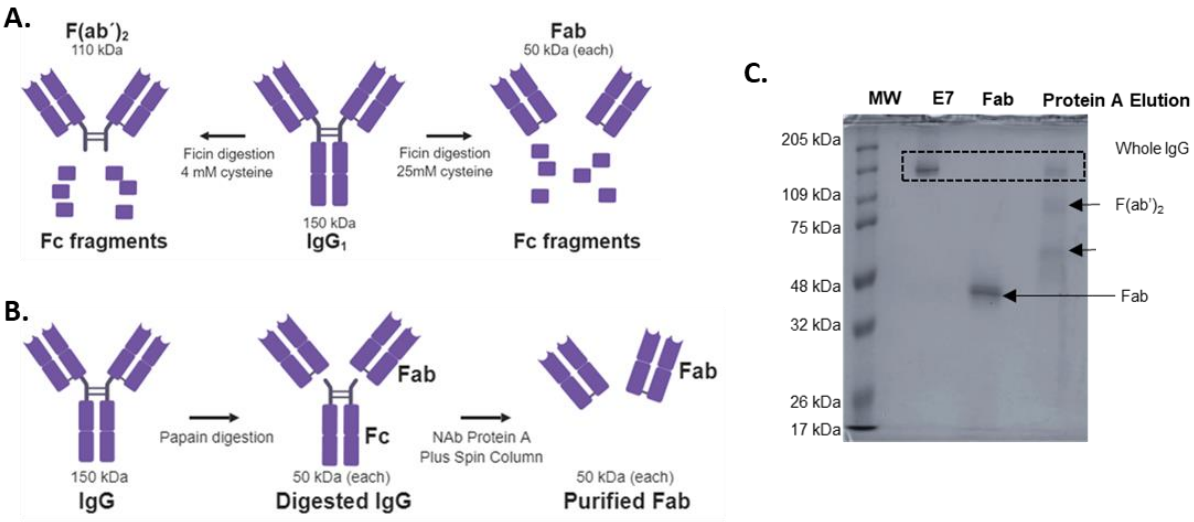

Figure 3.11. F(ab) fragment generation

A. *F(ab) fragment generation scheme from IgG_1 antibody with immobilized Ficin digestion.* ***B.*** *F(ab) fragment generation scheme from IgG_2 antibody with immobilized Papain digestion.* ***C.*** *Representative 10 % SDS-PAGE of E7 IgG_1. Non-reducing conditions were performed, not boiled and were not treated with beta-mercaptoethanol and stained with Coomassie Blue. (MW) molecular weight marker (kDa), (E7) Whole IgG_1, (F(ab)) protein A flow-through: resulting F(ab) fragment, (protein A elution) with no digested IgG_1, F(ab)2 fragments and Fc fragments.*

3.2.8 The anti-GPVI F(ab)-fragments prevent GPVI-induced platelet activation

Platelet activation can be measure by flowcytometry using anti-fibrinogen and anti P-selectin antibodies. Fibrinogen binds to the platelet plasma membrane due to the conformational change of the GPIIb/IIIa complex, while P-selectin is a component of the α-granules which is translocated to the surface of activated platelets after α-granules secretion.

F(ab) fragments of the IgGs were generated and then tested by flow cytometry and not by aggregometry, as done for their IgGs, due to the small amount obtained. Using flow cytometry, activated platelets were detected by determining both the amount of platelet bound fibrinogen, and the P-selectin exposure on the membrane (a marker of a-granule secretion).

F(ab) fragments were tested to detect whether they have a similar effect on platelet aggregation than their respective IgGs and further clarify whether the activation observed was due to the Fc region. We found that fibrinogen binding and the total level of P-selectin exposure (measured by the median fluorescent intensity) was the same as control when platelets were incubated with only the F(ab) fragments for all four IgGs. Additionally, none had any effect on PAR mediated activation, as it can be seen in Figure 3.12 when platelets are stimulated with 10 µM TRAP-6 and median fluorescent intensity is the same as controls.

Platelets pre-incubated with E7 F(ab) fragment and further stimulated with 3 µg/ml CRP showed the same levels of fibrinogen binding and P-selectin exposure such as no stimulated platelets (resting, Figure 3.12. A). This result matches with those obtained with its IgG form on aggregation experiments (Figure 3.4).

E2 and A9 F(ab) fragments display an inhibitory effect when platelets were stimulated with 3 µg/ml CRP (Figure 3.12. B, D). D3 F(ab) fragment significantly decreased fibrinogen median fluorescent intensity (Figure 3.12. C, $P< 0.05$). These results are opposite to the results obtained on aggregometry with their respective IgGs (Figure 3.7, E2; Figure 3.8, A9; Figure 3.7, D3).

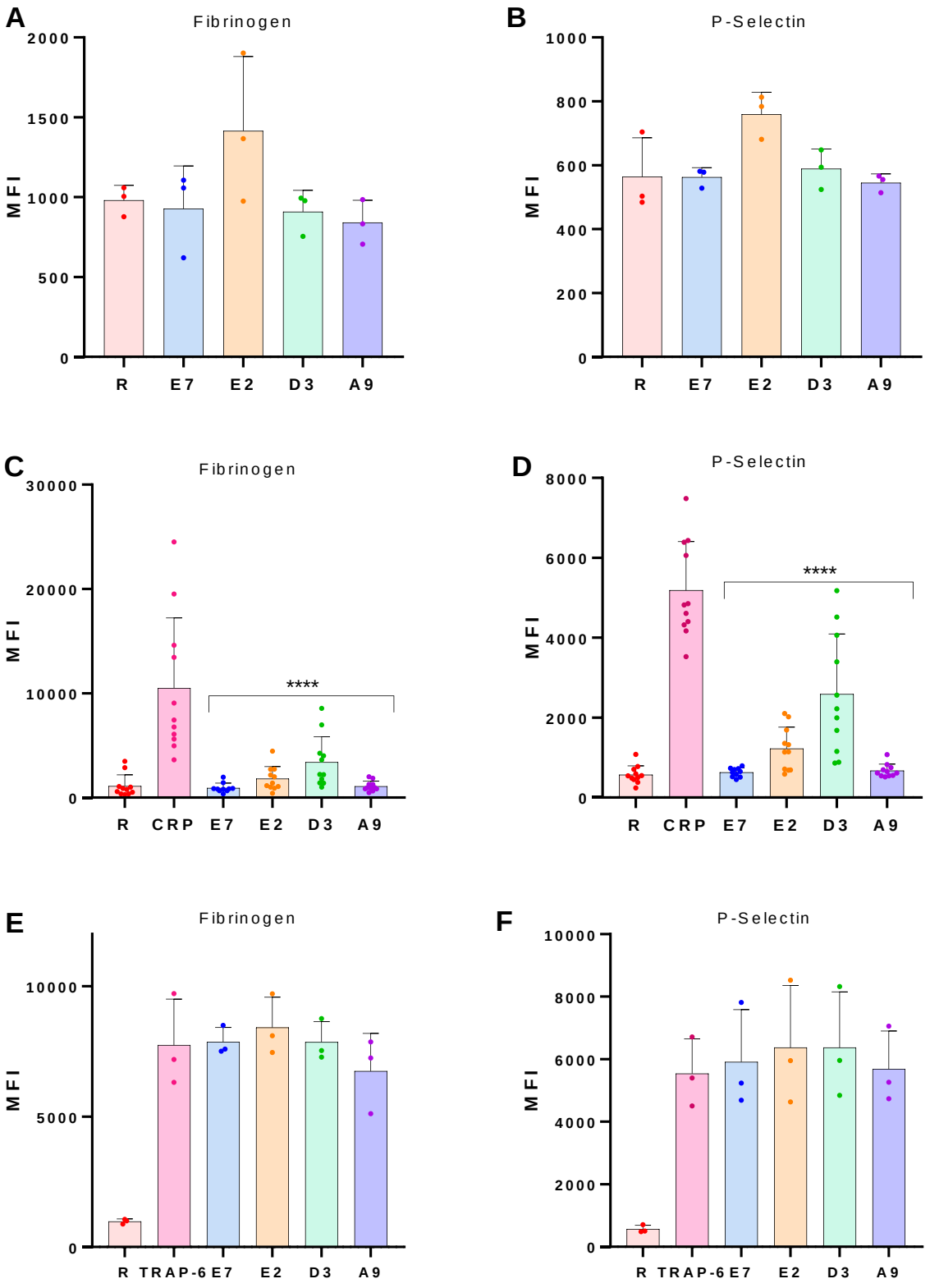

Figure 3.12. mAbs flow cytometry.

*PRP was incubated 10 minutes with F(ab) fragments (3 µg/mL) before stimulation with the agonist. Fibrinogen binding (**A. C. E.**) and P-selectin exposure (**B. D. F.**) were studied by flow cytometry. Bar graphs represent results of median fluorescent intensity (n = 3-11). Results are*

*shown as mean ± SD (*** p< 0.0001). Statistics have been calculated comparing each condition to with its control (**A./B.** resting, **C./D.** CRP, or **E./F.** TRAP-6) without the F(ab) fragment.*

3.2.9 Anti-GPVI F(ab)-fragments optimal concentration

The data above is a F(ab) fragment single concentration, in order to confirm that the effect is full and also identify a minimal dose that gives full inhibition, the optimal dilution of anti-GPVI F(ab)-fragments and dose-response were determined by flow cytometry. This is also useful if it were to be used *in vivo* as a drug.

F(ab) E7 and F(ab) A9 were seen to be inhibitory at 0.03 μg/mL (Figure 3.13. A-D) and between 0.3-1 μg/mL fibrinogen and P-selectin values were as the resting platelets.

F(ab) E2 also had a significant decrease at 0.03 μg/mL ($p < 0.05$). But it showed to be less potent, it was needed between 1-3 μg/mL to see full inhibition (Figure 3.13. E-F). However, higher concentrations of F(ab) E2 revealed to be less effective, as fibrinogen and P-selectin values were higher.

Median fluorescent intensity of fibrinogen binding in the presence of F(ab) D3 (Figure 3.13. G) presented a slightly significant decrease at 0.03 μg/mL ($p < 0.05$) and from 1 μg/mL fibrinogen binding values are similar to resting. On the other hand, P-selectin exposure was not a significant decrease until a higher concentration (0.3 μg/mL) (Figure 3.13. H). There is one donor that has higher values than the rest of the sample, sample size (n = 4-7) would be increased to have more reliable results.

JAQ1 F(ab) fragment (Figure 3.13. I) also presented a slightly significant decrease of fibrinogen binding at 0.03 μg/mL ($p < 0.05$). However, P-selectin exposure (Figure 3.13. J) was not significant decrease until the highest concentrations (10 μg/mL).

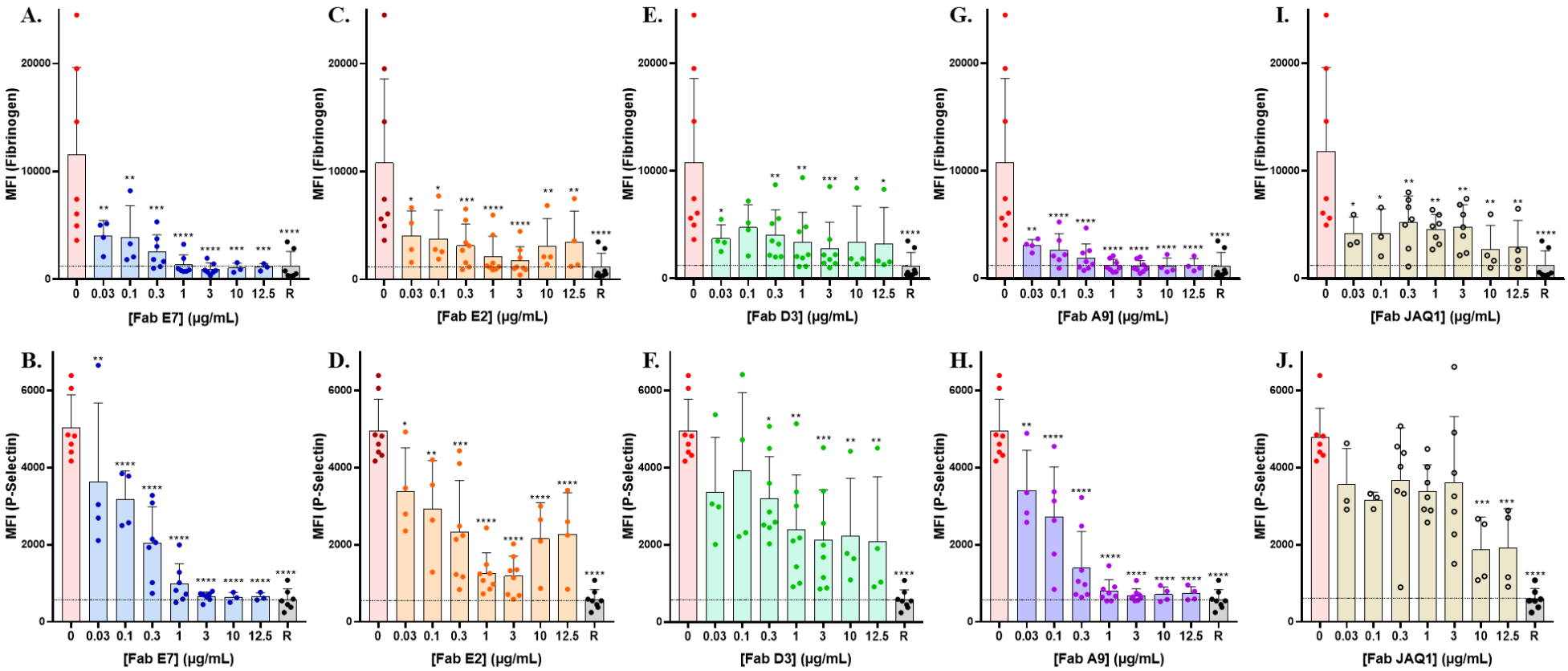

Figure 3.13. F(ab) fragments potency.

*PRP was incubated 10 minutes with increasing concentrations of the F(ab) fragments (from 0.03 to 12.5 µg/mL) before stimulation with 3 µg/mL of CRP. Fibrinogen binding (**A. C. E. G. I.**) and P-selectin exposure (**B. D. F. H. J.**) were studied by flow cytometry. Bar graphs represent results of median fluorescent intensity (n = 3-8). F(ab) E7 (**A.** fibrinogen, **B.** P-selectin), F(ab) E2 (**C.** fibrinogen, **D.** P-selectin), F(ab) D3 (**E.** fibrinogen, **F.** P-selectin), F(ab) A9 (**G.** fibrinogen, **H.** P-selectin), F(ab) JAQ1 (**I.** fibrinogen, **J.** P-selectin). Results are shown as mean ± SD (****p <0.0001, *** p< 0.001, ** p< 0.005, * p< 0.05). Statistics have been calculated comparing each condition to its control without the F(ab) fragment.*

3.3 Discussion

Human platelets express on their surface 1000–4000 copies of the low-affinity Fc receptor (FcR), FcγRIIA (CD32a), making platelets the richest source of FcγRIIA in the body (Karas et al., 1982). FcγRIIA binds the constant region of IgG, recognizing immune complexes (ICs) and IgG-opsonized cells with high avidity (Karas et al., 1982; Rosenfeld et al., 1985). The anti-hGPVI mAbs used in this work caused platelet aggregation, as expected by their bidding to the FcγRIIA receptor, this is the reason for testing in the presence of the anti-FcγRII mAb blocking IV.3. Differences observed between donors might be due to the difference in the number of receptor copies express on the surface of their platelets. Other factors that may influence these results are that platelets could be pre-activated in some degree during washing.

Following blockade of FcγRIIA, we found that the E7 is the only mAb that inhibited GPVI mediated aggregation when studied by aggregometry. Additionally, this inhibition was not overcome with high concentrations of agonist, suggesting that E7 is highly potent. Interestingly, the lag phase analysis showed that A9 increased the time between the addition of the agonist and the beginning of the aggregation indicating that it is delaying the response but not reducing the overall extent of the response. The fact that this only happens when platelets are stimulated with CRP but not with collagen suggest that A9 might be binding near to the CRP binding site which supports the hypothesis that CRP and collagen share some binding residues but they have different binding site (Lecut et al., 2004a). A9 could be slowing down CRP binding by steric impediment or binding CRP binding site and competing for the binding site with the CRP, giving as a result a delay on aggregation start.

Stimulation with thrombin showed that the antibodies are not interfering with PAR receptor-mediated aggregation, showing a specific effect on GPVI.

F(ab) fragments were generated to test their functional effect and avoid aggregation produced by the Fc portion. The advantage of the F(ab) fragment is that we are able to eliminate non-specific binding between Fc portions of antibodies and Fc receptors on immune cells and they penetrate tissues more efficiently due to their smaller size (Nelson, 2010) and can bind to hidden epitopes not accessible to whole antibodies. F(ab) fragments are monovalent, binding only to one epitope meanwhile the whole antibodies are bivalent and bind two epitopes.

We did not test the F(ab) fragments by aggregometry due to the large amount of F(ab) required for these experiments. Therefore, we used flow cytometry as an alternative which can be used to measure markers of platelet aggregation and secretion but with much smaller volumes and numbers of cells. Platelets incubated only with the F(ab) fragments (E7, E2, D3 and A9) did not show any difference with respect to controls (Figure 3.12). This, together with the aggregometry results of the mAbs in presence of IV.3, allow us to conclude that platelet activation shown on aggregation traces with the full mAbs is due to activation though the FcγRIIA receptor by the Fc regions of the mAbs and not by receptor clustering.

F(ab) fragment generation led us to confirm that E7 F(ab) fragment was still inhibiting GPVI. Surprisingly, we found that pre-incubation with E2, D3 and A9 F(ab) fragments showed an inhibitory effect, differing from to the whole mAbs. One reason for this could be that as F(ab) fragments are smaller they are not excluded from an epitope on GPVI which the full mAbs might be. Or maybe they bind to different/hidden epitopes. In the

case of E2 and D3 this could also be owing to the concentration of IV.3 used on aggregation assays was not enough to fully prevent aggregation by the FcγRIIA receptor. There is also a hight variability between donors what might indicate that FcγRIIA receptor expression levels are also factor influencing these differences. Quantitative studies of FcγRIIA receptor expression levels on platelets showed a variation of 2.8 fold (Tomiyama et al., 1992) while GPVI expression levels are tightly regulated, varying by no more than 1.5-fold (Best et al., 2003). Results with the D3 F(ab) fragment should be also interpreted with the caveat that the D3 F(ab) fragment preparation was not well purified due to a technical issue with the kit, and it is therefore a mix of the IgG and the F(ab) fragment.

Stimulation with TRAP-6 provides evidence that the F(ab) fragments did not interfere with PAR receptor-mediated aggregation and that F(ab) fragments inhibition is specific to GVPI.

A dose-response curve of the F(ab) fragments showed that best concentration to achieve full inhibition with E7, E2, and A9 F(ab) fragments is between 1-3 μg/mL. F(ab) E7 and A9 were the more effective and potent. Regarding, D3 F(ab), we can observe that one of the donors had higher values than the rest of the sample, this could be due to this donor is more sensitive to FcγRIIA receptor activation by the Fc regions of the IgG, as D3 F(ab) fragment preparation is a mix with the IgG because of deficient purification and it is a mix of the IgG and the F(ab) fragment. Nevertheless, the sample size (n = 3-8) should be increased to have more reliable results and obtaining a more homogeneous F(ab) fragment preparation will improve these results.

On the other hand, if we compare the fibrinogen binding to P-selectin exposure it can be seen that in the presence of the F(ab) fragments E2, D3 and JAQ1 the reduction in

fibrinogen binding is more pronounced than the reduction of P-selectin exposure. This may suggest that even if there is a sub-population of activated and secreting platelets, there may still be a global reduction in fibrinogen binding which translates to a reduction in platelet-platelet interactions resulting in smaller thrombi. This cannot be verified statistically here, but it will be interesting studying it.

Additionally, there are differences in platelet preparations that may influence the differences seen between the whole Abs and the F(ab) fragments. In the aggregometry experiments, platelets were isolated, and aggregations were conducted under stirring conditions. In contrast, flow-cytometry experiments were performed with PRP and no stirring.

3.4 Conclusions

This chapter shows the characterization of four new anti-GPVI mAbs and the production and characterization of their F (ab) fragments. Among the mAbs, E7 is the only inhibitory antibody and A9 could be competing with CRP for its binding site or adding some steric impediments to its binding, suggested by A9 increase in lag phase when platelets are stimulated by CRP. GPVI-mediated platelet activation was inhibited by all the four F(ab) fragments suggesting these have potential as a novel α-GPVI therapy. Where exactly this mAbs bind to GPVI will be investigated in the next section (Chapter 4. epitope mapping, structure function).

Chapter 4

Epitope mapping, structure function and crystallography

4 CHAPTER 4. EPITOPE MAPPING, STRUCTURE FUNCTION AND CRYSTALLOGRAPHY

4.1 Introduction

Four mAbs and their F(ab) fragments have been characterised for their effect on platelet function on the previous chapter (Chapter 3). Protein-based therapeutics, such as mAbs, need a thorough characterization on their activity, efficacy, and immunogenicity, which relay directly on their primary structure, post translational modifications, and higher order structure. Robust characterization and analysis of these characteristics needs to be demonstrated during development.

Regarding GPVI, how its structure relates to its function is not fully understood. This lack of knowledge is more patent when it comes to the question of monomer vs dimer and which conformation is responsible for signal transduction, with studies contradicting each other (see general introduction 1.3 GPVI). Therefore, it was important for this to elucidate whether the mAbs bound to monomeric and/or dimeric GPVI as this may underly their inhibitory action. Furthermore, we wanted to identify which domain(s) were involved in this binding as this would also potentially highlight their mechanism. Indeed, work in the previous chapter demonstrates that all the F(ab) fragments inhibit GPVI activation by CRP which led us to hypothesise that the mAbs binding site are within the collagen/CRP binding site or close to them at the D1 domain.

This chapter presents the structural characterization of GVPI interaction with our mAbs. This characterization will be carried out by bio-layer interferometry, crystallography, and epitope mapping.

4.1.1 Biolayer interferometry

Biolayer Interferometry (BLI) is a label-free technique that directly measures biomolecular interactions in real time. BLI measures the interference pattern in light reflected from an internal reference layer and a biomolecular layer due to binding events. The immobilisation of your molecule of interest on the biosensor surface can be achieved by a variety of interactions, e.g., biotin/streptavidin, antibody/anti-Fc, His-tag/Ni-NTA or GST/anti-GST (Sultana and Lee, 2015). One of the advantages of this technique compared with others (e.g., Biacore) is the small amount of sample that it required (nanomoles).

The instrument used for BLI was an Octet K2 system (ForteBio Inc.). This multichannel device can perform 2 assays in parallel in 96-well plates with a final sample volumes of 180/200 μL and can measure binding of molecules down to 150 Da and affinities from millimolar to picomolar concentrations.

Biosensors need to be pre-hydrated in the experiment buffer for at least 30 minutes before the experiment. The Data Acquisition software allows the user to design the experiment in advance. Binding kinetic experiments consist in 5 steps which are illustrated in Figure 4.1. First step consists of an initial baseline using the assay buffer. Secondly, the ligand is immobilized at the surface of the biosensor (loading), followed by a second baseline to assess assay drift, and determine the loading level of ligand. Then, the biosensors with the loading ligand are immersed into a solution with the binding molecule (analyte) and the association is measured. Finally, biosensors are moved into a new buffer solution without analyte to measure the disassociation.

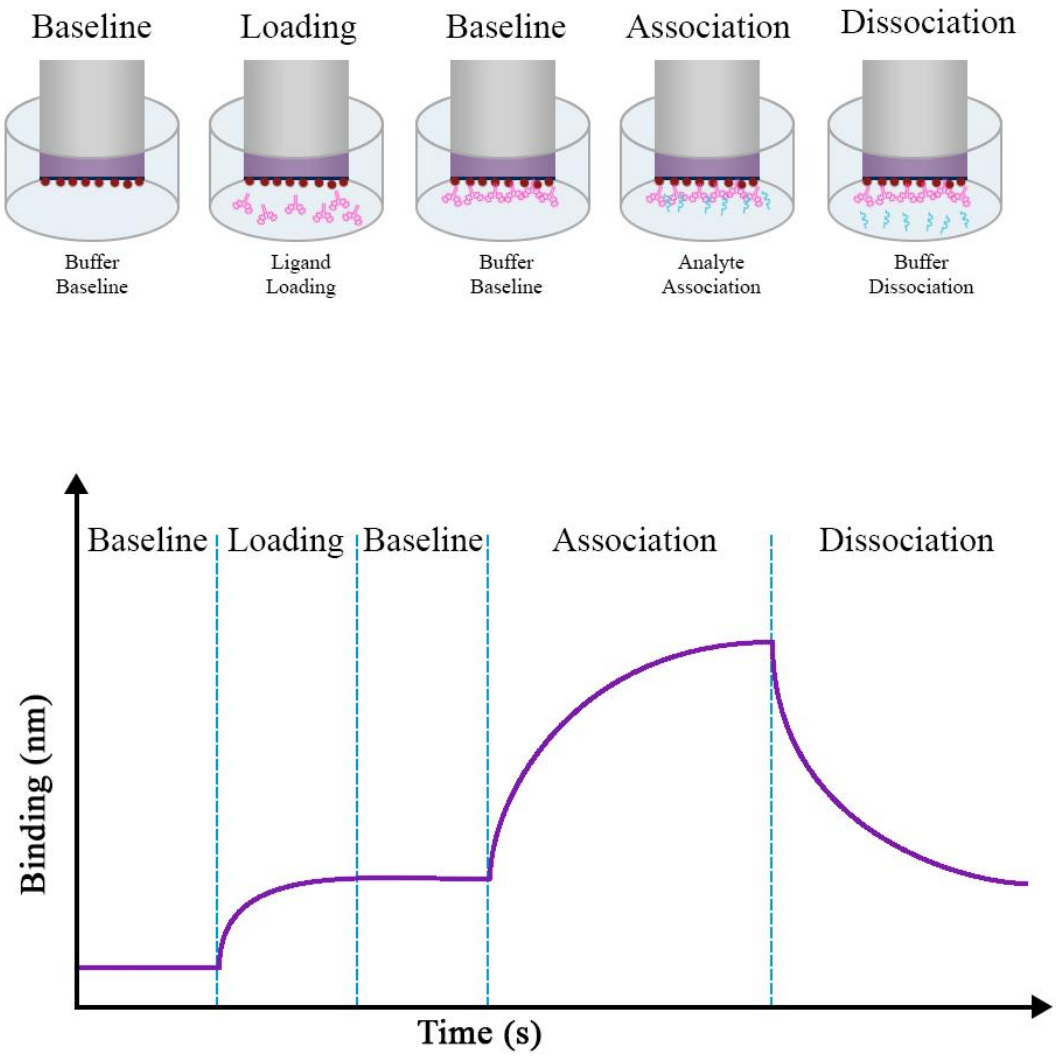

Figure 4.1. BLI scheme.

On the top schematic representation of the process. Buffer baseline, ligand immobilization on the biocompatible surface (loading), baseline, analyte binding (association), and dissociation in buffer. On the bottom, the typical trace graph with the steps of the experiment: baseline, loading, association, and dissociation.

Association and disassociation binding constants (k_a and k_d, respectively) and the affinity constant (K_D) are calculated by mathematical equations. The simplest model is a 1:1 interaction where one molecule of analyte interacts with one molecule of ligand and this reaction is described by the following equation:

$$A\,(ligand) + B(analyte) \underset{k_d}{\overset{k_a}{\rightleftharpoons}} AB(ligand - analyte\ complex)$$

k_a is the constant association rate and represents the number of AB complexes formed during association and is expressed in M^{-1} sec^{-1}. K_d is the disassociation constant and measure the stability of the complex or the decaying complexes per second is expressed in $seconds^{-1}$. K_D is the affinity or equilibrium disassociation constant and measures the strength of the binding and is expressed in molar units (M). To calculate the k_a and K_D, the concentration of analyte must be known.

$$k_D = \frac{[A] \cdot [B]}{[AB]} = \frac{k_d}{k_a}$$

Some ligands or analytes can be bivalent, such as antibodies, and the mathematical equation of the binding model are more complex corresponding with a 1:2 model:

$$A + B \underset{k_{d1}}{\overset{k_{a1}}{\rightleftarrows}} AB \rightarrow AB + B \underset{k_{d2}}{\overset{k_{a2}}{\rightleftarrows}} AB_2$$

This model assumes that the analyte can bind a second ligand due to the limited distances. The formation of the AB_2 complex is dependent on the formation of the AB ones. This avidity effect results in a slower apparent dissociation rata than would be expected if the interaction followed a 1:1 binding.

4.1.2 X-ray Crystallography

Single crystal X-ray diffraction is the most popular method for structural determination of proteins. Solving a protein structure has become easier in the last years thanks to the development in computing, automation of crystallization techniques and high-flux synchrotron sources to collect diffraction datasets (Ilari and Savino, 2017; Wlodawer et al., 2013). The fundamental principle of X-ray crystallography is based on Bragg's law. The atoms within the crystal structure diffract the X-ray beam in specific directions. Measuring the intensity of the diffraction spots, taken from multiple angels, the data can be processed to obtain an electron density map.

The first and the rate-limiting step in X-ray crystallography is obtaining diffraction-quality crystals. Furthermore, each sample has different and specific crystallization conditions making protein crystallization mainly a "trial and error" procedure (Ilari and Savino, 2017). A protein crystal consists of a repeating arrangement of molecules packed in the three-dimensional space (unit cell). The unit cell is the smallest repeating unit with crystal structure symmetry. Purified protein samples are trialled against a very broad range of crystallization conditions using commercial screenings. The amounts of protein required for setting up a broad range of screenings has decreased over time with the development of crystallization robots and the miniaturization of the crystallization apparatus, however, the process still required relatively large amounts of very pure protein compared to other analytical methods (Wlodawer et al., 2013).

The predominant method for protein crystallization is sitting drop vapour diffusion. The protein solution is mixed in a 1:1 ratio with the reservoir solution in a drop surrounded by the reservoir and place into an enclosed chamber, as showed in Figure 4.2. The vapor pressure is lower in the reservoir solution than in the protein drop, which results in a loss

of water that increases protein concentration within the drop. If the conditions are optimal protein crystals will form. There are many factors that influence the formation of the crystals, such as protein concentration and purity, pH, temperature, and the reservoir precipitants (Forsythe et al., 2002). Once the initial screening yields crystals further optimisations are required to obtain a diffraction-quality crystals.

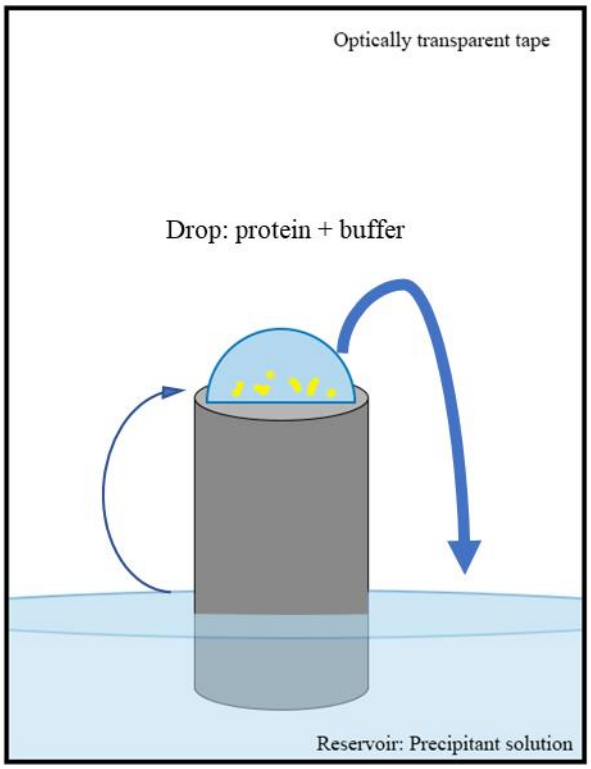

Figure 4.2. Crystallization by vapour diffusion.

In sitting drop vapour protein solution is mixed in a 1:1 ratio with the reservoir solution in a drop surrounded by the reservoir and place into an enclosed chamber sealed with tape. The vapor pressure is lower in the reservoir solution than in the protein drop, which results in a loss of water that increases protein concentration within the drop. If the conditions are optimal protein crystals will form.

X-ray crystallographic structure determination workflow can be divided in 5 steps:

1. Sample preparation: obtaining highly pure protein of interest (>95%), usually is recommended starting with a concentration of 10 mg/mL.
2. Crystal plate setup: protein and crystallization (reservoir) buffer are mixed and distributed into a 96-well plate.
3. Crystallization: proteins are crystallized under specific conditions.
4. Data collection: protein crystals are exposed to an X-ray beam to produce a unique diffraction pattern to the protein structure.
5. Phasing, model building and refinement: the diffraction pattern is analysed with specialized software to determine the protein's 3D structure.

4.1.3 Epitope mapping

Multiple methods can be used to map the interaction between a protein and an antibody. The most commonly used method due to the level of accuracy is X-ray crystallography, this is one of the approaches that we have tried to map GPVI interface interaction with some of its antibodies also in this chapter. However, X-ray crystallography is a long process that requires lots of optimisation to obtain diffraction-quality crystals. In the meantime, a faster and more straightforward approach is to analyse the binding of the antibodies to a mutated form of GPVI. Loss of binding to a particular mutant suggests that the mutated portion contains an epitope or part of it. An even more compelling approach would be making target mutants with structurally related protein such as an orthologue, in this case mouse GPVI, this is called orthologue epitope mapping. Here, recombinant human and mouse GPVI chimeras will be developed to delimit with regions the mAbs bind. Although crystallography would give a much greater level of detail in determining the epitope, the chimera approach is rapid, both requiring fewer steps and being less prone to issues with protein purification and stability.

4.1.4 Aims

The aims of this chapter are:

- to produce and purified recombinant GPVI to be used on BLI and crystallography studies.
- to establish whether the mAbs are monomer and/or dimeric specific.
- to delimit the binding region.
- to determine GPVI-F(ab) fragment complex structure, by co-crystallising GPVI-F(ab) fragment complex.

4.2 Results

4.2.1 GPVI expression and purification

BLI and crystallography experiments require the production of large amounts of highly purified protein. Recombinant GPVI was produced by transient transfection (see methods) of Lenti-X 293T cells with GPVI Fc SigPlg vector and secreted to the growth medium. The Lenti-X 293T cell line was chosen as a highly transfectable derivative of human embryonic kidney 293 cells, which also supports high levels protein expression and contains the simian virus 40 (SV40) large T antigen, that binds to SV40 enhancers of expression vectors increasing protein production (Xu et al., 2018). Furthermore, as mammalian cells, they can produce mammalian post-transcriptional modifications, such as glycosylations and phosphorylation (Durocher and Butler, 2009).

Lenti-X 293T cells were transfected with polyethylenimine 'Max' (PEI 'Max') a stable cationic polymer which condenses DNA into positively charged particles leading to DNA released into the cytoplasm without compromising cell viability, obtaining high transfection efficiency (Longo et al., 2013). In parallel with the GPVI expression construct, a GFP expression construct was co-transfected to allow us to measure transfection efficiency rapidly by fluorescence microscopy (Figure 4.3).

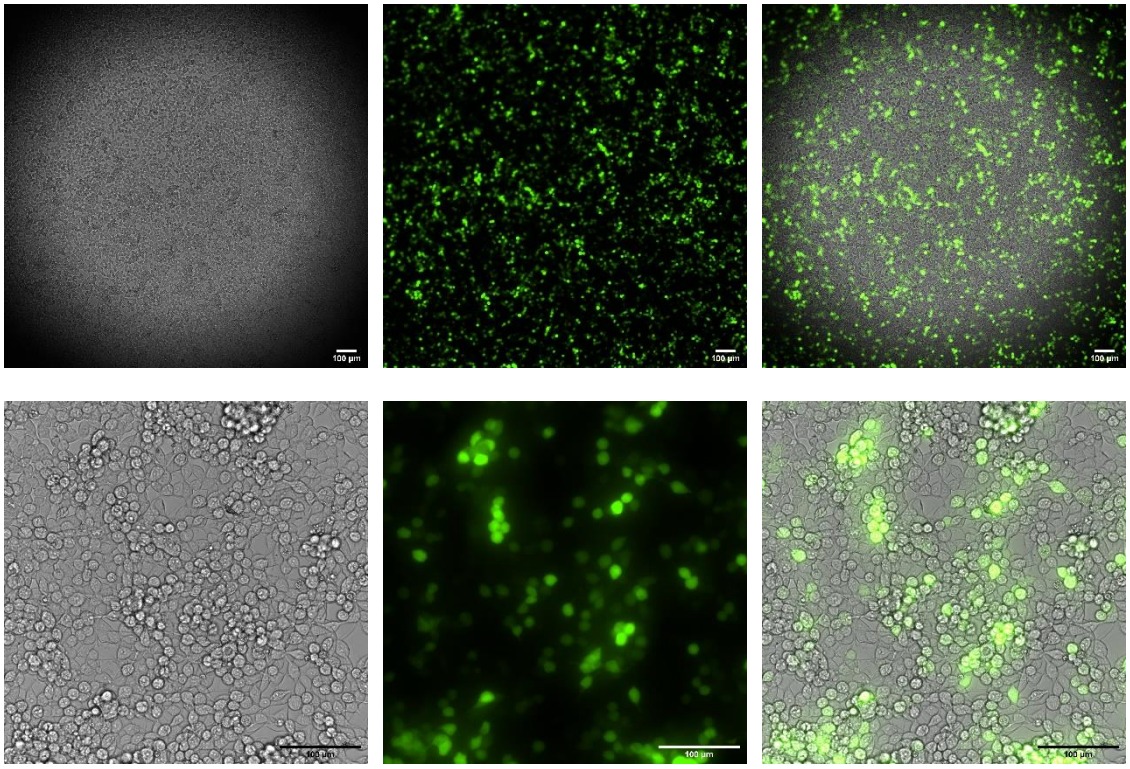

Figure 4.3. Transfection efficiency

Transfection efficiency was measure by transfecting in parallel with a GFP construct, bar: 100 µm.

Cell-culture medium containing GPVI-Fc was purified by protein-A affinity chromatography (Figure 4.4). To increase the yield the medium was passed through the column twice and unbound protein was removed by a washing step. Finally, bound protein was eluted with glycine (pH = 1.3), usually obtaining ~1mg of protein out of 100 mL of cell-culture medium. The eluted protein was then analysed by SDS-PAGE and Coomassie staining (Figure 4.5, A, D). The use of ultra-low IgG DMEM medium allows us to obtain a highly pure recombinant GPVI-Fc that, as a Fc-tagged proteins, is expressed as a homodimer (Shimamoto et al., 2012). This is visible as a single band, approximately 150 kDa (Figure 4.5, D lane 1). Dimeric GPVI-Fc for BLI experiments was further purified by gel filtration.

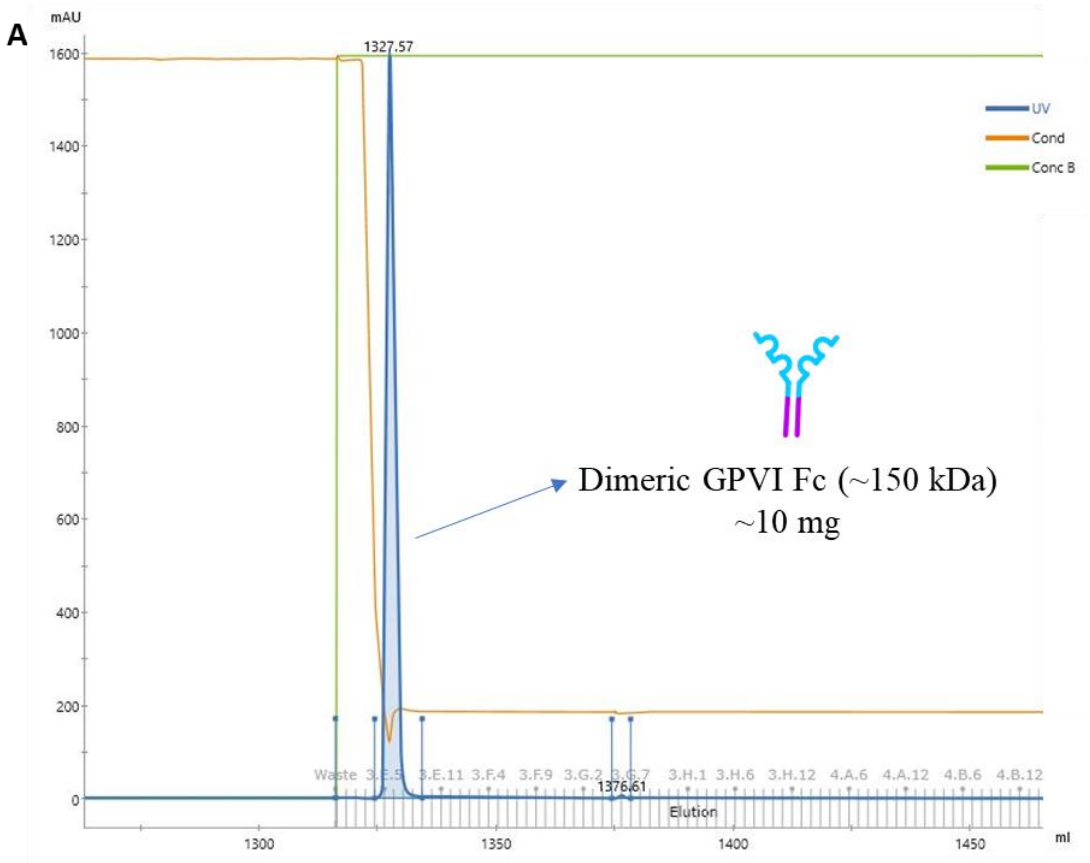

Figure 4.4. GPVI IMAC purification chromatogram.

Displaying absorbance at 280 nm (mAU, blue trace), conductivity (orange trace) and concentration of glycine (green trace), plotted against elution volume. ***A.*** *Dimeric GPVI Fc purification chromatogram with a 5 mL HiTrap™ Protein A column to remove non-specific proteins.*

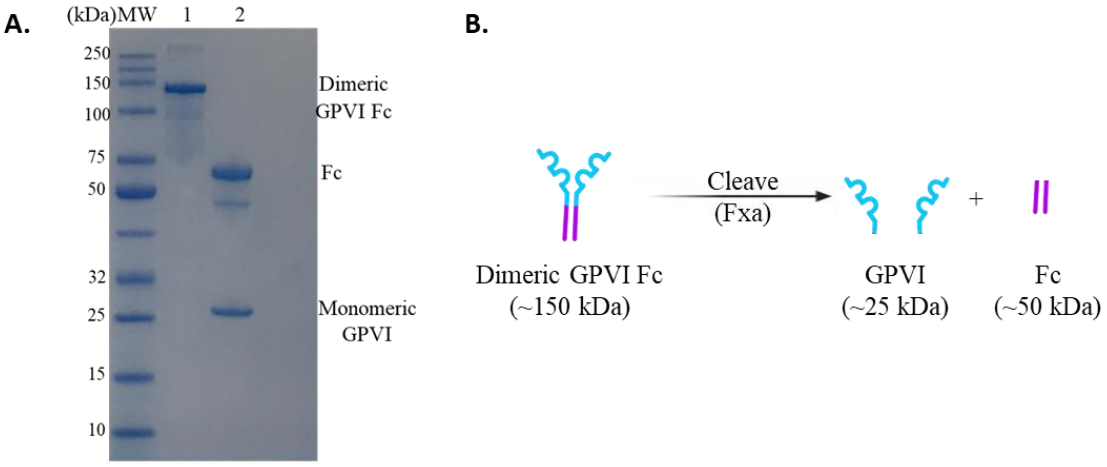

Figure 4.5. GPVI purification SDS-PAGE and FXa cleave scheme.

A. *SDS-PAGE of dimeric GPVI IMAC purification separated on a 4-12% Bis-Tris NuPAGE gel and stained with InstantBlue Coomassie. (MW) Molecular weight marker (kDa). (1) Dimeric*

GPVI elution from (~150 kDa), (2) Fc (~50 kDa), FXa (~43 kDa), GPVI (~25 kDa) after FXa cleave. B. Scheme showing Fc cleave by Factor Xa protease.

Monomeric GPVI was subsequently obtained by cleaving the Fc region with Factor Xa protease (FXa, Figure 4.5) and then purified by affinity chromatography with HiTrap Protein A HP column. The cleaved Fc region was attached to the column and the monomeric GPVI was in the flow-through during the sample application (Figure 4.6). Monomeric GPVI was further purified by SEC (Size Exclusion Chromatography) using Superdex 75 Increase 10/300 GL column, usually obtaining between 4 - 2 mg.

Monomeric GPVI used for crystallography was used straight away on SEC buffer. Final dimeric and monomeric GPVI to be used for BLI was dialyzed into PBS buffer (24 h, with two changes to refresh) frozen with liquid nitrogen and stored at -80°C. Samples were concentrated using a VIVA spin column 10,000 MWCO and concentrations were measured by nanodrop and adjusted with extinction coefficient.

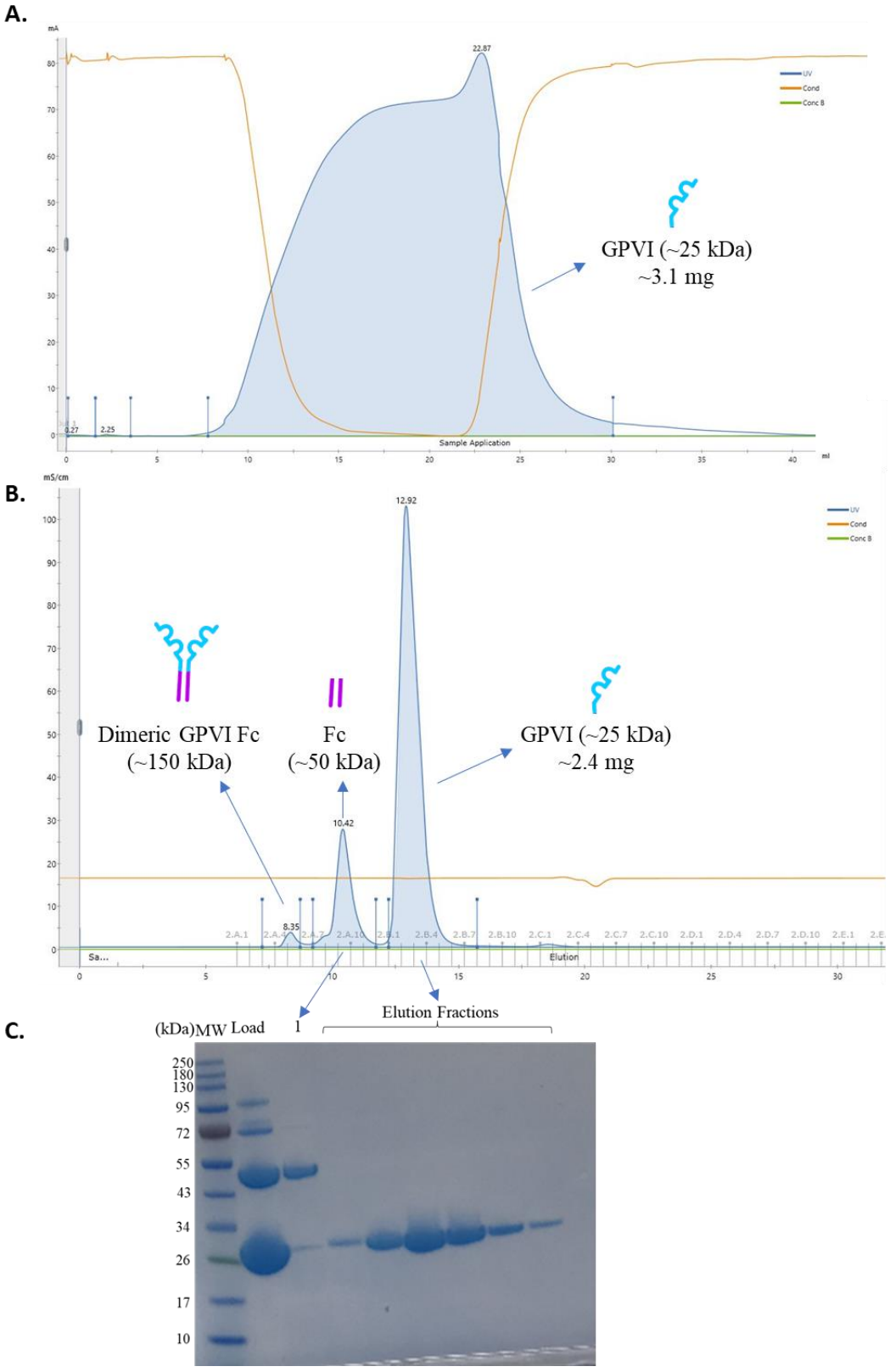

Figure 4.6. Monomeric GPVI purification chromatograms.

Displaying absorbance at 280 nm (mAU, blue trace), conductivity (mS/cm, orange trace) and concentration of glycine (green trace), plotted against elution volume. ***A.*** *Monomeric GPVI purification chromatogram with protein A column, after Fc cleave, GPVI is collected from the*

flow- through during sample application. ***B.*** *SEC purification chromatogram of monomeric GPVI for further purification to remove non-cleaved GPVI and/or Fc remaining portions.* ***C.*** *SDS-PAGE of SEC purification (**B**). separated on a 4-12% Bis-Tris NuPAGE gel (Invitrogen) and stained with InstantBlue Coomassie (Expedeon). (MW) Molecular weight marker (kDa), (Load) Load sample into SEC column, (1) sample from the 2nd elution peak on the SEC chromatogram (Fc portion), (fractions) fractions of the 3rd peak on the SEC chromatogram (**B.**).*

4.2.2 All mAbs bind both monomeric and dimeric GPVI with equal affinity

Whether mAbs bind monomeric or/and dimeric GPVI was measured using BLI (described previously in this chapter). This experiment was carried out on a ForteBio Octet® RED96 System using anti-mouse Fc biosensor probes. Anti-GPVI mAbs (10μg/mL) were immobilized on to the biosensor (via their Fc tail) and the recombinant monomeric or dimeric GPVI solutions were loaded onto a 96-well plate (7.5 nM and 5 nM, respectively).

Binding of the mAbs to recombinant monomeric or dimeric GPVI was measured. We found that there was as no differential binding to monomeric or dimeric form, all mAbs bind to both. Processed data was fitted to 1:1 Langmuir Model (Figure 4.7 A), but dimeric GPVI gave binding profiles typical of a 1:2 stoichiometry (Figure 4.7 B) with likely high avidity as evidenced by the very slow dissociation rates. K_D (nM) results of mAbs to monomeric GPVI are shown on Table 4.1 with their error. A9 and E7 seem to have higher affinity (lower K_D) to monomeric GPVI than the rest of the antibodies with 0.5 and 0.9 nM, respectively.

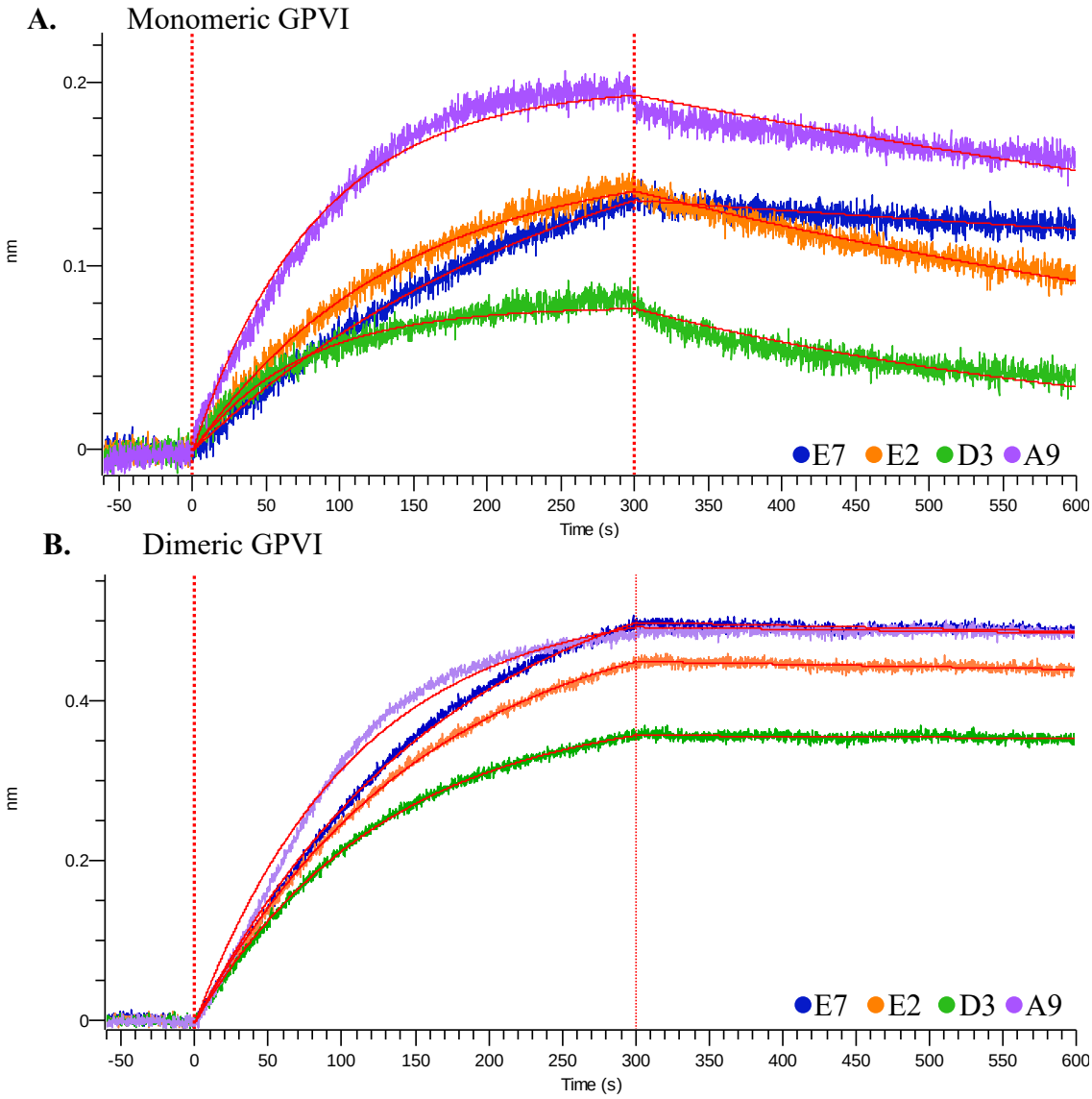

Figure 4.7. mAbs BLI traces.

*Binding of antibodies E7, E2, D3 and A9 to monomeric GPVI (**A**) and dimeric GPVI (**B**) was measured by ForteBio Octet. Data was reference subtracted, aligned to the start of association and interstep corrected to association. The processed data was fitted using the 1:1 Langmuir Model (**A**) or the 1:2 Model (**B**) with full, local settings.*

Loading (10 µg/ml)	Sample	Conc. (nM)	Response	K_D (nM)	K_D Error (nM)
E7	Mono GPVI	7.5	0.13	0.9	0.02
E2			0.14	1.86	0.02
D3			0.08	1.82	0.03
A9			0.2	0.53	0.01
E7	Dimer GPVI	5	0.49	0.73	0.53
E2			0.44	0.33	0.45
D3			0.35	0.54	0.14
A9			0.48	4.24	3.47

Table 4.1. Binding affinity results of mAbs to monomeric and dimeric GPVI.

Reported by the equilibrium dissociation constant (K_D in nM) with their error.

4.2.3 GPVI crystallography

In order to understand the relationship between structure and function, we undertook crystallographic studies with the aim to generate co-crystals of GPVI and the mAbs. We decided to use F(ab) fragments rather than full length antibody as these smaller ligands would be more likely to crystallise due to reduced dynamic variability. The E2 and E7 F(ab) fragments were chosen for these studies because, in addition to us showing here that they inhibit platelet function downstream of GPVI, parallel studies in the Neiswandt laboratory have shown that these F(ab) fragments are also inhibitory in flow adhesion models (Navarro et al., 2021) and in a humanised mouse model of thrombosis (unpublished data, personal oral communication). A third F(ab) fragment (E12), not tested in the previous chapter, but also of interest for other projects in the Nieswandt laboratory was also added to the crystal screen. The F(ab) fragments for this aspect of the project we all generated by technicians in the Nieswandt lab; as a support role for the spin-out company Emfret Analytics Würzburg, Germany, they have a routine method for

high yield production of F(ab) fragments which is required for these kind of crystallographic screens.

4.2.3.1 E12 new anti-GPVI inhibitory mAb

Prior to using the E12 antibody in the crystallographic screening, we confirmed that it was inhibiting GPVI similarly to the other mAbs by LTA. Human washed platelets ($4x10^8$/mL) were pre-treated for 10 minutes at 37°C with IV.3 (3 μg/mL) (FcγRIIA blocker) and, an additional, 5 minutes with E12 IgG (10 μg/mL) prior to stimulation with 3 or 10 μg/mL of GPVI agonist CRP or collagen. Platelet aggregation was significantly inhibited by E12 mAb (Figure 4.8). The final aggregation percentage was significantly reduced from 92% to 12% ± 4.2% ($p \leq 0.0001$) when platelets were pre-treated with 3 μg/mL IV.3 and stimulated with 3 μg/mL CRP (Figure 4.8). Similar results were also observed after increasing CRP concentration to 10 μg/mL (92% to 12% ± 6.2%, $p \leq 0.0001$, Figure 4.8). When platelets were stimulated with collagen the final percentage was also significantly inhibitory and dose dependent (25 % ± 4.6 %, when stimulated with 3 μg/mL of collagen and 37 % ± 4.8 % with 10 μg/mL of collagen, $p \leq 0.0001$). Thrombin stimulation was tested to confirm that the inhibition by E12 IgG was specific to GPVI-mediated activation. As expected, E12 did not have a significant effect on thrombin induced platelet aggregation. All these data confirmed that E12 inhibits GPVI activation. This appears to be comparable to the level of inhibition seen with E7 (Figure 3.4).

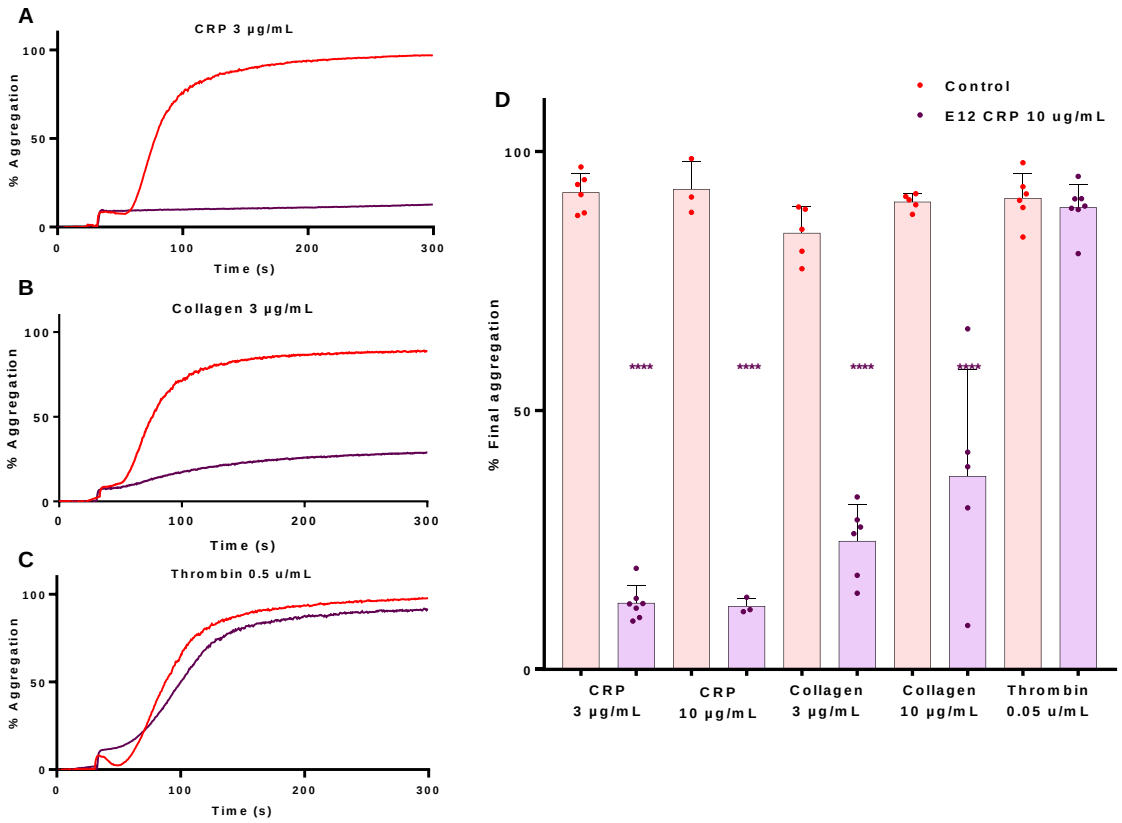

Figure 4.8. Representative aggregation traces of human washed platelets with E12.

*Human washed platelets (4×10^8/mL) preincubated for 10 minutes with 3 µg/mL of mAb IV.3 (FcγRIIA blocker) prior to incubation with E12 (10 µg/mL) for 5 minutes. Platelet aggregation was induced by the respective agonist (**A.** CRP 3 µg/mL, **B.** Collagen 3 µg/mL and **C.** Thrombin 0.5 u/mL) and it was monitored using LTA for an additional 5 minutes. **D.** Quantified aggregation values for human washed platelets in presence of E12 (10 µg/mL) with IV.3 (3 µg/mL). Statistical significance was calculated using one-way ANOVA for multiple comparisons with the Sidak post-test. Data are shown as mean ± SD and are representative of 3-7 experiments. ****$p \leq 0.0001$.*

4.2.3.2 GPVI-F(ab) fragment complex purification.

The chosen F(ab) fragments (E12, E7 and E2) were used to co-crystallise with the extracellular portion of GPVI (monomeric GPVI purified in part 4.2.1). The F(ab) fragments were the limiting factor, so GPVI was added in a 1.5-2-fold excess. After 5 minutes incubation this mix was loaded into a gel filtration column equilibrated with SEC buffer to separate the complex from the unbound GPVI. As shown in Figure 4.9 A, three distinct peaks were eluted from the column. Samples from these peaks were analysed using SDS-PAGE to identify which proteins were present. The first peak represents the void column volume and typically contains aggregated proteins which explains their apparent large molecular weight. A sample from this peak shows the presence of both GPVI and F(ab) in agreement with this (Figure 4.9 B). The second peak also contains both proteins which suggests that these are the native complex of GPVI and F(ab), and the third peak contains only GPVI. The fractions with the complex were spin concentrated to 5-12 mg/mL. Commercially available crystallisation screens tested are shown at Table 4.2.Table 4.2. Summary table of the crystal screens used in the attempts to crystallise the GPVI-F(ab) fragment complexes. This crystallisation screens allow to test several buffers, salts and precipitants changing concentrations and pH values to identify potential conditions for crystal growth.

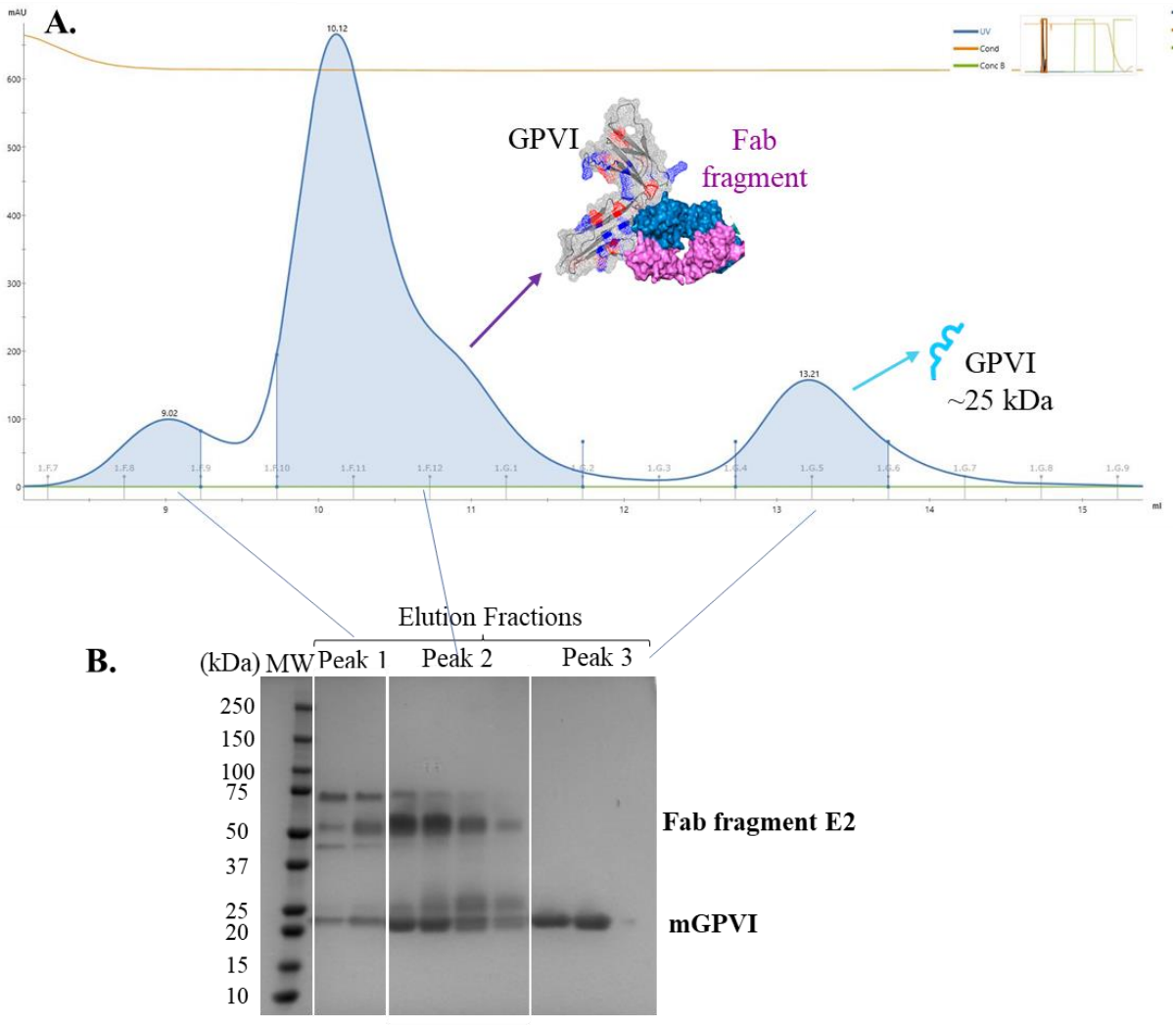

Figure 4.9. Representative GPVI-F(ab) fragment complex purification chromatogram.

Displaying absorbance at 280 nm (mAU, blue trace), conductivity (orange trace) and concentration of glycine (green trace), plotted against elution volume. ***A.*** *Representative SEC* purification chromatogram of *monomeric GPVI in complex with F(ab) fragment E2 to separate unbound portions.* ***B.*** *SDS-PAGE of SEC purification fractions (**A**). separated on a 10 % Bis-Tris PAGE gel and stained with Gel Code Blue Safe Stain (Thermo).*

Protein complex	Protein concentration	Screen	Well with crystals
GPVI-E12	5 mg/mL	Morpheus	None
		Proplex	
		Ligand friendly	
		Wizard classic	D11
		Wizard PEG ion	None
		SG1	
		PACT standard	
		LMB	
GPVI-E7	5 mg/mL	Morpheus	None
		Wizard PEG ion	
GPVI-E2	12 mg/mL	Morpheus	None
		Proplex	
		Wizard classic	
		Wizard PEG ion	
		Ligand friendly	
		LMB	

Table 4.2. Summary table of the crystal screens used in the attempts to crystallise the GPVI-F(ab) fragment complexes.

All crystals were grown at 20°C and took between 6-8 weeks to fully form.

Attempts to co-crystallise the GPVI with the F(ab) fragments largely were unsuccessful although a few crystals were obtained. The only conditions that did yield crystals were 2.5 M Sodium Chloride 100 mM Imidazole/ Hydrochloric Acid, pH 8.0, 200 Mm Zinc Acetate in D11 of the Wizard PEG ion screen (Figure 4.10). Crystals were collected and sent to the synchrotron. However, crystals gave no X-ray diffraction or poor diffraction. These results strongly suggested that the crystals were salts rather than protein in nature.

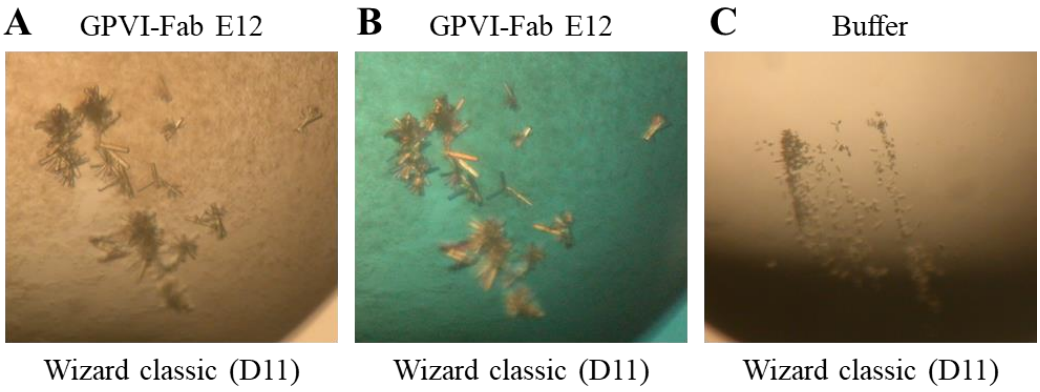

Figure 4.10. Crystals from the GPVI-F(ab) E12 Wizard PEG ion screen.

A. *Rod like crystals from D11 produce in presence of 2.5 M Sodium Chloride 100 mM Imidazole/ Hydrochloric Acid, pH 8.0, 200 Mm Zinc Acetate and* ***B.*** *same crystals under polarizing filter.* ***C.*** *D11 control well without protein complex.*

In an attempt to understand why we failed to obtain any crystals; the F(ab) fragments were analysed by SDS-PAGE to check their quality. F(ab) fragments usually run at 50 kDa under non-reducing conditions and they will resolve into two bands around 30-25 kDa under reducing conditions. The F(ab) E12 however, was not observed as a single band at 50 kDa which suggested that during shipping and storage, the conditions may have led to degradation of the F(ab) fragments (Figure 4.11).

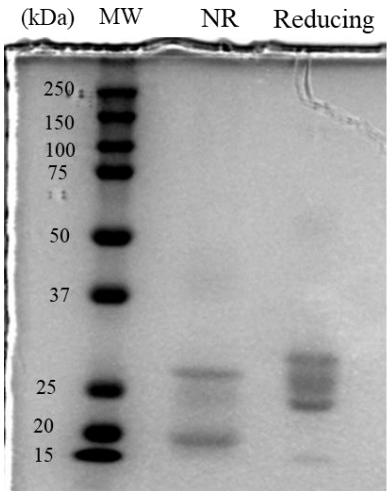

Figure 4.11. F(ab) E12 SDS-PAGE.

SDS-PAGE of F(ab) E12 separated on a 10 % Bis-Tris PAGE gel in non-reducing (lane 2) and reducing conditions (lane 3) and stained with Gel Code Blue Safe Stain.

4.2.4 Design and molecular cloning of GPVI chimeras

In order to map the mAbs binding site, expression vectors with the chimeric sequences of GPVI (Figure 8.3) and mouse GPVI were designed and generated using the human (GenBank accession number AB035073.1) and mouse GPVI sequences (GenBank NM_001163014.1) from GenBank. A full-length human GPVI pEF6a construct was kindly provided by Dr Mike Tomlinson (University of Birmingham, UK). GPVI chimeras and full-length mouse GPVI constructs were generated by designing and inserting their sequences into the pEF6a mammalian expression vector. Human-mouse chimera (termed as hm from here on) consist of full-length human GPVI in which the second IgG-like extracellular domain (D2) was replaced by the mouse one (Figure 8.5). the mouse-human chimera (mh) consists of full-length human GPVI in which the first IgG-like extracellular domain (D1) was replace by the mouse sequence (Figure 8.6). DNA and aa sequences can be found in Appendix.

Hm, mh and mouse sequences were inserted into the pEF6a mammalian expression vector by the Gibson Assembly (NEBuilder HiFi DNA Assembly commercial master mix, NEB). The Gibson Assembly consists of a single reaction method for assembling multiple overlapping DNA molecules by three DNA enzymes, a 5′ exonuclease, a DNA polymerase and a DNA ligase .(Gibson et al., 2009). Hm, mh and mouse sequences were prepared for the assembly by PCR with primers containing a 17/18 bp overlap complementary to the pEF6a vector (Table 2.8). The pEF6a vector was prepared for the reaction by restriction with KpnI and NotI. Cartoon representations of the constructs are shown in Figure 8.3. Successfully amplified PCR products were purified from both template DNA and reaction reagents, followed by their insertion into their appropriate,

linearized vectors. Correct insertion was then confirmed by sequencing with the T7 primer (chromatograms can be found at appendix, Figure 8.5, Figure 8.6 and Figure 8.7).

4.2.5 mAbs bind GPVI ligand binding domain D1

The chimeric GPVIs, human and mouse GPVI as controls were then used to identify the epitope of the mAbs. Together with a FcRɣ chain expression plasmid (required for GPVI expression at membrane surface) (Berlanga et al., 2002; Mori et al., 2008; Tomlinson et al., 2007), were transfected and expressed into Lenti-X 293T cells. Cells were incubated at 37°C, 5% CO_2 for 48 h prior to experiments with the mAbs.

E12, E7, E2, D3 and A9 mAbs where tested for their ability to bind to chimeric GPVIs by flow cytometry (Figure 4.12). Rat anti-mouse antibody (JAQ1, NB this also binds to human GPVI) and a commercial anti-human GPVI PE conjugated antibody was used as positive controls for human and mouse GPVI and for human GPVI, respectively (Figure 4.12 A and B). Mouse and rat IgGs, and secondary antibodies were also used as negative controls (Figure 8.8, appendix).

We found that the commercial anti-human GPVI PE conjugated antibody bound to both the human GPVI and the hm GPVI chimera, meaning that its binding site is within the D1 domain (Figure 4.12. A). JAQ1 antibody bound to mouse and hm better than to human and mh GPVI (Figure 4.12. B). Flow cytometry experiments revealed that all tested anti-GPVI mAbs bind hm and human GPVI, suggesting that the epitope on GPVI is located within the human D1 GPVI domain (Figure 4.12).

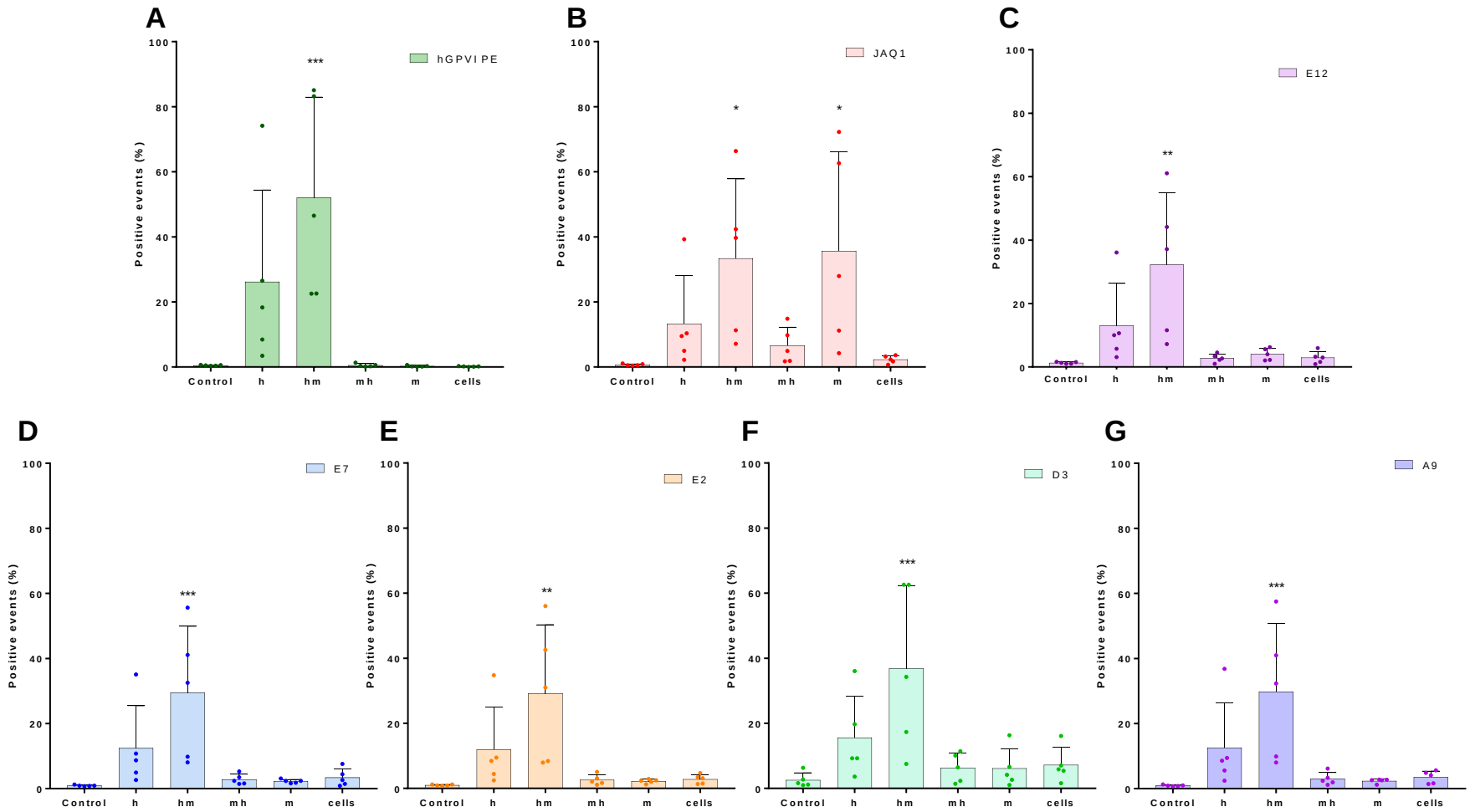

Figure 4.12. mAbs bind GPVI domain D1.

*Lenti-X 293T cells expressing human (h), human D1 mouse D2 (hm), mouse D1human D2 (mh) and mouse GPVI. Controls are cells transfected with empty vectors (Control) and cells are non-transfected (cells). Samples were incubated with the corresponding GPVI antibody and a secondary Alexa Fluor 488 (when necessary) before the flow cytometric analysis. The percentage of positive events was plotted against the cells expressing the different GPVI and analysed using a one-way ANOVA with Dunnett's multiple comparation test. Data are shown as mean ± SD and are representative of five independent experiments. *p ≤ .05 **p ≤ .01, ***p ≤ .001.*

JAQ1 was the only mAb which bound to mouse GPVI (as has been previously published (Nieswandt et al., 2000). However, the level of binding of JAQ1 to the mh GPVI chimera was low (only slightly higher than the non-specific values seen when testing the secondary abs alone (not shown)). This led to some uncertainty as to whether this particular chimera was being correctly expressed or not. All four GPVI constructs were tagged with both a Myc-tag and a poly-His-tag at their C-terminal end. To confirm that the mh GPVI chimera was being expressed we performed a small-scale flow cytometry experiment in the presence of saponin (a detergent-like molecule, which solubilizes mainly membrane cholesterol and allows antibodies to penetrate the cytoplasm) with anti-Myc antibody (Figure 4.13). These data showed that there was a significant level of expression of the mh GPVI chimera which suggests that the lack of signal with the mAbs is due to a genuine lack of binding and not a lack of expression. The commercial anti-human GPVI PE conjugated antibody was included as a negative control and again confirmed a lack of binding.

Furthermore, a portion of the cells were used to generate a lysate for analysis by SDS-PAGE and western blotting with a specific antibody against the Myc-tag. As show in Figure 4.13. GPVI expression on Lenti-X 293T cells., a GPVI band at ~75 kDa (Figure 4.13), can be seen for all four GPVI constructs.

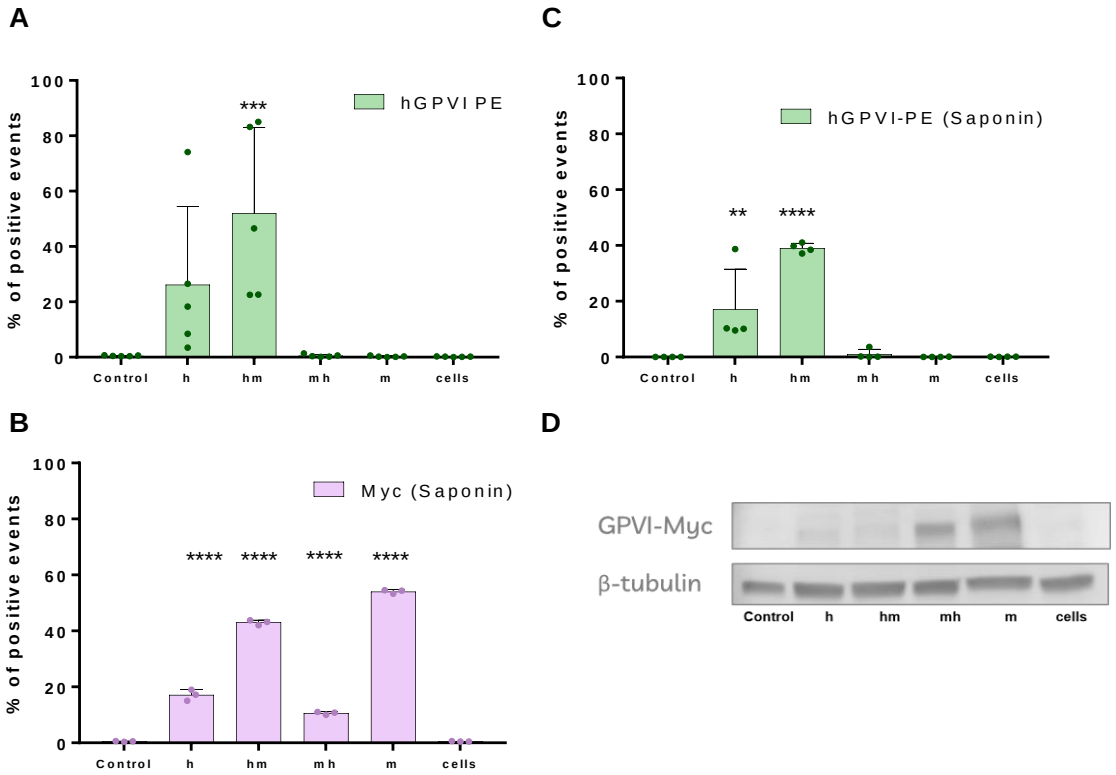

Figure 4.13. GPVI expression on Lenti-X 293T cells.

*Lenti-X 293T cells expressing human (h), human D1 mouse D2 (hm), mouse D1human D2 (mh) and mouse GPVI. Controls are cells transfected with empty vectors (Control) and cells are non-transfected (cells). Samples were incubated with (**B**) Myc antibody in presence of Saponin and a secondary Alexa Fluor 488 or (**A** and **C**) the commercial anti-human GPVI PE conjugated antibody before the flow cytometric analysis. The percentage of positive events was plotted against the cells expressing the different GPVI and analysed using a one-way ANOVA with Dunnett's multiple comparation test. Data are shown as mean ± SD and are representative of 3-5 independent experiments. **$p \leq 0.01$, ***$p \leq 0.001$, ****$p \leq 0.0001$. **D.** Western blot analysis of GPVI chimeras labelled with Alexa Fluor® 488 via the Myc-tag resolved using reducing conditions. Imaged with Typhoon FLA 9500, LD488 laser.*

4.3 Discussion

Using three different techniques, bio-layer interferometry, crystallography, and mutagenesis (epitope mapping) the structural characterization of the interaction of GPVI with our mAbs was attempted to be addressed. In order to accomplish this, first step was the production of recombinant GPVI. GPVI production was achieved in mammalian cells (Lenti-X 293T) due to their ability to produce mammalian post-transcriptional modifications, such as glycosylation and phosphorylation (Durocher and Butler, 2009) and to secrete the protein into the growth medium, which allows a simpler purification. Recombinant GPVI was obtained with good yields (~ 1 mg of dimeric GPVI per 100 mL).

Once monomeric and dimeric GPVI were produced we could proceed with the function-structure relationship experiments. Using Bio-layer interferometry (BLI) we studied mAbs binding to monomeric/dimeric GPVI. These affinity assays provided an initial comparison of the affinity of the mAbs to monomeric and dimeric GPVI, showing that they bind with similar affinities to both. Moreover, A9 and E7 presented higher affinity (lower K_D) to monomeric GPVI than the others mAbs which may explain why these two antibodies prevent aggregation on functional studies. However, these K_Ds are indicative only, and more optimizations would be needed to obtain a reliable K_Ds and obtaining more accurate results avoiding avidity with dimeric GPVI. Although these results are not absolute, they are relative, allowing us to conclude that the mechanism of inhibition is not through prevention of clustering, as mAbs do not have preference for either of the forms.

Recombinant monomeric GPVI was used in order to attempt to produce GPVI crystals in complex with three F(ab) fragments, E12, E7 and E2. GPVI has previously been crystallised before, alone in 0.9M ammonium sulphate, 8% MPD and 20% glycerol (Horii

et al., 2006), and in complex with a nanobody, in 0.2 M calcium acetate, 0.1 M sodium cacodylate, pH 6.5, and 18% PEG8K (Slater et al., 2021). The large differences between these two crystallization buffers did not allow any prediction for the crystallization buffer for our attempts to generate crystals from the GPVI-F(ab) fragment complex. Therefore, commercial screens were tested (Table 4.2) in an attempt to co-crystallised GPVI with our F(ab) fragments. The only crystals obtained (in complex with F(ab) E12) showed no signs of diffraction or poor diffraction corresponding with salt diffraction patterns, most likely due to the high salt concentrations in the buffers (2500 mM sodium chloride 100 mM imidazole/ hydrochloric acid, pH 8.0, 200 mM zinc acetate) and not due to the protein complex. This is a common problem on crystallography studies. Another cause that may have interfered with complex crystallization was sample purity. We were aiming to obtain single bands when the complex was run on an SDS-PAGE gel after SEC purification (Figure 4.9), but the gel shows multiple bands. These impurities most likely came from the F(ab) fragments, as monomeric GPVI was highly pure after SEC purification (Figure 4.6). The F(ab) fragment quality may have been sub-optimal due either an issue with their synthesis, or due to the time between production and use, or other issues with shipping and storage conditions, all of which may have led to some degradation below a threshold required for crystallography, as it is showed at Figure 4.11. Different approaches can be implemented in order to solve these setbacks, such as shipping monomeric GPVI instead of the F(ab) fragments that are more sensitive or producing the F(ab) fragments *in situ* where the complex is going to be set up.

Crystallography is the most commonly used method due to the level of accuracy. Nevertheless, as it is a long process with lots of optimisation that not always can be achieved. Parallel with crystallographic studies, we ran epitope mapping studies in order to obtain more information about the structural interaction of our mAbs with GPVI. To

this end, recombinant human and mouse GPVI chimeras were successfully generated and expressed on Lenti-X 293T cells. These chimeras have helped to identify that the mAbs bind to the D1 domain of GPVI. The D1 domain of GPVI is the ligand binding domain and the binding of the mAbs to this domain is highly suggestive that the inhibitory mechanism is through direct blockage of ligand binding (Lecut et al., 2004a; Smethurst et al., 2004). This findings are in line with other GPVI inhibitory mAbs, and more recently, nanobodies, previously published in the literature, that also bind to GPVI D1, such as, mAb 9O12 (Lecut et al., 2004a), mAb 10B12 (Smethurst et al., 2004) or the nanobody Nb2 (Slater et al., 2021). GPVI accommodates two distinct binding sites with different affinities for collagen and CRP, where the collagen-binding site is likely to contain a CRP-binding site where they compete with each other for the binding (Morton et al., 1995; Schulte et al., 2001). The rat mAb JAQ1 was the first mAb found to be specific to the CRP-binding site on mouse GPVI given that its inhibitory effect was overcome with high concentrations of collagen (Schulte et al., 2001). Our studies with GPVI chimeras and JAQ1 revealed that the mouse D2 domain GPVI might be implicated in JAQ1 binding to GPVI providing some stability, due to the fact that JAQ1 bound to human-mouse (hm) and mouse GPVI but not mouse-human (mh) GVPI chimera (Figure 4.12). This may be related with the replacement of lysine (K, single-letter amino acid code, positive charge, in human) for glutamine (E, negative charge, in mouse) at position 59 in domain 1, the change of arginine 117 (R, positive charge, in human) for proline (no charge, in mouse) in domain 2 and the change of arginine 166 (R, positive charge, in human) for serine (S, negatively charge, in mouse) in domain 2, Figure 4.14, that have been previously reported to support CRP binding (Smethurst et al., 2004). The K59E mutation is the only one reported to disrupt CRP binding and that change on mouse GPVI has been suggested to be the reason why mouse GPVI has lower affinity than human

GPVI for CRP (Smethurst et al., 2004). Regarding our mAbs (E12, E7, E2, D3 and A9), all of them are binding GPVI D1 and no contribution of D2 is observed of the key mutations. All mAbs are able to bind to the D1 GPVI domain close to the collagen-CRP binding site or on their surroundings, likely making steric hindrances. An alternate possibility is that their binding causes conformational changes within GPVI that drastically decreases the accessibility of the CRP-binding site. One example of this would be the Nb2, which binds to GPVI D1 near the CRP binding site (Figure 4.14) and induces a small conformational change in D1 (Slater et al., 2021). Further studies making new chimeras by alanine substitution approach with a focus on the surroundings of K59, could shed light on the epitope binding of our mAbs.

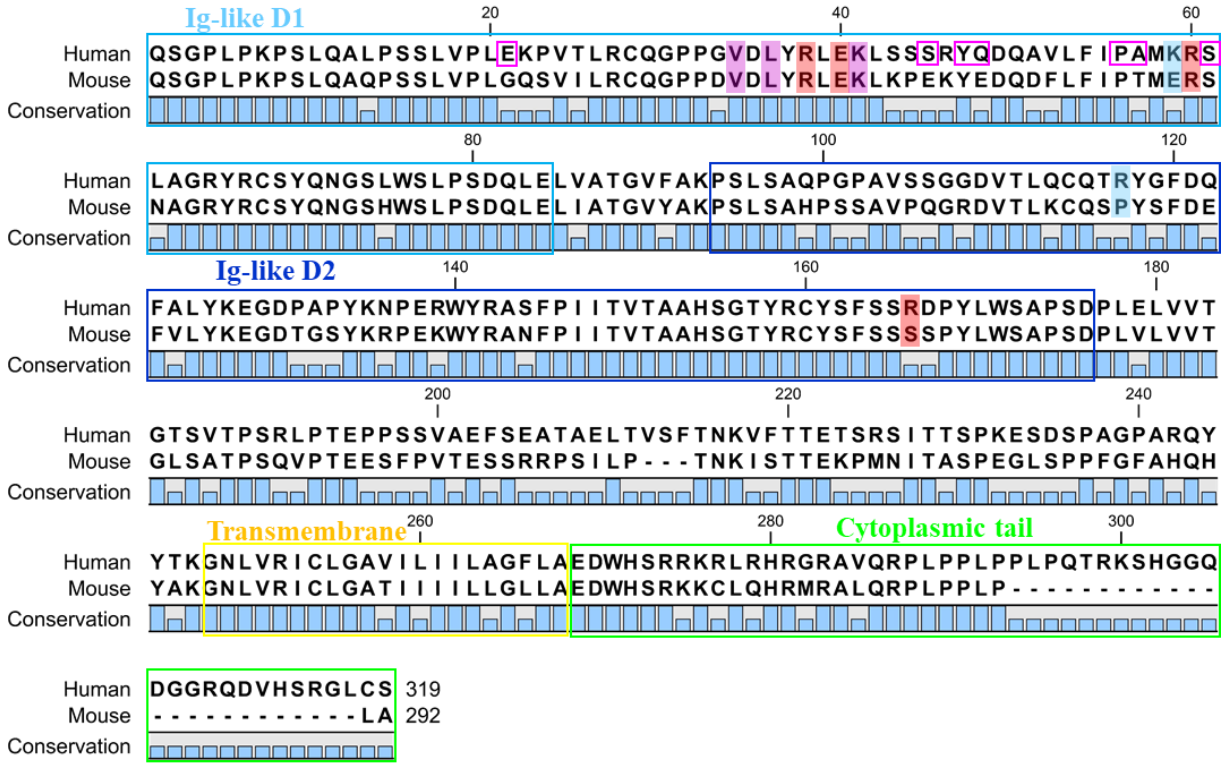

Figure 4.14. Sequence alignment of human and mouse GPVI.

Collagen-CRP binding more relevant residues found on literature are highlight (red, residues implicated on collagen binding; blue, residues implicated on CRP binding and purple, residues that contribute to both)(Lecut et al., 2004a; O'Connor et al., 2006; Smethurst et al., 2004).

Protein sequences were aligned using CLC Viewer. Magenta squares show residues interacting with the inhibitory nanobody, Nb2 (Slater et al., 2021).

4.4 Conclusions

This chapter attempts to characterize the structural interactions of GPVI with our anti-GPVI mAbs (E12, E7, E2, D3 and A9) using three complementary approaches bio-layer interferometry, crystallography, and epitope mapping. BLI showed that none of the mAbs are mono or dimer specific, crystallographic studies were not successful and will need more optimisations and GPVI chimeras helped to delimit the mAbs-GPVI binding region to the GPVI D1, the ligand binding domain. Additional studies will be needed to accomplish the full structural characterization of these mAbs with GPVI in order to achieve robust characterization which protein-based therapeutics need to demonstrate during development.

.

Chapter 5

Generation of anti-G6b-B Affimers

5 CHAPTER 5. GENERATION OF ANTI-G6B-B AFFIMERS

5.1 Introduction

In the previous chapter, we have tested and characterized some mAbs developed in preparation for this project at the University of Wurzburg. However, a further aim of this project was to generate new biologics targeting platelet glycoprotein receptors within the GPVI pathway. To this end, a second focus for our efforts was on the platelet glycoprotein G6b-B. G6b-B constitutively inhibits platelet activation by the (hem)ITAM-bearing receptors GPVI and CLEC-2 (Mori et al., 2008). G6b-B is constitutively phosphorylated under resting conditions (Senis et al., 2007) which suggests that it may play an important role preventing activation of circulating platelets. G6b-B is highly expressed on the cell surface, and it is restricted to platelets and megakaryocytes (Lewandrowski et al., 2009). Potentially, this provides high specificity and low risk of off-target effects in other cell types. However, very few studies have explored the impact of G6b-B stimulation. G6b-B cross-linking with polyclonal antibodies was shown to exert inhibition of both platelet activation and aggregation in vitro (Newland et al., 2007). Its potential as a target for antiplatelet therapy has been further discusses in our review (Soriano Jerez et al., 2021). All these together make G6b-B a novel candidate that may provide a selective approach to downregulate ITAM dependent platelet activation (GPVI) and study whether G6b-B stimulation could lead to less reactive platelets, reducing the risk, or severity of thrombosis.

In the general introduction we have discussed different biologics than can be used for therapies (Biologics). As a part of this project, in this chapter we developed new biologics (Affimers binding G6b-B) that will be helpful to determine if it is a good target for

downregulate GPVI. We decided to develop Affimers due to their advantages on time development, among others, further discussed in next section (5.1.1Affimers).

5.1.1 Affimers

Affimers are small binding proteins (12-14 kDa) based on human Stefin A or a consensus sequence of Cystatin A in plants (Adhiron) that bind to target proteins with high affinity (nM range). Affimers were first reported in 2005 by Woodman et al. when they developed the initial states of a scaffold based on human SteA to contain peptide aptamers (Woodman et al., 2005). Human Stefin A, also called cystatin A, is a small single-chain protein (98 amino acids), which inhibits members of the cathepsin family of proteases, and it meets the desired features of a scaffold protein (Woodman et al., 2005): known structure, highly stable, flexible that its folding is not affected by the insertion of peptides, biologically neutral, by removing the natural cysteine protease inhibitor function (Stadler et al., 2011), and able to fold identically in any expression systems (both prokaryotic and eukaryotic).

In 2014 a new protein scaffold, related in structure, was engineered by Tiede et al. This new protein scaffold is a synthetic protein based on a consensus sequence of plant phytocystatins, a small protein inhibitors of cysteine proteases (100 aa), called Adhiron (Tiede et al., 2014). The Adhirons also meet all the desired features of a good scaffold for peptide presentation: small, monomeric, high solubility and high stability and the lack of disulfide bonds and glycosylation sites. In spite of the fact that they have low sequence homology their structure is very similar (Figure 5.1) and binding proteins derived from these two scaffolds are referred to collectively as Affimer proteins, and we will refer to them consequently.

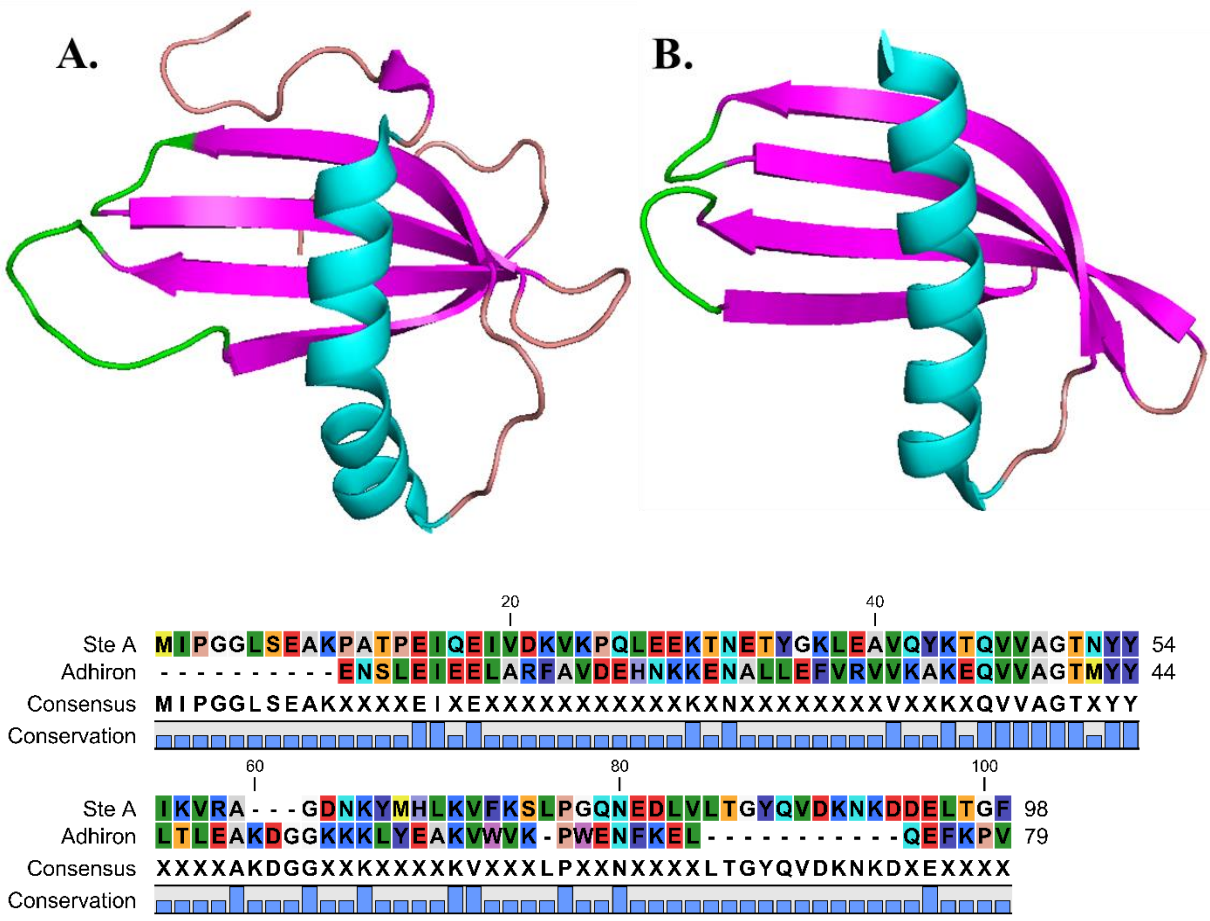

Figure 5.1. Cartoon diagram and sequence alignment of the two different Affimer scaffolds. *In green are shown the variable loops.* ***A****. stefin A scaffold (PDB ID: 1NB5).* ***B.*** *Adhiron scaffold (PDB ID: 4N6T). At the bottom, sequence alignment of both scaffolds. Images were generated using PyMol and protein sequences were aligned using CLC Viewer.*

The structure of the Affimers consist of a αβ roll structure comprising a four anti-parallel β -sheet which are wrapped around a central α-helix (the characteristic cystatin family fold) (Figure 5.1). The inner two β-strands, β2 and β3, are coiled smoothly, but the outer two β-strands, β1 and β4, are twisted with three β-bulges. Together, these bulges produce a tight coiling of the β-sheet, allowing it to wrap around the helix (Irene et al., 2012; Martin et al., 1995). Engineered peptide aptamers or randomized amino acid sequences are displayed at two variable peptide regions: loops between two β-strands, β1 and β2 (loop 1); and β3 and β4 (loop 2), replacing the inhibitory sequences of the Cystatin proteins (Tiede et al., 2014). The Affimer structure is compact with limited unstructured

loops which is consistent with the very high melting temperature (Tm = 101°C) of the consensus protein (Tiede et al., 2014).

Affimer proteins are screened for binding to target molecules using phage display. Phage display technology was developed more than 30 years ago (Smith, 1985) and has become one of the most extensively used methods *in vitro*. This method detects protein interactions using bacteriophages to identify binders. In the phage display technique, the gene of the protein of interest (in this case the Affimer sequences) is inserted into a phage coat protein gene, leading to the phage to display the protein on the outside. The phages containing the gene for the protein (Affimer) that bind to the screened protein are sequenced, and the coding regions are subcloned into expression vectors. This method allows selection of highly specific Affimer clones that are able to discriminate between protein isoforms (Tang et al., 2017). Affimers which bind to a target protein are identified by a series of phage-display library screenings (Figure 5.2). At University of Leeds, the BioScreening Technology Group has generated two highly complex phage display libraries each containing more than 10 billion Affimer proteins. The binding Affimers are further confirmed to specifically find the target protein by phage ELISA. Then, the DNA coding sequences for the Affimers are amplified by PCR and subcloned into a prokaryotic expression vector fused with C-terminal tags and purified by IMAC (Tiede et al., 2014). The *in vitro* screening of Affimer proteins including phage ELISA and sequencing of positive clones usually takes 3-4 weeks. The full development time is approximately 3 months, which is comparatively low compared to the typical production times for antibodies or nanobodies.

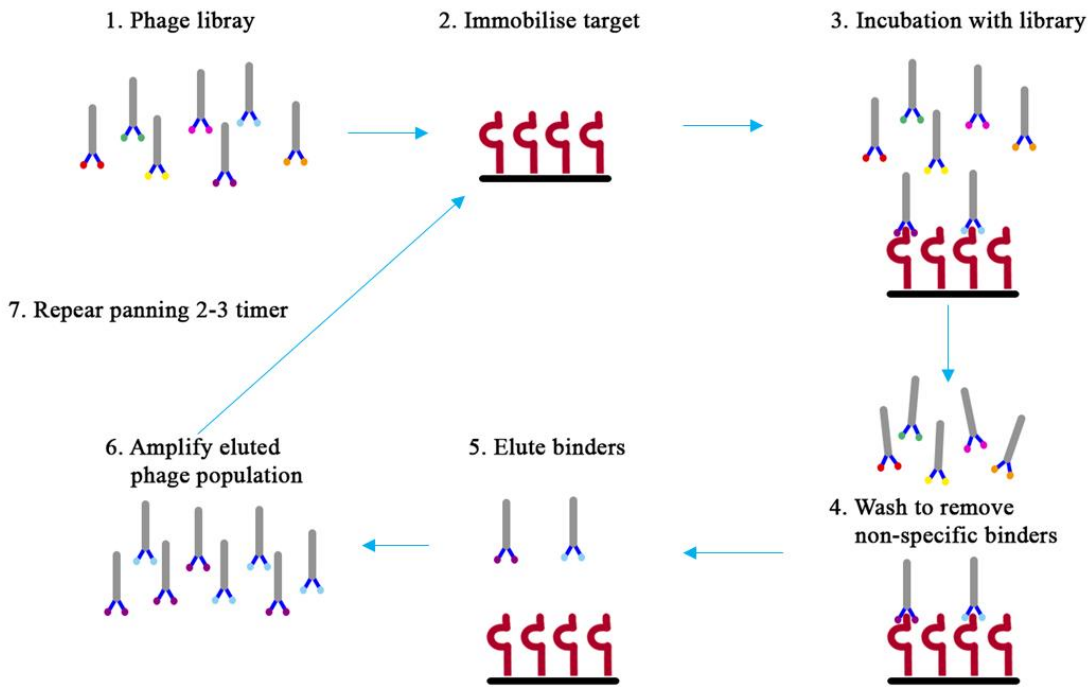

Figure 5.2. Phage display Affimer selection process scheme.

Affimers meet a number of advantages compared with other high affinity proteins that are listed below:

1. Versatile. Affimers can be developed from two different scaffolds from different species which means that each of them can be more beneficial depending on the final application. For example, Affimers derived from human Stefin A would be more suitable for therapeutics, as they are less likely to induce immune responses than the plant one.

2. Easy to engineer. Affimers are small, monomeric, lack disulphide bonds and can be easy manipulated to generate fusion proteins, bi- or polymeric Affimer reagents. They can also be easily labelled with biotin, enzymes or fluorophores for multiple applications and assay formats by introducing specific cysteine residues at the C-terminus. Maleimide groups have high reactivity with reduced sulfhydryls which

allows the formation of a thioether bond and therefore easy crosslinking, labelling and protein modification for different applications (Johnson et al., 2008).

3. *In vitro* screening. Synthetic libraries replace animal immunisation and allows for the screening of toxic and non-immunogenic molecules.

4. Quick development times. Screening, including phage ELISA and sequencing of positive clones normally takes between 3-4 weeks.

5. Easy production in prokaryotic expression systems. Affimers can be produced in *E. coli*, the most cost- and time-saving expression system, obtaining a high yield.

6. Specific. The level of Affimer specificity and the technique used for Affimer isolation is ideal for isolating reagents with high specificity.

7. Stable. Affimers are stable within a wide range of temperatures (melting temperature up to 101°C) and pH.

8. Small size. Affimers have an average weight of 12 kDa which allows them to easily penetrate tissues and access epitopes in densely packed subcellular structures of cells more readily than antibodies (Tiede et al., 2017). They also position fluorophore labels closer to their target increasing spatial resolution in super-resolution microscopy.

9. Non-immunogenic. Affimer scaffolds have been shown to have low immunogenicity using a peripheral blood mononuclear cell test (Avacta, 2017), which means that they are not like likely to provoke an undesirable immune response.

Affimer characteristics make them suitable for a wide range of applications, such as diagnostic tools, pull-downs, affinity fluorescence and *in vivo* and cell imaging, formation of magnetic nanoparticles, biosensor, modulators of protein functions, western blotting, detection of small molecules, crystallization chaperones, and affinity purifications (Tiede et al., 2017).

5.1.2 Hypothesis

G6b-B activating Affimers will downregulate ITAM signalling downstream of GPVI and CLEC-2. This downregulation may potentially modulate platelet function and lead to reduced bleeding risk compared to current antiplatelet drugs.

5.1.3 Aims

To this end, the aims of this part of the project are:

- to express and purify G6b-B to be used for *in vitro* screening of Affimer proteins by our collaborators at University of Leeds to obtain positive binders.
- to clone into a bacterial expression vector, overexpress, and purify the top candidate Affimers.
- to test selected Affimers on platelet function assays to identify their possible applications.

5.2 Results

5.2.1 Recombinant G6b-B expression and purification

G6b-B Fc-fusion was express and purified in the same way as GPVI Fc-fusion (Methods 2.2.5.5.). In short, recombinant G6b-B was produced in mammalian Lenti-X 293T cells following transient transfection. Transfection efficiency was assessed by co-transfection of a GFP expression construct (Figure 4.3). Secreted protein was filtered, purified by affinity chromatography (Figure 5.3), SEC chromatography, and analysed by SDS-PAGE gels (10%) to identify fractions containing the recombinant protein with an expected apparent molecular weight of ~50 kDa (reducing conditions). Coomassie staining showed the distinctive G6b-B doublet which is a result of the N-glycosylation (de Vet et al., 2001; Mazharian et al., 2012) (Figure 5.4). Samples were dialyzed into PBS and concentrated. The final concentration was measured using a nanodrop and adjusted applying the Beer-Lambert law, obtaining 6.45 mg and 12 mg in two different batches. Once the G6b-B Fc-fusion protein was ready, screening for G6b-B binding Affimers was carried out at the University of Leeds by the BioScreening Technology Group.

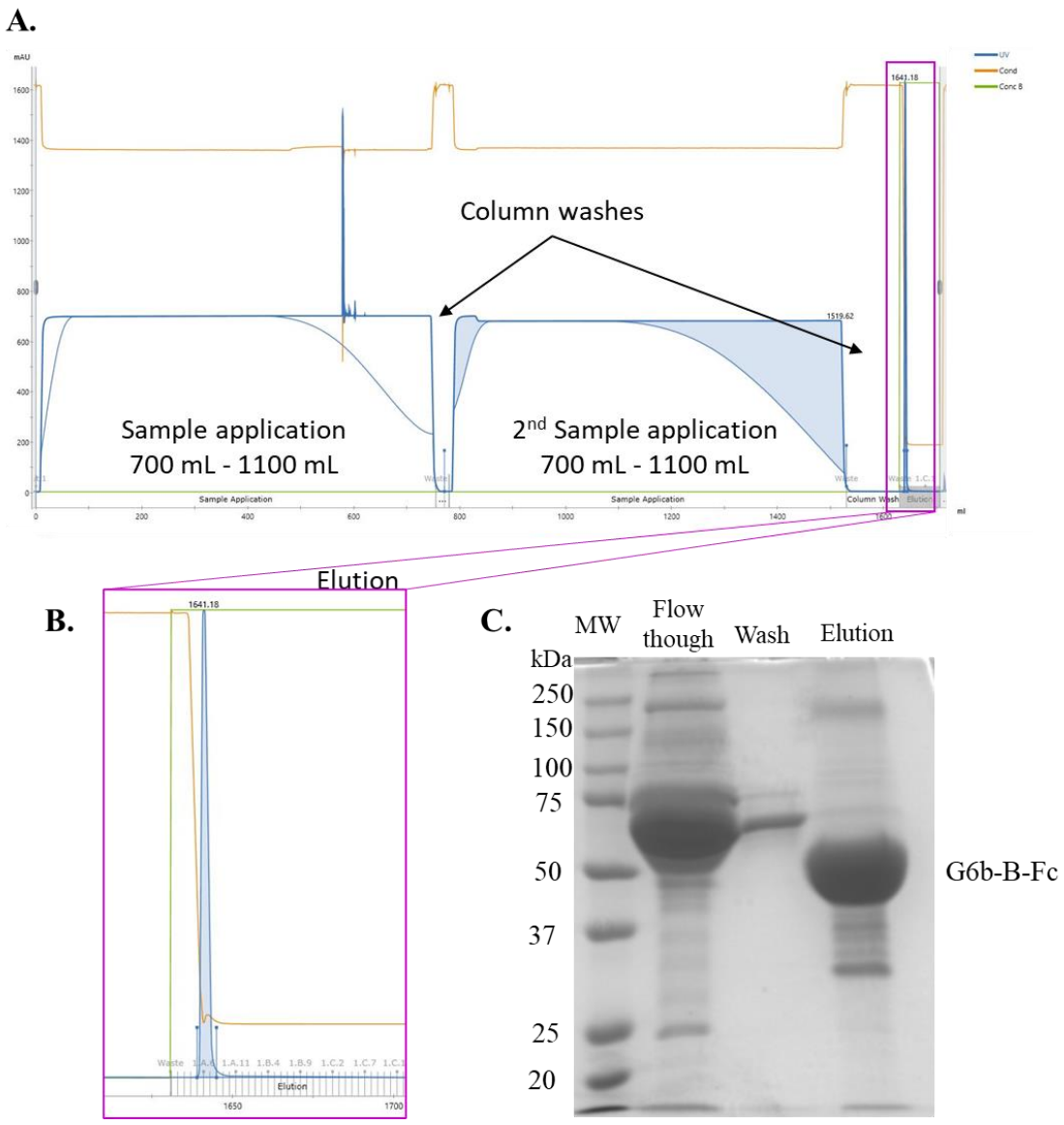

Figure 5.3. G6b-B purification affinity chromatogram.

Displaying absorbance at 280 nm (mAU, blue trace), conductivity (orange trace) and concentration of glycine (green trace), plotted against elution volume. ***A.*** *Dimeric G6b-B Fc purification chromatogram with a 5 mL HiTrap™ Protein A column with all the followed steps, including two sample applications with a column wash after each of them and protein elution.* ***B.*** *Amplification of the protein elution section showing a single peak.* ***C.*** *Coomassie staining of 10% polyacrylamide gel.*

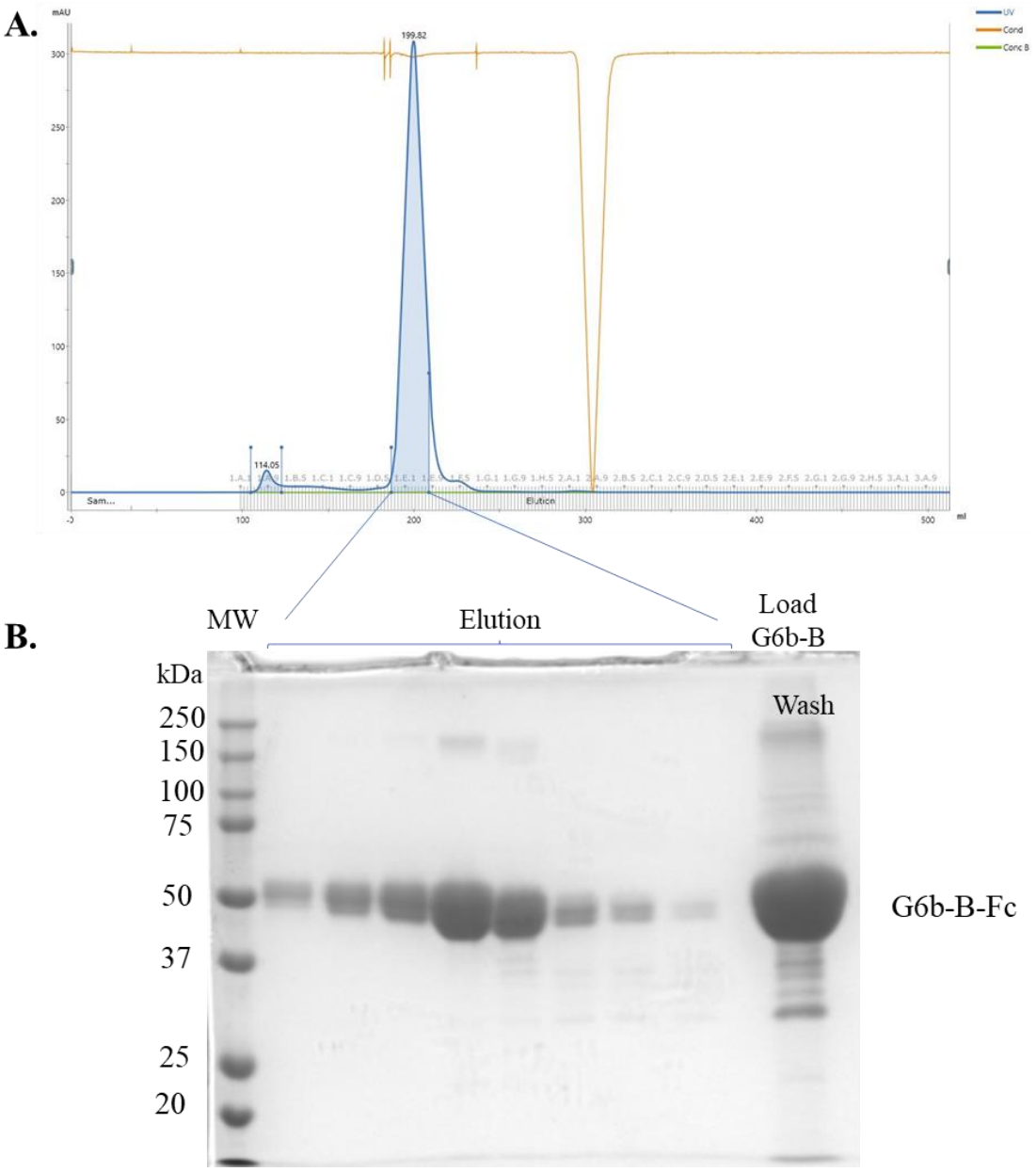

Figure 5.4. G6b-B SEC purification.

Displaying absorbance at 280 nm (mAU, blue trace), conductivity (orange trace) and concentration of glycine (green trace), plotted against elution volume. ***A.*** *Dimeric G*6b-B *Fc purification chromatogram with* ***B.*** *Coomassise staining of 10% polyacrylamide gel in reducing conditions showing (MW) Molecular weight marker (kDa), all the elution fractions and the load protein from affinity purification.*

5.2.2 Affimer sequence cloning into a *E. Coli* expression vector

Affimer screening for G6b-B was carried out at the University of Leeds by the BioScreening Technology Group. Human IgG1 Fc recombinant protein (Invitrogen) was used during the screening to discard non-specific binders due to the Fc portion. From forty-eight binding clones, forty were found to bind specifically to G6b-B (Figure 5.5). These binding clones were sequenced and only three unique binders were found: Affimers 2, 24 and 34. The other thirty-five resulted to be the same one (Affimer 2). The sequences of these three G6b-B binding Affimers were supplied in phage expression vectors. Sequence alignment of the Affimers showed that Affimers 2 and 24 have a similar variable region (Figure 5.5), which suggests that they may bind to the same epitope. Affimer 34 lacks the second variable region, which may mean that it has less contact sites with G6b-B.

The three G6b-B binding Affimers were sub-cloned into the pET11a-derived bacterial expression vector using a commercial version of the Gibson Assembly method (NEBuilder HiFi DNA Assembly commercial master mix, NEB). Affimer sequences were prepared for the assembly by PCR (Figure 5.6. B.) with primers containing a 17/18 bp overlap complementary to the pET11a-derived vector and amplification using one of two reverse primers that would generate proteins with or without a C-terminal cysteine for downstream functionalization (Table 2.8). The pET11a-derived vector was prepared for the reaction by restriction with NheI and NotI (Figure 5.6. A.). Cartoon representations of the constructs are shown in Figure 8.4. Successfully amplified PCR products were purified from both template DNA and reaction reagents, followed by their insertion into the linearized vector. Correct insertion was then confirmed by sequencing with the T7 primer.

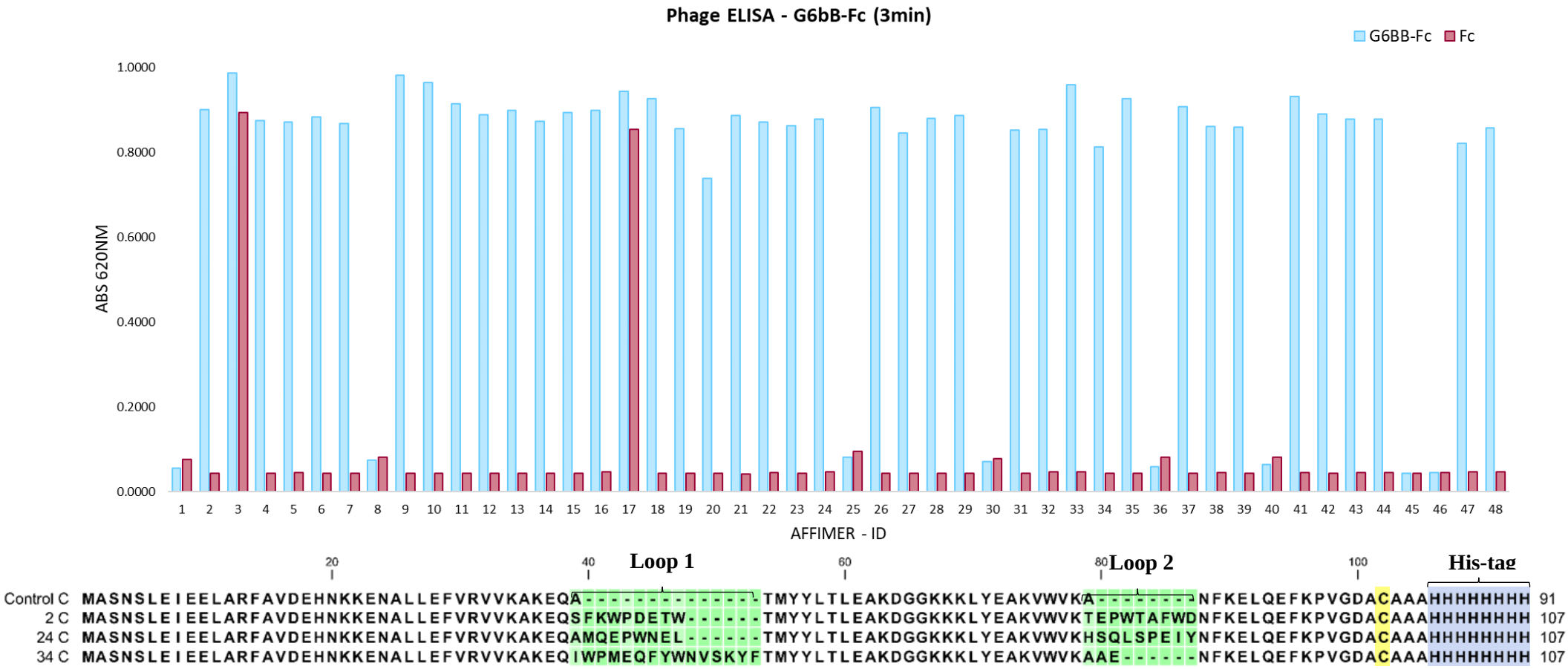

Figure 5.5*. Isolation and characterisation of G6b-B binding Affimers.*

Phage ELISA for 48 monoclonal Affimers isolated against G6b-B-Fc. Non-specific binders to the Fc portion were tested through binding to Human IgG1 Fc recombinant protein (Fc). At the bottom, sequence alignment of binding Affimers. Protein sequences were aligned using CLC Viewer, in green are shown the variable loops, in yellow the cysteine for functionalization and in blue the His-tag for purification.

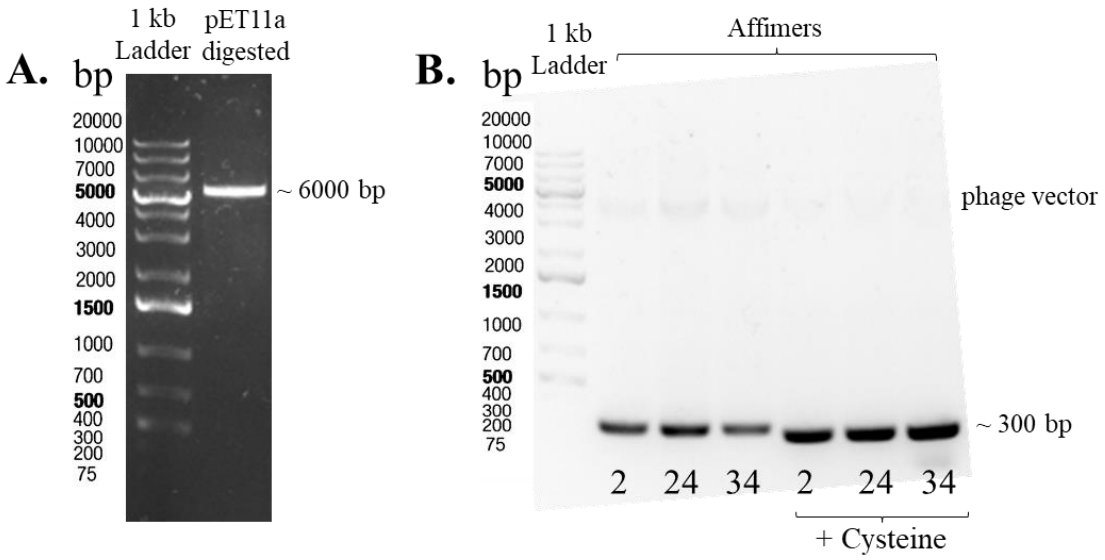

Figure 5.6. Affimers agarose gels.

A. *pET11a-derived vector was linearized by restriction with NheI and NotI and separated on a 1 % agarose gel alongside a 1kb plus DNA ladder.* ***B.*** *Affimers PCR amplification products without or with a C-terminal cysteine with the predicted size of ~ 300 bp.*

5.2.3 Affimers production and purification

Affimers were cloned into a pET11a-derived vector in frame with a N-terminal 8x His tag for Ni^{2+}-NTA affinity purification. Affimers were expressed using the T7 Express Competent *E. coli* strain (NEB) an enhanced BL21 derivative suitable for high efficiency transformation and protein expression. This strain contains the T7 RNA Polymerase in the lac operon which allows the bacteria to produce protein using the plasmid under the control of an IPTG inducible T7 promotor. Affimer constructs were transformed by heat shock method as described (Methods 2.1.10.1). Single colonies were used as started cultures in LB medium supplemented with Ampicillin which were used for inoculating large scale expression cultures and stored as glycerol stocks. Expression was induced with 0.1 mM IPTG at 0.6-0.8 OD_{600}. Cells were harvested after overnight incubation at 25°C, 150 rpm, post-induction. Cells were lysed and incubated at 50°C for 20 minutes to heat denature non-specific proteins, as previously described (Methods 2.1.12.3). Affimers

express in the soluble fraction (Tiede et al., 2014), after centrifugation the supernatant was filtered and purified using GE healthcare Ni-NTA affinity column as previously described (Methods 2.1.12.3). Affimers were eluted by increasing the imidazole concentration in the buffer, the chromatograms contained one elution peak at ~1200 milli-absorbance units (mAU), this peak has a long tail that is due to the presence of high concentrations of imidazole. Affimers elution samples were analysed by SDS-PAGE corresponding with the thick 12-14 kDa band (Figure 5.7. B). Affimers with the unpaired cysteine residues showed dimers and oligomers, compared with the single band obtained in the Affimers without the unpaired cysteine (Figure 5.7. B). However, the proportion is really low compared with the monomers. Affimers were further purified by SEC chromatography. Affimers came as a single peak (Figure 5.8.) corresponding with the thick ~13 kDa band (Figure 5.7.). However, Affimers with the unpaired cysteine residues, presented 3 elution peaks corresponding with trimers (~36 kDa), dimers with (~28 kDa) and the monomer (~12kDa) showed on Figure 5.9. Affimer oligomerization was expected due to the unpaired cysteine residues. This might suggest that DTT concertation within the sample buffer was not enough to fully reduce the Affimers.

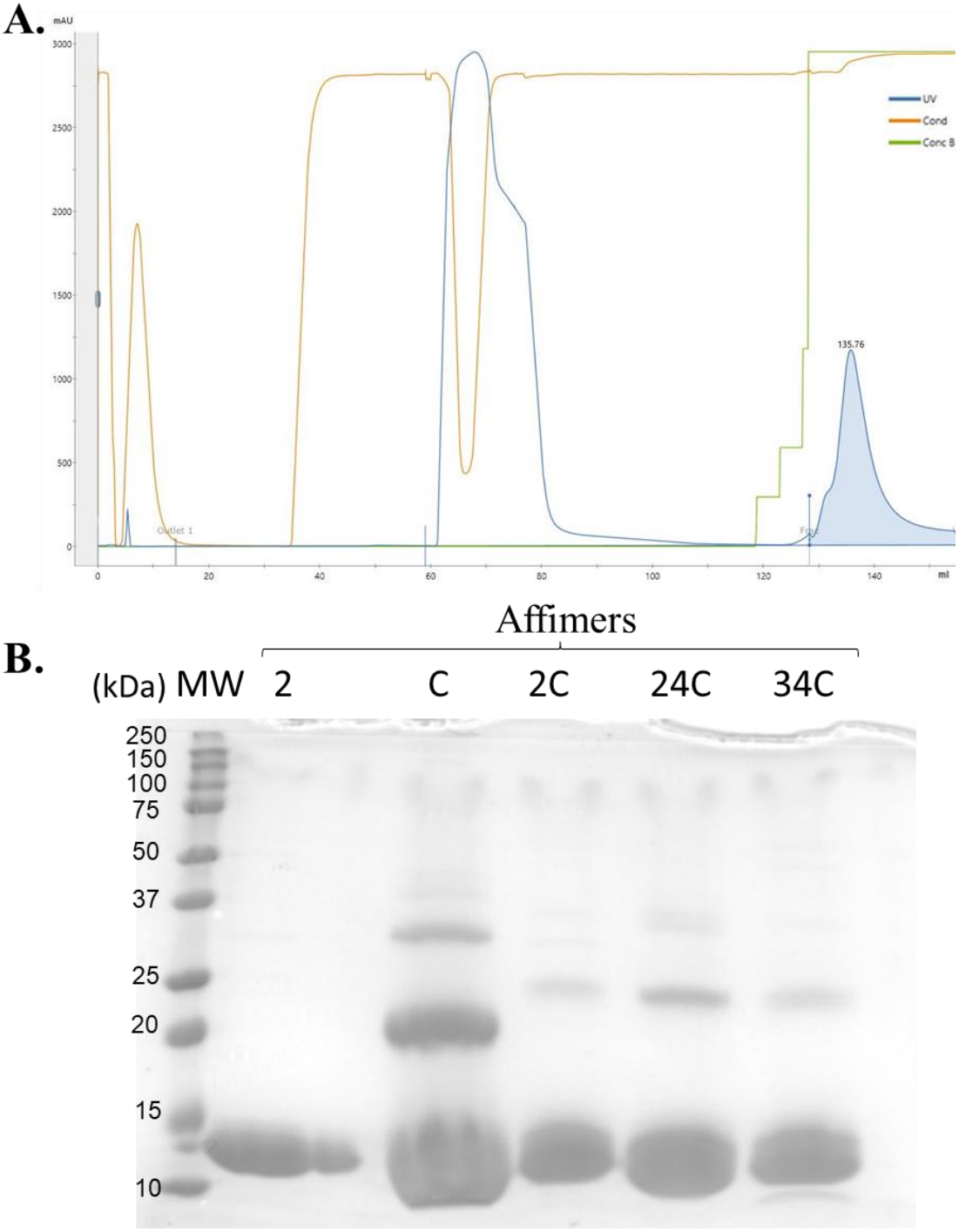

Figure 5.7. IMAC chromatography of His-tagged Affimers.

Soluble protein after lysis and heat denaturation was filtered and load on to a 5 mL HisTrap excel column. ***A.*** *Representative Affimer IMAC chromatogram, corresponding to the control Affimer with cysteine. Absorbance at 280 nm (blue trace), conductivity (orange trace) and concentration of imidazole (green trace) are plotted against elution volume (mL). Fist peak corresponds to non-specific proteins, second with the Affimer.* ***B.*** *Representative SDS-PAGE of Affimers purification after IMAC and stained with Coomassise. (MW) Molecular weight marker (kDa), 2, C, 2C, 24C,*

34C are the Affimers 2, control Affimer containing cysteine and the Affimers containing cysteine, respectively.

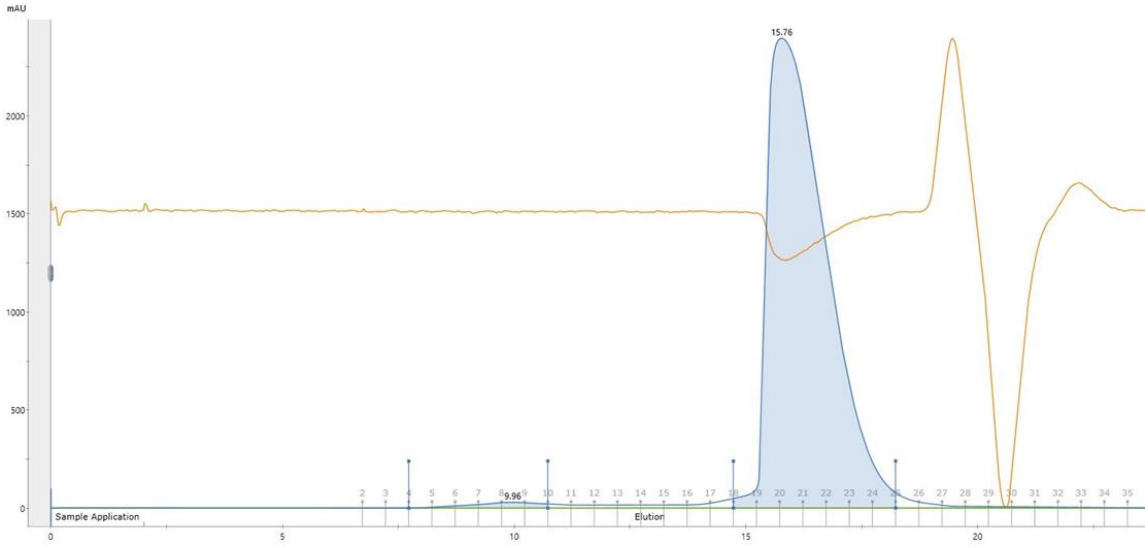

Figure 5.8. SEC chromatography of Affimer 2.

SEC purification chromatogram of Affimer 2. Absorbance at 280 nm (blue trace) and conductivity (orange trace) are plotted against elution volume (mL). Single peak corresponding with the Affimer 2.

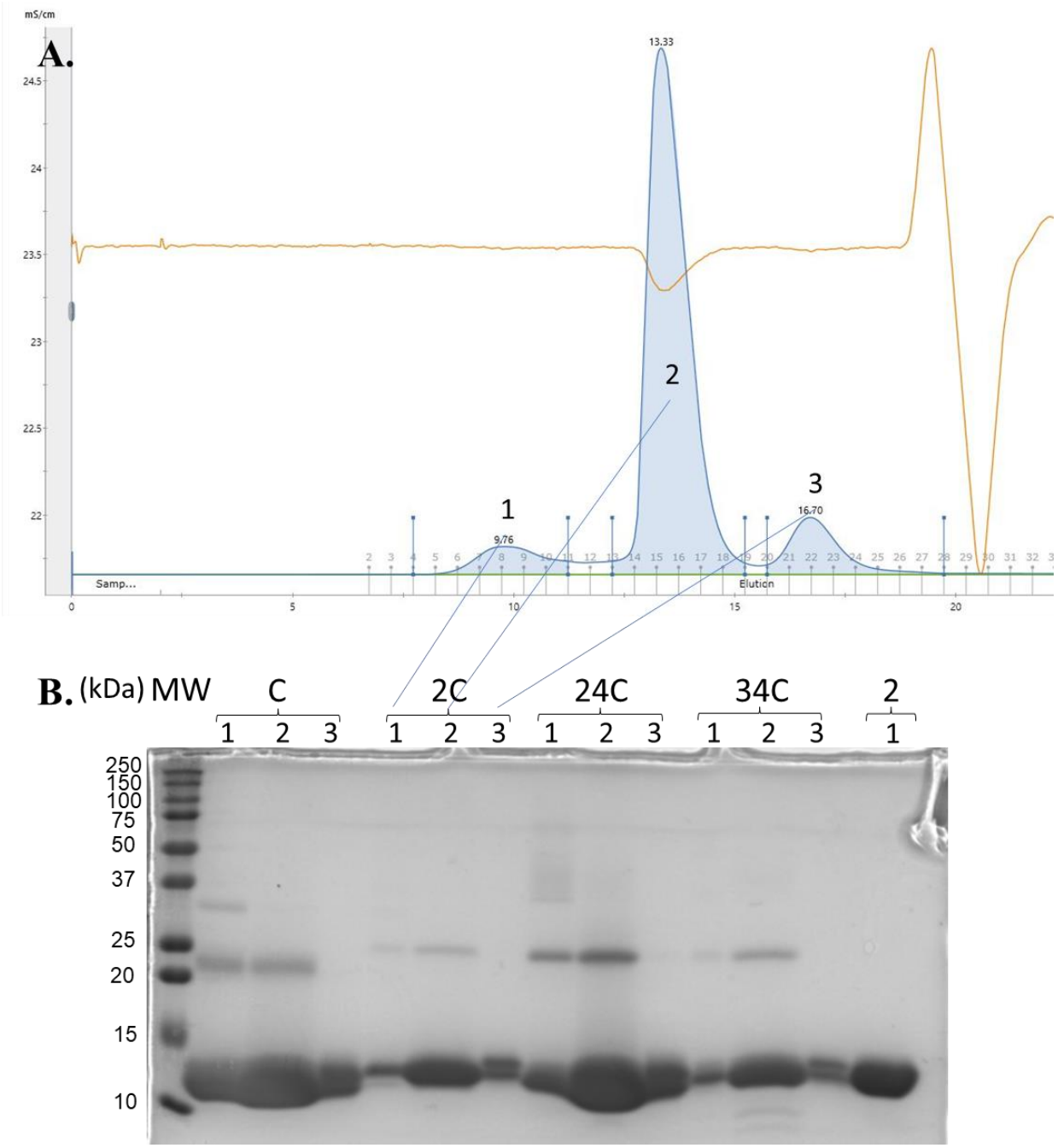

Figure 5.9. SEC chromatography of Affimer with unpaired cysteine.

Representative SEC purification chromatogram of Affimers with unpaired cysteine residue. Absorbance at 280 nm (blue trace) and conductivity (orange trace) are plotted against elution volume (mL). Peaks corresponding with trimers, dimers or monomers. ***B.*** *Representative SDS-PAGE of Affimers purification after SEC and stained with Coomassie. (MW) Molecular weight marker (kDa), Control Affimer containing cysteine (C), 2C, 24C, 34C are the respective Affimers containing cysteine and 2 is Affimer 2.*

5.2.4 Anti G6b-B affimers do not affect platelet aggregation

The anti G6b-B affimers were tested on plate-based aggregometry (PBA). PBA is an alternative method to the LTA carried on a 96-well plate with the advantages that it allows measure more sample at the same with less washed platelets. PBA measures absorbance at 405 nm (Chan et al., 2018; Fratantoni and Poindexter, 1990) giving the final % of aggregation as an end point, this is the main difference with LBA, which is real time.

The effect of the G6b-B affimers on GPVI mediated aggregation was studied on washed platelets ($4x10^8$/mL) incubated 20 minutes with increasing concentration of the Affimers (3, 10, 30, 100 μg/mL) before stimulation with CRP (1/3 μg/mL), collagen (1/3 μg/mL) or thrombin (0.05 units/mL). Sample plate was shaken for 5 minutes, and absorbance was measure at 405 nm. None of the tested concentrations had significant effect on platelet aggregation (Figure 5.10).

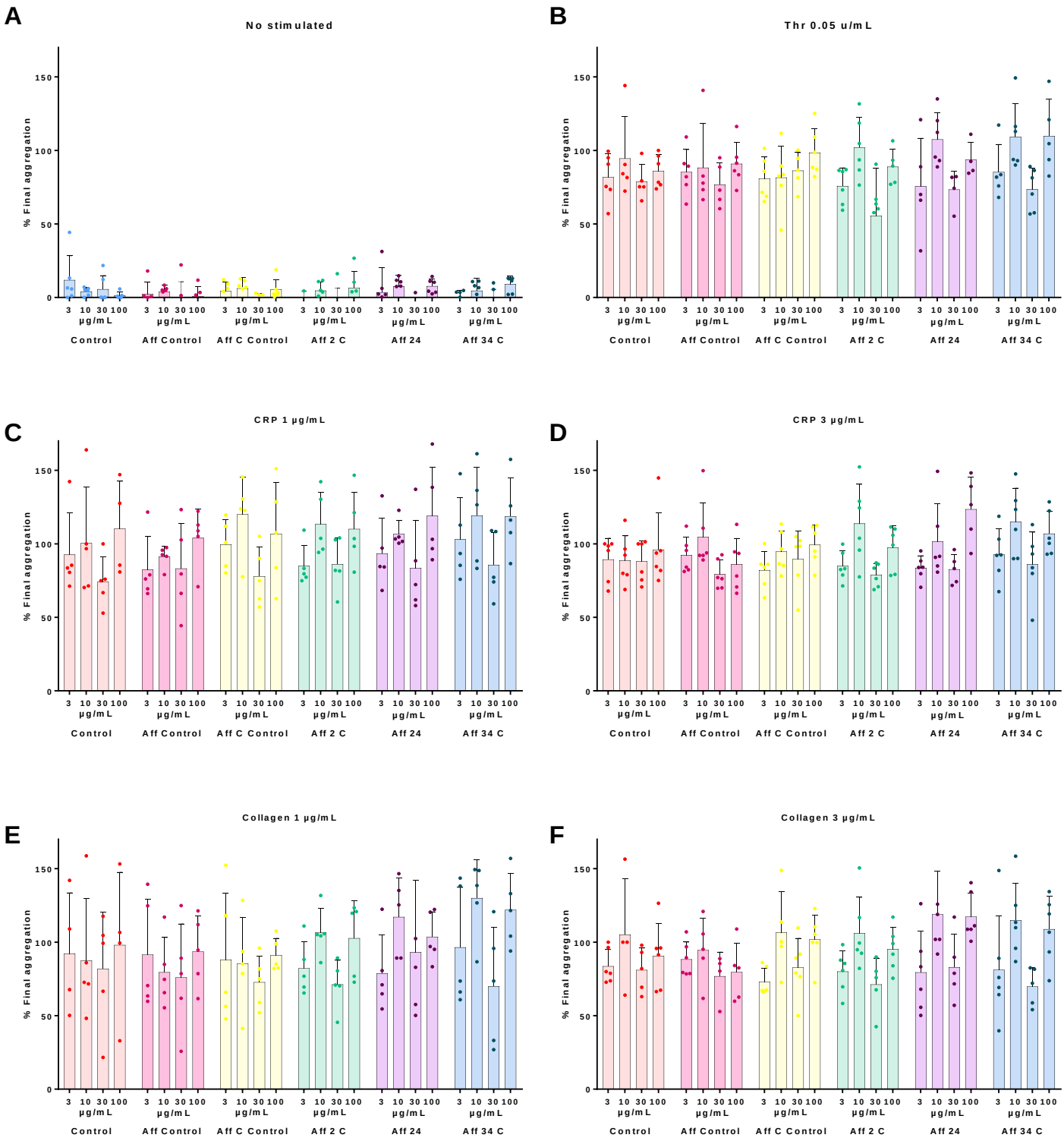

Figure 5.10. G6b-B binding Affimers have no effect on platelet activation tested by PBA. *Washed platelets (4×10^8 cells/ml) were incubated for 20 minutes with increasing concentration of the Affimers (3, 10, 30, 100 µg/mL) before no stimulation (**A.**) or stimulation with (**B**) thrombin (0.05 units/mL), CRP (1/3 µg/mL, **C** and **D,** respectively) and collagen (1/3 µg/mL **E** and **F,** respectively) for 5 minutes. None of the tested concentrations had significant effect calculated using one-way ANOVA with Dunnett's post-test. Data are shown as mean ± SD and are representative of five experiments.*

5.2.5 Affimers do not significantly affect fibrinogen binding and P-selectin exposure

Anti-G6b-B Affimers were also tested for they ability to modify "inside-out" signalling in platelets. This was accomplished using flow cytometry to measure the fibrinogen binding to integrin αIIbβ3 in activated platelets and the P-selectin translocation to the membrane during α-granules released.

PRP was incubated with the higher dose of the Affimers (100 μg/mL) or their controls and the FITC Fibrinogen and PE/Cy5 anti-human P-selectin (CD62P) antibodies for 15 minutes. Then, platelets were stimulated with the GPVI agonist (CRP, 3 μg/mL), to test their ability to modulate GPVI signalling. They were stimulated with thrombin receptor activating peptide-6 (TRAP-6 10 μM), to test for any effect on PAR receptors, and were left unstimulated to confirm that the Affimers do not directly activate platelets. Following incubation for 20 minutes in the dark the reaction was stopped by fixing the samples with 0.2% formyl saline and measured using a BD Accuri C6 Plus flow cytometer. Affimers did not have significant effect on platelets activation on any of the tested conditions (Figure 5.11).

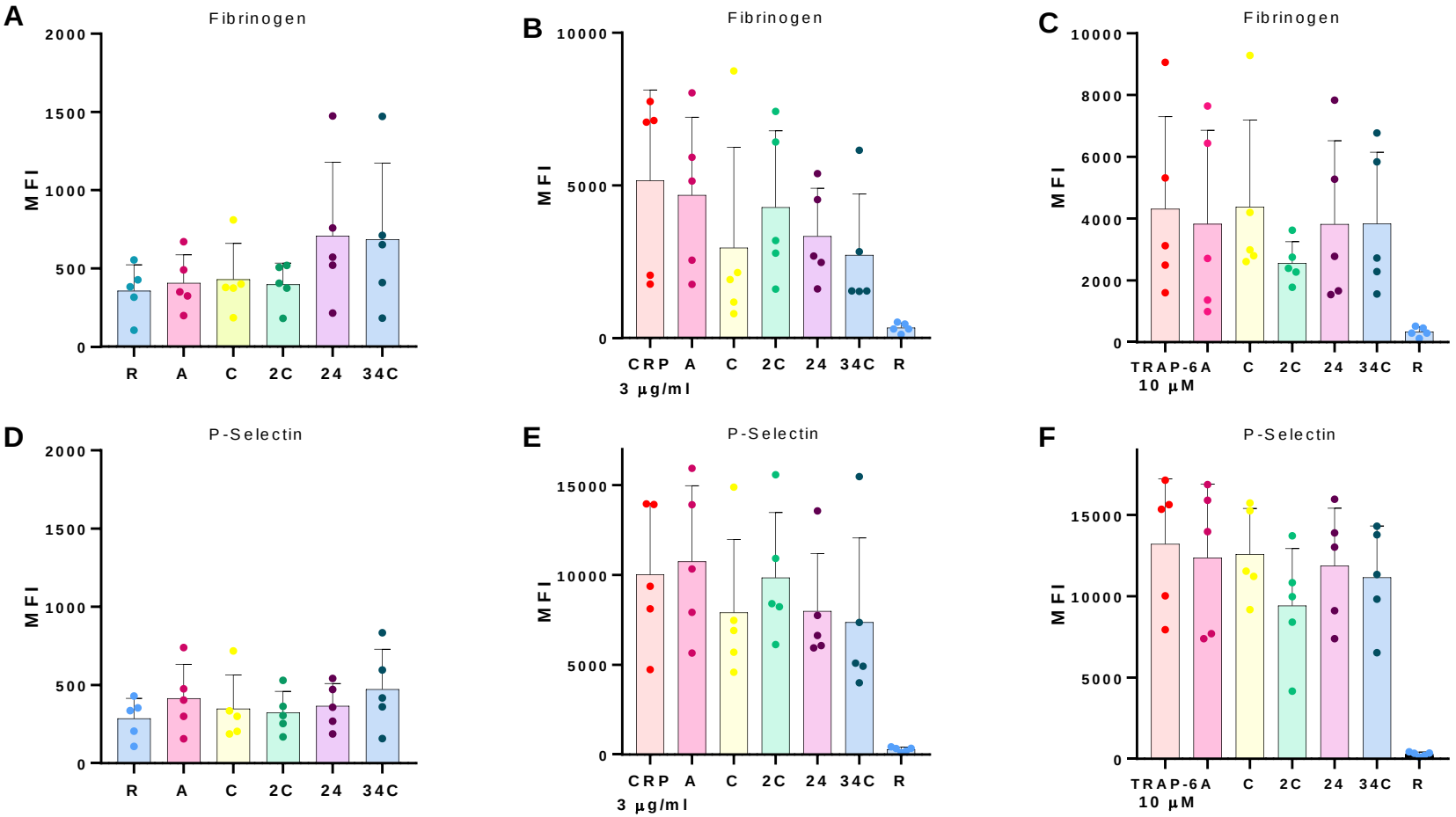

Figure 5.11. G6b-B affimers did not have significant effect on fibrinogen binding and P-selectin exposure in PRP.

*PRP was incubated with the Affimers (Affimer 2 with cysteine residue, 2C, Affimer 24, 24, Affimer 34 with cysteine residue, 34C at 100 µg/mL) or with the controls (Resting platelets, R, Control Affimer, A, Control Affimer with cysteine residue, C, at 100 µg/mL) and FITC anti-human Fibrinogen antibody to measure fibrinogen binding (**A, B, C**) and PE/Cy5 anti-human CD62P antibody to measure P-selectin exposure (**D, E, F**) for 15 minutes. Samples were stimulated with 3 µg/ml CRP (**B**, **E**), 10 µM TRAP-6 (**C, F**) or not stimulate (**A, D**) for 20 minutes in darkness, before been analysed by flow cytometry. The median fluorescence intensity (MFI) was plotted against the Affimers and analysed using a one-way ANOVA with Dunnett's post-test. Data are shown as mean ± SD and are representative of five independent experiments.*

5.2.6 Fluorescent labelling of Affimers

PBA and flow cytometry assays suggested that anti-G6b-B Affimers do not have an activatory effect on G6b-B sufficient to inhibit platelet activation through GPVI pathway or PAR receptors. We wanted to explore whether they had an effect in different models of platelet function and whether they could be used as a tool for labelling G6b-B. For this purpose, Affimers were functionalized with a dye (Alexa Fluor 488) by the single cysteine residue that we inserted before the His-tag. Alexa Fluor 488 C5 Maleimide was used to functionalise the Affimers owing to the high reactivity of maleimide groups with sulfhydryls. Functionalised fluorescent Affimers were tested using flow cytometry to confirm that the reaction was successful and that they bind to G6b-B in platelets. Flow cytometry results showed that Affimer 24 and 34 had significant levels of binding to G6b-B compare with the control Affimer (C, Figure 5.12). Affimer 2 shows an insignificant increased that could represent either that Affimer to does not bind well or that is poorly labelled.

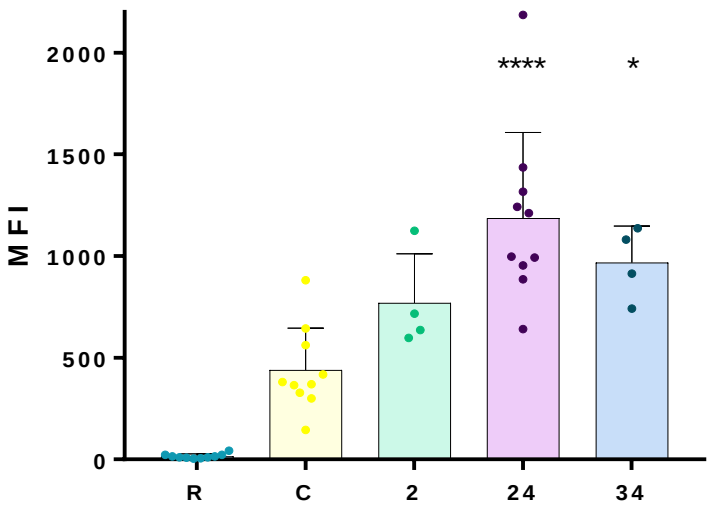

Figure 5.12. Fluorescent Affimers bind platelets.

PRP was incubated the Affimers (100 µg/mL) (Resting platelets, R, Control Affimer with cysteine residue, C) for 15 minutes. Samples were fixed with 0.2% formyl saline, before been analysed by flow cytometry. The median fluorescence intensity (MFI) was plotted against the Affimers and

*analysed using a one-way ANOVA with Dunnett's post-test. Data are shown as mean ± SD, n= 4-10. *p ≤ 0.05, ****p ≤ 0.0001.*

5.2.7 Potential role of Affimer 24 in thrombus formation under flow

Under resting conditions G6b-B is constitutively phosphorylated (Senis et al., 2007), indicating that it may play an important role preventing activation of circulating platelets. PBA and flow cytometry assays with the anti-G6b-B Affimers suggested that they are not strong enough to inhibit platelet activation through the GPVI pathway. Nevertheless, this do not rule out the possibility that they could modulate thrombus formation. To this end, thrombus formation was monitored in hirudin-anticoagulated whole blood over a CRP or Perlecan coated microspots. CRP was used because it is GPVI ligand GPVI and Perlecan is a large basement membrane heparan sulphate proteoglycan on the vessel-wall, which have been proposed to facilitate G6b-B activation, resulting in the inhibition of platelet activation (Vogtle et al., 2019).

CRP and perlecan were coated to the surface in the presence of vWF (native human vWF) to allow for GPIb-V-IX mediate trapping of platelets, but it do not activate platelets (Jooss et al., 2019). Whole blood was incubated for 10 minutes with Affimer 24, or the control Affimer with cysteine, at 37°C. Perfusion through microspot-containing flow chambers was performed at a wall shear rate of 150 s^{-1} over 3.5 minutes at 37°C. Formed thrombi were stained for PS (phosphatidylserine) exposure (which is required for coagulation factor binding, yellow) and P-selectin (CD62P, red), the residual label was removed by rinsing with HEPES buffer (pH 7.45) containing 2 mM $CaCl_2$ and 1 U/mL heparin (Figure 5.13). The experiments were performed in duplicate, using blood obtained from 3 different healthy donors.

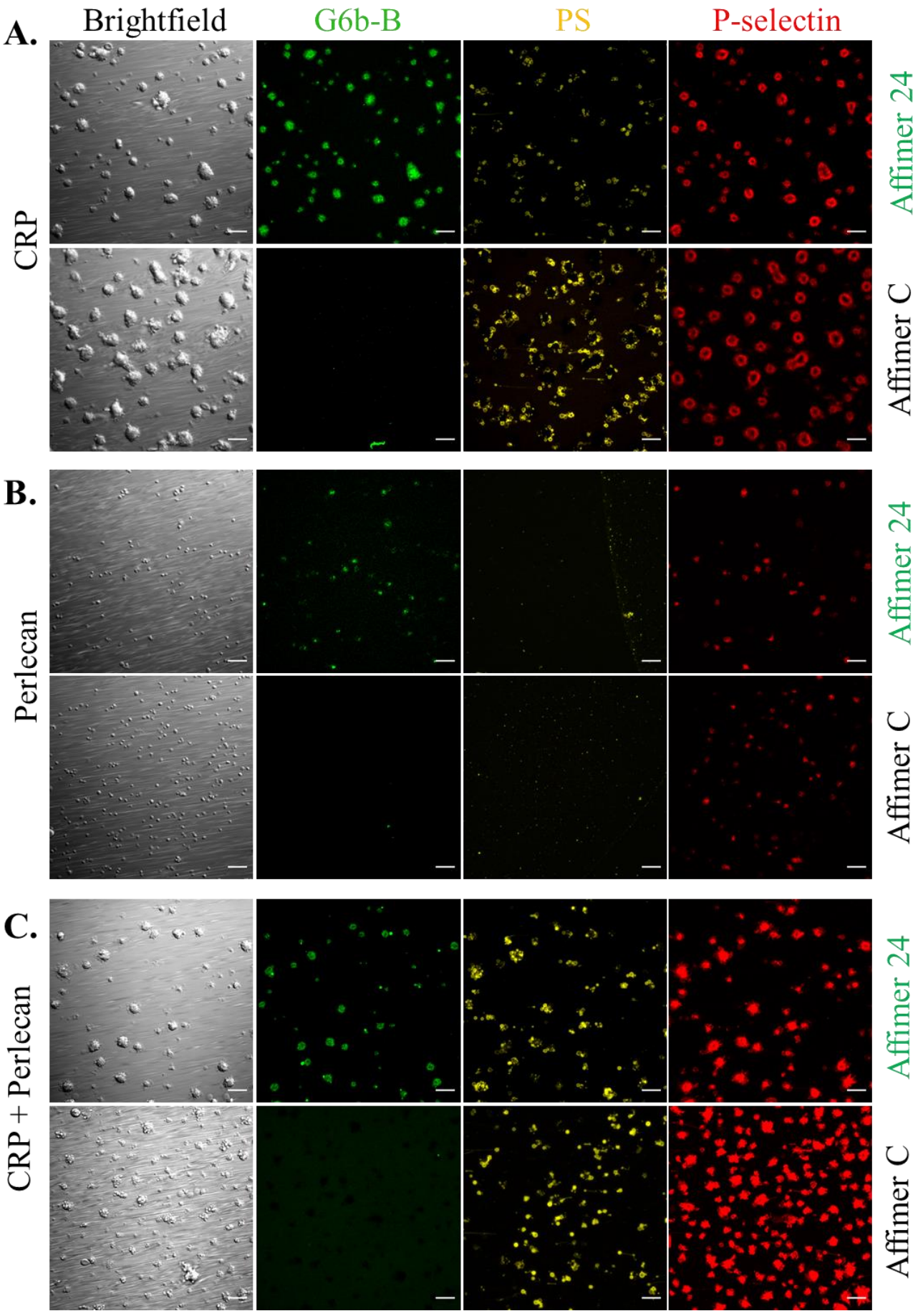
A.
Brightfield
G6b-B
PS
P-selectin
CRP
Affimer 24
Affimer C
B.
Perlecan
Affimer 24
Affimer C
C.
CRP + Perlecan
Affimer 24
Affimer C

Figure 5.13. In vitro flow assay in presence of the anti-G6b-B Affimer.
*Thrombus formation on immobilized (**A**) CRP (250 µg/mL), and VWF (12.5 ug/mL µg/mL), (**B**) Perlecan (25 ug/mL) and vWF (12.5 µg/mL) or (**C**) CRP (250 µg/mL) + Perlecan (25 ug/mL) and VWF (12.5 ug/mL µg/mL). Hirudin-anticoagulated whole blood was incubated 10 minutes at 37°C with Affimer 24 or the negative control Affimer and perfused for 5 minutes at a shear rate of 150 s^{-1} (37°C). Representative microscopic images of bright-field and the three fluorescent images of Affimer 24 (green), PS (phosphatidylserine) exposure (yellow) and P-selectin (red) at the end stage are shown. Scale bars represent 20 µm. Images by Isabella Provenzale.*

Thrombi produced by CRP usually are large with aggregated platelets with high levels of activation markers, such as PS and P-selectin (Jooss et al., 2019). However, brightfield and fluorescent endpoint images suggest that the thrombi in presence of Affimer 24 were fewer, smaller, and more contracted compared with the control. PS exposure appeared to be limited but in contrast P-selectin was higher compare with the control (Figure 5.13 A).

Coated surfaces with perlecan did not produce thrombi, only single platelets, but these were activated platelets as showing by the P-selectin exposure. There was not PS exposure which suggests that the platelets were not strongly activated. It seems that the presence of Affimer 24 lightly decrease the number of adhered platelets (Figure 5.13 B).

Mixed coated surfaces with CRP and perlecan in the presence of Affimer 24 showed fewer and more contracted thrombi compared with the control. PS exposure also appears to be lower in some donors when treated with Affimer 24 (Figure 5.13 C).

Nevertheless, these are preliminary data, the sample number (n=3) for this experiment will need to be increased in order to conclude any effect of Affimer 24 on thrombus formation. The work in this experiment was performed in collaboration with Isabella Provenzale, as part of the TAPAS European consortium.

5.3 Discussion

This chapter successfully achieved the overexpression and purification of G6b-B in mammalian cells that was used as a target for phage display screening and selection process of anti-G6b-B Affimers. The selected Affimers were cloned into a *E. coli* expression vector, overexpressed, purified, functionalised with a fluorophore and finally, tested in platelet function assays, as a first approach to identify their possible applications.

Affimer selection led to the discovery of 3 unique G6b-B binding hits (Affimer 2, 24 and 34). Sequencing showed that Affimers 2 and 24 have a similar variable region (Figure 5.5), which suggests that they may bind to the same epitope. Affimer 34 lacks the second variable region, as it can be seen on its predicted structure model at Figure 5.14. In theory, two binding sites are more likely to have better recognition, however Affimer 34 has a large first variable region, so binding may still be possible.

Affimer production and purification is a standard method well developed by Tiede *et al.* However, Affimers containing the functional cysteine tend to form multimers due to disulphide formation although this issue is alleviated if the cysteine is labelled with the functional tag, which our case was an Alexa fluorophore.

Due to the established role of G6b-B in regulating GPVI, our G6B-b binding Affimers were tested for their ability to bind to G6b-B and then inhibit platelet activation through GPVI activation pathway by plate-based aggregometry (PBA) and flow cytometry. None of the Affimers displayed a significative inhibitory effect when platelets were stimulated by CRP, although there was a slight decrease in P-selectin exposure and fibrinogen binding in some donors with Affimers 24 and 34 (Figure 5.10). Although this was statistically insignificant, the variability between donors warrants further work as there

may be a link between receptor expression level (G6b-B or GPVI) and inhibition. However, due to time limitations we can only speculate beyond these preliminary tests with low sample numbers that there is a feasible effect of G6b-B Affimers. Sample number, and correlations with receptor expression levels would need to be increased and more functional studies will need to be done to identify any significative effects.

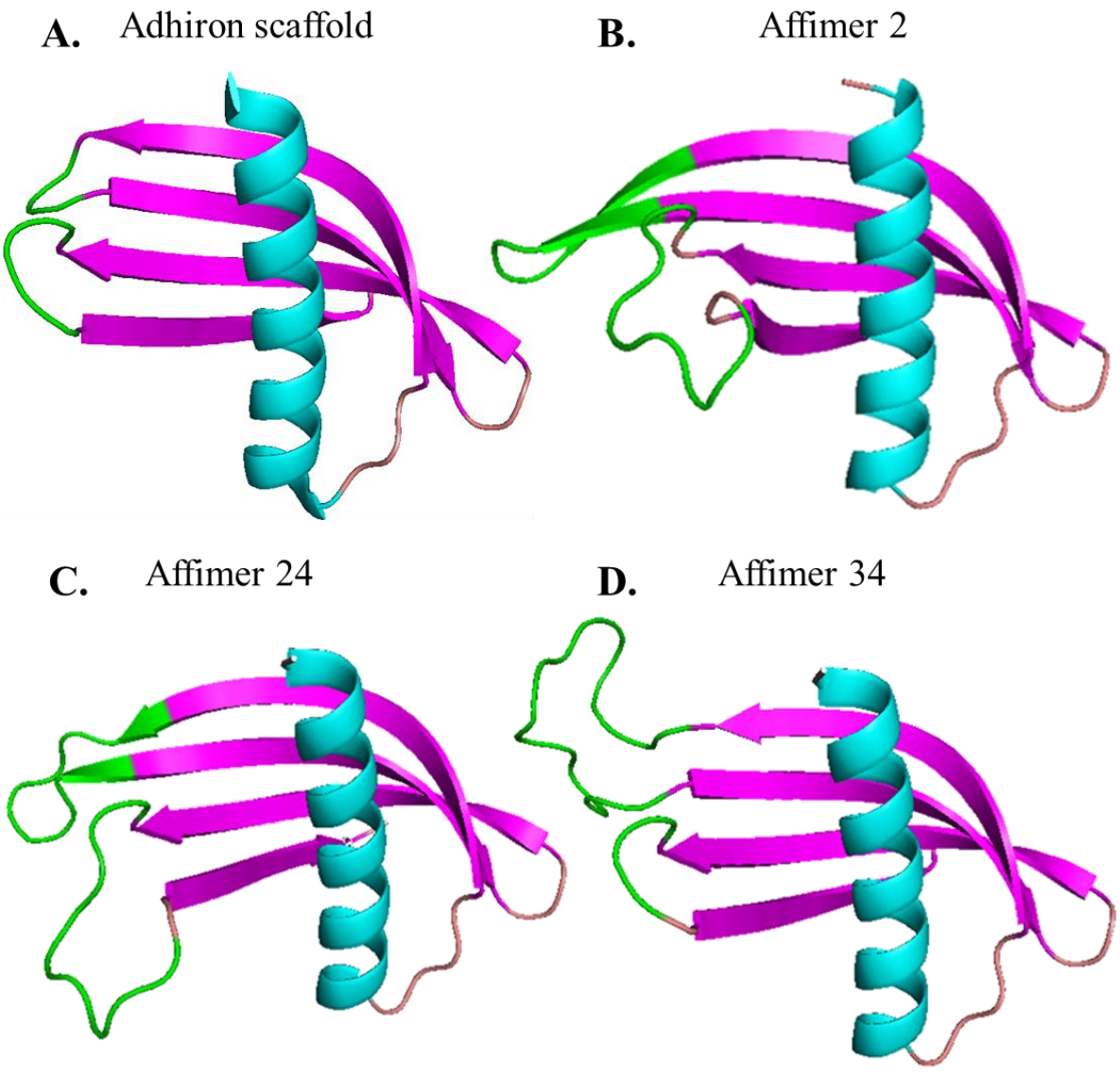

Figure 5.14*. Cartoon diagram of the predicted Affimers structure.*
A. *Adhiron scaffold (PDB ID: 4N6T).* ***B.*** *G6b-B binding Affimer 2.* ***C.*** *G6b-B binding Affimer 24.* ***D.*** *G6b-B binding Affimer 34. In green are highlight the two variable regions. Structures were predicted with the online tool: Swiss-model, a protein structure homology-modelling server, using*

Adhiron scaffold (4N6T) as a template. In green are shown the variable loops. Images were generated using PyMol.

The Affimers were functionalized with the conjugation of Alexa Fluor 488 to the Cys containing versions. This provided us with a new tool to visualize G6b-B, the equivalent of which is not available commercially. Flow cytometry testing with these labelled Affimers allowed us to conclude that Affimer 24 bound significatively better to G6b-B than Affimer 34 and 2. This was the reason why we selected Affimer 24 to perform a preliminary *in vitro* thrombus formation under flow studies. These preliminary studies were undertaken to explore the possibility of using Affimers not only as an anti-platelet therapy, but also as an imagining tool to detect G6b-B. We were aiming to see less thrombi formation and platelets less reactive. Perlecan was included because it is an heparan sulphate proteoglycan present on the vessel-wall, which have been proposed to activate G6b-B (Vogtle et al., 2019).

These initial experiments showed that Affimer 24 may have a small effect on thrombus size on CRP coated surfaces (both CRP alone or in combination with Perlecan) where we could observe fewer and smaller, more contracted thrombi compared to treatment with control Affimer. Phosphatidylserine (PS) exposure also appears to be lower in some donors when treated with Affimer 24. However, robust quantification is required, and the sample number will need to be increased to be able to conclude an effect of Affimer 24 in thrombus formation. Future replicates will shed light on the potential effect of Affimer 24 on thrombus formation and where the other two Affimers (2 and 34), have antithrombotic effect.

5.4 Conclusions

Here we presented the first attempt of targeting an inhibitory receptor to inhibit the platelet function. New anti- G6b-B Affimers were successfully generated, and preliminary functional studies were carried out to determine their potential as anti-platelet therapy by preventing GPVI activation. Affimers might be a plausible alternative to conventional mAbs because they not only have high affinity but also improve all the weaknesses of the mAbs and F(ab), such as that they are not available for oral therapy. Promising results were obtained with Affimer 24, which showed a potential on decreasing thrombi size on *in vitro* thrombus formation studies. Future research will conclude whether these Affimers could stimulate platelets to make them less reactive and therefore reducing thrombosis.

Chapter 6

General Discussion

6 CHAPTER 6. GENERAL DISCUSSION

6.1 Discussion

This study was focused on the characterization and development of new biologics targeting GPVI-mediated pathway molecules (GPVI and G6b-B) in order to overcome the bleeding risk of current antithrombotics, which target other platelet activation pathways crucial for haemostasis. On the activatory side of the GPVI pathway this was addressed by directly targeting the GPVI glycoprotein with novel monoclonal antibodies (mAbs) and their F(ab) fragments. These were developed prior to the start of this project by Emfret Analytics Würzburg, Germany, and characterized functionally and partially structurally in this study. On the inhibitory side of the pathway this was attempted by targeting the ITIM-receptor G6b-B with Affimers developed during the course of this project.

6.1.1 Activatory side of the GPVI pathway

Of the five tested mAbs, only E7 and E12 (the latter also known as EMF-1) showed complete inhibition of GPVI-mediated platelet activation. In contrast, all the tested F(ab) fragments (E7, E2, D3 and A9) inhibited GPVI-mediated platelet activation, suggesting that they have potential as a novel anti-GPVI therapy.

mAb A9 did not prevent CRP aggregation but delayed it, and at low collagen doses caused some reduction in platelet aggregation in some donors only, but this light inhibitory effect was overcome with high concentrations of collagen. This is similar to the data reported with the rat mAb JAQ1 which was found to be specific to the CRP-binding site on mouse GPVI as its inhibitory effect was overcome with high concentrations of collagen (Schulte et al., 2001). This, together with, the epitope mapping studies which identified binding to

the D1 domain, this led us to suggest that mAb A9 is likely binding to the collagen/CRP binding site and may be competing with collagen/CRP for binding. Because the A9 F(ab) fragment completely blocked platelet aggregation, even with low agonist concentration (it was one of the most potent F(ab) fragments tested) it seems likely that the ab fragment has better access/higher affinity for its epitope due to less steric hindrance compared to the full length mAb. It would be interesting in the future structural studies of A9 F(ab) fragment in complex with GPVI.

The next questions to address regarding the inhibitory mechanism of these mAbs and their F(ab) fragments will be: Is mAbs inhibitory mechanism due to internalization of the receptor or shedding? Would these mAbs be able to prevent thrombus formation? Can they prevent fibrin(ogen) binding and therefore preventing thrombus stabilization? Can these mAbs affect collagen binding and GPVI clustering/association with other proteins and signalling (tyrosine phosphorylation)? *Ex vivo* thrombus formation under flow in coated surfaces with the GPVI agonist and with components of the extracellular matrix (in order to address the thrombus formation in a more physiological way) and the use of GPVI humanized mouse models will be good approaches to address their therapeutic potential.

A GPVI humanized mouse model will be able to model the *in vivo* human responses to the mAbs more accurately than in other mouse models. Furthermore, it provides a preclinical tool to assess the antithrombotic potential of these biologics *in vivo*, evaluate them in terms of efficacy and safety, and may help to design future clinical studies.

Another student from TAPAS consortium has explored some of these in parallel with this project. They focussed on the E12 F(ab) fragment, also known as EMF-1 Fab, such as

testing them in a GPVI humanized mouse model (unpublished data). A recent publication from Navarro *et al*., showed that blocking GPVI with the EMF-1 Fab led to smaller, unstable thrombi, reduced platelet adhesion and a near total blockade of PS (phosphatidylserine, marker of collagen-induced GPVI signalling) exposure on a collagen coated surface (Navarro et al., 2021).

Regarding the GPVI-mAbs/F(ab) fragment structural interaction, studies with monomeric and dimeric GPVI suggested that the mechanism of inhibition is not through preventing GPVI dimerization/clustering because they did not have preferential binding for any of them. Nevertheless, these studies were performed with recombinant GPVI; dimeric GPVI is achieved by Fc region dimerisation, which may differ from GPVI dimers found on the platelet membrane.

During this project we were unable to produce crystals with good crystallographic properties for X-ray diffraction. There are lot of reasons why GPVI-F(ab)-fragment complex did not yield crystals. One of the reasons may be that the quality of the F(ab) fragment preparation may have been below a threshold required (i.e., some degradation) for crystallography. On the other side, the F(ab) fragments are bigger than GPVI, so one of the reasons could be that the orientation of GPVI and F(ab) is less favourable for crystallization. Finding the perfect conditions and concentrations for generating the crystals will require more time and optimizations. However, there are cases where complexes have not been able to form crystals with good qualities for crystallography.

Chimeric GPVI proteins helped us to confirm that these mAbs were inhibiting GPVI platelet activation by a direct interaction with the ligand binding site, which suggested that they could be binding directly to the collagen/CRP binding site or the surrounding

amino acids, preventing ligand binding by allosteric impediment. Future work on GPVI chimeras would be generating other chimeras with smaller regions on the D1 domain, for example, changing regions of 5-10 amino acids at a time within the D1 domain, from amino acid 30 to 80, that have previously been implicated on collagen and CRP binding (Lecut et al., 2004a; Smethurst et al., 2004). It would be interesting to make chimeras on the surroundings of K59, previously reported to be essential for CRP binding (Smethurst et al., 2004), and even a single point mutations, such as, K59 to study whether A9 binding to GPVI is affected by this mutation and therefore, it would be binding within the area of CRP binding site.

The GPVI K59E, R117P and R166S mutations have been previously reported to support CRP binding by mutagenesis experiments with the K59E mutation being the only one reported to disrupt CRP binding (Smethurst et al., 2004). However, if we look at the GPVI 3D structure bound to triple-helical collagen peptides (Figure 6.1), just released this March in Blood by Feitsma et al. (Feitsma et al., 2022) (PDB: 5OU8) it can be seen that the amino acids proposed to be important in mutation studies do not lie within the binding site. Therefore, these residues are not likely to directly be involve in binding but maybe allosteric modulators. Moreover, as CRP is the binding portion of collagen to GPVI, then the CRP binding site in the crystal structure may represent the collagen binding site. Feitsma et al. have identified W76, R38 and E40 as the essential residues for binding to fibrillar collagens and CRP (Feitsma et al., 2022). However, in the majority of the GPVI crystal structures to date the D1-D2 angle is rigid (Feitsma et al., 2022; Horii et al., 2006; Slater et al., 2021), so this does not discard the possibility that other residues within the D2 domain may be contributing to the binding, directly or by allosteric contributions.

Future work will shed light in this matter, one possibility would be to address GPVI structure by structural cryo-electron microscopy. This approach would bring the possibility to study GPVI in the context of the platelet membrane, without any modification on GPVI and in complex with its ligands, this will help not only to understand GPVI interaction with its ligands but also address the controversy whether GPVI is a monomer, a dimer or both.

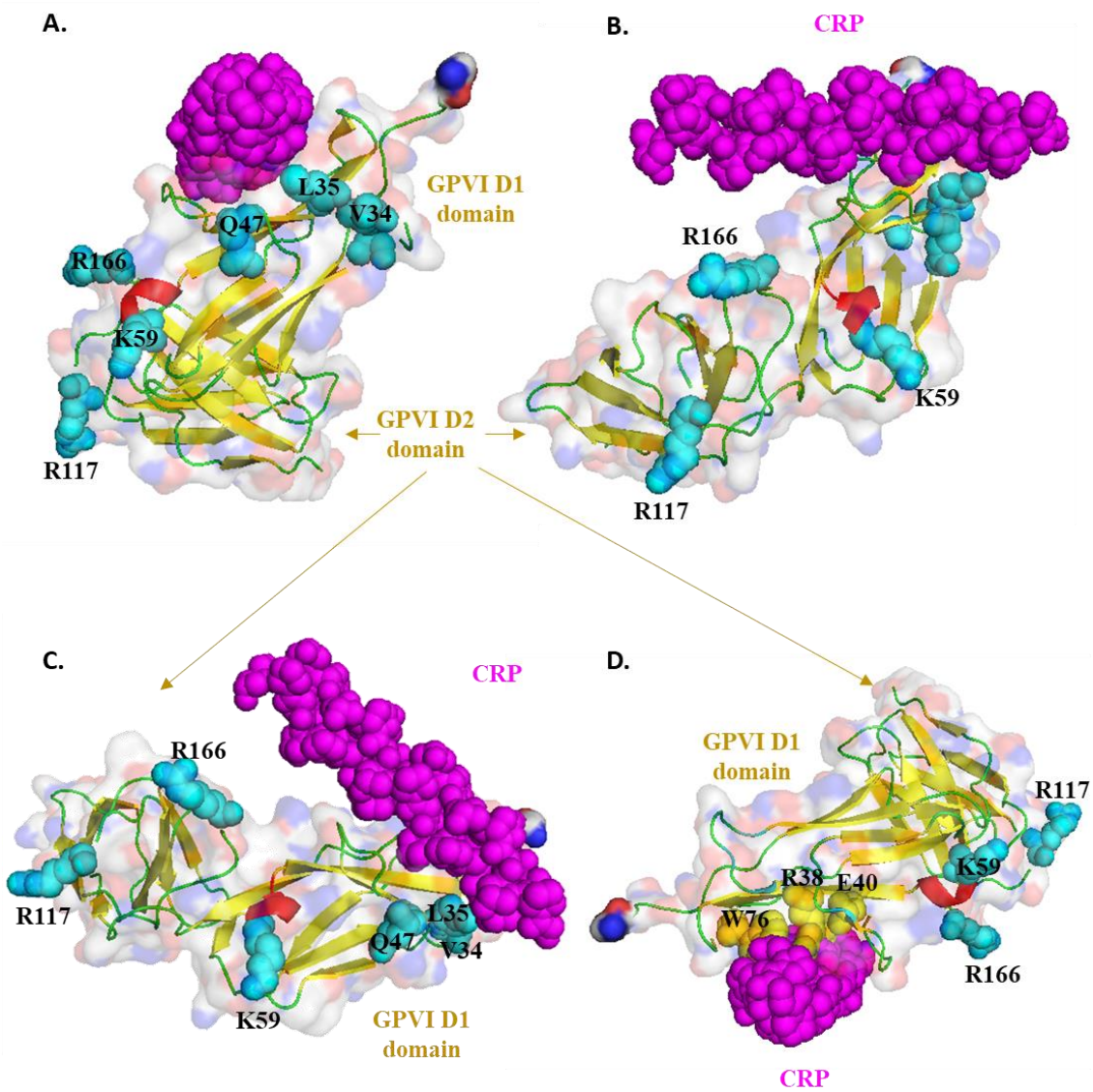

Figure 6.1. GPVI structure in complex with triple-helical collagen peptides.

GPVI has been represented in cartoon and mesh surface with low opacity. In blue can be found residues previously proposed to contribute to collagen/CRP binding, in magenta CRP from

*different points of view (**A**, **B**, **C**), and (**D**) in yellow the residues interacting with CRP (R38, E40, W76). Images were generated using PyMol (PDB ID: 5OU8) (Feitsma et al., 2022).*

6.1.2 Inhibitory side of the GPVI pathway

The potential antithrombotic effect of G6b-B and whether G6b-B stimulation could lead to less reactive platelets, reducing the risk, or severity of thrombosis has not been extensively studied so far. Only a few references can be found in the literature, such as the finding that G6b-B cross-linking with polyclonal antibodies caused inhibition of platelet activation and aggregation *in vitro* (Newland et al., 2007). One of the advantages of G6b-B as a potentially effective and safe antithrombotic target relies on the fact that it is highly expressed on the platelet cell surface, and this is restricted to platelets and megakaryocytes. Potentially, this provides high specificity and low risk of off-target effects in other cell types. Additionally, G6b-B is a cell-surface receptor, as is GPVI, which increases the chances of successful drug delivery, as the drug does not have to cross the membrane to reach the target.

There are no studies so far on potential differences in G6b-B expression levels between individuals, it would be interesting to explore whether this variation exits and if this has some implication, such as, a relation between higher expression of G6b-B and less tendency to thrombotic events. There is a precedent for this with the other platelet ITIM-receptor, PECAM-1. PECAM-1 expression levels on human platelets surface vary extensively from 5,000 up to 20,000 copies/cell in around 20% of the population, and high levels of expression are associated with a decrease in platelet response to CRP-XL, ADP and thrombin (Jones et al., 2009). Investigating whether this variation exist in G6b-B would be useful to know and might support the notion that stimulation of G6b-B could be used therapeutically.

We explored the possibility of targeting G6b-B with different biologics, such as mAbs, nanobodies, Aptamers or Affimers. We decided to proceed with the approach of targeting

G6b-B with Affimers because they met all the requirements for a good therapeutic and had some advantages to the classic mAbs, such as being good for oral delivery and having shorter development times than other biologics, such as nanobodies.

Three Affimers were identified to bind G6b-B. Functional studies so far showed that these three Affimers do not induce G6b-B to inhibit platelet activation through the GPVI activation pathway in classical *in vitro* platelet function assays (namely aggregometry). However, preliminary *in vitro* flow studies with Affimer 24 showed that they might influence thrombus size on CRP coated surfaces. More investigation is needed to fully understand this new biologics. New methodologies developed within the fields of thrombosis can help to a better characterize this Affimers, such as the "occlusive thrombosis-on-a-chip" microfluidic device developed at Harper's lab for investigating the effect of anti-thrombotic drugs with patient's blood *ex vivo* (Berry et al., 2021).

Which is the affinity of this Affimers to G6b-B? BLI experiments would give insights of their affinities. Which epitope of G6b-B do they bind? Affimers structure is easy to generate by protein structure homology-modelling using the Adhiron scaffold as a template, molecular docking with G6b-B structure can give an approximation of their binding epitopes in shorter times than crystallographic studies.

Are Affimers able to cluster G6b-B in order to activate it? The small size of Affimers could make them unlikely to cause receptor clustering and therefore they are less likely to act as agonists. Can we modify Affimers to achieve receptor clustering? Affimers are easy to engineer which opens the possibility to fuse Affimers binding different or the same epitope within G6b-B to activate it, or even the possibility to generate a bispecific Affimer. These could potentially target more than one receptor to generate stronger

responses. For example, a dimeric Affimer binding both PECAM-1 and G6b-B. This would allow selective activation of PECAM-1 on platelets, together with the activation of G6b-B promoting upregulation of ITIM signalling to downregulate platelet activation by ITAM-receptors signalling.

In the same way as the GPVI mAbs/F(ab) fragments, it would also be interesting to generate to study the pharmacokinetics of this biologics *in vivo*, a humanized G6b-B mouse modes to assess the antithrombotic potential of these biologics *in vivo*, evaluate them in terms of efficacy and safety.

Further research is needed to explore these ideas, and fully determine the potential success of targeting inhibitory pathways as anti-platelet therapy.

6.2 Conclusions

In conclusion, in this thesis we provided an insight of the first functional and structural characterization of new mAbs targeting GPVI, with some of them having potential to be good candidates for antiplatelet therapy. The fact that the collagen/CRP binding site within GPVI is a large area decreases the chances of inhibiting this interaction with small molecules, making biologics the most suitable strategy to prevent its activation.

Additionally, we attempt for the first time to target G6b-B as antiplatelet therapy by developing Affimers against it. Further research is needed to explore whether G6b-B stimulation could lead to platelets less reactive reducing the risk, or severity of thrombotic disease without causing substantial bleeding.

7 BIBLIOGRAPHY

2010. Cardiovascular Disability: Updating the Social Security Listings. Chapter 7 Ischemic Heart Disease. *In* Cardiovascular Disability: Updating the Social Security Listings, Washington (DC).

(FDA), U.S.F.a.D.A. 2018. What Are "Biologics" Questions and Answers.

Aarts, P.A., S.A. van den Broek, G.W. Prins, G.D. Kuiken, J.J. Sixma, and R.M. Heethaar. 1988. Blood platelets are concentrated near the wall and red blood cells, in the center in flowing blood. *Arteriosclerosis*. 8:819-824.

Adachi, T., and Y. Nakamura. 2019. Aptamers: A Review of Their Chemical Properties and Modifications for Therapeutic Application. *Molecules*. 24.

Al-Tamimi, M., E.E. Gardiner, J.Y. Thom, Y. Shen, M.N. Cooper, G.J. Hankey, M.C. Berndt, R.I. Baker, and R.K. Andrews. 2011. Soluble glycoprotein VI is raised in the plasma of patients with acute ischemic stroke. *Stroke*. 42:498-500.

Al-Tamimi, M., F.T. Mu, J.F. Arthur, Y. Shen, M. Moroi, M.C. Berndt, R.K. Andrews, and E.E. Gardiner. 2009. Anti-glycoprotein VI monoclonal antibodies directly aggregate platelets independently of FcgammaRIIa and induce GPVI ectodomain shedding. *Platelets*. 20:75-82.

Albelda, S.M., P.D. Oliver, L.H. Romer, and C.A. Buck. 1990. EndoCAM: a novel endothelial cell-cell adhesion molecule. *J Cell Biol*. 110:1227-1237.

Alberts, B.J., A.; Lewis, J.; Raff, M.; Roberts, K.; and Walter, P.;. 2002. Molecular Biology of the Cell. 4th edition.

Alshehri, O.M., C.E. Hughes, S. Montague, S.K. Watson, J. Frampton, M. Bender, and S.P. Watson. 2015. Fibrin activates GPVI in human and mouse platelets. *Blood*. 126:1601-1608.

Andrews, R.K., K. Suzuki-Inoue, Y. Shen, D. Tulasne, S.P. Watson, and M.C. Berndt. 2002. Interaction of calmodulin with the cytoplasmic domain of platelet glycoprotein VI. *Blood*. 99:4219-4221.

Arman, M., and K. Krauel. 2015. Human platelet IgG Fc receptor FcgammaRIIA in immunity and thrombosis. *J Thromb Haemost*. 13:893-908.

Arthur, J.F., S. Dunkley, and R.K. Andrews. 2007. Platelet glycoprotein VI-related clinical defects. *Br J Haematol*. 139:363-372.

Avacta. 2017. No immunogenicity issues for Affimer technology.

Banerji, P.G., J.B. Chatterjea, and P.C. Sengupta. 1964. Megakaryocytes in the Lungs. *Bull Calcutta Sch Trop Med*. 12:160-161.

Bartunek, J., E. Barbato, G. Heyndrickx, M. Vanderheyden, W. Wijns, and J.B. Holz. 2013. Novel antiplatelet agents: ALX-0081, a Nanobody directed towards von Willebrand factor. *J Cardiovasc Transl Res*. 6:355-363.

Baumgartner, H.R. 1977. Platelet interaction with collagen fibrils in flowing blood. I. Reaction of human platelets with alpha chymotrypsin-digested subendothelium. *Thromb Haemost*. 37:1-16.

Bender, M., I. Hagedorn, and B. Nieswandt. 2011. Genetic and antibody-induced glycoprotein VI deficiency equally protects mice from mechanically and FeCl(3) -induced thrombosis. *J Thromb Haemost*. 9:1423-1426.

Berlanga, O., D. Tulasne, T. Bori, D.C. Snell, Y. Miura, S. Jung, M. Moroi, J. Frampton, and S.P. Watson. 2002. The Fc receptor gamma-chain is necessary and sufficient to initiate signalling through glycoprotein VI in transfected cells by the snake C-type lectin, convulxin. *Eur J Biochem*. 269:2951-2960.

Berry, J., F.J. Peaudecerf, N.A. Masters, K.B. Neeves, R.E. Goldstein, and M.T. Harper. 2021. An "occlusive thrombosis-on-a-chip" microfluidic device for investigating the effect of anti-thrombotic drugs. *Lab Chip*. 21:4104-4117.

Best, D., Y.A. Senis, G.E. Jarvis, H.J. Eagleton, D.J. Roberts, T. Saito, S.M. Jung, M. Moroi, P. Harrison, F.R. Green, and S.P. Watson. 2003. GPVI levels in platelets: relationship to platelet function at high shear. *Blood*. 102:2811-2818.

Bhunia, S.S., A. Misra, I.A. Khan, S. Gaur, M. Jain, S. Singh, A. Saxena, T. Hohlfield, M. Dikshit, and A.K. Saxena. 2017. Novel Glycoprotein VI Antagonists as Antithrombotics: Synthesis, Biological Evaluation, and Molecular Modeling Studies on 2,3-Disubstituted Tetrahydropyrido(3,4-b)indoles. *J Med Chem*. 60:322-337.

Bigalke, B., K. Stellos, T. Geisler, E. Kremmer, P. Seizer, A.E. May, S. Lindemann, A. Melms, A. Luft, and M. Gawaz. 2010. Expression of platelet glycoprotein VI is associated with transient ischemic attack and stroke. *Eur J Neurol*. 17:111-117.

Billadeau, D.D., and P.J. Leibson. 2002. ITAMs versus ITIMs: striking a balance during cell regulation. *J Clin Invest*. 109:161-168.

Bird, R.E., K.D. Hardman, J.W. Jacobson, S. Johnson, B.M. Kaufman, S.M. Lee, T. Lee, S.H. Pope, G.S. Riordan, and M. Whitlow. 1988. Single-chain antigen-binding proteins. *Science*. 242:423-426.

Blair, P., and R. Flaumenhaft. 2009. Platelet alpha-granules: basic biology and clinical correlates. *Blood Rev*. 23:177-189.

Born, G.V. 1962. Aggregation of blood platelets by adenosine diphosphate and its reversal. *Nature*. 194:927-929.

Boudreau, L.H., A.C. Duchez, N. Cloutier, D. Soulet, N. Martin, J. Bollinger, A. Pare, M. Rousseau, G.S. Naika, T. Levesque, C. Laflamme, G. Marcoux, G. Lambeau, R.W. Farndale, M. Pouliot, H. Hamzeh-Cognasse, F. Cognasse, O. Garraud, P.A. Nigrovic, H. Guderley, S. Lacroix, L. Thibault, J.W. Semple, M.H. Gelb, and E. Boilard. 2014. Platelets release mitochondria serving as substrate for bactericidal group IIA-secreted phospholipase A2 to promote inflammation. *Blood*. 124:2173-2183.

Bourne, J.H., M. Colicchia, Y. Di, E. Martin, A. Slater, L.T. Roumenina, J.D. Dimitrov, S.P. Watson, and J. Rayes. 2021. Heme induces human and mouse platelet activation through C-type-lectin-like receptor-2. *Haematologica*. 106:626-629.

Brooks, D.G., W.Q. Qiu, A.D. Luster, and J.V. Ravetch. 1989. Structure and expression of human IgG FcRII(CD32). Functional heterogeneity is encoded by the alternatively spliced products of multiple genes. *J Exp Med*. 170:1369-1385.

Buchwald, P. 2010. Small-molecule protein-protein interaction inhibitors: therapeutic potential in light of molecular size, chemical space, and ligand binding efficiency considerations. *IUBMB Life*. 62:724-731.

Bultmann, A., Z. Li, S. Wagner, M. Peluso, T. Schonberger, C. Weis, I. Konrad, K. Stellos, S. Massberg, B. Nieswandt, M. Gawaz, M. Ungerer, and G. Munch. 2010. Impact of glycoprotein VI and platelet adhesion on atherosclerosis--a possible role of fibronectin. *J Mol Cell Cardiol*. 49:532-542.

Burkhart, J.M., M. Vaudel, S. Gambaryan, S. Radau, U. Walter, L. Martens, J. Geiger, A. Sickmann, and R.P. Zahedi. 2012. The first comprehensive and quantitative analysis of human platelet protein composition allows the comparative analysis of structural and functional pathways. *Blood*. 120:e73-82.

Burshtyn, D.N., W. Yang, T. Yi, and E.O. Long. 1997. A novel phosphotyrosine motif with a critical amino acid at position -2 for the SH2 domain-mediated activation of the tyrosine phosphatase SHP-1. *J Biol Chem*. 272:13066-13072.

Bye, A.P., A.J. Unsworth, and J.M. Gibbins. 2016. Platelet signaling: a complex interplay between inhibitory and activatory networks. *J Thromb Haemost*. 14:918-930.

Camilletti, A., N. Moretti, G. Giacchetti, E. Faloia, D. Martarelli, F. Mantero, and L. Mazzanti. 2001. Decreased nitric oxide levels and increased calcium content in platelets of hypertensive patients. *Am J Hypertens*. 14:382-386.

Carolyn S. Feldkamp, J.L.C. 1996. 2 - IMMUNE FUNCTION AND ANTIBODY STRUCTURE. *In* Immunoassay. T.K.C. Eleftherios P. Diamandis, editor. 5-24.

Chames, P., M. Van Regenmortel, E. Weiss, and D. Baty. 2009. Therapeutic antibodies: successes, limitations and hopes for the future. *Br J Pharmacol*. 157:220-233.

Chan, M.V., P.C. Armstrong, and T.D. Warner. 2018. 96-well plate-based aggregometry. *Platelets*. 29:650-655.

Chance, R.E., and B.H. Frank. 1993. Research, development, production, and safety of biosynthetic human insulin. *Diabetes Care*. 16 Suppl 3:133-142.

Chiu, M.L., D.R. Goulet, A. Teplyakov, and G.L. Gilliland. 2019. Antibody Structure and Function: The Basis for Engineering Therapeutics. *Antibodies (Basel)*. 8.

Clark, J.C., F.N. Damaskinaki, Y.F.H. Cheung, A. Slater, and S.P. Watson. 2021a. Structure-function relationship of the platelet glycoprotein VI (GPVI) receptor: does it matter if it is a dimer or monomer? *Platelets*. 32:724-732.

Clark, J.C., R.A.I. Neagoe, M. Zuidscherwoude, D.M. Kavanagh, A. Slater, E.M. Martin, M. Soave, D. Stegner, B. Nieswandt, N.S. Poulter, J. Hummert, D.P. Herten, M.G. Tomlinson, S.J. Hill, and S.P. Watson. 2021b. Evidence that GPVI is Expressed as a Mixture of Monomers and Dimers, and that the D2 Domain is not Essential for GPVI Activation. *Thromb Haemost*. 121:1435-1447.

Clemetson, J.M., J. Polgar, E. Magnenat, T.N. Wells, and K.J. Clemetson. 1999. The platelet collagen receptor glycoprotein VI is a member of the immunoglobulin superfamily closely related to FcalphaR and the natural killer receptors. *J Biol Chem*. 274:29019-29024.

Cohen, J.A., and C.H. Leeksma. 1956. Determination of the life span of human blood platelets using labelled diisopropylfluorophosphonate. *J Clin Invest*. 35:964-969.

Colas, P., B. Cohen, T. Jessen, I. Grishina, J. McCoy, and R. Brent. 1996. Genetic selection of peptide aptamers that recognize and inhibit cyclin-dependent kinase 2. *Nature*. 380:548-550.

Cosemans, J.M., M.J. Kuijpers, C. Lecut, S.T. Loubele, S. Heeneman, M. Jandrot-Perrus, and J.W. Heemskerk. 2005. Contribution of platelet glycoprotein VI to the thrombogenic effect of collagens in fibrous atherosclerotic lesions. *Atherosclerosis*. 181:19-27.

Coxon, C.H., M.J. Geer, and Y.A. Senis. 2017. ITIM receptors: more than just inhibitors of platelet activation. *Blood*. 129:3407-3418.

D'Ambrosio, D., K.L. Hippen, S.A. Minskoff, I. Mellman, G. Pani, K.A. Siminovitch, and J.C. Cambier. 1995. Recruitment and activation of PTP1C in negative regulation of antigen receptor signaling by Fc gamma RIIB1. *Science*. 268:293-297.

Daeron, M. 1995. Intracytoplasmic sequences involved in the biological properties of low-affinity receptors for IgG expressed by murine macrophages. *Braz J Med Biol Res*. 28:263-274.

Daeron, M. 1997. Fc receptor biology. *Annu Rev Immunol*. 15:203-234.

de Vet, E.C., B. Aguado, and R.D. Campbell. 2001. G6b, a novel immunoglobulin superfamily member encoded in the human major histocompatibility complex, interacts with SHP-1 and SHP-2. *J Biol Chem*. 276:42070-42076.

de Vet, E.C., S.A. Newland, P.A. Lyons, B. Aguado, and R.D. Campbell. 2005. The cell surface receptor G6b, a member of the immunoglobulin superfamily, binds heparin. *FEBS Lett*. 579:2355-2358.

Duggan, S. 2018. Caplacizumab: First Global Approval. *Drugs*. 78:1639-1642.

Duran-Saenz, N.Z., A. Serrano-Puente, P.I. Gallegos-Flores, B.D. Mendoza-Almanza, E.L. Esparza-Ibarra, S. Godina-Gonzalez, I.E. Gonzalez-Curiel, J.L. Ayala-Lujan, M. Hernandez-Barrales, C.F. Cueto-Villalobos, S.Y. Frausto-Fierros, L.A. Burciaga-Hernandez, and G. Mendoza-Almanza. 2022. Platelet Membrane: An Outstanding Factor in Cancer Metastasis. *Membranes (Basel)*. 12.

Durocher, Y., and M. Butler. 2009. Expression systems for therapeutic glycoprotein production. *Curr Opin Biotechnol*. 20:700-707.

Dutting, S., M. Bender, and B. Nieswandt. 2012. Platelet GPVI: a target for antithrombotic therapy?! *Trends Pharmacol Sci*. 33:583-590.

Elaskalani, O., I. Khan, M. Morici, C. Matthysen, M. Sabale, R.N. Martins, G. Verdile, and P. Metharom. 2018. Oligomeric and fibrillar amyloid beta 42 induce platelet aggregation partially through GPVI. *Platelets*. 29:415-420.

EMA, E.M.A. 2021. Biological medicine.

Esparza-Ibarra, E.L., J.L. Ayala-Lujan, B. Mendoza-Almanza, I. Gonzalez-Curiel, S. Godina-Gonzalez, M. Hernandez-Barrales, and G. Mendoza-Almanza. 2021. The Platelet Role in Severe and Fatal Forms of COVID-19. *Curr Mol Med*.

Ezumi, Y., T. Uchiyama, and H. Takayama. 2000. Molecular cloning, genomic structure, chromosomal localization, and alternative splice forms of the platelet collagen receptor glycoprotein VI. *Biochem Biophys Res Commun*. 277:27-36.

Falati, S., S. Patil, P.L. Gross, M. Stapleton, G. Merrill-Skoloff, N.E. Barrett, K.L. Pixton, H. Weiler, B. Cooley, D.K. Newman, P.J. Newman, B.C. Furie, B. Furie, and J.M. Gibbins. 2006. Platelet PECAM-1 inhibits thrombus formation in vivo. *Blood*. 107:535-541.

Faulds, D., and E.M. Sorkin. 1994. Abciximab (c7E3 Fab). A review of its pharmacology and therapeutic potential in ischaemic heart disease. *Drugs*. 48:583-598.

Feitsma, L.J., H.C. Brondijk, G.E. Jarvis, D. Hagemans, D.G. Bihan, N.E. Jerah, M. Versteeg, R.W. Farndale, and E.G. Huizinga. 2022. Structural insights into collagen-binding by platelet receptor Glycoprotein VI. *Blood*.

Florian, P., P. Wonerow, S. Harder, K. Kuczka, M. Dubar, and J. Graff. 2017. Anti-GPVI Fab SAR264565 effectively blocks GPVI function in ex vivo human platelets under arterial shear in a perfusion chamber. *Eur J Clin Pharmacol*. 73:949-956.

Forsythe, E.L., D.L. Maxwell, and M. Pusey. 2002. Vapor diffusion, nucleation rates and the reservoir to crystallization volume ratio. *Acta Crystallogr D Biol Crystallogr*. 58:1601-1605.

Fosgerau, K., and T. Hoffmann. 2015. Peptide therapeutics: current status and future directions. *Drug Discov Today*. 20:122-128.

Foster, H., C. Wilson, J.S. Gauer, R.G. Xu, M.J. Howard, I.W. Manfield, R. Ariens, K. Naseem, L.R. Vidler, H. Philippou, and R. Foster. 2022. A Comparative Assessment Study of Known Small-molecule GPVI Modulators. *ACS Med Chem Lett*. 13:171-181.

Fratantoni, J.C., and B.J. Poindexter. 1990. Measuring platelet aggregation with microplate reader. A new technical approach to platelet aggregation studies. *Am J Clin Pathol*. 94:613-617.

Fuster, V., L. Badimon, J.J. Badimon, and J.H. Chesebro. 1992a. The pathogenesis of coronary artery disease and the acute coronary syndromes (1). *N Engl J Med*. 326:242-250.

Fuster, V., L. Badimon, J.J. Badimon, and J.H. Chesebro. 1992b. The pathogenesis of coronary artery disease and the acute coronary syndromes (2). *N Engl J Med*. 326:310-318.

Gardiner, E.E., J.F. Arthur, M.L. Kahn, M.C. Berndt, and R.K. Andrews. 2004. Regulation of platelet membrane levels of glycoprotein VI by a platelet-derived metalloproteinase. *Blood*. 104:3611-3617.

Gardiner, E.E., D. Karunakaran, Y. Shen, J.F. Arthur, R.K. Andrews, and M.C. Berndt. 2007. Controlled shedding of platelet glycoprotein (GP)VI and GPIb-IX-V by ADAM family metalloproteinases. *J Thromb Haemost*. 5:1530-1537.

Gibbins, J.M. 2002. The negative regulation of platelet function: extending the role of the ITIM. *Trends Cardiovasc Med*. 12:213-219.

Gibson, D.G., L. Young, R.Y. Chuang, J.C. Venter, C.A. Hutchison, 3rd, and H.O. Smith. 2009. Enzymatic assembly of DNA molecules up to several hundred kilobases. *Nat Methods*. 6:343-345.

Giles, C. 1981. The platelet count and mean platelet volume. *Br J Haematol*. 48:31-37.

Gitz, E., A.Y. Pollitt, J.J. Gitz-Francois, O. Alshehri, J. Mori, S. Montague, G.B. Nash, M.R. Douglas, E.E. Gardiner, R.K. Andrews, C.D. Buckley, P. Harrison, and S.P. Watson. 2014. CLEC-2 expression is maintained on activated platelets and on platelet microparticles. *Blood*. 124:2262-2270.

Grozovsky, R., K.M. Hoffmeister, and H. Falet. 2010. Novel clearance mechanisms of platelets. *Curr Opin Hematol*. 17:585-589.

Gurbel, P.A., A. Myat, J. Kubica, and U.S. Tantry. 2016. State of the art: Oral antiplatelet therapy. *JRSM Cardiovasc Dis*. 5:2048004016652514.

Gurevich, E.V., and V.V. Gurevich. 2014. Therapeutic potential of small molecules and engineered proteins. *Handb Exp Pharmacol*. 219:1-12.

Hamers-Casterman, C., T. Atarhouch, S. Muyldermans, G. Robinson, C. Hamers, E.B. Songa, N. Bendahman, and R. Hamers. 1993. Naturally occurring antibodies devoid of light chains. *Nature*. 363:446-448.

Harris, L.J., S.B. Larson, K.W. Hasel, and A. McPherson. 1997. Refined structure of an intact IgG2a monoclonal antibody. *Biochemistry*. 36:1581-1597.

Hawiger, J. 1987. Macromolecules that link platelets following vessel wall injury. *Ann N Y Acad Sci*. 509:131-141.

Hermann, T., and D.J. Patel. 2000. Adaptive recognition by nucleic acid aptamers. *Science*. 287:820-825.

Herter, J.M., J. Rossaint, and A. Zarbock. 2014. Platelets in inflammation and immunity. *J Thromb Haemost*. 12:1764-1775.

Hofmann, I., M.J. Geer, T. Vogtle, A. Crispin, D.R. Campagna, A. Barr, M.L. Calicchio, S. Heising, J.P. van Geffen, M.J.E. Kuijpers, J.W.M. Heemskerk, J.A. Eble, K. Schmitz-Abe, E.A. Obeng, M. Douglas, K. Freson, C. Pondarre, R. Favier, G.E. Jarvis, K. Markianos, E. Turro, W.H. Ouwehand, A. Mazharian, M.D. Fleming, and Y.A. Senis. 2018. Congenital macrothrombocytopenia with focal myelofibrosis due to mutations in human G6b-B is rescued in humanized mice. *Blood*. 132:1399-1412.

Holinstat, M. 2017. Normal platelet function. *Cancer Metastasis Rev*. 36:195-198.

Holliger, P., and P.J. Hudson. 2005. Engineered antibody fragments and the rise of single domains. *Nat Biotechnol*. 23:1126-1136.

Horii, K., M.L. Kahn, and A.B. Herr. 2006. Structural basis for platelet collagen responses by the immune-type receptor glycoprotein VI. *Blood*. 108:936-942.

Ilari, A., and C. Savino. 2017. A Practical Approach to Protein Crystallography. *Methods Mol Biol*. 1525:47-78.

Induruwa, I., S.M. Jung, and E.A. Warburton. 2016. Beyond antiplatelets: The role of glycoprotein VI in ischemic stroke. *Int J Stroke*. 11:618-625.

Induruwa, I., M. Moroi, A. Bonna, J.D. Malcor, J.M. Howes, E.A. Warburton, R.W. Farndale, and S.M. Jung. 2018. Platelet collagen receptor Glycoprotein VI-dimer recognizes fibrinogen and fibrin through their D-domains, contributing to platelet adhesion and activation during thrombus formation. *J Thromb Haemost*. 16:389-404.

Inoue, O., K. Suzuki-Inoue, O.J. McCarty, M. Moroi, Z.M. Ruggeri, T.J. Kunicki, Y. Ozaki, and S.P. Watson. 2006. Laminin stimulates spreading of platelets through integrin alpha6beta1-dependent activation of GPVI. *Blood*. 107:1405-1412.

Irene, D., T.Y. Chung, B.J. Chen, T.H. Liu, F.Y. Li, J.T. Tzen, C.I. Wang, and C.L. Chyan. 2012. Solution structure of a phytocystatin from Ananas comosus and its molecular interaction with papain. *PLoS One*. 7:e47865.

Isakov, N. 1997. Immunoreceptor tyrosine-based activation motif (ITAM), a unique module linking antigen and Fc receptors to their signaling cascades. *J Leukoc Biol*. 61:6-16.

Italiano, J.E., Jr., P. Lecine, R.A. Shivdasani, and J.H. Hartwig. 1999. Blood platelets are assembled principally at the ends of proplatelet processes produced by differentiated megakaryocytes. *J Cell Biol*. 147:1299-1312.

Jandrot-Perrus, M., S. Busfield, A.H. Lagrue, X. Xiong, N. Debili, T. Chickering, J.P. Le Couedic, A. Goodearl, B. Dussault, C. Fraser, W. Vainchenker, and J.L. Villeval. 2000. Cloning, characterization, and functional studies of human and mouse glycoprotein VI: a platelet-specific collagen receptor from the immunoglobulin superfamily. *Blood*. 96:1798-1807.

Johnson, S., D. Evans, S. Laurenson, D. Paul, A.G. Davies, P. Ko Ferrigno, and C. Walti. 2008. Surface-immobilized peptide aptamers as probe molecules for protein detection. *Anal Chem*. 80:978-983.

Jones, C.I., S.F. Garner, L.A. Moraes, W.J. Kaiser, A. Rankin, C. Bloodomics, W.H. Ouwehand, A.H. Goodall, and J.M. Gibbins. 2009. PECAM-1 expression and activity negatively regulate multiple platelet signaling pathways. *FEBS Lett*. 583:3618-3624.

Jooss, N.J., I. De Simone, I. Provenzale, D.I. Fernandez, S.L.N. Brouns, R.W. Farndale, Y.M.C. Henskens, M.J.E. Kuijpers, H. Ten Cate, P.E.J. van der Meijden, R. Cavill, and J.W.M. Heemskerk. 2019. Role of Platelet Glycoprotein VI and Tyrosine Kinase Syk in Thrombus Formation on Collagen-Like Surfaces. *Int J Mol Sci*. 20.

Jung, S.M., M. Moroi, K. Soejima, T. Nakagaki, Y. Miura, M.C. Berndt, E.E. Gardiner, J.M. Howes, N. Pugh, D. Bihan, S.P. Watson, and R.W. Farndale. 2012. Constitutive dimerization of glycoprotein VI (GPVI) in resting platelets is essential for binding to collagen and activation in flowing blood. *J Biol Chem*. 287:30000-30013.

Jung, S.M., K. Tsuji, and M. Moroi. 2009. Glycoprotein (GP) VI dimer as a major collagen-binding site of native platelets: direct evidence obtained with dimeric GPVI-specific Fabs. *J Thromb Haemost*. 7:1347-1355.

Kang, Y., M.S. Son, and T.T. Hoang. 2007. One step engineering of T7-expression strains for protein production: increasing the host-range of the T7-expression system. *Protein Expr Purif*. 55:325-333.

Karas, S.P., W.F. Rosse, and R.J. Kurlander. 1982. Characterization of the IgG-Fc receptor on human platelets. *Blood*. 60:1277-1282.

Kearney, K.J., N. Pechlivani, R. King, C. Tiede, F. Phoenix, R. Cheah, F.L. Macrae, K.J. Simmons, I.W. Manfield, K.A. Smith, B.E.J. Spurgeon, K.M. Naseem, R.A.S. Ariens, M.J. McPherson, D.C. Tomlinson, and R.A. Ajjan. 2019. Affimer proteins as a tool to modulate fibrinolysis, stabilize the blood clot, and reduce bleeding complications. *Blood*. 133:1233-1244.

Kleinschnitz, C., M. Pozgajova, M. Pham, M. Bendszus, B. Nieswandt, and G. Stoll. 2007. Targeting platelets in acute experimental stroke: impact of glycoprotein Ib, VI, and IIb/IIIa blockade on infarct size, functional outcome, and intracranial bleeding. *Circulation*. 115:2323-2330.

Labelle, M., S. Begum, and R.O. Hynes. 2011. Direct signaling between platelets and cancer cells induces an epithelial-mesenchymal-like transition and promotes metastasis. *Cancer Cell*. 20:576-590.

Lebozec, K., M. Jandrot-Perrus, G. Avenard, O. Favre-Bulle, and P. Billiald. 2017. Design, development and characterization of ACT017, a humanized Fab that blocks platelet's glycoprotein VI function without causing bleeding risks. *MAbs*. 9:945-958.

Lecut, C., V. Arocas, H. Ulrichts, A. Elbaz, J.L. Villeval, J.J. Lacapere, H. Deckmyn, and M. Jandrot-Perrus. 2004a. Identification of residues within human glycoprotein VI involved in the binding to collagen: evidence for the existence of distinct binding sites. *J Biol Chem*. 279:52293-52299.

Lecut, C., A. Schoolmeester, M.J. Kuijpers, J.L. Broers, M.A. van Zandvoort, K. Vanhoorelbeke, H. Deckmyn, M. Jandrot-Perrus, and J.W. Heemskerk. 2004b. Principal role of glycoprotein VI in alpha2beta1 and alphaIIbbeta3 activation during collagen-induced thrombus formation. *Arterioscler Thromb Vasc Biol*. 24:1727-1733.

Lee, R.H., and W. Bergmeier. 2016. Platelet immunoreceptor tyrosine-based activation motif (ITAM) and hemITAM signaling and vascular integrity in inflammation and development. *J Thromb Haemost*. 14:645-654.

Lee, T.Y., C.C. Chang, W.J. Lu, T.L. Yen, K.H. Lin, P. Geraldine, J.Y. Li, and J.R. Sheu. 2017. Honokiol as a specific collagen receptor glycoprotein VI antagonist on human platelets: Functional ex vivo and in vivo studies. *Sci Rep*. 7:40002.

Lefrancais, E., G. Ortiz-Munoz, A. Caudrillier, B. Mallavia, F. Liu, D.M. Sayah, E.E. Thornton, M.B. Headley, T. David, S.R. Coughlin, M.F. Krummel, A.D. Leavitt, E. Passegue, and M.R. Looney. 2017. The lung is a site of platelet biogenesis and a reservoir for haematopoietic progenitors. *Nature*. 544:105-109.

Levine, R.F., P. Shoff, Z.C. Han, and A. Eldor. 1990. Circulating megakaryocytes and platelet production in the lungs. *Prog Clin Biol Res*. 356:41-52.

Lewandrowski, U., S. Wortelkamp, K. Lohrig, R.P. Zahedi, D.A. Wolters, U. Walter, and A. Sickmann. 2009. Platelet membrane proteomics: a novel repository for functional research. *Blood*. 114:e10-19.

Li, W., X. Tang, W. Yi, Q. Li, L. Ren, X. Liu, C. Chu, Y. Ozaki, J. Zhang, and L. Zhu. 2013. Glaucocalyxin A inhibits platelet activation and thrombus formation preferentially via GPVI signaling pathway. *PLoS One*. 8:e85120.

Locke, D., H. Chen, Y. Liu, C. Liu, and M.L. Kahn. 2002. Lipid rafts orchestrate signaling by the platelet receptor glycoprotein VI. *J Biol Chem*. 277:18801-18809.

Lockyer, S., K. Okuyama, S. Begum, S. Le, B. Sun, T. Watanabe, Y. Matsumoto, M. Yoshitake, J. Kambayashi, and N.N. Tandon. 2006. GPVI-deficient mice lack collagen responses and are protected against experimentally induced pulmonary thromboembolism. *Thromb Res*. 118:371-380.

Longo, P.A., J.M. Kavran, M.S. Kim, and D.J. Leahy. 2013. Transient mammalian cell transfection with polyethylenimine (PEI). *Methods Enzymol*. 529:227-240.

Loyau, S., B. Dumont, V. Ollivier, Y. Boulaftali, L. Feldman, N. Ajzenberg, and M. Jandrot-Perrus. 2012. Platelet glycoprotein VI dimerization, an active process inducing receptor competence, is an indicator of platelet reactivity. *Arterioscler Thromb Vasc Biol*. 32:778-785.

Makurvet, F.D. 2021. Biologics vs. small molecules: Drug costs and patient access. *Medicine in Drug Discovery*. Volume 9.

Mammadova-Bach, E., V. Ollivier, S. Loyau, M. Schaff, B. Dumont, R. Favier, G. Freyburger, V. Latger-Cannard, B. Nieswandt, C. Gachet, P.H. Mangin, and M. Jandrot-Perrus. 2015. Platelet glycoprotein VI binds to polymerized fibrin and promotes thrombin generation. *Blood*. 126:683-691.

Mangin, P.H., M.B. Onselaer, N. Receveur, N. Le Lay, A.T. Hardy, C. Wilson, X. Sanchez, S. Loyau, A. Dupuis, A.K. Babar, J.L. Miller, H. Philippou, C.E. Hughes, A.B. Herr, R.A. Ariens, D. Mezzano, M. Jandrot-Perrus, C. Gachet, and S.P. Watson. 2018. Immobilized fibrinogen activates human platelets through glycoprotein VI. *Haematologica*. 103:898-907.

Manne, B.K., T.M. Getz, C.E. Hughes, O. Alshehri, C. Dangelmaier, U.P. Naik, S.P. Watson, and S.P. Kunapuli. 2013. Fucoidan is a novel platelet agonist for the C-type lectin-like receptor 2 (CLEC-2). *J Biol Chem*. 288:7717-7726.

Martin, J.R., C.J. Craven, R. Jerala, L. Kroon-Zitko, E. Zerovnik, V. Turk, and J.P. Waltho. 1995. The three-dimensional solution structure of human stefin A. *J Mol Biol*. 246:331-343.

Matus, V., G. Valenzuela, C.G. Saez, P. Hidalgo, M. Lagos, E. Aranda, O. Panes, J. Pereira, X. Pillois, A.T. Nurden, and D. Mezzano. 2013. An adenine insertion in exon 6 of human GP6 generates a truncated protein associated with a bleeding disorder in four Chilean families. *J Thromb Haemost*. 11:1751-1759.

Mazharian, A., Y.J. Wang, J. Mori, D. Bem, B. Finney, S. Heising, P. Gissen, J.G. White, M.C. Berndt, E.E. Gardiner, B. Nieswandt, M.R. Douglas, R.D. Campbell, S.P. Watson, and Y.A. Senis. 2012. Mice lacking the ITIM-containing receptor G6b-B exhibit macrothrombocytopenia and aberrant platelet function. *Sci Signal*. 5:ra78.

Meng, D., M. Luo, and B. Liu. 2021. The Role of CLEC-2 and Its Ligands in Thromboinflammation. *Front Immunol*. 12:688643.

Miura, Y., M. Ohnuma, S.M. Jung, and M. Moroi. 2000. Cloning and expression of the platelet-specific collagen receptor glycoprotein VI. *Thromb Res*. 98:301-309.

Miura, Y., T. Takahashi, S.M. Jung, and M. Moroi. 2002. Analysis of the interaction of platelet collagen receptor glycoprotein VI (GPVI) with collagen. A dimeric form of GPVI, but not the monomeric form, shows affinity to fibrous collagen. *J Biol Chem*. 277:46197-46204.

Mohan, G., S.V. Malayala, P. Mehta, and M. Balla. 2020. A Comprehensive Review of Congenital Platelet Disorders, Thrombocytopenias and Thrombocytopathies. *Cureus*. 12:e11275.

Mori, J., A.C. Pearce, J.C. Spalton, B. Grygielska, J.A. Eble, M.G. Tomlinson, Y.A. Senis, and S.P. Watson. 2008. G6b-B inhibits constitutive and agonist-induced signaling by glycoprotein VI and CLEC-2. *J Biol Chem*. 283:35419-35427.

Moroi, M., S.M. Jung, M. Okuma, and K. Shinmyozu. 1989. A patient with platelets deficient in glycoprotein VI that lack both collagen-induced aggregation and adhesion. *J Clin Invest*. 84:1440-1445.

Morton, L.F., P.G. Hargreaves, R.W. Farndale, R.D. Young, and M.J. Barnes. 1995. Integrin alpha 2 beta 1-independent activation of platelets by simple collagen-like peptides: collagen tertiary (triple-helical) and quaternary (polymeric) structures are sufficient alone for alpha 2 beta 1-independent platelet reactivity. *Biochem J*. 306 (Pt 2):337-344.

Muyldermans, S. 2013. Nanobodies: natural single-domain antibodies. *Annu Rev Biochem*. 82:775-797.

Nagy, M., G. Perrella, A. Dalby, M.F. Becerra, L. Garcia Quintanilla, J.A. Pike, N.V. Morgan, E.E. Gardiner, J.W.M. Heemskerk, L. Azocar, J.F. Miquel, D. Mezzano, and S.P. Watson. 2020. Flow studies on human GPVI-deficient blood under coagulating and noncoagulating conditions. *Blood Adv*. 4:2953-2961.

Navarro, S., D. Stegner, B. Nieswandt, J.W.M. Heemskerk, and M.J.E. Kuijpers. 2021. Temporal Roles of Platelet and Coagulation Pathways in Collagen- and Tissue Factor-Induced Thrombus Formation. *Int J Mol Sci*. 23.

Nelson, A.L. 2010. Antibody fragments: hope and hype. *MAbs*. 2:77-83.

Newland, S.A., I.C. Macaulay, A.R. Floto, E.C. de Vet, W.H. Ouwehand, N.A. Watkins, P.A. Lyons, and D.R. Campbell. 2007. The novel inhibitory receptor G6B is expressed on the surface of platelets and attenuates platelet function in vitro. *Blood*. 109:4806-4809.

Newman, P.J. 1999. Switched at birth: a new family for PECAM-1. *J Clin Invest*. 103:5-9.

Newman, P.J., M.C. Berndt, J. Gorski, G.C. White, 2nd, S. Lyman, C. Paddock, and W.A. Muller. 1990. PECAM-1 (CD31) cloning and relation to adhesion molecules of the immunoglobulin gene superfamily. *Science*. 247:1219-1222.

Ngo, H.X., and S. Garneau-Tsodikova. 2018. What are the drugs of the future? *Medchemcomm*. 9:757-758.

Nieswandt, B., W. Bergmeier, V. Schulte, K. Rackebrandt, J.E. Gessner, and H. Zirngibl. 2000. Expression and function of the mouse collagen receptor glycoprotein VI is strictly dependent on its association with the FcRgamma chain. *J Biol Chem*. 275:23998-24002.

Nieswandt, B., I. Pleines, and M. Bender. 2011. Platelet adhesion and activation mechanisms in arterial thrombosis and ischaemic stroke. *J Thromb Haemost*. 9 Suppl 1:92-104.

Nieswandt, B., V. Schulte, W. Bergmeier, R. Mokhtari-Nejad, K. Rackebrandt, J.P. Cazenave, P. Ohlmann, C. Gachet, and H. Zirngibl. 2001. Long-term antithrombotic protection by in vivo depletion of platelet glycoprotein VI in mice. *J Exp Med*. 193:459-469.

Novinska, M., V. Rathore, D. Newman, and P. Newman. 2007. Chapter 11—Pecam-1 Platelets. Academic Press.

Nurbhai, S., K.J. Roberts, T.M. Carlton, L. Maggiore, M.F. Cubitt, K.P. Ray, J. Reckless, H. Mohammed, P. Irving, T.T. MacDonald, A. Vossenkamper, M.R. West, G.C. Parkes, and J.S. Crowe. 2019. Oral Anti-Tumour Necrosis Factor Domain Antibody V565 Provides High Intestinal Concentrations, and Reduces Markers of Inflammation in Ulcerative Colitis Patients. *Sci Rep*. 9:14042.

Nusca, A., D. Tuccinardi, S. Pieralice, S. Giannone, M. Carpenito, L. Monte, M. Watanabe, I. Cavallari, E. Maddaloni, G.P. Ussia, S. Manfrini, and F. Grigioni. 2021. Platelet Effects of Anti-diabetic Therapies: New Perspectives in the Management of Patients with Diabetes and Cardiovascular Disease. *Front Pharmacol*. 12:670155.

O'Brien, J.R. 1961. The adhesiveness of native platelets and its prevention. *J Clin Pathol*. 14:140-149.

O'Connor, M.N., P.A. Smethurst, R.W. Farndale, and W.H. Ouwehand. 2006. Gain- and loss-of-function mutants confirm the importance of apical residues to the primary interaction of human glycoprotein VI with collagen. *J Thromb Haemost*. 4:869-873.

Onselaer, M.B., A.T. Hardy, C. Wilson, X. Sanchez, A.K. Babar, J.L.C. Miller, C.N. Watson, S.K. Watson, A. Bonna, H. Philippou, A.B. Herr, D. Mezzano, R.A.S. Ariens, and S.P. Watson. 2017. Fibrin and D-dimer bind to monomeric GPVI. *Blood Adv*. 1:1495-1504.

Pasquet, J.M., B. Gross, L. Quek, N. Asazuma, W. Zhang, C.L. Sommers, E. Schweighoffer, V. Tybulewicz, B. Judd, J.R. Lee, G. Koretzky, P.E. Love, L.E. Samelson, and S.P. Watson. 1999. LAT is required for tyrosine phosphorylation of phospholipase cgamma2 and platelet activation by the collagen receptor GPVI. *Mol Cell Biol*. 19:8326-8334.

Patil, S., D.K. Newman, and P.J. Newman. 2001. Platelet endothelial cell adhesion molecule-1 serves as an inhibitory receptor that modulates platelet responses to collagen. *Blood*. 97:1727-1732.

Porath, J., and P. Flodin. 1959. Gel filtration: a method for desalting and group separation. *Nature*. 183:1657-1659.

Poulter, N.S., A.Y. Pollitt, D.M. Owen, E.E. Gardiner, R.K. Andrews, H. Shimizu, D. Ishikawa, D. Bihan, R.W. Farndale, M. Moroi, S.P. Watson, and S.M. Jung. 2017. Clustering of glycoprotein VI (GPVI) dimers upon adhesion to collagen as a mechanism to regulate GPVI signaling in platelets. *J Thromb Haemost*. 15:549-564.

Rayes, J., S.P. Watson, and B. Nieswandt. 2019. Functional significance of the platelet immune receptors GPVI and CLEC-2. *J Clin Invest*. 129:12-23.

Reininger, A.J., I. Bernlochner, S.M. Penz, C. Ravanat, P. Smethurst, R.W. Farndale, C. Gachet, R. Brandl, and W. Siess. 2010. A 2-step mechanism of arterial thrombus formation induced by human atherosclerotic plaques. *J Am Coll Cardiol*. 55:1147-1158.

Rendu, F., and B. Brohard-Bohn. 2001. The platelet release reaction: granules' constituents, secretion and functions. *Platelets*. 12:261-273.

Reth, M. 1989. Antigen receptor tail clue. *Nature*. 338:383-384.

Reverdatto, S., D.S. Burz, and A. Shekhtman. 2015. Peptide aptamers: development and applications. *Curr Top Med Chem*. 15:1082-1101.

Riba, R., C.E. Hughes, A. Graham, S.P. Watson, and K.M. Naseem. 2008. Globular adiponectin induces platelet activation through the collagen receptor GPVI-Fc receptor gamma chain complex. *J Thromb Haemost*. 6:1012-1020.

Robinson, M.J., D. Sancho, E.C. Slack, S. LeibundGut-Landmann, and C. Reis e Sousa. 2006. Myeloid C-type lectins in innate immunity. *Nat Immunol*. 7:1258-1265.

Rosenfeld, S.I., R.J. Looney, J.P. Leddy, D.C. Phipps, G.N. Abraham, and C.L. Anderson. 1985. Human platelet Fc receptor for immunoglobulin G. Identification as a 40,000-molecular-weight membrane protein shared by monocytes. *J Clin Invest*. 76:2317-2322.

Rosenfeld, S.I., D.H. Ryan, R.J. Looney, C.L. Anderson, G.N. Abraham, and J.P. Leddy. 1987. Human Fc gamma receptors: stable inter-donor variation in quantitative expression on platelets correlates with functional responses. *J Immunol*. 138:2869-2873.

Ross, R. 1993. The pathogenesis of atherosclerosis: a perspective for the 1990s. *Nature*. 362:801-809.

Roth, G.A., G.A. Mensah, C.O. Johnson, G. Addolorato, E. Ammirati, L.M. Baddour, N.C. Barengo, A.Z. Beaton, E.J. Benjamin, C.P. Benziger, A. Bonny, M. Brauer, M. Brodmann, T.J. Cahill, J. Carapetis, A.L. Catapano, S.S. Chugh, L.T. Cooper, J. Coresh, M. Criqui, N. DeCleene, K.A. Eagle, S. Emmons-Bell, V.L. Feigin, J. Fernandez-Sola, G. Fowkes, E. Gakidou, S.M. Grundy, F.J. He, G. Howard, F. Hu, L. Inker, G. Karthikeyan, N. Kassebaum, W. Koroshetz, C. Lavie, D. Lloyd-Jones, H.S. Lu, A. Mirijello, A.M. Temesgen, A. Mokdad, A.E. Moran, P. Muntner, J. Narula, B. Neal, M. Ntsekhe, G. Moraes de Oliveira, C. Otto, M. Owolabi, M. Pratt, S. Rajagopalan, M. Reitsma, A.L.P. Ribeiro, N. Rigotti, A. Rodgers, C. Sable, S. Shakil, K. Sliwa-Hahnle, B. Stark, J. Sundstrom, P. Timpel, I.M. Tleyjeh, M. Valgimigli, T. Vos, P.K. Whelton, M. Yacoub, L. Zuhlke, C. Murray, V. Fuster, and G.-N.-J.G.B.o.C.D.W. Group. 2020. Global Burden of Cardiovascular Diseases and Risk Factors, 1990-2019: Update From the GBD 2019 Study. *J Am Coll Cardiol*. 76:2982-3021.

Rubinstein, E., C. Boucheix, R.E. Worthington, and R.C. Carroll. 1995. Anti-platelet antibody interactions with Fc gamma receptor. *Semin Thromb Hemost*. 21:10-22.

Ruggeri, Z.M. 2002. Platelets in atherothrombosis. *Nat Med*. 8:1227-1234.

Schroeder, H.W., Jr., and L. Cavacini. 2010. Structure and function of immunoglobulins. *J Allergy Clin Immunol*. 125:S41-52.

Schulte, V., D. Snell, W. Bergmeier, H. Zirngibl, S.P. Watson, and B. Nieswandt. 2001. Evidence for two distinct epitopes within collagen for activation of murine platelets. *J Biol Chem*. 276:364-368.

Seizer, P., O. Borst, H.F. Langer, A. Bultmann, G. Munch, Y. Herouy, K. Stellos, B. Kramer, B. Bigalke, B. Buchele, M.G. Bachem, D. Vestweber, T. Simmet, M. Gawaz, and A.E. May. 2009. EMMPRIN (CD147) is a novel receptor for platelet GPVI and mediates platelet rolling via GPVI-EMMPRIN interaction. *Thromb Haemost*. 101:682-686.

Selvadurai, M.V., and J.R. Hamilton. 2018. Structure and function of the open canalicular system - the platelet's specialized internal membrane network. *Platelets*. 29:319-325.

Senis, Y.A., R. Antrobus, S. Severin, A.F. Parguina, I. Rosa, N. Zitzmann, S.P. Watson, and A. Garcia. 2009. Proteomic analysis of integrin alphaIIbbeta3 outside-in signaling reveals Src-kinase-independent phosphorylation of Dok-1 and Dok-3 leading to SHIP-1 interactions. *J Thromb Haemost*. 7:1718-1726.

Senis, Y.A., M.G. Tomlinson, A. Garcia, S. Dumon, V.L. Heath, J. Herbert, S.P. Cobbold, J.C. Spalton, S. Ayman, R. Antrobus, N. Zitzmann, R. Bicknell, J. Frampton, K.S. Authi, A. Martin, M.J. Wakelam, and S.P. Watson. 2007. A comprehensive proteomics and genomics analysis reveals novel transmembrane proteins in human platelets and mouse megakaryocytes including G6b-B, a novel immunoreceptor tyrosine-based inhibitory motif protein. *Mol Cell Proteomics*. 6:548-564.

Severin, S., C.A. Nash, J. Mori, Y. Zhao, C. Abram, C.A. Lowell, Y.A. Senis, and S.P. Watson. 2012. Distinct and overlapping functional roles of Src family kinases in mouse platelets. *J Thromb Haemost*. 10:1631-1645.

Shimamoto, G., C. Gegg, T. Boone, and C. Queva. 2012. Peptibodies: A flexible alternative format to antibodies. *MAbs*. 4:586-591.

Sidorenko, S.P., and E.A. Clark. 2003. The dual-function CD150 receptor subfamily: the viral attraction. *Nat Immunol*. 4:19-24.

Slater, A., Y. Di, J.C. Clark, N.J. Jooss, E.M. Martin, F. Alenazy, M.R. Thomas, R.A.S. Ariens, A.B. Herr, N.S. Poulter, J. Emsley, and S.P. Watson. 2021. Structural characterization of a novel GPVI-nanobody complex reveals a biologically active domain-swapped GPVI dimer. *Blood*. 137:3443-3453.

Slater, A., G. Perrella, M.B. Onselaer, E.M. Martin, J.S. Gauer, R.G. Xu, J.W. Heemskerk, R.A.S. Ariens, and S.P. Watson. 2018. Does fibrin(ogen) bind to monomeric or dimeric GPVI, or not at all? *Platelets*:1-9.

Smethurst, P.A., L. Joutsi-Korhonen, M.N. O'Connor, E. Wilson, N.S. Jennings, S.F. Garner, Y. Zhang, C.G. Knight, T.R. Dafforn, A. Buckle, I.J. MJ, P.G. De Groot, N.A. Watkins, R.W. Farndale, and W.H. Ouwehand. 2004. Identification of the primary collagen-binding surface on human glycoprotein VI by site-directed mutagenesis and by a blocking phage antibody. *Blood*. 103:903-911.

Smethurst, P.A., D.J. Onley, G.E. Jarvis, M.N. O'Connor, C.G. Knight, A.B. Herr, W.H. Ouwehand, and R.W. Farndale. 2007. Structural basis for the platelet-collagen interaction: the smallest motif within collagen that recognizes and activates platelet Glycoprotein VI contains two glycine-proline-hydroxyproline triplets. *J Biol Chem*. 282:1296-1304.

Smith, G.P. 1985. Filamentous fusion phage: novel expression vectors that display cloned antigens on the virion surface. *Science*. 228:1315-1317.

Soriano Jerez, E.M., J.M. Gibbins, and C.E. Hughes. 2021. Targeting platelet inhibition receptors for novel therapies: PECAM-1 and G6b-B. *Platelets*. 32:761-769.

Stadler, L.K., T. Hoffmann, D.C. Tomlinson, Q. Song, T. Lee, M. Busby, Y. Nyathi, E. Gendra, C. Tiede, K. Flanagan, S.J. Cockell, A. Wipat, C. Harwood, S.D. Wagner, M.A. Knowles, J.J. Davis, N. Keegan, and P.K. Ferrigno. 2011. Structure-function studies of an engineered scaffold protein derived from Stefin A. II: Development and applications of the SQT variant. *Protein Eng Des Sel*. 24:751-763.

Steevels, T.A., G.H. Westerlaken, M.R. Tijssen, P.J. Coffer, P.J. Lenting, J.W. Akkerman, and L. Meyaard. 2010. Co-expression of the collagen receptors leukocyte-associated immunoglobulin-like receptor-1 and glycoprotein VI on a subset of megakaryoblasts. *Haematologica*. 95:2005-2012.

Stegner, D., E.J. Haining, and B. Nieswandt. 2014. Targeting glycoprotein VI and the immunoreceptor tyrosine-based activation motif signaling pathway. *Arterioscler Thromb Vasc Biol*. 34:1615-1620.

Stephens, G., Y. Yan, M. Jandrot-Perrus, J.L. Villeval, K.J. Clemetson, and D.R. Phillips. 2005. Platelet activation induces metalloproteinase-dependent GP VI cleavage to down-regulate platelet reactivity to collagen. *Blood*. 105:186-191.

Stockinger, H., S.J. Gadd, R. Eher, O. Majdic, W. Schreiber, W. Kasinrerk, B. Strass, E. Schnabl, and W. Knapp. 1990. Molecular characterization and functional analysis of the leukocyte surface protein CD31. *J Immunol*. 145:3889-3897.

Sugiyama, T., M. Okuma, F. Ushikubi, S. Sensaki, K. Kanaji, and H. Uchino. 1987. A novel platelet aggregating factor found in a patient with defective collagen-induced platelet aggregation and autoimmune thrombocytopenia. *Blood*. 69:1712-1720.

Sultana, A., and J.E. Lee. 2015. Measuring protein-protein and protein-nucleic Acid interactions by biolayer interferometry. *Curr Protoc Protein Sci*. 79:19 25 11-19 25 26.

Suzuki-Inoue, K., G.L. Fuller, A. Garcia, J.A. Eble, S. Pohlmann, O. Inoue, T.K. Gartner, S.C. Hughan, A.C. Pearce, G.D. Laing, R.D. Theakston, E. Schweighoffer, N. Zitzmann, T. Morita, V.L. Tybulewicz, Y. Ozaki, and S.P. Watson. 2006. A novel

Syk-dependent mechanism of platelet activation by the C-type lectin receptor CLEC-2. *Blood*. 107:542-549.

Suzuki-Inoue, K., D. Tulasne, Y. Shen, T. Bori-Sanz, O. Inoue, S.M. Jung, M. Moroi, R.K. Andrews, M.C. Berndt, and S.P. Watson. 2002. Association of Fyn and Lyn with the proline-rich domain of glycoprotein VI regulates intracellular signaling. *J Biol Chem*. 277:21561-21566.

Suzuki Inoue, K., O. Inoue, and Y. Ozaki. 2010. [Identification of the novel platelet activation receptor CLEC-2 and Its pathological and physiological roles]. *Rinsho Byori*. 58:1193-1202.

Tang, A.A., C. Tiede, D.J. Hughes, M.J. McPherson, and D.C. Tomlinson. 2017. Isolation of isoform-specific binding proteins (Affimers) by phage display using negative selection. *Sci Signal*. 10.

Taylor, L., S.R. Vasudevan, C.I. Jones, J.M. Gibbins, G.C. Churchill, R.D. Campbell, and C.H. Coxon. 2014. Discovery of novel GPVI receptor antagonists by structure-based repurposing. *PLoS One*. 9:e101209.

Tiede, C., R. Bedford, S.J. Heseltine, G. Smith, I. Wijetunga, R. Ross, D. AlQallaf, A.P. Roberts, A. Balls, A. Curd, R.E. Hughes, H. Martin, S.R. Needham, L.C. Zanetti-Domingues, Y. Sadigh, T.P. Peacock, A.A. Tang, N. Gibson, H. Kyle, G.W. Platt, N. Ingram, T. Taylor, L.P. Coletta, I. Manfield, M. Knowles, S. Bell, F. Esteves, A. Maqbool, R.K. Prasad, M. Drinkhill, R.S. Bon, V. Patel, S.A. Goodchild, M. Martin-Fernandez, R.J. Owens, J.E. Nettleship, M.E. Webb, M. Harrison, J.D. Lippiat, S. Ponnambalam, M. Peckham, A. Smith, P.K. Ferrigno, M. Johnson, M.J. McPherson, and D.C. Tomlinson. 2017. Affimer proteins are versatile and renewable affinity reagents. *Elife*. 6.

Tiede, C., A.A. Tang, S.E. Deacon, U. Mandal, J.E. Nettleship, R.L. Owen, S.E. George, D.J. Harrison, R.J. Owens, D.C. Tomlinson, and M.J. McPherson. 2014. Adhiron: a stable and versatile peptide display scaffold for molecular recognition applications. *Protein Eng Des Sel*. 27:145-155.

Tomiyama, Y., T.J. Kunicki, T.F. Zipf, S.B. Ford, and R.H. Aster. 1992. Response of human platelets to activating monoclonal antibodies: importance of Fc gamma RII (CD32) phenotype and level of expression. *Blood*. 80:2261-2268.

Tomlinson, M.G., S.D. Calaminus, O. Berlanga, J.M. Auger, T. Bori-Sanz, L. Meyaard, and S.P. Watson. 2007. Collagen promotes sustained glycoprotein VI signaling in platelets and cell lines. *J Thromb Haemost*. 5:2274-2283.

Tuerk, C., and L. Gold. 1990. Systematic evolution of ligands by exponential enrichment: RNA ligands to bacteriophage T4 DNA polymerase. *Science*. 249:505-510.

Ungerer, M., Z. Li, C. Baumgartner, S. Goebel, J. Vogelmann, H.P. Holthoff, M. Gawaz, and G. Munch. 2013. The GPVI-Fc fusion protein Revacept reduces thrombus formation and improves vascular dysfunction in atherosclerosis without any impact on bleeding times. *PLoS One*. 8:e71193.

Ungerer, M., K. Rosport, A. Bultmann, R. Piechatzek, K. Uhland, P. Schlieper, M. Gawaz, and G. Munch. 2011. Novel antiplatelet drug revacept (Dimeric Glycoprotein VI-Fc) specifically and efficiently inhibited collagen-induced platelet aggregation without affecting general hemostasis in humans. *Circulation*. 123:1891-1899.

van der Meijden, P.E.J., and J.W.M. Heemskerk. 2019. Platelet biology and functions: new concepts and clinical perspectives. *Nat Rev Cardiol*. 16:166-179.

Verschoor, A., and H.F. Langer. 2013. Crosstalk between platelets and the complement system in immune protection and disease. *Thromb Haemost*. 110:910-919.

Vivier, E., and M. Daeron. 1997. Immunoreceptor tyrosine-based inhibition motifs. *Immunol Today*. 18:286-291.

Vogtle, T., S. Sharma, J. Mori, Z. Nagy, D. Semeniak, C. Scandola, M.J. Geer, C.W. Smith, J. Lane, S. Pollack, R. Lassila, A. Jouppila, A.J. Barr, D.J. Ogg, T.D. Howard, H.J. McMiken, J. Warwicker, C. Geh, R. Rowlinson, W.M. Abbott, A. Eckly, H. Schulze, G.J. Wright, A. Mazharian, K. Futterer, S. Rajesh, M.R. Douglas, and Y.A. Senis. 2019. Heparan sulfates are critical regulators of the inhibitory megakaryocyte-platelet receptor G6b-B. *Elife*. 8.

Voors-Pette, C., K. Lebozec, P. Dogterom, L. Jullien, P. Billiald, P. Ferlan, L. Renaud, O. Favre-Bulle, G. Avenard, M. Machacek, Y. Pletan, and M. Jandrot-Perrus. 2019. Safety and Tolerability, Pharmacokinetics, and Pharmacodynamics of ACT017, an Antiplatelet GPVI (Glycoprotein VI) Fab. *Arterioscler Thromb Vasc Biol*. 39:956-964.

Washington, A.V., R.L. Schubert, L. Quigley, T. Disipio, R. Feltz, E.H. Cho, and D.W. McVicar. 2004. A TREM family member, TLT-1, is found exclusively in the alpha-granules of megakaryocytes and platelets. *Blood*. 104:1042-1047.

Watson, S.P., J.M. Herbert, and A.Y. Pollitt. 2010. GPVI and CLEC-2 in hemostasis and vascular integrity. *J Thromb Haemost*. 8:1456-1467.

WHO. 2021a. Cardiovascular diseases (CVDs).

WHO, W.H.O. 2021b. 22nd World Health Organization model lists of essential medicines.

Wlodawer, A., W. Minor, Z. Dauter, and M. Jaskolski. 2013. Protein crystallography for aspiring crystallographers or how to avoid pitfalls and traps in macromolecular structure determination. *FEBS J*. 280:5705-5736.

Wonerow, P., A. Obergfell, J.I. Wilde, R. Bobe, N. Asazuma, T. Brdicka, A. Leo, B. Schraven, V. Horejsi, S.J. Shattil, and S.P. Watson. 2002. Differential role of glycolipid-enriched membrane domains in glycoprotein VI- and integrin-mediated phospholipase Cgamma2 regulation in platelets. *Biochem J*. 364:755-765.

Woodman, R., J.T. Yeh, S. Laurenson, and P. Ko Ferrigno. 2005. Design and validation of a neutral protein scaffold for the presentation of peptide aptamers. *J Mol Biol*. 352:1118-1133.

Xu, D.H., X.Y. Wang, Y.L. Jia, T.Y. Wang, Z.W. Tian, X. Feng, and Y.N. Zhang. 2018. SV40 intron, a potent strong intron element that effectively increases transgene expression in transfected Chinese hamster ovary cells. *J Cell Mol Med*. 22:2231-2239.

Yeung, J., and M. Holinstat. 2012. Newer agents in antiplatelet therapy: a review. *J Blood Med*. 3:33-42.

Yousuf, O., and D.L. Bhatt. 2011. The evolution of antiplatelet therapy in cardiovascular disease. *Nat Rev Cardiol*. 8:547-559.

Zeiler, M., M. Moser, and M. Mann. 2014. Copy number analysis of the murine platelet proteome spanning the complete abundance range. *Mol Cell Proteomics*. 13:3435-3445.

Zhang, S., Y. Liu, X. Wang, L. Yang, H. Li, Y. Wang, M. Liu, X. Zhao, Y. Xie, Y. Yang, S. Zhang, Z. Fan, J. Dong, Z. Yuan, Z. Ding, Y. Zhang, and L. Hu. 2020. SARS-CoV-2 binds platelet ACE2 to enhance thrombosis in COVID-19. *J Hematol Oncol*. 13:120.

Zheng, Y.M., C. Liu, H. Chen, D. Locke, J.C. Ryan, and M.L. Kahn. 2001. Expression of the platelet receptor GPVI confers signaling via the Fc receptor gamma -chain

in response to the snake venom convulxin but not to collagen. *J Biol Chem*. 276:12999-13006.

8 APPENDIX

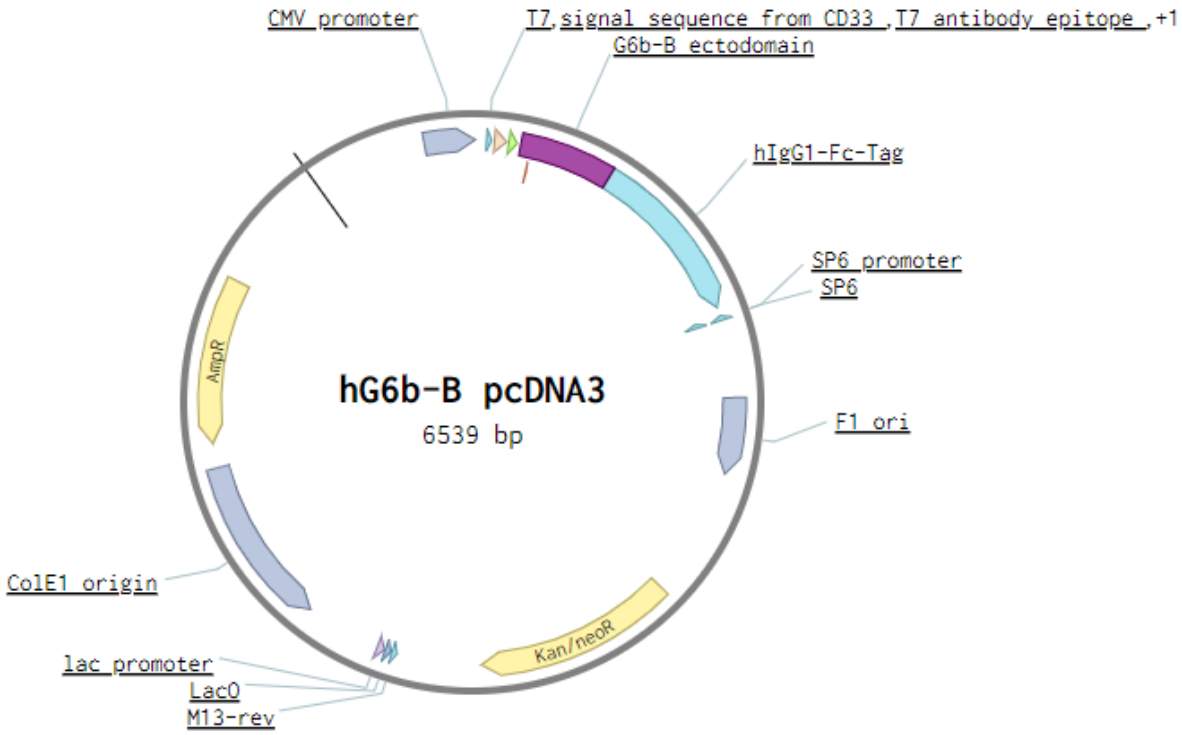

Figure 8.1. Plasmid map of hG6b-B pcDNA3.

G6b-B is in frame with hIgG-Fc-tag sequence upstream. Image generated with the online tool Benchling. Plasmid kindly provided by Prof Michael Douglas (University of Birmingham, UK).

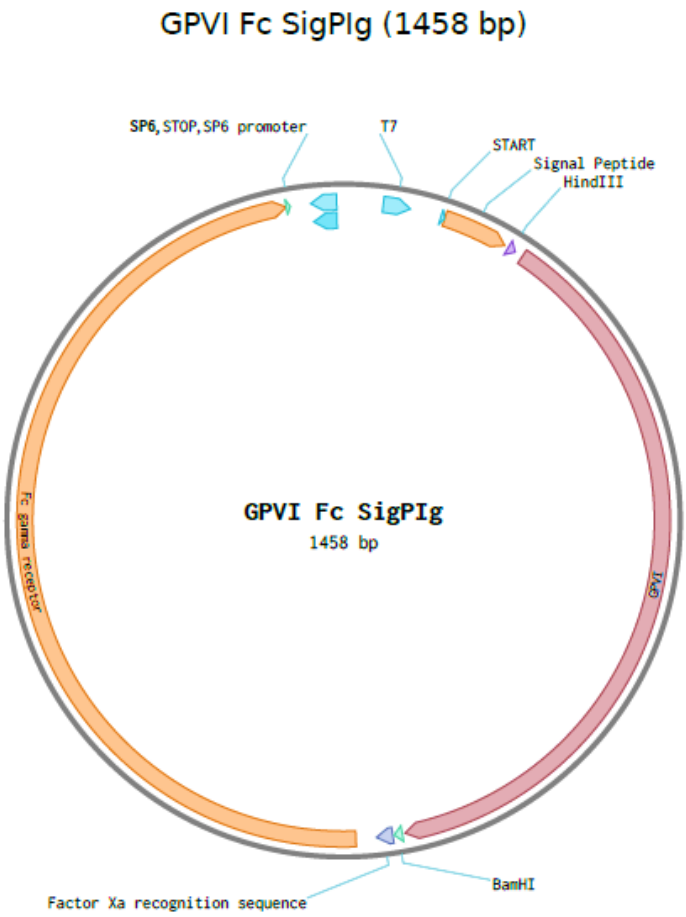

Figure 8.2. GPVI-Fc SigpIg+ expression vector.

SigpIg+ mammalian expression vector with GPVI ectodomain sequence inserted encoding an N-terminal CD33 signal sequence and a C-terminal human IgG1-Fc sequence. Plasmid kindly provided by Prof. Andrew Herr (Cincinnati Children's Hospital).

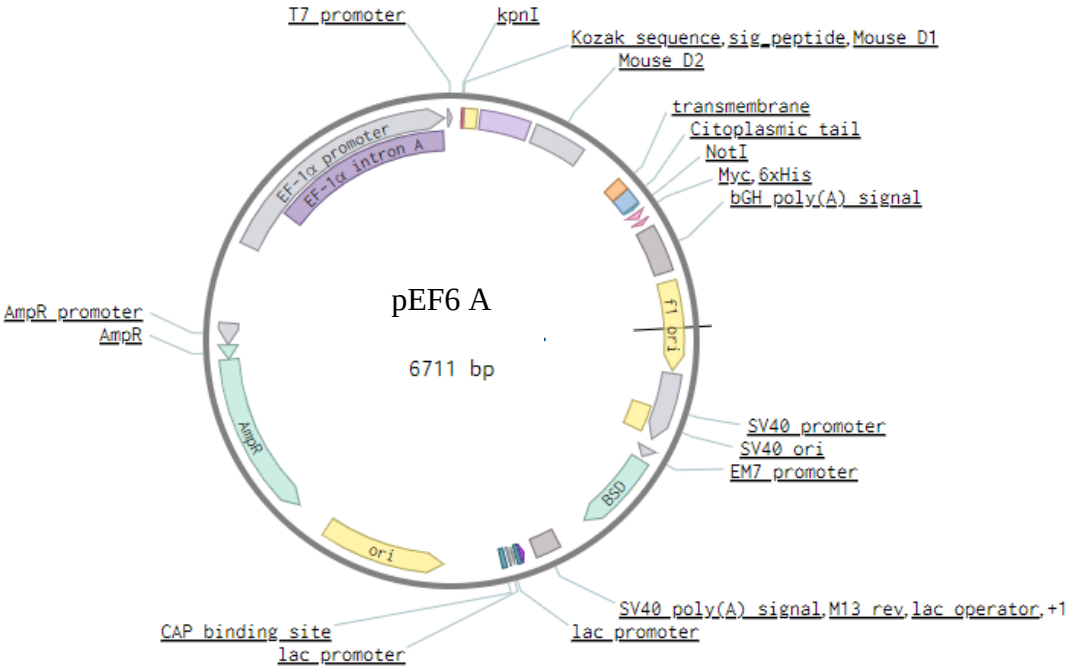

Figure 8.3. pEf6 A plasmid.

Chimera representative vector with GPVI sequence inserted between restriction sites KpnI and NotI. Image generated with the online tool Benchling.

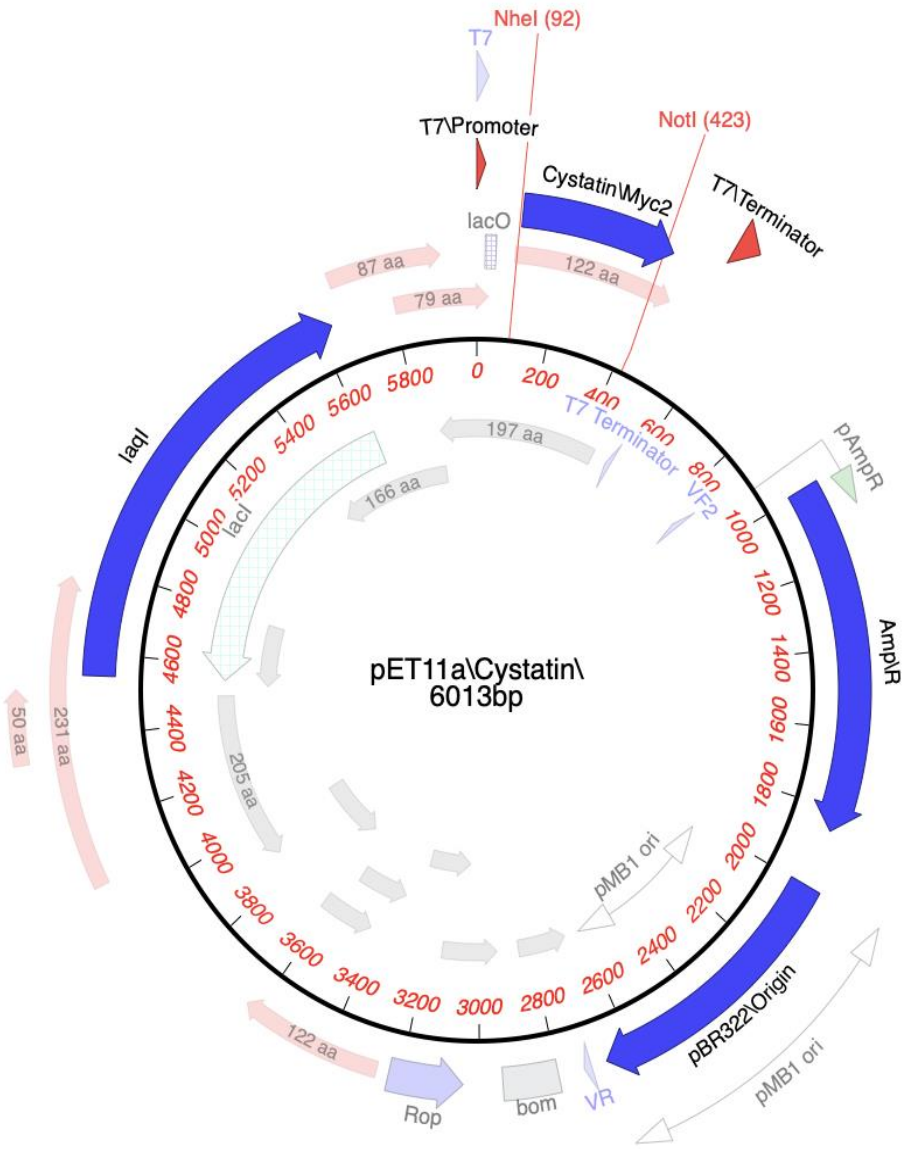

Figure 8.4. Plasmid map of pET11a.

Affimers were cloned in frame into the vector containing a His-tag sequence upstream. Image kindly provided by Dr. Christian Tiede (University of Leeds, UK).

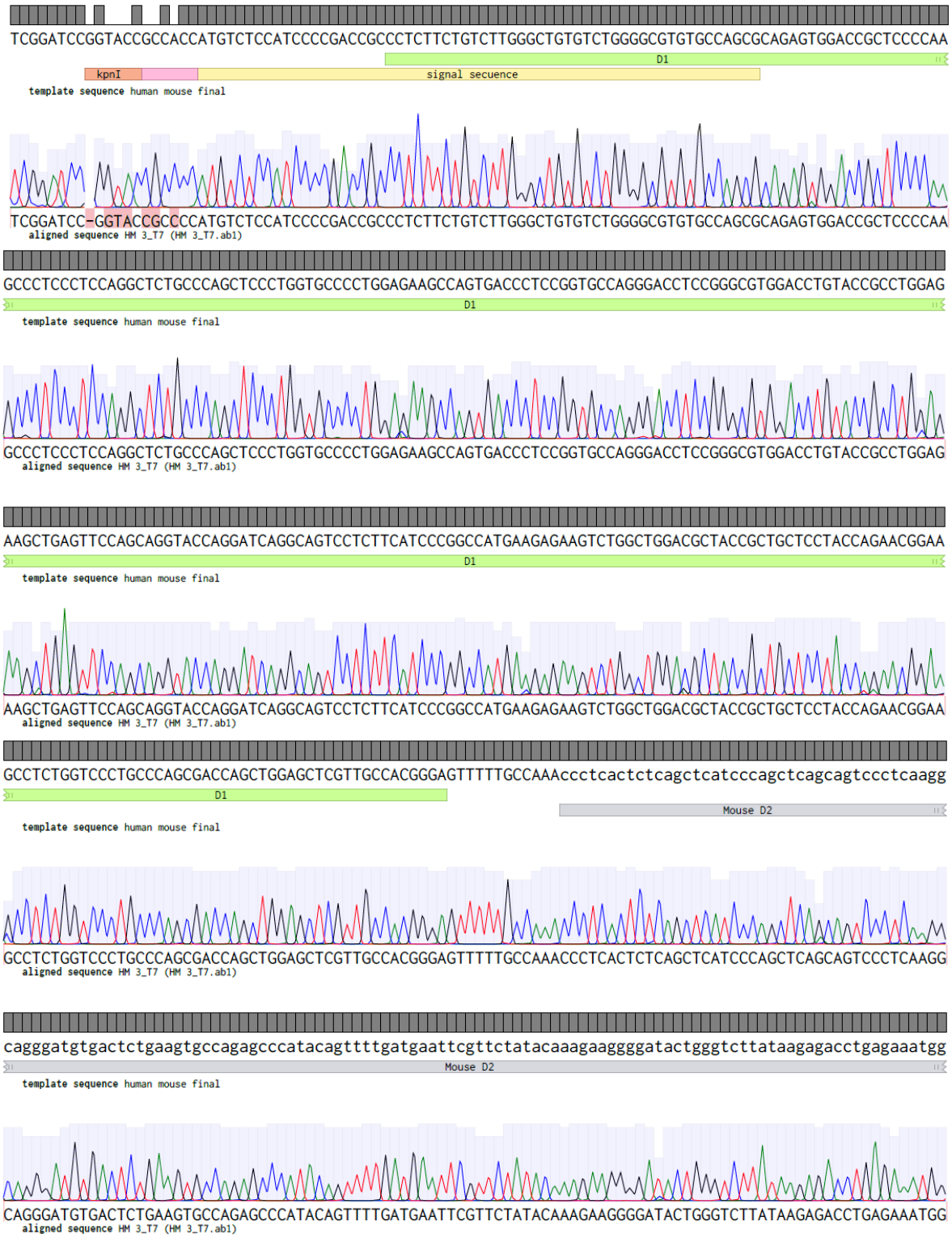
TCGGATCCGGTACCGCCACCATGTCTCCATCCCCGACCGCCCTCTTCTGTCTTGGGCTGTGTCTGGGGCGTGTGCCAGCGCAGAGTGGACCGCTCCCCAA
D1
kpnI
signal secuence
template sequence human mouse final
TCGGATCC-GGTACCGCCCCATGTCTCCATCCCCGACCGCCCTCTTCTGTCTTGGGCTGTGTCTGGGGCGTGTGCCAGCGCAGAGTGGACCGCTCCCCAA
aligned sequence HM 3_T7 (HM 3_T7.ab1)
GCCCTCCCTCCAGGCTCTGCCCAGCTCCCTGGTGCCCCTGGAGAAGCCAGTGACCCTCCGGTGCCAGGGACCTCCGGGCGTGGACCTGTACCGCCTGGAG
D1
template sequence human mouse final
GCCCTCCCTCCAGGCTCTGCCCAGCTCCCTGGTGCCCCTGGAGAAGCCAGTGACCCTCCGGTGCCAGGGACCTCCGGGCGTGGACCTGTACCGCCTGGAG
aligned sequence HM 3_T7 (HM 3_T7.ab1)
AAGCTGAGTTCCAGCAGGTACCAGGATCAGGCAGTCCTCTTCATCCCGGCCATGAAGAGAAGTCTGGCTGGACGCTACCGCTGCTCCTACCAGAACGGAA
D1
template sequence human mouse final
AAGCTGAGTTCCAGCAGGTACCAGGATCAGGCAGTCCTCTTCATCCCGGCCATGAAGAGAAGTCTGGCTGGACGCTACCGCTGCTCCTACCAGAACGGAA
aligned sequence HM 3_T7 (HM 3_T7.ab1)
GCCTCTGGTCCCTGCCCAGCGACCAGCTGGAGCTCGTTGCCACGGGAGTTTTTGCCAAAccctcactctcagctcatcccagctcagcagtccctcaagg
D1
Mouse D2
template sequence human mouse final
GCCTCTGGTCCCTGCCCAGCGACCAGCTGGAGCTCGTTGCCACGGGAGTTTTTGCCAAACCCTCACTCTCAGCTCATCCCAGCTCAGCAGTCCCTCAAGG
aligned sequence HM 3_T7 (HM 3_T7.ab1)
cagggatgtgactctgaagtgccagagcccatacagttttgatgaattcgttctatacaaagaaggggatactgggtcttataagagacctgagaaatgg
Mouse D2
template sequence human mouse final
CAGGGATGTGACTCTGAAGTGCCAGAGCCCATACAGTTTTGATGAATTCGTTCTATACAAAGAAGGGGATACTGGGTCTTATAAGAGACCTGAGAAATGG
aligned sequence HM 3_T7 (HM 3_T7.ab1)

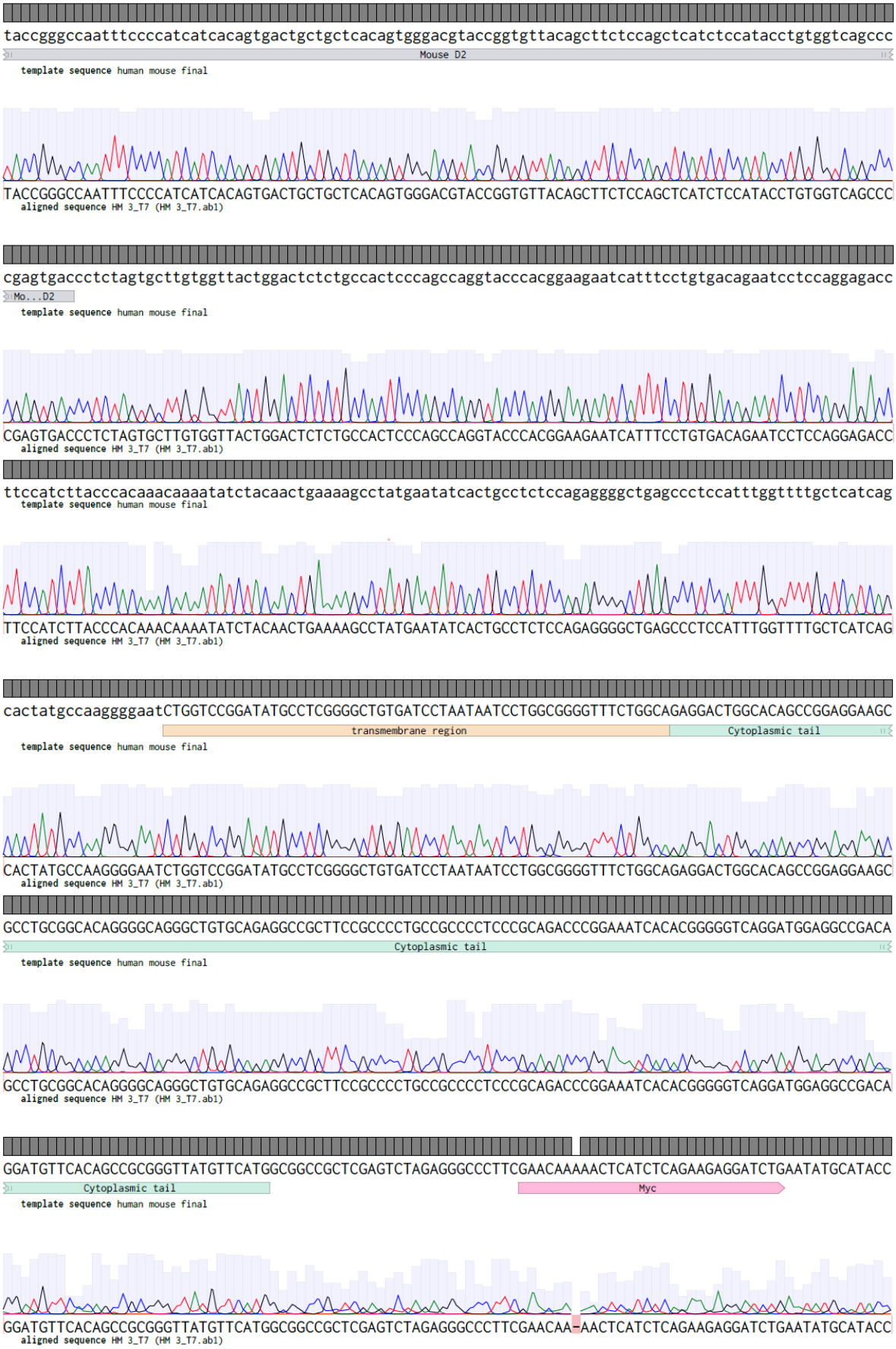

Figure 8.5. Human-Mouse (HM) sequencing results.

pEFa vector map with hm sequence (human mouse final) compare with sequencing results obtained with the T7 forward primer (HM 3_T7). Protein structural features and sequencing traces are shown.

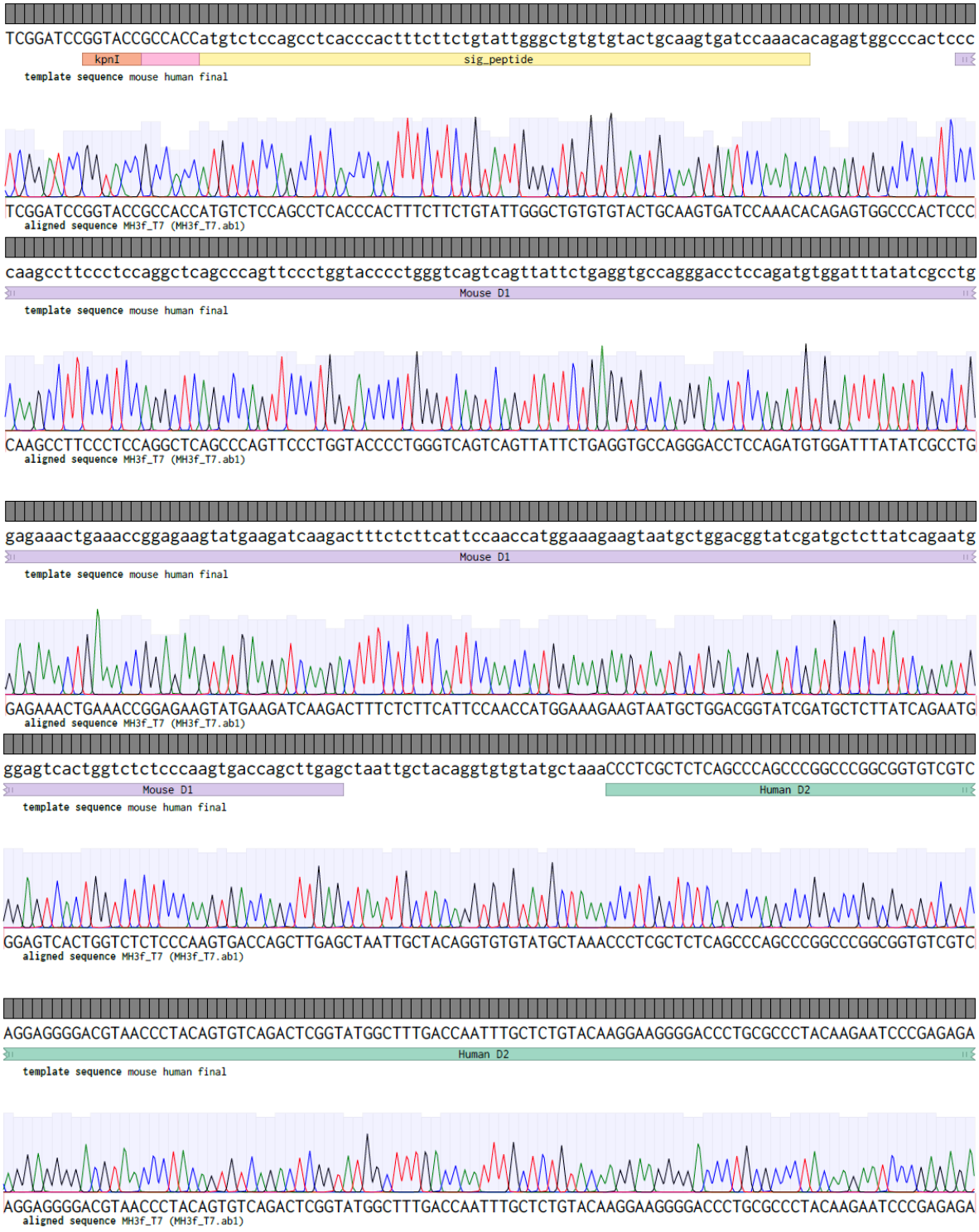
TCGGATCCGGTACCGCCACCatgtctccagcctcacccactttcttctgtattgggctgtgtgtactgcaagtgatccaaacacagagtggcccactccc
kpnI
sig_peptide
template sequence mouse human final
TCGGATCCGGTACCGCCACCATGTCTCCAGCCTCACCCACTTTCTTCTGTATTGGGCTGTGTGTACTGCAAGTGATCCAAACACAGAGTGGCCCACTCCC
aligned sequence MH3f_T7 (MH3f_T7.ab1)
caagccttccctccaggctcagcccagttccctggtacccctgggtcagtcagttattctgaggtgccagggacctccagatgtggatttatatcgcctg
Mouse D1
template sequence mouse human final
CAAGCCTTCCCTCCAGGCTCAGCCCAGTTCCCTGGTACCCCTGGGTCAGTCAGTTATTCTGAGGTGCCAGGGACCTCCAGATGTGGATTTATATCGCCTG
aligned sequence MH3f_T7 (MH3f_T7.ab1)
gagaaactgaaaccggagaagtatgaagatcaagactttctcttcattccaaccatggaaagaagtaatgctggacggtatcgatgctcttatcagaatg
Mouse D1
template sequence mouse human final
GAGAAACTGAAACCGGAGAAGTATGAAGATCAAGACTTTCTCTTCATTCCAACCATGGAAAGAAGTAATGCTGGACGGTATCGATGCTCTTATCAGAATG
aligned sequence MH3f_T7 (MH3f_T7.ab1)
ggagtcactggtctctcccaagtgaccagcttgagctaattgctacaggtgtgtatgctaaaCCCTCGCTCTCAGCCCAGCCCGGCCCGGCGGTGTCGTC
Mouse D1
Human D2
template sequence mouse human final
GGAGTCACTGGTCTCTCCCAAGTGACCAGCTTGAGCTAATTGCTACAGGTGTGTATGCTAAACCCTCGCTCTCAGCCCAGCCCGGCCCGGCGGTGTCGTC
aligned sequence MH3f_T7 (MH3f_T7.ab1)
AGGAGGGGACGTAACCCTACAGTGTCAGACTCGGTATGGCTTTGACCAATTTGCTCTGTACAAGGAAGGGGACCCTGCGCCCTACAAGAATCCCGAGAGA
Human D2
template sequence mouse human final
AGGAGGGGACGTAACCCTACAGTGTCAGACTCGGTATGGCTTTGACCAATTTGCTCTGTACAAGGAAGGGGACCCTGCGCCCTACAAGAATCCCGAGAGA
aligned sequence MH3f_T7 (MH3f_T7.ab1)

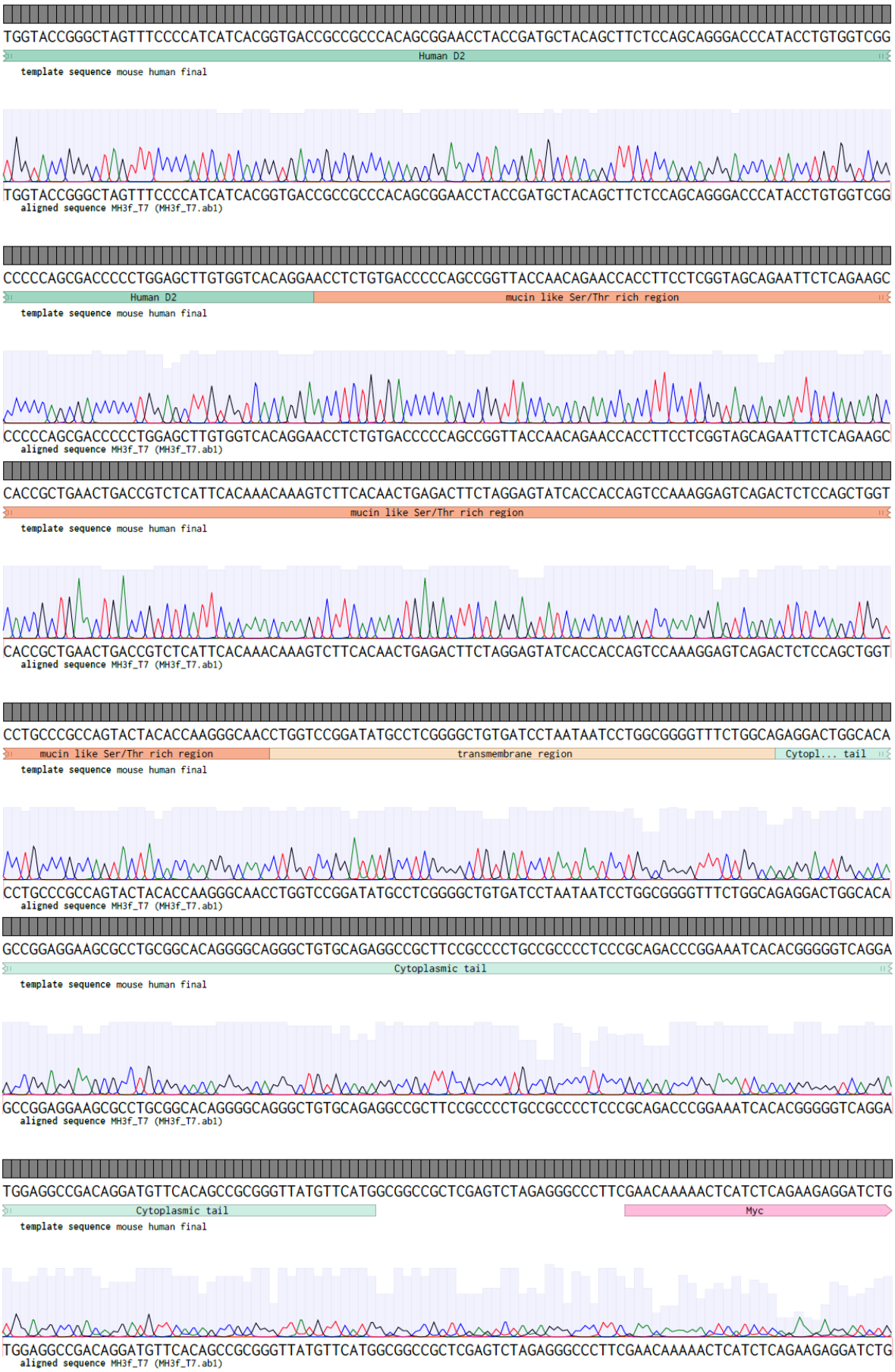
TGGTACCGGGCTAGTTTCCCCATCATCACGGTGACCGCCGCCCACAGCGGAACCTACCGATGCTACAGCTTCTCCAGCAGGGACCCATACCTGTGGTCGG
Human D2
template sequence mouse human final
TGGTACCGGGCTAGTTTCCCCATCATCACGGTGACCGCCGCCCACAGCGGAACCTACCGATGCTACAGCTTCTCCAGCAGGGACCCATACCTGTGGTCGG
aligned sequence MH3f_T7 (MH3f_T7.ab1)
CCCCCAGCGACCCCCTGGAGCTTGTGGTCACAGGAACCTCTGTGACCCCCAGCCGGTTACCAACAGAACCACCTTCCTCGGTAGCAGAATTCTCAGAAGC
Human D2
mucin like Ser/Thr rich region
template sequence mouse human final
CCCCCAGCGACCCCCTGGAGCTTGTGGTCACAGGAACCTCTGTGACCCCCAGCCGGTTACCAACAGAACCACCTTCCTCGGTAGCAGAATTCTCAGAAGC
aligned sequence MH3f_T7 (MH3f_T7.ab1)
CACCGCTGAACTGACCGTCTCATTCACAAACAAAGTCTTCACAACTGAGACTTCTAGGAGTATCACCACCAGTCCAAAGGAGTCAGACTCTCCAGCTGGT
mucin like Ser/Thr rich region
template sequence mouse human final
CACCGCTGAACTGACCGTCTCATTCACAAACAAAGTCTTCACAACTGAGACTTCTAGGAGTATCACCACCAGTCCAAAGGAGTCAGACTCTCCAGCTGGT
aligned sequence MH3f_T7 (MH3f_T7.ab1)
CCTGCCCGCCAGTACTACACCAAGGGCAACCTGGTCCGGATATGCCTCGGGGCTGTGATCCTAATAATCCTGGCGGGGTTTCTGGCAGAGGACTGGCACA
mucin like Ser/Thr rich region
transmembrane region
Cytopl... tail
template sequence mouse human final
CCTGCCCGCCAGTACTACACCAAGGGCAACCTGGTCCGGATATGCCTCGGGGCTGTGATCCTAATAATCCTGGCGGGGTTTCTGGCAGAGGACTGGCACA
aligned sequence MH3f_T7 (MH3f_T7.ab1)
GCCGGAGGAAGCGCCTGCGGCACAGGGGCAGGGCTGTGCAGAGGCCGCTTCCGCCCCTGCCGCCCCTCCCGCAGACCCGGAAATCACACGGGGGTCAGGA
Cytoplasmic tail
template sequence mouse human final
GCCGGAGGAAGCGCCTGCGGCACAGGGGCAGGGCTGTGCAGAGGCCGCTTCCGCCCCTGCCGCCCCTCCCGCAGACCCGGAAATCACACGGGGGTCAGGA
aligned sequence MH3f_T7 (MH3f_T7.ab1)
TGGAGGCCGACAGGATGTTCACAGCCGCGGGTTATGTTCATGGCGGCCGCTCGAGTCTAGAGGGCCCTTCGAACAAAAACTCATCTCAGAAGAGGATCTG
Cytoplasmic tail
Myc
template sequence mouse human final
TGGAGGCCGACAGGATGTTCACAGCCGCGGGTTATGTTCATGGCGGCCGCTCGAGTCTAGAGGGCCCTTCGAACAAAAACTCATCTCAGAAGAGGATCTG
aligned sequence MH3f_T7 (MH3f_T7.ab1)

Figure 8.6. Mouse-human sequencing results.

pEFa vector map with hm sequence (mouse human final) compare with sequencing results obtained with the T7 forward primer (MH3f_T7). Protein structural features and sequencing traces are shown.


TCGGATCCGGTACCGCCACCatgtctccagcctcacccactttcttctgtattgggctgtgtgtactgcaagtgatccaaacacagagtggcccactccc
kpnI
sig_peptide
template sequence mouse final
TCGGATCCGGTACCGCCACCATGTCTCCAGCCTCACCCACTTTCTTCTGTATTGGGCTGTGTGTACTGCAAGTGATCCAAACACAGAGTGGCCCACTCCC
aligned sequence M2f_T7 (M2f_T7.ab1)
caagccttccctccaggctcagcccagttccctggtaccctgggtcagtcagttattctgaggtgccagggacctccagatgtggatttatatcgcctg
Mouse D1
template sequence mouse final
CAAGCCTTCCCTCCAGGCTCAGCCCAGTTCCCTGGTACCCCTGGGTCAGTCAGTTATTCTGAGGTGCCAGGGACCTCCAGATGTGGATTTATATCGCCTG
aligned sequence M2f_T7 (M2f_T7.ab1)
gagaaactgaaaccggagaagtatgaagatcaagactttctcttcattccaaccatggaaagaagtaatgctggacggtatcgatgctcttatcagaatg
Mouse D1
template sequence mouse final
GAGAAACTGAAACCGGAGAAGTATGAAGATCAAGACTTTCTCTTCATTCCAACCATGGAAAGAAGTAATGCTGGACGGTATCGATGCTCTTATCAGAATG
aligned sequence M2f_T7 (M2f_T7.ab1)
ggagtcactggtctctcccaagtgaccagcttgagctaattgctacaggtgtgtatgctaaaccctcactctcagctcatcccagctcagcagtccctca
Mouse D1
Mouse D2
template sequence mouse final
GGAGTCACTGGTCTCTCCCAAGTGACCAGCTTGAGCTAATTGCTACAGGTGTGTATGCTAAACCCTCACTCTCAGCTCATCCCAGCTCAGCAGTCCCTCA
aligned sequence M2f_T7 (M2f_T7.ab1)
aggcagggatgtgactctgaagtgccagagcccatacagttttgatgaattcgttctatacaaagaaggggatactgggtcttataagagacctgagaaa
Mouse D2
template sequence mouse final
AGGCAGGGATGTGACTCTGAAGTGCCAGAGCCCATACAGTTTTGATGAATTCGTTCTATACAAAGAAGGGGATACTGGGTCTTATAAGAGACCTGAGAAA
aligned sequence M2f_T7 (M2f_T7.ab1)

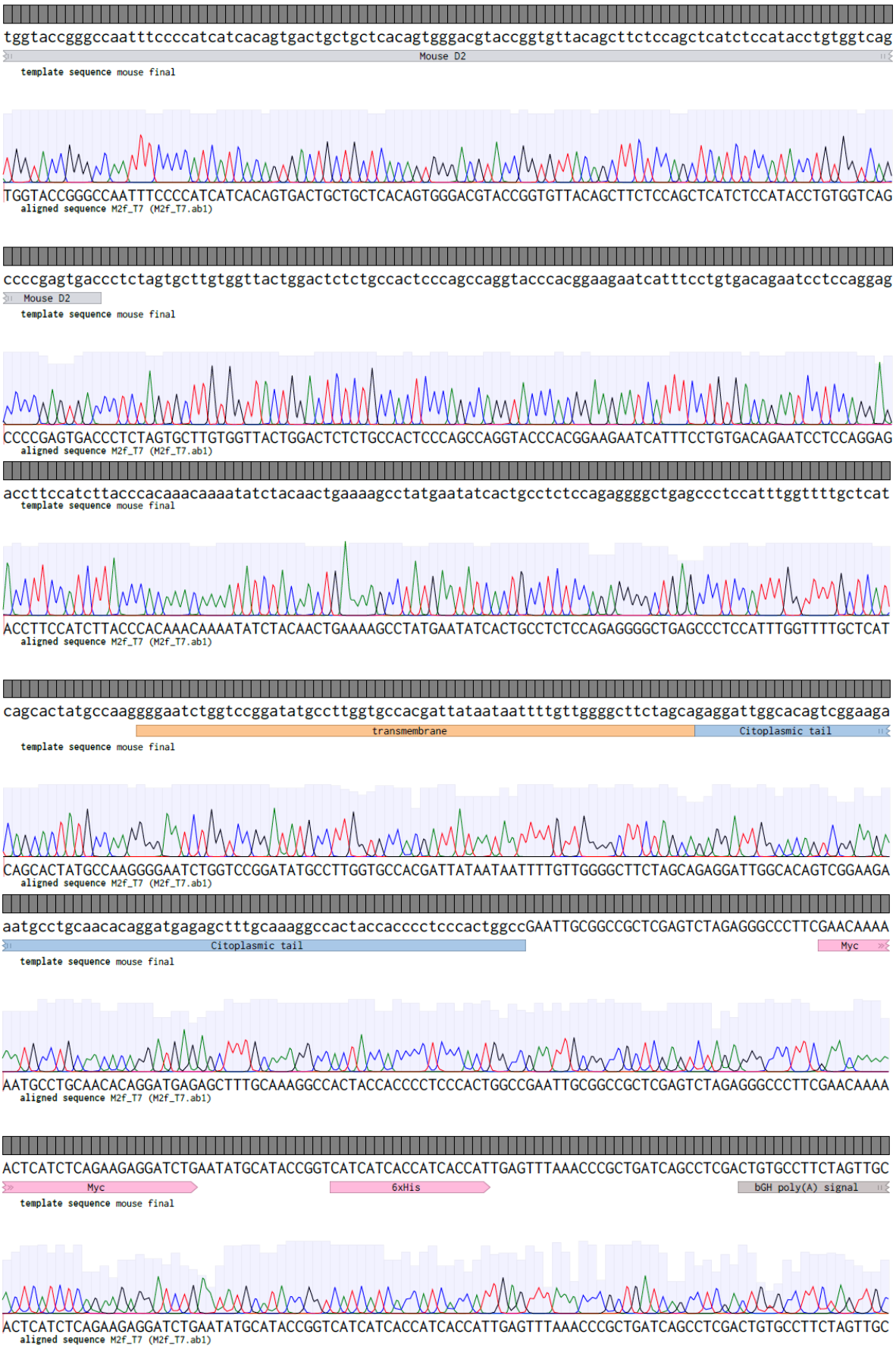

Figure 8.7. Mouse sequencing results.

pEFa vector map with mouse sequence (mouse final) compare with sequencing results obtained with the T7 forward primer (M2f_T7). Protein structural features and sequencing traces are shown.

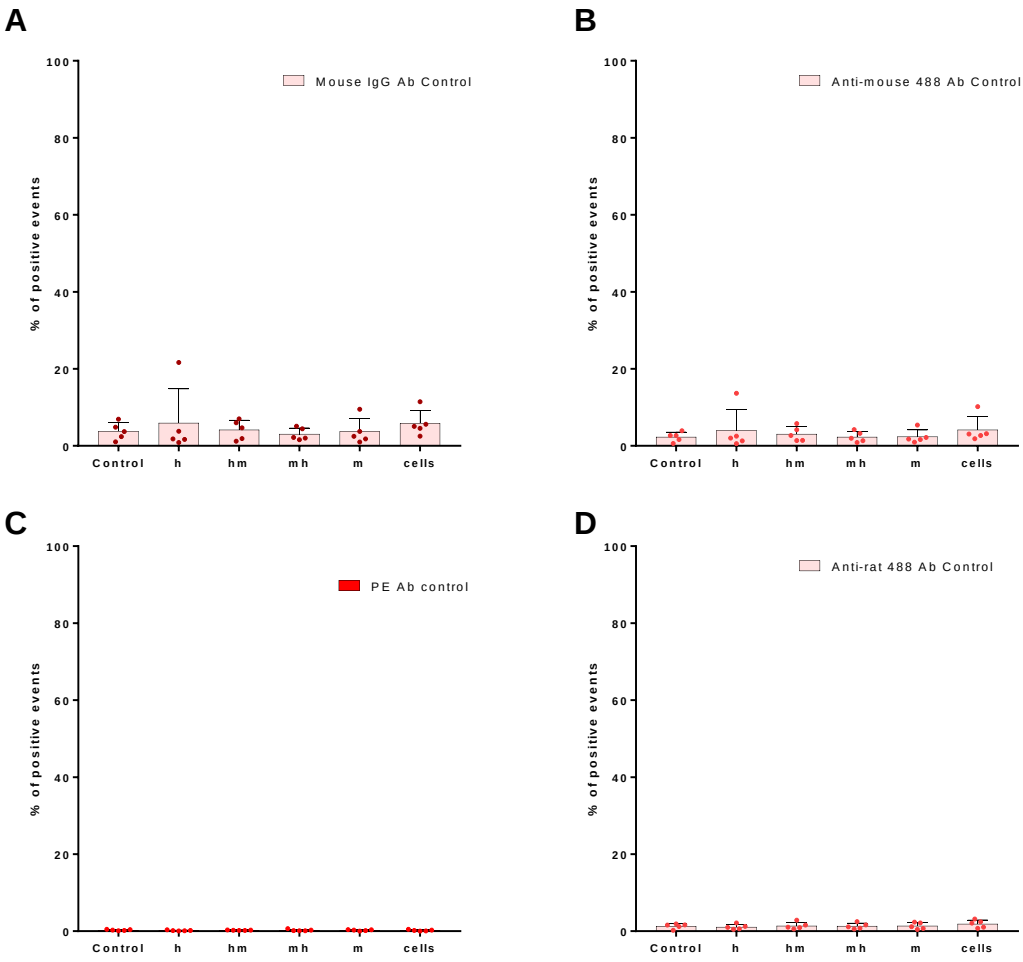

Figure 8.8. IgGs and secondary antibodies controls.

Lenti-X 293T cells expressing human (h), human D1 mouse D2 (hm), mouse D1human D2 (mh) and mouse GPVI. Controls are cells transfected with empty vectors (Control) and cells are non-transfected (cells). Samples were incubated with secondary and control antibodies before the flow cytometric analysis. The percentage of positive events was plotted against the cells expressing the different GPVI and analysed using a one-way ANOVA with Dunnett's multiple comparation test. Data are shown as mean ± SD and are representative of five independent experiments.